Metabolic Survival Strategies of Fe(II) Oxidation Coupled to Nitrate Reduction in the Chemolithoautotrophic Enrichment Cultures

Dissertation

der Mathematisch-Naturwissenschaftlichen Fakultät

der Eberhard Karls Universität Tübingen

zur Erlangung des Grades eines

Doktors der Naturwissenschaften

(Dr. rer. nat.)

vorgelegt von

M.Sc. Yu-Ming Huang

aus Taoyuan, Taiwan

Tübingen

2021

Gedruckt mit Genehmigung der Mathematisch-Naturwissenschaftlichen Fakultät der Eberhard Karls Universität Tübingen.

Tag der mündlichen Qualifikation:	07.10.2021
Dekan:	Prof. Dr. Thilo Stehle
1. Berichterstatter:	Jun.-Prof. Dr. Sara Kleindienst
2. Berichterstatter:	Prof. Dr. Karl Forchhammer

Table of Contents

Acknowledgements

I appreciate the financial support of the Deutsche Forschungsgemeinschaft (DFG) and the help from lots of people! Foremost, I would like to thank my supervisors, Jun-Prof. Dr. Sara Kleindienst and Prof. Dr. Andreas Kappler, for offering me the opportunity to work on this topic and to spend the great time in the Microbial ecology and Geomicrobiology group in a lovely city, Tübingen. Sara and Andreas were always accessible and very supportive when I faced difficulties throughout different phases of my PhD, even during Sara's parental leave. Both of them helped me enormously during the publication manuscript preparation process, it was great to work with and learn from them.

I also want to thank Prof. Dr. Karl Forchhammer and Prof. Dr. Klaus Hantke, who gave me several nice ideas during my committee meetings and helped me to evaluate the results and to plan further steps every year throughout my PhD. I appreciate the post-doctoral supervisors: Dr. Nia Blackwell, Dr. Daniel Straub and Dr. Adrian Langarica-Fuentes, who supported me a lot during Sara's parental leave and provided a lot of fruitful inputs for this study. I enjoyed many enlightening discussions with these supervisors, from which I have gained knowledge, skills and am greatly inspired to be even more curious and enthusiastic towards science.

I would like to extend my thanks to other supportive post-doctoral researchers: Dr. Casey Bryce, Dr. Sergey Abramov and Dr. Katharine (Kate) Thompson. Casey helps me a lot in the beginning of my PhD phase, she also helped me plan my PhD and for the sampling trip in Bremen, together with Timm Bayer and Lea Sauter. Sergey and Kate helped me a lot during the final phase of my PhD. They gave me advices to interpret the data and review the manuscripts.

I also want to express my appreciation to every team member in the Microbial Ecology and Geomicrobiology group. The relationship with those colleagues became friendships, which made me feel relaxed during any stressful periods! Particularly, I appreciate the support and company of my previous office mates, Constantin App, Saskia Rughöft, Chao Peng and my master student, Nicole Smith, as well as my current office mates, Franziska Schädler and Adrian. I appreciate Anh Van Le, Christopher Schwerdhelm, Markus Maisch, Ankita Chauhan, Monique Patzner and Timm Bayer that they always bring me joy whenever I walk at the hallway or work in the lab. I thank Natalia Jakus, Jianrong Huang and Stefanie Becker who work on similar projects as I do, so that I can discuss my results with them and get some input and suggestions. Anjela Thon and other MolBio group members, gave me a lot of valuable suggestions and feedback during the group seminar presentation. I would also like to thank Shun Li and Wiebke Ruschmeier the

sediment sampling in Bremen and enrichment set up for culture BP, which is the starting material for part of this study. I want to thank Katrin Wunsch for all of her help of DAPI cell count, Hanna Joss for DOC measurements and Stefan Fischer for conducting scanning electron microscopy. I am grateful to laboratory technicians Ellen Röhm, Lars Grimm and Franziska Schädler for their great technical supports and enormous efforts to keep the lab organized. I am thankful to Elisabetha Kraft, Marion Schäffling, Wolfgang Bott and Iris Dreher and Ulrich Nasarek for their administrative and IT help that enabled me to focus on my study. I would like to thank Dr. Ulf Lüder, Yuge, Jianrong, Verena Nikeleit, Natalia, Stefanie, Kate, Sergey, Dr. Muammar Mansor, Dr. Manuel Schad, Adrian and Abdelhakim Boudrioua for proofreading this thesis. My time in Tübingen was very enjoyable due to many friends that participated in my life. I thank my good friends Yuge Bai, Xiaohua Han, Dandan Chen and Zhen Yang for sharing leisure time, traveling together in Spain and bring me so much laugh and joy. I am grateful to Jing He, Chao Peng, and Lu Lu for helping me before and after I got this PhD position to integrate in the research groups in Tübingen. I also appreciate my friend Pei-Hua Tsai in the US and the friends in Taiwan. Even though they are far away on the other side of the Earth, their care and encouragement always supported me.

Also, there are so many others that I should thank, without them, I might have never been able to pursue a PhD degree. First, Prof. Dr. Chiu-Chung Young and Prof. Dr. Chang-Hsien Yang, who are my supervisors and offered me the opportunity to work in their labs during my bachelor and master, respectively. Dr. Asif Hameed and Wen-Hsuan Ko, who patiently taught me all of the basic biochemistry and biotechnology laboratory skills, during my bachelor and master, respectively.

Last but not least, I would like to thank my family, my parents, which makes me able to follow my heart and be proud of who I am with their unconditional love, care and support; my sister, who always supports me with company and tasty Taiwanese food when I feel homesick; my brother and his family, whenever I saw my cute nephew, he can always relieve my stress. Moreover, I want to thank my boyfriend, who understands me and shares my happiness and sadness. I also want to thank his parents and sister for treating me as a part of the family, to travel and to celebrate holidays together. Their company and care make my life abroad much easier and enjoyable!

Abstract

Chemical and microbial iron (Fe) redox processes play important roles in changing the fate of many contaminants (e.g. arsenic, cadmium) and nutrients. Fe(II)-oxidizing bacteria (FeOB) are widespread in the environment, being able to utilize several different electron acceptors, including nitrate. Autotrophic nitrate-reducing FeOB can remove nitrate and fix carbon, which leads to the production of greenhouse gases, i.e. nitrous oxide and carbon dioxide. Nitrate-reducing FeOB have been found in various types of environments such as freshwater sediments and groundwater, where they can potentially contribute to the removal of nitrate. To date, the autotrophic growth of nitrate-reducing FeOB is poorly investigated. The most prominent model system to study these microbes are enrichment cultures, i.e. mixed microbial communities performing nitrate reduction coupled to Fe(II) oxidation (NRFeOx) via metabolic exchange within the community. For example, enrichment cultures KS and BP from freshwater sediment in Bremen, Germany and culture AG from groundwater in Altingen, Germany were reported as autotrophic nitrate-reducing FeOB enrichment cultures.

The studies in chapter 2 and 3 provide evidence that individual species in the nitrate-reducing FeOB enrichment cultures KS and BP perform Fe(II) oxidation, denitrification, carbon fixation and oxidative phosphorylation, and further propose interspecies interaction in each enrichment culture. In chapter 3, we report the geochemistry, the community relative abundance, the existence, and activity of the microorganisms in the original sampling site of BP culture. In addition to these results, we compared and analyzed the taxonomic position of three, so far, unclassified *Gallionellaceae* spp., that dominate in all currently existing autotrophic nitrate-reducing FeOB enrichment cultures, KS, BP, and AG. In chapter 4, we further classified these *Gallionellaceae* spp. as representatives of novel candidate taxa and proposed *Candidatus* (*Ca.*) names, '*Ca.* Ferrigenium straubiae' sp. nov., '*Ca.* Ferrigenium bremense' sp. nov. and '*Ca.* Ferrigenium altingense' sp. nov. for bacteria growing in cultures KS, BP, and AG, respectively. The mechanisms, ecology, and environmental implications of microbial anaerobic Fe(II) oxidation were discussed in chapter 5.

Meta-omic (i.e., metagenomics, metatranscriptomics, and metaproteomics) analyses were applied to both cultures KS and BP. For culture KS, the meta-omic analyses demonstrated that *Gallionellaceae* sp. and *Rhodanobacter* sp. were the key players performing Fe(II) oxidation coupled to denitrification under anoxic autotrophic conditions.

'*Ca.* Ferrigenium straubiae' might oxidize Fe(II), fix CO_2, perform partial denitrification and produce nitric oxide (NO). The *Rhodanobacter* sp. may use the organic carbon fixed by '*Ca.* Ferrigenium straubiae' and help '*Ca.* Ferrigenium straubiae' to further detoxify the NO. This indicates that '*Ca.* Ferrigenium straubiae' and *Rhodanobacter* sp. in culture KS are interdependent. In culture BP, the dominant '*Ca.* Ferrigenium bremense' might play a similar role as '*Ca.* Ferrigenium straubiae'. However, '*Ca.* Ferrigenium bremense' only possess the genes encoding nitrite reductase (*nirK*/*S*) and nitric oxide reductase (*norBC*). Therefore, the initiation and completion of the denitrification pathway by this species would require cooperation with other community members, e.g. the *Noviherbaspirillum* sp. and *Thiobacillus* sp., which possess the missing denitrification genes. In theory, the *Noviherbaspirillum* sp. and *Thiobacillus* sp. in culture BP have the ability to proceed NRFeOx autotrophically, i.e. all genes and transcripts potentially involved in metal oxidation (e.g. *cyc2* or *mtoA*), denitrification and carbon fixation (e.g. *rbcL*) were detected. In addition to NRFeOx, the detection of the transcripts and partial proteins of cbb_3- and aa_3-type cytochrome *c* in both enrichment culture KS and BP, suggest that '*Ca.* Ferrigenium straubiae' and '*Ca.* Ferrigenium bremense' have an adaptation for growing under microoxic conditions. In '*Ca.* Ferrigenium altingense' (culture AG), the genes encoding cbb_3- and aa_3-type types cytochrome *c* were also detected. However, these three enrichment cultures KS, BP, and AG were grown under anoxic autotrophic conditions. We proposed the further experiments to provide the evidence for the microaerophilic lifestyle of these three *Ca. Gallionellaceae* spp. in chapter 6.

As for the environmental relevance, '*Ca.* Ferrigenium bremense' accounted for approximately 0.13% relative abundance *in situ*. The other flanking members in culture BP were also detected *in situ* except for the *Noviherbaspirillum* sp. Additionally, 36 distinct *Gallionellaceae* taxa were detected *in situ*, suggesting that the diversity of microorganisms affiliated to *Gallionellaceae* that can potentially contribute to NRFeOx might be even higher than currently known. Overall, the studies in this dissertation improve our understanding of the metabolic mechanism of microbial survival strategies of nitrate-reducing FeOB in the enrichment cultures and its original environment, and could serve as the foundation for the further studies of nitrate-reducing FeOB and for the application of nitrate-reducing FeOB for the decontamination of polluted environments.

Zusammenfassung

Chemische und mikrobielle Eisen (Fe)-Redoxprozesse spielen eine wichtige Rolle zum Verbleib vieler Schadstoffe (z.B. Arsen, Cadmium) und Nährstoffe in der Umwelt. Fe(II)-oxidierende Bakterien (FeOB) sind in der Umwelt weit verbreitet und können mehrere verschiedene Elektronenakzeptoren, einschließlich Nitrat, nutzen. Autotrophe nitratreduzierende FeOB können Nitrat abbauen und Kohlenstoff fixieren, was zur Produktion von Treibhausgasen, z.B. Lachgas und Kohlenstoffdioxid, führt. Nitratreduzierende FeOB wurden in verschiedenen Gebieten wie Süßwassersedimenten und Grundwasser gefunden und als mögliche Behandlung für Nitratverunreinigungen in Aquiferen und Abwässern untersucht. Bis heute ist das autotrophe Wachstum von nitratreduzierenden FeOB nur wenig erforscht. Das prominenteste Modellsystem zur Untersuchung dieser Mikroben sind Anreicherungskulturen, d.h mikrobielle Gemeinschaften, die Nitratreduktion gekoppelt an die Fe(II)-Oxidation (NRFeOx) gemeinsam durchführen. Zum Beispiel wurden die Anreicherungskulturen KS und BP aus einem Süßwassersediment in Bremen, Deutschland, und die Kultur AG aus dem Grundwasser in Altingen, Deutschland, als autotrophe nitratreduzierende FeOB-Anreicherungskulturen berichtet.

Die Studien in Kapitel 2 und 3 belegen die Fähigkeit zur Durchführung von Fe(II)-Oxidation, Denitrifikation, Kohlenstofffixierung und oxidativer Phosphorylierung in den einzelnen Spezies in den nitratreduzierenden FeOB-Anreicherungskulturen KS und BP, und deuten außerdem auf Interaktionen zwischen den Spezies jeder Anreicherungskultur hin. In Kapitel 3 berichten wir über die Geochemie, die relative Häufigkeit in der Gemeinschaft sowie über die Existenz und Aktivität der Mikroorganismen in der ursprünglichen Probenahmestelle der Kultur BP. Zusätzlich zu diesen Ergebnissen verglichen und analysierten wir die taxonomische Position von drei bisher nicht klassifizierten *Gallionellaceae* spp., die alle derzeit existierenden autotrophen nitratreduzierenden FeOB-Anreicherungskulturen, KS, BP und AG, dominieren. In Kapitel 4 haben wir diese *Gallionellaceae* spp. als Vertreter neuer Kandidatentaxa klassifiziert und die *Candidatus* (*Ca.*)-Namen "*Candidatus* Ferrigenium straubiae" sp. nov., "*Candidatus* Ferrigenium bremense" sp. nov. und "*Candidatus* Ferrigenium altingense" sp. nov. für die in den Kulturen KS, BP und AG wachsenden Bakterien vorgeschlagen.

Die Mechanismen, Ökologie und Umweltauswirkungen der mikrobiellen anaeroben Fe(II)-Oxidation wurden in Kapitel 5 diskutiert.

Die Metaomics-Analysen (d.h. Metagenomics, Metatranscriptomics und Metaproteomics) wurde auf die beiden Kulturen KS und BP angewendet. Für die Kultur KS zeigte die Metaomics-Analyse, dass *Gallionellaceae* sp. und *Rhodanobacter* sp. die Hauptakteure bei der Fe(II)-Oxidation in Verbindung mit Denitrifikation unter anoxischen autotrophen Bedingungen waren. '*Ca*. Ferrigenium straubiae' könnte Fe(II) oxidieren, CO_2 fixieren, eine partielle Denitrifikation durchführen und Stickstoffoxid (NO) produzieren. *Rhodanobacter* sp. könnte den von '*Ca.* Ferrigenium straubiae' fixierten organischen Kohlenstoff nutzen und '*Ca.* Ferrigenium straubiae' bei der weiteren Entgiftung des NO helfen. Dies deutet darauf hin, dass '*Ca.* Ferrigenium straubiae' und *Rhodanobacter* sp. in der Kultur KS voneinander abhängig sind. In der Kultur BP könnte das dominante '*Ca.* Ferrigenium bremense' eine ähnliche Rolle spielen wie '*Ca.* Ferrigenium straubiae'. Jedoch besitzt '*Ca.* Ferrigenium bremense' nur die Gene, die für Nitritreduktase (*nirK*/*S*) und Stickoxidreduktase (*norBC*) kodieren. Daher würde die Initiierung und Vervollständigung des Denitrifikationsweges durch diese Spezies die Zusammenarbeit mit anderen Mitgliedern der Gemeinschaft erfordern, z.B. mit *Noviherbaspirillum* sp. und *Thiobacillus* sp., die die fehlenden Denitrifikationsgene besitzen. Theoretisch haben die *Noviherbaspirillum* sp. und *Thiobacillus* sp. in der Kultur BP die Fähigkeit, die NRFeOx autotroph durchzuführen, d.h. es wurden alle Gene und Transkripte nachgewiesen, die potentiell an der Metalloxidation (z.B. *cyc2* oder *mtoA*), Denitrifikation und Kohlenstofffixierung (z.B. *rbcL*) beteiligt sind. Der Nachweis der Transkripte und Teilproteine des cbb_3- und aa_3-Typs von Cytochrom *c* sowohl in der Anreicherungskultur KS als auch in BP lässt neben NRFeOx darauf schließen, dass '*Ca.* Ferrigenium straubiae' und '*Ca.* Ferrigenium bremense' eine Anpassung an das Wachstum unter mikrooxischen Bedingungen aufweisen könnten. In '*Ca.* Ferrigenium altingense' (Kultur AG) wurden auch die Gene, die für die Cytochrom *c*-Typen cbb_3 und aa_3 kodieren, nachgewiesen. Die drei Anreicherungskulturen KS, BP und AG wurden jedoch unter anoxischen autotrophen Bedingungen kultiviert. In Kapitel 6 schlagen wir weitere Experimente mit den drei *Candidatus Gallionellaceae* spp. vor, die ihre Fähigkeit zur mikroaerophilen Lebensweise untersuchen.

Was die Umweltrelevanz betrifft, macht '*Ca.* Ferrigenium bremense' 0,13 % der relativen Abundanz *in situ* aus. Die anderen flankierenden Mitglieder in der Kultur BP wurden mit Ausnahme von *Noviherbaspirillum* sp. auch *in situ* nachgewiesen. Darüber hinaus wurden 36 verschiedene *Gallionellaceae*-Taxa *in situ* nachgewiesen, was darauf hindeutet, dass die Vielfalt der mit *Gallionellaceae* verbundenen Mikroorganismen, die potenziell zu NRFeOx beitragen können, noch größer sein könnte als derzeit bekannt. Insgesamt haben die Untersuchungen in dieser Dissertation unser Verständnis des Stoffwechselmechanismus der mikrobiellen Überlebensstrategien von nitratreduzierenden FeOB in den Anreicherungskulturen und ihrer ursprünglichen Umgebung verbessert und könnten als Grundlage für den Einsatz von nitratreduzierenden FeOB zur Dekontamination verschmutzter Umgebungen dienen.

1. Introduction

1.1. Microbial iron cycling in the environment

Iron (Fe) is the fourth most abundant element in the Earth's crust (Clarke and Washington, 1924) and is an essential element for living organisms since it is incorporated as a cofactor in many enzymes (Ilbert and Bonnefoy, 2013). Oxidation of ferrous iron [Fe(II)] and reduction of ferric iron [Fe(III)] contribute to biogeochemical carbon, nitrogen, oxygen and sulfur cycles and can be mediated by specific microorganisms within soils and sediments (Cornell and Schwertmann, 1996). Fe can be used as an energy and electron source or electron sink by a broad diversity of bacteria and archaea (Fig. 1.1) (Bird *et al.*, 2011; Melton *et al.*, 2014). In many habitats, e.g. hot, cold, freshwater, marine, terrestrial, aquatic, contaminated or pristine, these microorganisms play important roles in Fe redox cycling (Ehrlich *et al.*, 2015; Kappler *et al.*, 2021).

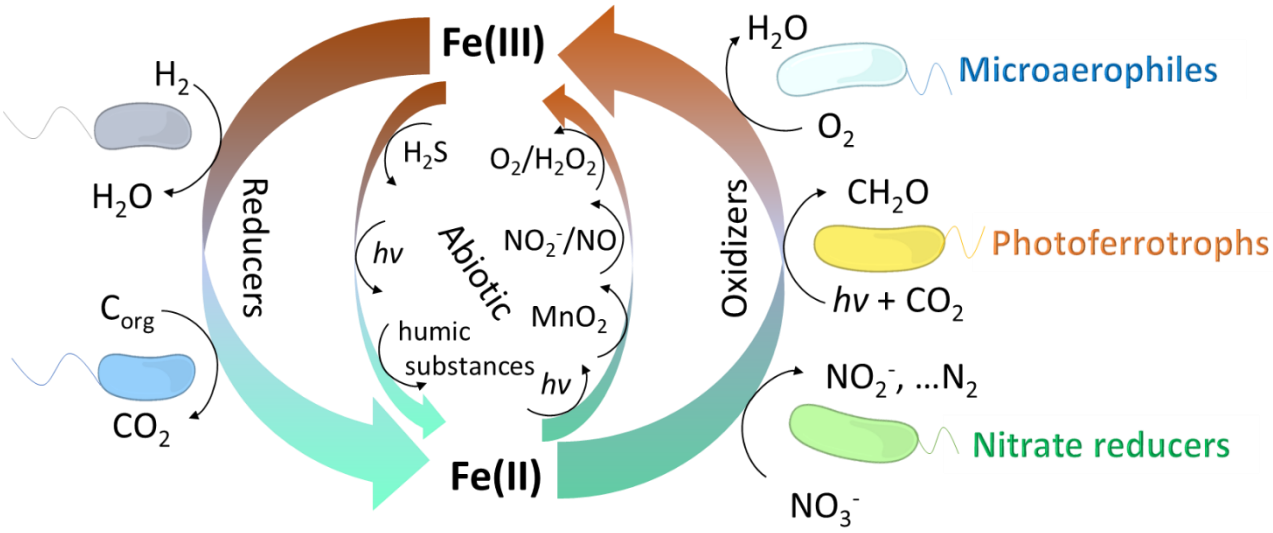

Fig. 1.1: Microbial and abiotic Fe cycling in the environment

Several microorganisms, e.g. *Shewanella* spp. (Myers and Nealson, 1990; Hau and Gralnick, 2007) and *Geobacter* spp. (Lovley and Phillips, 1988; Lovley *et al.*, 2011) can reduce Fe(III) with different electron donors, such as H_2, acetate, lactate and humic substances (Fig. 1.1). Compared to Fe(III), Fe(II) is more bioavailable, since it is relatively soluble at circumneutral pH; however, it gets rapidly oxidized by O_2, resulting in the

formation of poorly soluble Fe(III) (oxyhydr)oxides (Davison and Seed, 1983). Whereas, Fe(II) is more stable with O_2 at low pH and ambient temperature (Porsch and Kappler, 2011). There are some well-studied acidophilic autotrophic Fe(II)-oxidizing bacteria (FeOB), such as *Acidithiobacillus ferrooxidans* (previously called *Thiobacillus ferrooxidans*) (Temple and Colmer, 1951) and *Leptospirillum ferriphilum* (Coram and Rawlings, 2002) isolated from acid mine drainage, demonstrating the presence of FeOB under extreme conditions. At neutral pH conditions, neutrophilic FeOB can use both dissolved and solid Fe(II) as an electron donor (Ehrenberg, 1838), under either oxic conditions, i.e., microaerophilic and acidophilic FeOB, or anoxic conditions, i.e., nitrate-reducing and phototrophic FeOB (Widdel *et al.*, 1993; Straub *et al.*, 1996; Hedrich *et al.*, 2011; Emerson, 2012). There are three physiological types of neutrophilic FeOB, i.e. microaerophiles, photoferrotrophs and nitrate-reducing Fe(II) oxidizers (Fig. 1.1).

Microaerophilic FeOB were often found in oxic/anoxic interfaces with low oxygen concentrations (<50 µM) (Emerson and Moyer, 1997; Emerson, 2012). Microaerophilic FeOB grow lithoautotrophically using Fe(II) as an electron donor and O_2 as electron acceptor (Equation 1) (Emerson *et al.*, 2010). These bacteria are members of Betaproteobacteria in freshwater, including *Gallionella*, *Sideroxydans*, *Ferrigenium*, *Ferriphaselus*, *Ferritrophicum* and *Leptothrix* (Emerson *et al.*, 2010; Khalifa *et al.*, 2018), or the marine Zetaproteobacteria, e.g. *Mariprofundus* spp. and *Ghiorsea* spp. (Emerson *et al.*, 2010; Chan *et al.*, 2016; Mori *et al.*, 2017).

$$4Fe^{2+} + O_2 + 10H_2O \rightarrow 4Fe(OH)_3 + 8H^+ \quad (1)$$

Photoautotrophic FeOB (Photoferrotrophs) use light as energy and Fe(II) as electron donor to fix bicarbonate into organic carbon (Equation 2). There are three photoautotrophic FeOB: (i) purple sulfur bacteria, e.g. phylum Gammaproteobacteria, represented by the *Thiodictyon* spp. (Winogradsky, 1888; Peduzzi *et al.*, 2012); (ii) purple non-sulfur bacteria, e.g. phylum Alphaproteobacteria, including *Rhodobacter ferrooxidans* SW2 (Ehrenreich and Widdel, 1994), *Rhodopseudomonas palustris* TIE-1 (Jiao *et al.*, 2005) and two marine strains (*Rhodovulum iodosum* and *Rhodovulum robiginosum*) (Straub *et al.*, 1999); (iii) green sulfur bacteria represented by *Chlorobium*

ferrooxidans strain KoFox (Heising *et al.*, 1999), and the marine *Chlorobium* sp. strain N1 (Llirós *et al.*, 2015) are all members of the family *Chlorobiaceae*.

$$4Fe^{2+} + HCO_3^- + 10H_2O + hv \rightarrow CH_2O + 4Fe(OH)_3 + 7H^+ \quad (2)$$

Fe(II) oxidation coupled to the reduction of nitrate to N_2 under anoxic conditions was first described by Straub *et al.* (1996) (Equation 3). In general, several microbes were proposed as nitrate-reducing FeOB, such as *Thiobacillus denitrificans*, various members of the genera *Acidovorax* and a *Marinobacter*-related isolate (Straub *et al.*, 1996; Edwards *et al.*, 2003; Kappler *et al.*, 2005; Beller *et al.*, 2006b; Chakraborty *et al.*, 2011; Carlson *et al.*, 2013). However, most of them are mixotrophic FeOB, i.e. they require additional carbon sources to survive and reproduce. Only a minority of the nitrate-reducing FeOB are chemolithoautotrophic bacteria, which perform Fe(II) oxidation coupled to CO_2 fixation for biomass production and to energy generation by nitrate reduction, such as culture KS (Blöthe and Roden, 2009; Bryce *et al.*, 2018; Tominski *et al.*, 2018b). The existence of the chemolithoautotrophic nitrate-reducing FeOB is under debate. Therefore, more detailed description is in the following paragraphs.

$$10Fe^{2+} + 2NO_3^- + 24H_2O \rightarrow 10Fe(OH)_3 + N_2 + 18H^+ \quad (3)$$

1.2. Microbial Fe(II) oxidation coupled to nitrate reduction

Nitrate (NO_3^-) is widely used in fertilizers. At high concentrations, nitrate can contaminate water sources, e.g. groundwater, rivers or lakes, causing severe health issues (Widdison and Burt, 2008). Denitrification (Equation 4), the complete reduction of nitrate to dinitrogen (N_2) by microbes, can reduce environmental nitrate contamination. However, incomplete denitrification and carbon utilization may have more detrimental than beneficial effects: by producing greenhouse gases such as nitrous oxide (N_2O) and carbon dioxide (CO_2), it can further increase environmental pollution (Intergovernmental Panel on Climate Change, 2015). Thus, complete denitrification and CO_2 fixation are beneficial for both air and water decontamination.

$$NO_3^- \rightarrow NO_2^- \rightarrow NO \rightarrow N_2O \rightarrow N_2 \quad (4)$$

Neutrophilic nitrate reduction coupled to Fe(II) oxidation (NRFeOx) is known to be an important biochemical process in natural environments, such as soils, sediments and aquifers (Hafenbradl *et al.*, 1996; Straub *et al.*, 1996; Benz *et al.*, 1998; Straub and Buchholz-Cleven, 1998; Straub *et al.*, 2004; Shelobolina *et al.*, 2012; Laufer *et al.*, 2015; Laufer *et al.*, 2016; Bryce *et al.*, 2018; Jakus *et al.*, 2021), and was studied as a treatment for contaminated groundwater (Su *et al.*, 2016; Zhang *et al.*, 2016; Kiskira *et al.*, 2017) and wastewater treatment systems (i.e. constructed wetlands) (Song *et al.*, 2016). Nitrate-reducing FeOB could grow under different conditions: heterotrophic, with organic carbon as sole energy and carbon source; mixotrophic, with Fe(II) in addition to organic carbon as energy, electron and carbon source; and autotrophic, with Fe(II) as sole energy and electron source. Based on several laboratory studies on autotrophic and mixotrophic nitrate-reducing FeOB (ZoBell, 1944; Rabus and Widdel, 1995; Straub *et al.*, 1996; Buchholz-Cleven *et al.*, 1997; Edwards *et al.*, 2003; Beller *et al.*, 2006b; Kumaraswamy *et al.*, 2006; Weber *et al.*, 2006; Su *et al.*, 2015; Zhang *et al.*, 2015; Zhou *et al.*, 2016), it was proposed that true autotrophic nitrate-reducing Fe(II) oxidizing cultures (i) do not require an additional organic carbon source, (ii) can maintain Fe(II) oxidation over three transfers without organic carbon addition, (iii) confirm growth of cells with only Fe(II), nitrate and CO_2 provided, and (iv) show CO_2 uptake by incorporating labelled CO_2 into biomass during Fe(II) oxidation (Bryce *et al.*, 2018). To date, only enrichment culture KS has been the example of a stable autotrophic nitrate-reducing Fe(II)-oxidizing bacterial culture that fits all of the above criteria (Straub *et al.*, 1996; He *et al.*, 2016; Tominski *et al.*, 2018a; Tominski *et al.*, 2018b). In addition, except the fifth criteria, the novel enrichment culture BP (Huang *et al.*, 2021b) and the novel enrichment culture AG (Jakus *et al.*, 2021) fit four of the above criteria. Autotrophic nitrate-reducing Fe(II) oxidizers have the ability to fix carbon dioxide (CO_2) and to oxidize Fe(II) coupled with complete or incomplete denitrification. Thus, NRFeOx could influence the fate of the groundwater pollutant nitrate and the greenhouse gases nitrous oxide (N_2O) and carbon dioxide (CO_2). Cultures KS and BP originate from a freshwater ecosystem in Bremen, Germany (Straub *et al.*, 1996; Huang *et al.*, 2021b). Under autotrophic growth conditions (i.e. using Fe(II) and nitrate) and under heterotrophic conditions (i.e. using acetate and nitrate), the community members of culture KS were analyzed (He *et al.*, 2016; Tominski *et al.*, 2018a).

Culture KS was dominated by an unclassified FeOB *Gallionellaceae* sp. with almost 96% relative abundance of 16S rRNA gene sequence and flanked with several denitrifiers, i.e. *Rhodanobacter* sp. and *Bradyrhizobium* sp. under autotrophic conditions (He *et al.*, 2016). The top closely related organisms to the unclassified *Gallionellaceae* sp. in culture KS are the microaerophilic FeOB, *Ferrigenium kumadai* with 16S rRNA gene sequence identity of 96.45% (Khalifa *et al.*, 2018) and *Sideroxydans lithotrophicus* ES-1 with 16S rRNA gene sequence identity of 95.23% (Emerson and Moyer, 1997) as well as another unclassified *Gallionellaceae* sp. with 16S rRNA gene sequence identity of 97.88% (Huang *et al.*, 2021b) from culture BP, which originates from the same environment as culture KS. Despite several cultivation attempts, the unclassified *Gallionellaceae* sp. of culture KS has so far not yet been isolated (He *et al.*, 2016; Tominski *et al.*, 2018a). Furthermore, microorganisms of the family *Gallionellaceae* were widely found in a variety of natural environments, such as sediments (Straub *et al.*, 1996), aquifers (Jewell *et al.*, 2016), wetland soil (Wang *et al.*, 2009), groundwater (Emerson and Moyer, 1997) and metal-rich mine water discharge (Fabisch *et al.*, 2016). Several observations pointed towards an involvement of *Gallionellaceae* spp. in NRFeOx processes in different habitats (Emerson *et al.*, 2016; Jewell *et al.*, 2016; Bethencourt *et al.*, 2020). There is an increasing number of available genomes derived from omics studies of so far uncultured members of the family *Gallionellaceae* (Jewell *et al.*, 2016; Kadnikov *et al.*, 2016; Bethencourt *et al.*, 2020). These FeOB in the family *Gallionellaceae* have the potential of partial denitrification coupled to Fe(II) oxidation, which demonstrates the importance of classifying new taxa of these not-yet isolated species. In addition, the key FeOB of the stable nitrate-reducing Fe(II)-oxidizing cultures that exist to date (i.e. cultures KS, BP and AG) remain to be classified, especially considering that they are frequently used as model systems to study autotrophic nitrate reduction coupled to Fe(II) oxidation.

1.3. Meta-omics of nitrate-reducing Fe(II) oxidizers

Meta-omic (metagenomic, metatranscriptomic and metaproteomic) analysis is often used for exploring the genetic, transcript and protein potential of a certain microbial metabolism, electron transfer pathways in microorganisms and microbial interactions (Wilmes *et al.*, 2015; He *et al.*, 2016; McAllister *et al.*, 2020). In the metagenome-

assembled genomes (MAGs) produced during the analysis of culture KS, several genes encoding protein complexes were found, which potentially are involved in extracellular electron transfer pathways during Fe(II) oxidation (He *et al.*, 2016). Among the genes were *cyc2,* encoding for the outer membrane cytochrome *c*, which has been detected in marine microaerophiles (McAllister *et al.*, 2020; Keffer *et al.*, 2021), *pcoAB*, encoding for the porin-cytochrome *c* protein complexes, which are known for catalyzing Fe(II) oxidation in *Pseudomonas aeruginosa* (Huston *et al.*, 2002), and the *mtoAB* gene cluster, which has been detected in several microaerophiles, including *Gallionella lithotrophicus* ES-2 and *Sideroxydans lithotrophicus* ES-1 (Carlson *et al.*, 2012; Emerson *et al.*, 2013; He *et al.*, 2016; Bethencourt *et al.*, 2020). Yet, the genes and proteins ultimately involved in NRFeOx have remained largely unknown. Furthermore, in culture KS, the genes encoding for the nitrate reductase (*narGHI*), the nitrite reductase (*nirKS*), the nitric oxide reductase (*norBC*) and the nitrous oxide reductase (*nosZ*) for full denitrification were only found in the MAGs of the heterotrophic organisms, i.e., the *Bradyrhizobium* sp. and *Rhodanobacter* sp. (He *et al.*, 2016). In contrast, only the genes *narGHI* and *nirK/S* were identified in the *Gallionellaceae* sp. MAG of culture KS (He *et al.*, 2016). Since the product of nitrite reduction, i.e. nitric oxide (NO), is generally toxic to organisms without NO detoxification genes (He *et al.*, 2016), this was unexpected. Therefore, it remained uncertain how the unclassified *Gallionellaceae* sp. in culture KS detoxify NO to survive. In addition to denitrification and Fe(II)-oxidizing genes, the carbon fixation gene, *rbcL*, encoding for a form II ribulose 1,5-bisphosphate carboxylase/oxygenase (RuBisCO) was detected in the *Gallionellaceae* sp. MAG, and the genes, *rbcS*, encoding form IC RuBisCO were identified in the *Rhizobium* sp., *Bradyrhizobium* sp., and *Rhodanobacter* sp. MAGs in culture KS (He *et al.*, 2016). Unlike the *Bradyrhizobium* sp., the unclassified *Gallionellaceae* sp. in culture KS was further reported that it is able to fix CO_2 during Fe(II) oxidation, confirming its chemolithoautotrophic lifestyle (Tominski *et al.*, 2018b). Moreover, the high oxygen affinity genes (i.e., encoding cbb_3-type cytochrome *c* oxidase) along with the low oxygen affinity genes (i.e., encoding aa_3-type cytochrome *c* oxidase), which require low and high oxygen concentrations to be activated, respectively (Arai *et al.*, 2014; He *et al.*, 2016) were detected in unclassified *Gallionellaceae* spp. from culture

KS. This reveals that the unclassified *Gallionellaceae* spp. in culture KS might be a microaerophilic Fe(II)-oxidizer, which is able to respire oxygen (He *et al.*, 2016).

1.4. Objective of this study

Based on previous work, several mechanisms were proposed for Fe(II) oxidation in culture KS (He *et al.*, 2016; Tominski *et al.*, 2018b). However, the role of the community members in culture KS for Fe(II) oxidation, denitrification, CO_2 fixation and oxygen respiration remained unclear. Besides culture KS, we explored a novel autotrophic nitrate-reducing Fe(II)-oxidizing enrichment culture, named culture BP (Bremen Pond), that originated from freshwater sediment in Bremen, Germany, and was obtained in 2015 from a pond close to the sampling site of culture KS.

Therefore, the goals of this thesis were:

(i) To identify and compare gene expression and protein production by members of cultures KS and BP under autotrophic and heterotrophic conditions (chapter 2 and 3).

(ii) To study the potential metabolism for Fe(II) oxidation, denitrification, carbon fixation and oxidative phosphorylation of cultures KS and BP (chapter 2 and 3).

(iii) To create a hypothesis of the interaction between the species based on the expressed genes and produced proteins, which enables survival under autotrophic NRFeOx conditions in cultures KS and BP (chapter 2 and 3).

(iv) To assess the *in-situ* diversity and relative abundance of potential key players involved in NRFeOx at the original habitat of culture BP (chapter 3).

(v) To compare and classify three unclassified *Gallionellaceae* spp. in cultures KS, BP and AG (chapter 4).

2. Meta-omics reveal *Gallionellaceae* and *Rhodanobacter* as interdependent key players for Fe(II) oxidation and nitrate reduction in the autotrophic enrichment culture KS

Yu-Ming Huang[a, b], Daniel Straub[a, c], Nia Blackwell[a], Andreas Kappler[b,d] and Sara Kleindienst[a]

[a] Microbial Ecology, Center for Applied Geoscience, University of Tuebingen, Germany
[b] Geomicrobiology, Center for Applied Geoscience, University of Tuebingen, Germany
[c] Quantitative Biology Center (QBiC), University of Tuebingen, Germany
[d] Cluster of Excellence: EXC 2124: Controlling Microbes to Fight Infections, University of Tübingen, Tübingen, Germany

Slightly modified version published in

Applied and Environmental Microbiology

Huang, Y., Straub, D., Blackwell, N., Kappler, A., and Kleindienst, S. (2021) Meta-omics reveal *Gallionellaceae* and *Rhodanobacter* as interdependent key players for Fe(II) oxidation and nitrate reduction in the autotrophic enrichment culture KS. https://doi.org/10.1128/AEM.00496-21

2.1. Abstract

Nitrate reduction coupled to Fe(II) oxidation (NRFeOx) has been recognized as an environmentally important microbial process in many freshwater ecosystems. However, well-characterized examples of autotrophic nitrate-reducing Fe(II)-oxidizing bacteria are rare and their pathway of electron transfer as well as their interaction with flanking community members remain largely unknown. Here, we applied meta-omics (i.e., metagenomics, metatranscriptomics and metaproteomics) to the nitrate-reducing Fe(II)-oxidizing enrichment culture KS, growing under autotrophic compared to heterotrophic conditions, and originating from a freshwater sediment. We constructed four metagenome-assembled genomes with an estimated completeness of ≥95%, including the key players of NRFeOx in culture KS, identified as the *Gallionellaceae* sp. and *Rhodanobacter* sp. The presence of *Gallionellaceae* sp. and *Rhodanobacter* sp. transcripts and proteins likely involved in Fe(II) oxidation (e.g., *mtoAB, cyc2, mofA*), denitrification (e.g., *napGHI*) and oxidative phosphorylation (e.g., respiratory chain complexes I-V), along with the *Gallionellaceae* sp. transcripts and proteins for carbon fixation (e.g., *rbcL*) were detected. Overall, our results indicate that in culture KS, the *Gallionellaceae* sp. and *Rhodanobacter* sp. are interdependent: while the *Gallionellaceae* sp. fixes CO_2 and provides organic compounds for the *Rhodanobacter* sp., the *Rhodanobacter* sp. likely detoxifies NO through NO reduction and completes denitrification, which cannot be done by the *Gallionellaceae* sp. alone. Additionally, the transcripts and partial proteins of cbb_3- and aa_3- type cytochrome *c* suggest the possibility for a microaerophilic lifestyle of the *Gallionellaceae* sp., yet culture KS grows under anoxic conditions. Our findings demonstrate that autotrophic NRFeOx is performed through cooperation among denitrifying and Fe(II)-oxidizing bacteria, which might resemble microbial interactions in freshwater environments.

2.2. Introduction

Neutrophilic nitrate reduction coupled to iron(II) [Fe(II)] oxidation (NRFeOx) by nitrate-reducing Fe(II)-oxidizing bacteria is known as a vital biochemical process in different natural environments, such as sediments and soils (Hafenbradl *et al.*, 1996; Straub *et al.*, 1996; Benz *et al.*, 1998; Straub and Buchholz-Cleven, 1998; Straub *et al.*, 2004; Shelobolina *et al.*, 2012; Laufer *et al.*, 2015; Laufer *et al.*, 2016; Bryce *et al.*, 2018). Nitrate-reducing Fe(II)-oxidizing bacteria can thrive under different conditions: autotrophic, with Fe(II) as sole energy and electron source; mixotrophic, with Fe(II) and additional organic carbon as energy, electron and carbon source; and heterotrophic, with organic carbon as sole energy and carbon source. Chemolithotrophic Fe(II)-oxidizing bacteria (FeOB) use both solid and dissolved Fe(II) as an electron donor (Ehrenberg, 1838), under either oxic conditions, i.e., microaerophilic FeOB, or anoxic conditions, i.e., nitrate-reducing FeOB (Widdel *et al.*, 1993; Straub *et al.*, 1996; Hedrich *et al.*, 2011; Emerson, 2012). Despite the current knowledge of NRFeOx, for instance, as studied using the autotrophic nitrate-reducing Fe(II)-oxidizing bacterial enrichment culture KS (Straub *et al.*, 1996), whether autotrophic NRFeOx can be performed by an individual strain or requires cooperation between different strains remains elusive (Liu *et al.*, 2019).

Culture KS originates from a freshwater ecosystem in Bremen, Germany, and was first published in 1996 (Straub *et al.*, 1996). The community composition of culture KS was analyzed under autotrophic growth conditions (using Fe(II) and nitrate) and under heterotrophic conditions (using acetate and nitrate) (He *et al.*, 2016; Tominski *et al.*, 2018a). Under autotrophic conditions, culture KS was found to be enriched for an unclassified FeOB *Gallionellaceae* sp., which dominated with almost 96% relative 16S rRNA gene sequence abundance. The most closely related organisms to this unclassified *Gallionellaceae* sp. are the microaerophilic FeOB, *Ferrigenium kumadai* An22 (16S rRNA gene sequence identity: 96.45%) (Khalifa *et al.*, 2018) and *Sideroxydans lithotrophicus* strain ES-1 (16S rRNA gene sequence identity: 95.23%) (Emerson and Moyer, 1997) as well as another unclassified *Gallionellaceae* sp. (16S rRNA gene sequence identity: 97.88%) (Huang *et al.*, 2021b) from the novel autotrophic NRFeOx enrichment culture BP that originates from the same environment as culture KS, i.e., a freshwater ecosystem in Bremen. However, despite elaborate cultivation attempts, the unclassified

Gallionellaceae sp. of culture KS has so far not been isolated (He *et al.*, 2016; Tominski *et al.*, 2018a).

Metagenomic analysis of culture KS, including metagenome-assembled genomes (MAGs), uncovered several genes encoding for protein complexes potentially involved in extracellular electron transfer (EET) pathways during neutrophilic Fe(II) oxidation (He *et al.*, 2016). Among the genes were those encoding for the outer membrane cytochrome *c* (*cyc2*) detected in marine microaerophiles (McAllister *et al.*, 2020; Keffer *et al.*, 2021), as well as the porin-cytochrome *c* protein complexes (PcoAB) known for Fe(II) oxidation in *Pseudomonas aeruginosa* (Huston *et al.*, 2002), and the *mtoAB* gene cluster shown in several microaerophiles, including *Gallionella* sp. strain ES-2 and *Sideroxydans* sp. strain ES-1 (Carlson *et al.*, 2012; Emerson *et al.*, 2013; He *et al.*, 2016; Bethencourt *et al.*, 2020). However, it remained largely unknown which genes and proteins are ultimately involved in NRFeOx. Furthermore, in culture KS, the full denitrification gene complex, which consists of the genes encoding for the nitrate reductase (*narGHI*), the nitrite reductase (*nirKS*), the nitric oxide reductase (*norBC*) and the nitrous oxide reductase (*nosZ*), was only found in the MAGs of the heterotrophic organisms, i.e., the *Bradyrhizobium* sp. and *Rhodanobacter* sp. (He *et al.*, 2016). In contrast, in the *Gallionellaceae* sp. MAG of culture KS, only the genes *narGHI* and *nirKS* were identified. This was unexpected since the product of nitrite reduction, nitric oxide (NO), is generally toxic to organisms without detoxification genes (He *et al.*, 2016). Therefore, it remained unclear how the unclassified *Gallionellaceae* sp. in culture KS deals with this toxic compound and survives under this condition. Apart from NRFeOx genes, the carbon fixation gene encoding for a form II ribulose 1,5-bisphosphate carboxylase/oxygenase (RuBisCO) was identified in the *Gallionellaceae* sp. MAG, and genes encoding form IC RuBisCO were identified in the *Rhizobium* sp., *Bradyrhizobium* sp., and *Rhodanobacter* sp. MAGs in culture KS (He *et al.*, 2016). It was further shown that, unlike the *Bradyrhizobium* sp., the unclassified *Gallionellaceae* sp. in culture KS is capable of CO_2 fixation during Fe(II) oxidation, confirming its chemolithoautotrophic lifestyle (Tominski *et al.*, 2018b). In addition, the unclassified *Gallionellaceae* sp. from culture KS possesses high oxygen affinity genes (i.e., encoding cbb_3-type cytochrome *c* oxidase) as well as low oxygen affinity genes (i.e., encoding aa_3-type cytochrome *c* oxidase), which require low

and high oxygen concentrations, respectively (Arai *et al.*, 2014; He *et al.*, 2016). This indicates that the unclassified *Gallionellaceae* sp. in culture KS might have the ability to respire oxygen, as a microaerophilic Fe(II)-oxidizer, however it remained unknown whether these cytochrome *c* oxidases are expressed.

Based on this previous work, several mechanisms were proposed for Fe(II) oxidation in culture KS. Yet, the individual role of the culture KS community members in Fe(II) oxidation, CO_2 fixation, reduction of the individual N species and potential oxygen respiration remained elusive. Therefore, the aims of this study were (i) to identify genes expressed and proteins produced by the FeOB and other community members of culture KS under autotrophic compared to heterotrophic conditions, (ii) to create a concept of interspecies interaction based on the expressed genes and proteins which enables survival under autotrophic NRFeOx conditions in culture KS and (iii) to obtain information from these expressed genes and produced proteins, allowing to develop potential isolation strategies of the unclassified *Gallionellaceae* sp. from culture KS for future studies. To answer these questions, we applied a meta-omics approach (i.e., metagenomics, metatranscriptomics and metaproteomics) to culture KS under autotrophic and heterotrophic conditions. The physiology of the culture and population dynamics in these experiments were furthermore determined by monitoring Fe(II), nitrate, and acetate consumption as well as cell counts and 16S rRNA gene amplicon sequencing.

2.3. Results and discussion

Physiology of culture KS

For the meta-omics approach, culture KS was grown under anoxic autotrophic or anoxic heterotrophic conditions. Under autotrophic conditions, 9.34 mM of Fe(II) was oxidized with an average Fe(II) oxidation rate of 3.25 mM/day during the exponential growth phase (i.e., between day 1 and 4; Fig. 2.1A). This co-occurred with a reduction of 2.18 mM of nitrate and an average nitrate reduction rate of 0.77 mM/day, without detectable nitrite production (Fig. 2.1A), suggesting either a potentially rapid consumption of nitrite by the enzyme nitrite reductase (NirK/S), or the involvement of nitrite in abiotic Fe(II) oxidation. The average $Fe(II)_{oxidized}/nitrate_{reduced}$ stoichiometric ratio was 4.28, indicative of autotrophic NRFeOx, albeit at a ratio that is slightly lower than the previously reported $Fe(II)_{oxidized}/nitrate_{reduced}$ ratios of 4.5-4.8 (Tominski *et al.*, 2018a). The theoretical stoichiometry, however, suggests that the $Fe(II)_{oxidized}/nitrate_{reduced}$ ratio should be around 5 or even greater than 5 if the electrons used for CO_2 fixation were also considered (Blöthe and Roden, 2009). We suggest two possible explanations for this phenomenon. First, the product of nitrate reduction might be not only the final end member of denitrification, i.e., N_2, but can also be one of the less reduced N-intermediates, i.e., NO or N_2O, which potentially leads to greenhouse gas emission. Second, heterotrophs might contribute to nitrate reduction not only using the electrons from Fe(II) but also from the trace amount of organic carbon present in Milli-Q water (determined at 2.17 mg/L; triplicate measurements) used for media preparation. In our experiments, cell numbers increased from 5.16×10^5 cells/mL to 2.82×10^7 cells/mL within 3 days (Fig. 2.1B). Given that 1 mg/L of dissolved organic carbon in Milli-Q water could in theory produce 2.5×10^6 cells/mL (see calculation in supplementary calculation 2.6.2), cell growth in our cultivation experiments clearly derive not only from the trace amount of organic carbon but mainly from the carbon fixation using electrons donated from Fe(II).

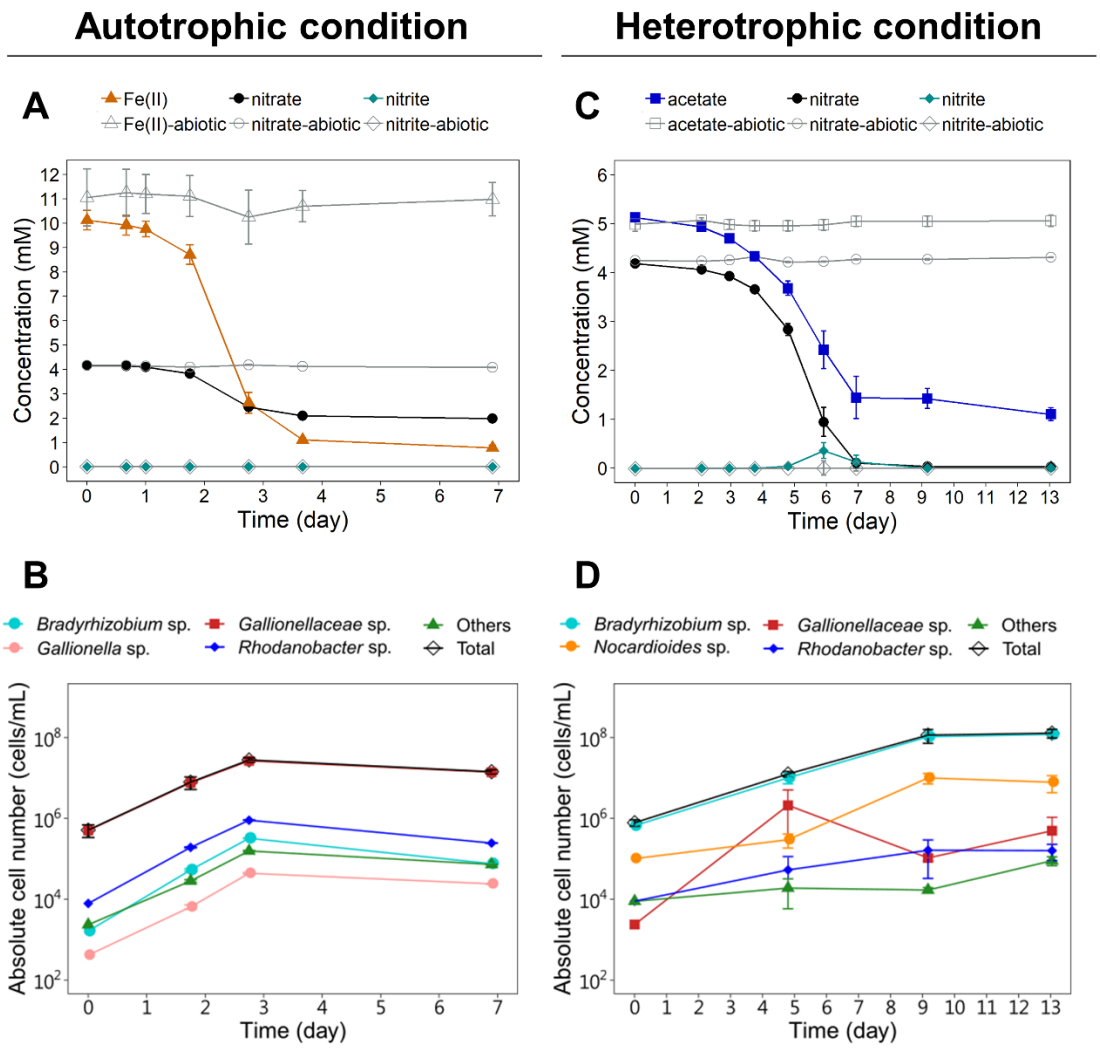

Fig. 2.1. Geochemistry of culture KS under autotrophic (left) and heterotrophic (right) conditions. Changes in Fe(II), nitrate and nitrite concentrations (A), acetate, nitrate and nitrite concentrations (C), estimated absolute cell numbers from total cell number (calculated with triplicate samples at all time points) and microbial community relative abundance of 16S rRNA gene amplicon sequencing (performed with triplicate samples, except for T0) (B and D), as monitored over time. Error bars represent the standard deviation of three to four replicates (day 0 had no replicates in 16S rRNA gene amplicon sequencing).

Under autotrophic growth conditions, the microbial community composition revealed that the unclassified *Gallionellaceae* sp. dominated with 95-98% relative 16S rRNA gene sequence abundance (Fig. 2.1B). Conversely, lower abundances were detected for the *Rhodanobacter* sp. (2-3%), *Bradyrhizobium* sp. (up to 1%), *Nocardioides* sp. (<1%), and another *Gallionella* sp. (<1%; Fig. 2.1B), in agreement with previous studies (Blöthe and Roden, 2009; He *et al.*, 2016; Tominski *et al.*, 2018a). The total cell numbers and the

relative abundance of the unclassified *Gallionellaceae* sp. were higher than in a previous growth and population dynamics study (Tominski *et al.*, 2018a), which reported total cell growth from 4×10^4 cells/mL to 2×10^6 cells/mL and an increase in the unclassified *Gallionellaceae* sp. relative abundance from 58% to 83% in 10 days (Tominski *et al.*, 2018a). In line with previous studies, the cell number increased 55 times over three days and the unclassified *Gallionellaceae* sp. always accounted for the majority of the microbial community during the process of NRFeOx (Fig. 2.1B). Therefore, under autotrophic growth conditions, culture KS appeared reproducible, with only slight fluctuations among the different transfers.

Under heterotrophic conditions, 4.02 mM of acetate was consumed with an average acetate oxidation rate of 0.72 mM/day during the exponential growth phase (i.e., between day 2 and day 7). This co-occurred with an average reduction of 4.16 mM of nitrate and an average nitrate reduction rate of 0.82 mM/day. Nitrite was detected between day 4 and day 9 at concentrations ranging from 0.04 to 0.36 mM (Fig. 2.1C), pointing towards inefficient enzymatic nitrite reduction of the dominating microbial populations. The average ratio yield $\text{acetate}_{\text{oxidized}}/\text{nitrate}_{\text{reduced}}$ of 0.99 was similar to previously reported ratios (0.9-1.4) (Tominski *et al.*, 2018a). Throughout the experiment, cell numbers increased from 7.85×10^5 cells/mL to 1.30×10^8 cells/mL within 9 days (Fig. 2.1D). The *Bradyrhizobium* sp. dominated under heterotrophic conditions with 85-97% relative 16S rRNA gene sequence abundance, while lower abundances were detected for the *Nocardioides* sp. (3-13%), unclassified *Gallionellaceae* sp. (<1%), *Rhodanobacter* sp. (<1%), and *Pseudomonas* sp. (<1%) (Fig. 2.1D). Thus, the unclassified *Gallionellaceae* sp. and *Rhodanobacter* sp. were still detectable, albeit at low relative abundance (i.e., 0.09-0.38% and 0.08-1.13%, respectively).

Our data confirmed the population dynamics of the unclassified *Gallionellaceae* sp. and *Bradyrhizobium* sp. under heterotrophic and autotrophic conditions in culture KS, which have previously been determined via fluorescence *in situ* hybridization (FISH) (Tominski *et al.*, 2018a), indicating that culture KS sustains a stable microbial consortium over time (i.e., several years). Our results also allowed to determine optimal sampling points for meta-omics analysis, i.e., during the exponential growth phase of culture KS under both autotrophic and heterotrophic conditions.

Overview of the four assembled MAGs in culture KS under autotrophic and heterotrophic conditions

Four high-quality MAGs of the *Gallionellaceae* sp., *Rhodanobacter* sp., *Bradyrhizobium* sp. and *Nocardioides* sp. were recovered from the metagenomic data from culture KS with estimated completeness of ≥95% and estimated contamination of 0% (Table 2.1).

Table 2.1. Summary of Metagenome-Assembled Genomes (MAGs)

	Gallionellaceae	***Rhodanobacter***	***Bradyrhizobium***	***Nocardioides***
Information of genome bins				
Estimated completeness (%)	99.3	95.3	95.3	96.6
Estimated contamination (%)	0	0	0	0
Genome size (bp)	2,659,708	3,841,026	6,667,305	4,380,799
No. contigs (scaffold)	5	5	1	3
Gene count	2610	3533	6605	4365
GC (%)	60.26	67.64	64.44	72.03
No. of CDS	2545	3458	6515	4297
Taxonomy ID	90627	75309	374	1839
IMG Submission ID	235568	235569	235570	235571
IMG Genome ID	2878407288	2878409899	2878413433	2878420039
GOLD Analysis Project ID	Ga0439409	Ga0439410	Ga0439411	Ga0439412
16S rRNA identity of closest related isolated species	*Ferrigenium kumadai* (96.45**%**) (Khalifa *et al.*, 2018)	*Rhodanobacter denitrificans* strain 2APBS1 (99.32**%**) (Prakash *et al.*, 2012)	*Bradyrhizobium neotropicale* BR 10247 (99.69**%**) (Zilli *et al.*, 2014)	*Nocardioides* sp. JS614 (99.10**%**) (Coleman *et al.*, 2011)
Community composition (exponential phase) (%)				
Autotrophic	96.42	2.47	0.63	0.04
Heterotrophic	0.12	0.08	96.74	2.87
Number of significantly changed (adjusted $p \leq 0.05$) transcripts under autotrophic conditions compared to heterotrophic conditions				
Total	2666	3259	420	928
Significant-up	2666	3258	287	0
Significant-down	0	1	133	928
Number of significantly changed proteins (adjusted $p \leq 0.05$) under autotrophic conditions compared to heterotrophic conditions				
Total	52	8	610	20
Significant-up	35	5	28	7
Significant-down	17	3	582	13

Several genes involved in carbon, nitrate, and oxygen metabolisms as well as in Fe(II) oxidation were identified (Fig. 2.2). Carbon metabolism pathway genes for the reductive pentose phosphate (CBB) cycle, the glycolysis pathway, tricarboxylic acid (TCA) cycle, and the pentose phosphate pathway (PPP) were identified in the four MAGs. Furthermore, the genes encoding RuBisCO were only identified in the MAGs of the *Gallionellaceae* sp. and *Bradyrhizobium* sp., but not in the *Rhodanobacter* sp., which is different from a previous report (He *et al.*, 2016). The lack of RuBisCO in the *Rhodanobacter* sp. might be explained by evolutionary gene loss over time, or incompleteness of the *Rhodanobacter* sp. MAG.

Regarding Fe(II) oxidation, the genes encoding for outer membrane and porin-cytochrome *c* proteins of putative EET systems, i.e., *cyc2*, *mtoAB, pcoAB*, and outer membrane multi-copper oxidases (an *ompB* homolog, *mofA*), were detected in the MAGs of the *Gallionellaceae* sp. and *Rhodanobacter* sp., suggesting that both organisms might have the ability to oxidize Fe(II). Concerning the further electron acceptor pathway in the periplasm and inner membrane, the dissimilatory nitrate reductase complex *narGHI* and nitrite reductase *nirKS* were detected in all of the four MAGs. The additional genes to complete denitrification, i.e., *norBC* and *nosZ*, were only detected in the MAGs of the *Rhodanobacter* sp., *Bradyrhizobium* sp. and *Nocardioides* sp. Another set of electron acceptors at the inner membrane of the cell are the oxidative phosphorylation complexes, i.e., the respiratory chain complexes I (NADH quinone oxidoreductase), II (succinate dehydrogenase), III (cytochrome bc_1 complex), IV (cbb_3- and aa_3- type cytochrome *c* oxidases) and V (F-type ATPase). We identified the genes encoding for these oxidative phosphorylation systems in all four MAGs.

To determine the nutritional requirements of the bacterial populations in culture KS, particularly for the *Gallionellaceae* sp., we examined the amino acid biosynthesis pathways. The *Gallionellaceae* sp. MAG in culture KS encodes the complete synthesis pathways for the essential amino acids, suggesting that the *Gallionellaceae* sp. does not depend on other organisms regarding amino acid biosynthesis, which is in line with a previous metagenomic study (He *et al.*, 2016).

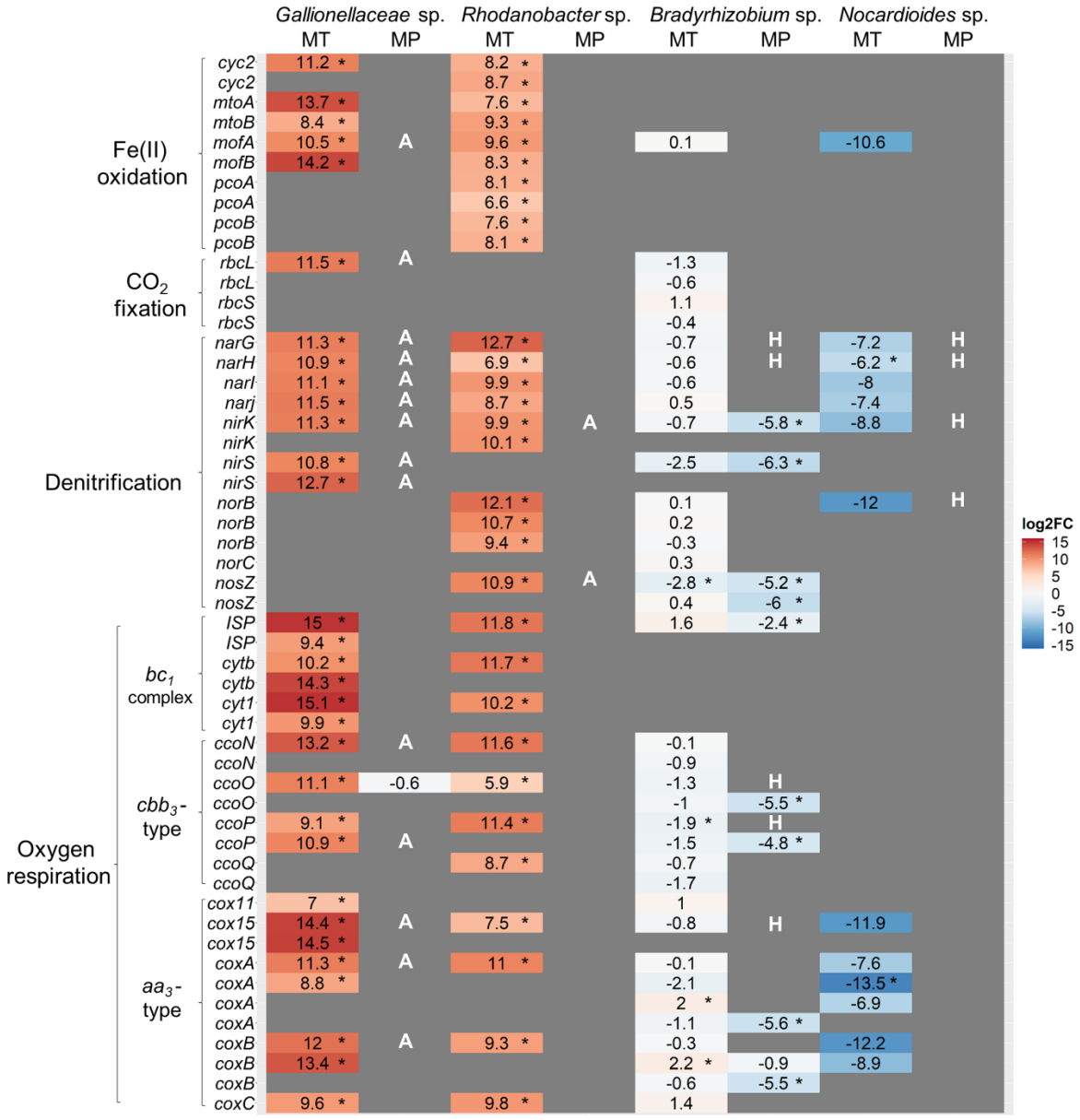

Fig. 2.2. Fold changes of normalized counts (log2) of key transcripts and proteins involved in Fe(II) oxidation, CO_2 fixation, acetate oxidation, denitrification and potential oxygen respiration under autotrophic conditions compared to heterotrophic conditions. Genes with several copy numbers are listed multiple times. MT: metatranscriptomic analysis; MP: metaproteomic analysis. A star "*" indicates significant changes (adjusted $p \leq 0.05$). A white "A" indicates the protein was only detected under autotrophic conditions. A white "H" indicates the protein was only detected under heterotrophic conditions.

Carbon fixation by the dominant *Gallionellaceae* sp. supports the survival of heterotrophic community members under autotrophic conditions

To advance the knowledge beyond the previous work (Blöthe and Roden, 2009; He *et al.*, 2016; Tominski, 2016; Nordhoff *et al.*, 2017; Tominski *et al.*, 2018a; Tominski *et al.*, 2018b), we now also performed metatranscriptomic and metaproteomic analyses, which has not been done with culture KS before. For a comparison of total transcript and protein abundances under autotrophic to heterotrophic conditions, differential abundance analysis was performed which were the main basis of our interpretations (Fig. 2.2). In addition, normalized gene expression per MAG (i.e., *Gallionellaceae* sp., *Rhodanobacter* sp., *Bradyrhizobium* sp. and *Nocardioides* sp.) was calculated for both growth conditions using housekeeping genes as reference, and resulting in normalized transcripts per kilobase million (TPM) (Fig. 2.3); however, these normalized results were interpreted with caution if data were obtained from one sample only out of triplicates (a value of 0 TPM was interpreted as missing data). The metatranscriptomic analysis revealed the presence of several transcripts associated with carbon metabolic pathways under autotrophic NRFeOx conditions. Some of those transcripts showed significantly higher abundances under autotrophic compared to heterotrophic conditions (Fig. 2.2): more specifically, the essential carbon fixation gene transcripts, encoding form II RuBisCO (*rbcL*), and form IC RuBisCO (*rbcL/S*), of the *Gallionellaceae* sp. and *Bradyrhizobium* sp., respectively (Fig. 2.2). However, of these carbon fixation genes only the *rbcL* transcript of the *Gallionellaceae* sp. was significantly ($p \leq 0.05$) more abundant under autotrophic conditions compared to heterotrophic conditions, and the RbcL protein of the *Gallionellaceae* sp. was only detected under autotrophic conditions (Fig. 2.2). In addition, the highest normalized gene expression of *rbcL* per MAG was calculated for the *Gallionellaceae* sp. under autotrophic conditions (4.78 averaged normalized TPM; Fig. 2.3) and under heterotrophic conditions (however, with data from one sample only). In previous studies, form II RuBisCO was found in the nitrate-reducing FeOB *Thiobacillus denitrificans* as well as the microaerophilic FeOB *Sideroxydans lithotrophicus* ES-1 and *Gallionella capsiferriformans* ES-2 (Beller *et al.*, 2006a; Emerson *et al.*, 2013). This gene usually has a low affinity to CO_2 and is adapted to high CO_2 and low O_2 environments; hence, it could function well under the anoxic, bicarbonate-buffered cultivation conditions

in culture KS (Badger and Bek, 2008; Emerson *et al.*, 2013). Form IC RuBisCO was mostly found in the microorganisms living in environments with oxic conditions and reduced levels of CO_2 (Badger and Bek, 2008). Based on our findings, the expression level of form IC RuBisCO in the *Bradyrhizobium* sp. might rather be low under anoxic conditions (see 0-0.18 averaged normalized TPM per MAG; Fig. 2.3), and this could explain why we were unable to detect the corresponding protein in our dataset (Fig. 2.2). Our meta-omics data demonstrate, at both transcriptional and protein levels, that the *Gallionellaceae* sp. is the key organism responsible for carbon fixation under autotrophic conditions in culture KS, supporting the hypothesis of Tominski *et al.* (2018b), based on uptake studies of ^{13}C-labeled bicarbonate (Tominski *et al.*, 2018b). In addition, under autotrophic conditions we detected most of the transcripts and some of the proteins involved in the CBB cycle, the TCA cycle, the glycolysis pathway, and the PPP from the *Gallionellaceae* sp. and *Rhodanobacter* sp. (Fig. 2.2 and Fig. 2.3). Based on these detected carbon metabolism pathways, we propose that the *Gallionellaceae* sp. may proceed carbon fixation to produce the key component, i.e., organic carbon, 3-phosphoglycerate, for heterotrophic community members to survive under autotrophic conditions. These heterotrophs may subsequently metabolize 3-phosphoglycerate in the TCA cycle for further energy generation (Fig. 2.2) and for their survival in culture KS under autotrophic conditions. Hence, our data demonstrate that metabolic cooperation among microbial community members likely plays an essential role in the organic carbon-limited cultivation of the autotrophic culture KS, which might resemble the conditions in an organic carbon-poor aquifer (Jewell *et al.*, 2016) or even in a more organic carbon-rich coastal marine sediment (Norsminde, Denmark) (Laufer *et al.*, 2016).

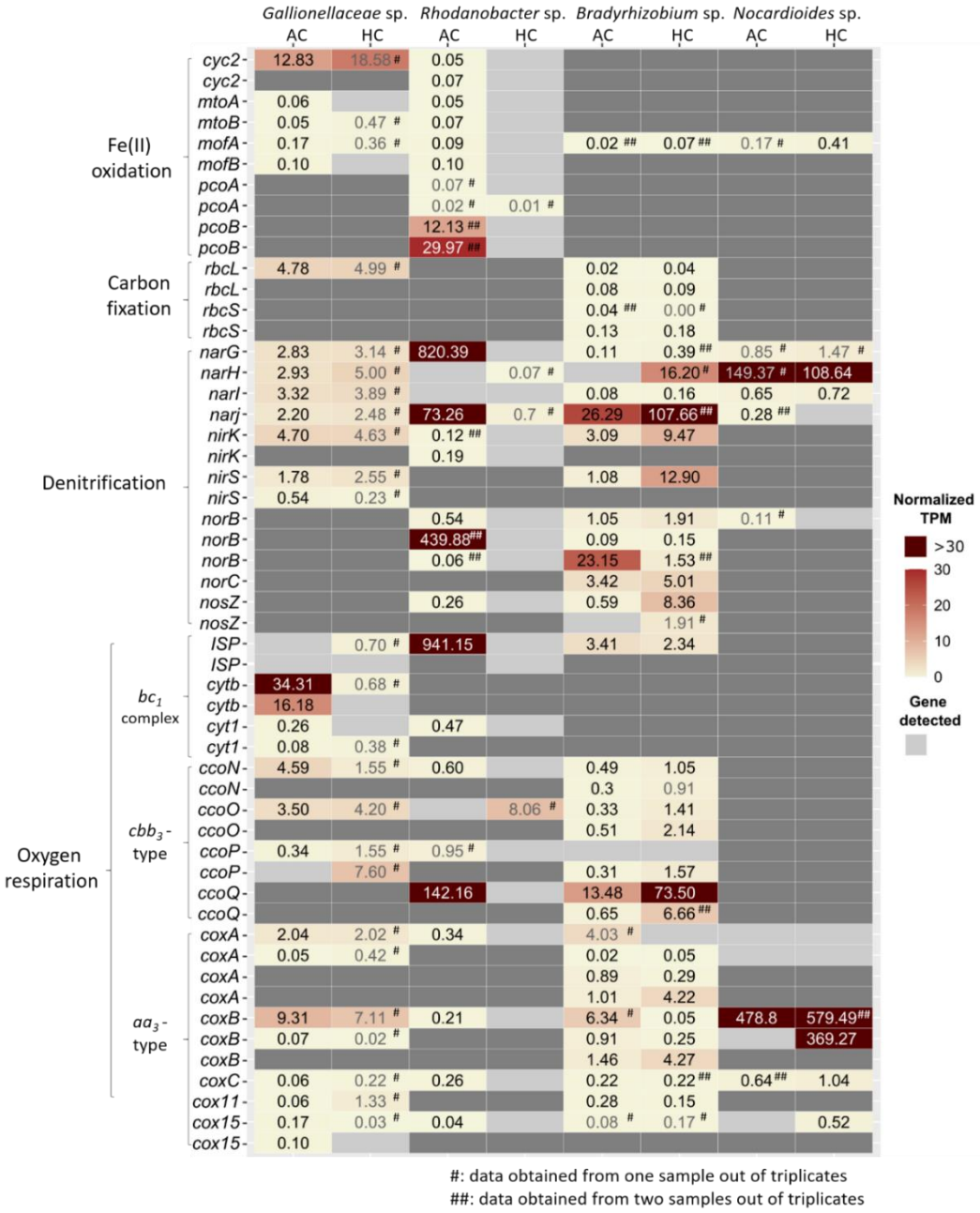

Fig. 2.3. Heatmap of normalized transcripts per kilobase million (TPM) of the *Gallionellaceae* sp., *Rhodanobacter* sp., *Bradyrhizobium* sp. and *Nocardioides* sp. metagenome-assembled genomes. Visualized are normalized TPM values for the pathways of Fe(II) oxidation, carbon fixation, denitrification and oxygen respiration. AC: autotrophic conditions; HC: heterotrophic conditions; #: data obtained from one sample out of triplicates (i.e. two data points out of three were 0 TPM and treated as missing data, therefore data have to be interpreted with caution also indicated by the gray font of these data); ##: data obtained from two samples out of triplicates; numbers without #: data obtained from all three triplicates; light gray-colored cell: no transcript of the identified gene detected among triplicate samples; dark gray-colored cell: no gene and no transcript detected.

The *Gallionellaceae* sp. and *Rhodanobacter* sp. likely perform Fe(II) oxidation in culture KS

The enzymatic Fe(II) oxidation by microaerophilic FeOB under pH-neutrophilic conditions has been proposed to occur at the outer membrane of the cell via EET instead of cytoplasmic Fe(II) oxidation to avoid intracellular mineral encrustation (Emerson and Moyer, 1997; Kappler *et al.*, 2005; Carlson *et al.*, 2013; Nordhoff *et al.*, 2017; Bryce *et al.*, 2018). Our transcriptomic data revealed that most of the detected putative EET system genes were expressed by the *Gallionellaceae* sp. and *Rhodanobacter* sp. (Fig. 2.2). For these two populations, the transcripts encoding Cyc2, MtoA, MtoB, Cytc1, Cytc2, Cytbc and MofA were detected at a significantly higher abundance under autotrophic conditions compared to heterotrophic conditions (Fig. 2.2). Additionally, in the *Rhodanobacter* sp., the transcripts encoding PcoA and PcoB were detected at significantly higher abundance levels under autotrophic conditions (Fig. 2.2). Furthermore, among the detected putative EET system transcripts highest normalized gene expression per MAG was calculated for the *cyc2* in the *Gallionellaceae* sp. (12.83 averaged normalized TPM; Fig. 2.3) and for the *pcoB* in the *Rhodanobacter* sp. (12.13 and 29.97 averaged normalized TPM of two *pcoB* copies; Fig. 2.3) under autotrophic conditions, respectively. The normalized gene expression of *cyc2* in the *Gallionellaceae* sp. was also high under heterotrophic conditions, however with data from one sample only. Homologs of the *mtoAB* and *cyc2* genes from the *Gallionellaceae* sp. in culture KS were found in the most closely related and publicly available genomes of *Sideroxydans lithotrophicus* ES-1 and *Gallionella capsiferriformans* ES-2 (Emerson *et al.*, 2013; He *et al.*, 2016; He *et al.*, 2017). MtoA and MtoB were shown to perform Fe(II) oxidation in the *Sideroxydans lithotrophicus* strain ES-1 (Liu *et al.*, 2012). Furthermore, the *cyc2* gene encoding the putative Fe oxidase was identified in several FeOB genomes (He *et al.*, 2017), *cyc2* transcripts were highly abundant *in situ* in *Zetaproteobacteria*-dominated Fe mats at marine hydrothermal vents (McAllister *et al.*, 2020), and *cyc2* transcripts as well as the Cyc2 protein were detected in the unclassified *Gallionellaceae* sp. of the novel autotrophic NRFeOx enrichment culture BP (Huang *et al.*, 2021b). Moreover, PcoA and PcoB were shown to use a broad range of redox substrates, and *pcoAB* homologs were widely identified in FeOB that have the genetic ability to oxidize Fe(II) (Huston *et al.*, 2002; He *et al.*, 2017), e.g., in *P.*

aeruginosa, for which the Fe(II) oxidation function of PcoA was demonstrated (Huston *et al.*, 2002). It was therefore hypothesized that homologs of *pcoAB* might function in Fe(II) oxidation in many *Betaproteobacteria* (Huston *et al.*, 2002; He *et al.*, 2017). The proteins MofA, MofB and MofC were identified in *Leptothrix discophora* SS-1, and were speculated to be involved in Mn(II) and Fe(II) oxidation (Corstjens *et al.*, 1992; Corstjens *et al.*, 1997; Brouwers *et al.*, 2000; El Gheriany *et al.*, 2009). Under our growth conditions, no Mn(II) was added besides the trace amounts that originated from trace metals in the growth medium (0.50 µM); thus, it is unlikely that Mn(II) is the main electron donor in the KS culture, and we propose that the detected putative EET system transcripts are directly involved in Fe(II) oxidation. At the proteome level, we detected only the OmpB homolog, MofA, which was assigned to the *Gallionellaceae* sp. MAG (Fig. 2.2). Even though we used a total protein extraction method, membrane proteins are difficult to extract (Singer, 1990) and we might have missed those EET proteins that reside in the membrane.

Collectively, the data from our meta-omics analyses combined with previous studies strengthen the concept that *cyc2*, *mtoAB*, *mofABC* and *pcoAB* might be involved in EET to oxidize Fe(II) in not only the *Gallionellaceae* sp. but also the *Rhodanobacter* sp. (Fig. 2.2 and Fig. 2.3). However, according to the metaproteomic data, the *Gallionellaceae* sp. might be the key FeOB potentially employing MofA to oxidize Fe(II) and to transfer electrons from Fe(II) to the periplasm via MofB and MofC (Corstjens *et al.*, 1992; Brouwers *et al.*, 2000; El Gheriany *et al.*, 2009; He *et al.*, 2017). Indeed, the isolated *Rhodanobacter* sp. from culture KS was unable to oxidize $FeCl_2$ and Fe(II)-EDTA either under autotrophic or mixotrophic conditions (Tominski, 2016). This indicates that the *Rhodanobacter* sp. might be dependent on the *Gallionellaceae* sp. to survive in culture KS under autotrophic conditions, as previously proposed (He *et al.*, 2016; Tominski *et al.*, 2018a).

With respect to the other flanking community members under both autotrophic and heterotrophic conditions, the only EET transcripts detected for the *Bradyrhizobium* sp. and *Nocardioides* sp. were those of *mofA* (Fig. 2.2). The results overall indicate that the *Gallionellaceae* sp. might not depend on the *Rhodanobacter* sp. for the process of electron donation, i.e., Fe(II) oxidation, but might depend on the *Rhodanobacter* sp. for other metabolic steps, e.g., for accepting electrons from oxidation of organic carbon

provided by the *Gallionellaceae* sp. at the periplasm and the inner membrane. Furthermore, in order to survive (and even grow) under carbon-limited and Fe(II)-rich conditions, heterotrophs such as the *Bradyrhizobium* sp. and *Nocardioides* sp. depend on the *Gallionellaceae* sp. that uses electrons from Fe(II) oxidation to fix carbon and, thus, provides organic compounds to the heterotrophs.

The *Rhodanobacter* sp. in culture KS likely detoxifies NO under autotrophic conditions

Among the processes able to accept the electrons donated by Fe(II) oxidation at the periplasm and the inner membrane of the bacterial populations in culture KS is the reduction of nitrate, also known as denitrification. The transcripts of the denitrification pathway genes, i.e., *narGHI* and *nirKS* of the *Gallionellaceae* sp. as well as *narGHI*, *nirK, norB* and *nosZ* of the *Rhodanobacter* sp., were detected at significantly higher abundances under autotrophic conditions (Fig. 2.2). The proteins NarGHI and NirKS of the *Gallionellaceae* sp. as well as NirK and NosZ of the *Rhodanobacter* sp. were detected only under autotrophic conditions (Fig. 2.2). The *Rhodanobacter* sp. expressed all three copies of the nitric oxide reductase (*norB*) gene. In addition, normalized gene expression per MAG revealed highly expressed *norB* in the *Rhodanobacter* sp. under autotrophic conditions (439.88 averaged normalized TPM; Fig. 2.3). Therefore, the *Rhodanobacter* sp. might play a role in NO detoxification which is critical for the survival of the *Gallionellaceae* sp. (Fig. 2.2). It was previously suggested that the NO produced by the *Gallionellaceae* sp. could be reduced either via biotic processes by flanking community members or via abiotic processes, i.e., nitric oxide reduction coupled to Fe(II) oxidation (He *et al.*, 2016). Based on our findings, the biotic process of NO detoxification by the *Rhodanobacter* sp. seems likely, and might be essential for the survival of the *Gallionellaceae* sp. in the presence of toxic NO. This implies that the lack of the *nor* gene could be the barrier that prevents isolation of the *Gallionellaceae* sp. from culture KS. Thus, constant removal of NO may help for the isolation of the *Gallionellaceae* sp. in culture KS. Furthermore, the product derived from NO reduction is a greenhouse gas, N_2O, which is harmful to the environment. The proteins required for completing the denitrification pathway - NosZ by the *Rhodanobacter* sp. and the other heterotrophic

community members - were detected in culture KS under autotrophic conditions, further highlighting the critical role of interspecies interactions in the process of reducing N_2O. In naturally occurring microbial communities, the process of complete denitrification is vital to decrease N_2O greenhouse gas emissions which derive from incomplete microbial denitrification.

Oxidative phosphorylation pathway under anoxic conditions

Oxidative phosphorylation could also take part in accepting the electrons and transfer the electrons at the inner membrane to generate cellular energy. The metatranscriptome analysis revealed the presence of significantly higher abundances of oxidative phosphorylation gene transcripts under autotrophic compared to heterotrophic conditions for both, the *Gallionellaceae* sp. and *Rhodanobacter* sp. (Fig. 2.2). In addition, normalized gene expression per MAG showed high expression of *cytB* in the *Gallionellaceae* sp. (up to 34.31 averaged normalized TPM; Fig. 2.3) and of *ccoQ* in the *Rhodanobacter* sp. (142.16 averaged normalized TPM) under autotrophic conditions, respectively. Interestingly, the *Gallionellaceae* sp. homologs proteins for the cbb_3- and aa_3- type cytochrome *c* oxidases of complex IV, which have high and low affinity to oxygen, respectively (Arai *et al.*, 2014), were detected under autotrophic conditions (Fig. 2.2). These cbb_3- and aa_3- type cytochrome *c* oxidases are typically found in microaerophilic FeOB, such as *Sideroxydans lithotrophicus* strain ES-1, and aerobic acidophilic FeOB, such as *Acidthiobacillus ferrooxidans* spp., respectively (Castelle *et al.*, 2008; Emerson *et al.*, 2013). Under heterotrophic conditions, only the transcripts of the *Bradyrhizobium* sp. genes encoding for the protein complexes II, IV and V were detected, and only a few of them had significantly higher abundances compared to autotrophic conditions (Fig. 2.2). Furthermore, normalized gene expression per MAG revealed high levels of *ccoQ* in the *Bradyrhizobium* sp. (0.65-73.50 averaged normalized TPM; Fig. 2.3) and of *coxB* in the *Nocardioides* sp. (369.27-579.49 averaged normalized TPM) under both growth conditions, respectively. These data suggest that under both growth conditions, oxidative phosphorylation with O_2 as electron acceptor might occur in culture KS. However, our growth experiments were performed under anoxic conditions using N_2/CO_2 in the headspace and amended with $FeCl_2$ prior to inoculation, which would have consumed

any atmosphere O_2 contamination during the preparation procedure. Hypothetically, there might be a similar mechanism as proposed for the nitric oxide reductase (Nod). Nod was suggested to produce oxygen and dinitrogen in aerobic methane oxidizing bacteria under anoxic conditions (Ettwig *et al.*, 2010) and the corresponding gene was widely detected in the environment (Ettwig *et al.*, 2010; Zhang *et al.*, 2018; Hu *et al.*, 2019; Zhu *et al.*, 2019). However, evidence of *nod* gene homologs was confirmed to be vague in culture KS and the most similar protein in culture KS, compared to the published *nod* genes, has only 34% amino acids identity (in the *Rhodanobacter* sp.). Hence, to confirm the production of O_2 by an enzyme similar to Nod or the production of reactive oxygen species such as hydroxyl radicals, superoxide, and hydrogen peroxide in the culture KS system, further physiological experiments are required, as already suggested in a previous study (Mumford *et al.*, 2016). Another possible scenario might be constitutive expression of the oxidative phosphorylation complex III genes.

Overall, the microorganisms in culture KS may in theory have a microaerophilic living style, and the electrons accepted from the EET system may not only be transferred to the denitrification pathway but also to the oxidative phosphorylation pathway (Fig. 2.4). Indeed, several microoxic cultivation approaches, e.g., gradient tube and zero-valent iron plate, were used to grow culture KS and to isolate the *Gallionellaceae* sp. (Blöthe and Roden, 2009; Tominski *et al.*, 2018a). It was found that under these microoxic conditions, the *Gallionellaceae* sp. grew for the first few transfers, but the growth was not as stable as the culture under autotrophic anoxic NRFeOx conditions (Tominski, 2016; Tominski *et al.*, 2018a), suggesting that the *Gallionellaceae* sp. prefers an autotrophic anoxic NRFeOx environment or requires the microbial network that thrives under these conditions.

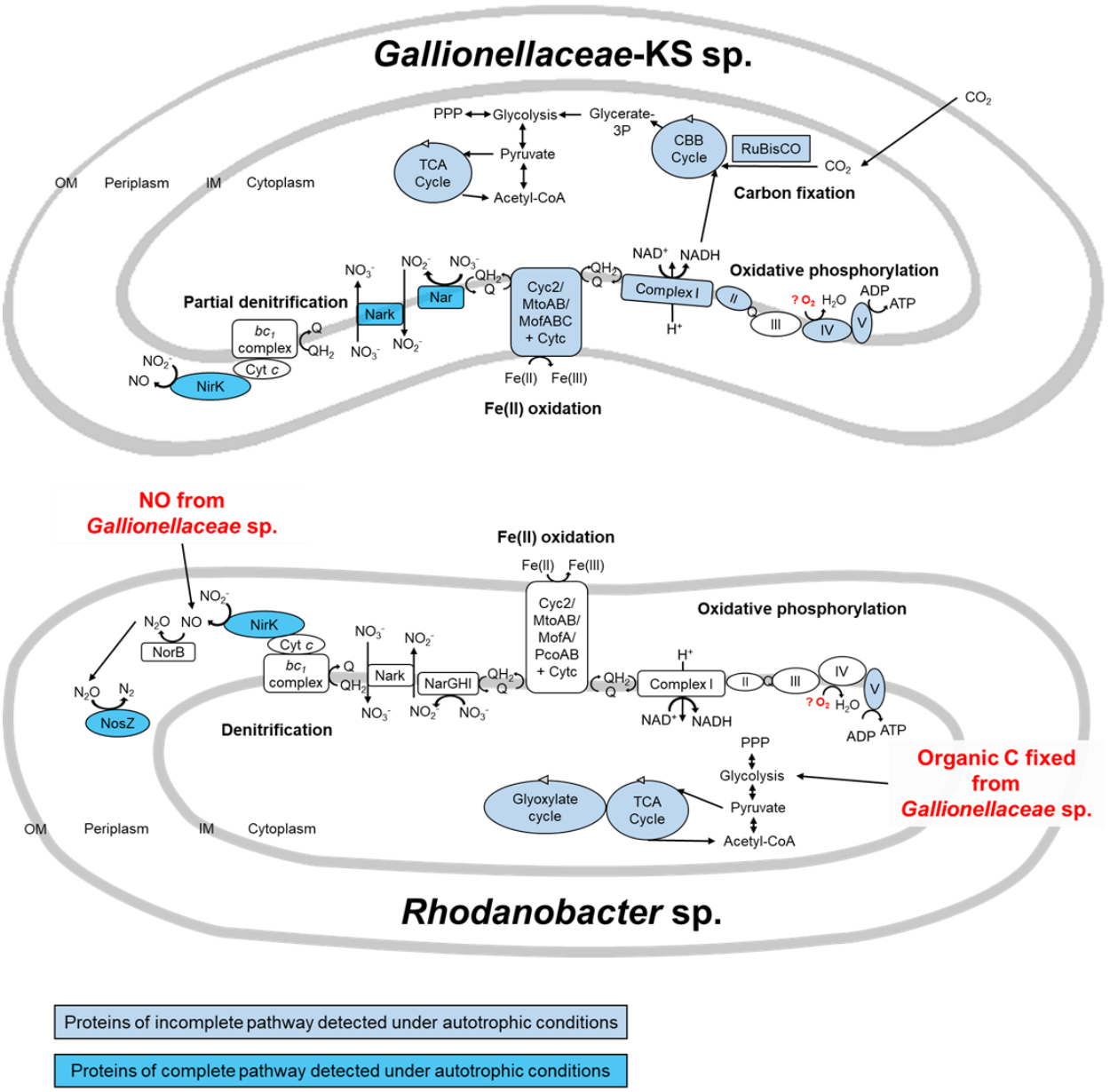

Fig. 2.4. Overview of the proposed microbial interactions of the *Gallionellaceae* sp. and *Rhodanobacter* sp. in culture KS under autotrophic conditions. The depicted putative reactions are based on the meta-omics data for extracellular electron transfer system, denitrification, carbon metabolism and oxidative phosphorylation in the *Gallionellaceae* sp. and *Rhodanobacter* sp. Most of the transcripts in this figure were detected under autotrophic conditions. Lighter blue color filling: incomplete pathway of proteins detected under autotrophic conditions; intense blue color filling: all proteins of the complete pathway detected under autotrophic conditions.

2.4. Conclusion

Overall, our meta-omics analysis demonstrated that the microbial mechanism of NRFeOx occurs in the neutrophilic, autotrophic enrichment culture KS at the transcript and protein levels. Based on this, both the *Gallionellaceae* sp. and *Rhodanobacter* sp. likely take part in the processes of Fe(II) oxidation and denitrification (Fig. 2.4). Carbon fixation by the *Gallionellaceae* sp. is probably required for the survival of the *Rhodanobacter* sp. (Fig. 2.4). In return, the *Rhodanobacter* sp. likely removes the toxic product, NO, that the *Gallionellaceae* sp. produces through incomplete denitrification (Fig. 2.4). This indicates that the *Gallionellaceae* sp. and *Rhodanobacter* sp. have established a symbiotic relationship to survive in the organic carbon source-limited but Fe(II)- and nitrate-rich environment of culture KS under autotrophic conditions. While we cannot provide direct proof of enzymatic NRFeOx and NO detoxification, our meta-omics analysis strengthens previous evidence of these mechanisms and sheds more light on the fascinating metabolisms and interdependencies of the microbial key players in culture KS. Furthermore, our meta-omics analysis revealed transcripts and proteins in culture KS that are an important basis for follow-up studies. For instance, our data provide hints on the conditions that might be required to isolate the nitrate-reducing Fe(II)-oxidizing *Gallionellaceae* sp. One promising approach employs a growth chamber with a periplasm membrane in between which might be used to grow the isolated *Rhodanobacter* sp. and the *Gallionellaceae* sp. via serial dilution from culture KS. This method would allow chemicals (e.g., organic carbon and NO) to pass through the membrane while separating the two species, resulting in a co-culture with complete pathways of NRFeOx and carbon fixation. Considering the environmental impact of microbial NRFeOx, a better knowledge of the physiology and the metabolism of members of the culture KS will be additionally valuable for the understanding of NRFeOx processes in the natural environment, particularly in organic carbon-limited but Fe(II)- and nitrate-containing habitats, such as aquifers. This knowledge may furthermore be used for treatment strategies of contaminated groundwater, wastewaters (Su *et al.*, 2016; Zhang *et al.*, 2016; Kiskira *et al.*, 2017) or constructed wetlands (i.e., wastewater treatment systems) (Song *et al.*, 2016).

2.5. Experimental proceedures

Cultivation, analytical methods and cell counts

Culture KS originates from a freshwater pond in Bremen, Germany (Straub *et al.*, 1996). Since then, culture KS has been transferred for more than 20 years under autotrophic conditions. For at least three years, culture KS was transferred with 1% (vol/vol) inoculum, including more than 10 transfers per year. The culture was grown in 58 mL serum bottles with 25 mL bicarbonate-buffered, anoxic, unfiltered medium, containing 10 mM $FeCl_2$, 4 mM $NaNO_3$, vitamins, and trace elements with a final pH of 6.9 to 7.2 (Hegler *et al.*, 2008; Blöthe and Roden, 2009). The incubation temperature was 28°C without light source and agitation, and the N_2/CO_2 ratio in the headspace was 90/10. Under heterotrophic conditions, 5 mM acetate was used instead of 10 mM $FeCl_2$ as electron donor. The analytic methods used to determine the concentrations of Fe(II), Fe(total), nitrate, nitrite and acetate as well as DAPI cell counts were described previously (Tominski *et al.*, 2018a).

Experimental setup for meta-omics

In order to achieve a high-quality metagenome, we used a hybrid approach with both, short read (Illumina) and long read (Nanopore) sequencing technologies. Also, to assemble genomes optimally that dominate either under autotrophic or heterotrophic growth conditions, we sequenced samples of both treatments. Therefore, metagenome samples were obtained at day 2 (Illumina) and 7 (Nanopore) under autotrophic conditions and at day 13 (Illumina) under heterotrophic conditions.

For the metatranscriptomics and metaproteomics analysis, both autotrophic and heterotrophic conditions were used with biological triplicates, respectively. Under autotrophic conditions, within 4 days on average 80% of Fe(II) was oxidized and 75% of nitrate was reduced. Therefore, samples under autotrophic conditions were taken at the 2^{nd} day (remaining Fe(II) and NO_3^- was 8.7 mM and 3.8 mM, respectively; 7.95×10^6 cells/mL). Under heterotrophic conditions, in a first step a pre-culture was grown for two transfers with 1% (vol/vol) inoculum for 10 days each, allowing more than seven generations under pre-culture conditions, considering an average doubling time of 1.5 days, to avoid carryover of signals from gene and protein expression under

autotrophic conditions. In a second step, the 3rd transfer under heterotrophic conditions was used for the experimental setup: within 7 days, 72% of acetate was oxidized and 97.5% of nitrate was reduced. Therefore, samples under heterotrophic conditions were taken at the 5th day (remaining: acetate - 3.68 mM; NO_3^- - 2.84 mM; NO_2^- - 0.04 mM; 5.29×10^7 cells/mL).

Biomass sampling

At the sampling time points, biomass of culture KS with total cell numbers ranging from 10^9 to 10^{10} cells was collected under sterile conditions on cellulose filters (mixed cellulose ester sterile filter membrane, 0.22 µm pore size, 47 mm filter diameter; Millipore) using vacuum filtration. The filters were cut into pieces and either stored in 15 mL falcon tubes at -80°C before proceeding with DNA and RNA extractions or stored in 50 mL falcon tubes at -80°C before proceeding with the protein extractions.

DNA and RNA co-extraction

DNA/RNA co-extraction was done according to the protocol of Lueders *et al.* (2004) with the following modifications: two tubes of “MP Bio Lysis Matrix E” beads were added into a 15 mL falcon tube including the filter pieces with the collected biomass. To disrupt the cells, 3.75 mL PB buffer (with 112.87 mM Na_2HPO_4 and 7.12 mM NaH_2PO_4) and 1.25 mL TNS buffer (with 500 mM Tris-HCL, 100 mM NaCl and 10% w/v SDS) were added, followed by bead beating for 4 minutes on the vortex adapter (maximum power) at room temperature (RT). The following centrifugation steps were all at maximum speed (7,197 ×g; Eppendorf Centrifuge 5430 with Rotor F35-6-30) at 4°C. All transfer steps were done on ice. The samples were centrifuged twice for 15 minutes and transferred to a new 15 mL falcon tube in between centrifugation steps, to obtain a clear supernatant. Then, the supernatant was split into new sterile 2 mL tubes (1 mL per tube) to proceed with phenol-chloroform-isoamyl alcohol and chloroform-isoamyl alcohol extractions according to Lueders *et al.* (2004). Subsequently, all aqueous phases were pooled again into a new 15 mL tube for polyethylene glycol (with 30% w/v polyethylene glycol 6000 and 1.6 M NaCl) precipitation overnight. From the ethanol-washing step, the extraction was done under a clean bench. The ethanol was removed carefully with a pipette with filter tips and

the pellet was dried at RT for ca. 10 minutes. The DNA/RNA pellet was dissolved in 20-50 µl diethyl pyrocarbonate (DEPC) treated water with Invitrogen™ Ambion™ RNase inhibitor (40 Unit/µl, 1 ul RNase inhibitor/ 40 µl), at RT for 30 min. For RNA samples, DNA digestion with TURBO DNA-free™ Kit was performed following the users' manual protocol for rigorous treatment. Successful DNA removal was confirmed by 30-cycle PCR using universal bacterial primers (see below). All samples were stored at -80°C before sequencing.

Protein extraction

Protein extraction was performed according to the "Protein extraction method B" from Spät *et al.* (2015) with the following modifications: 5 mL and 2 mL lysis buffer were added to the samples from autotrophic and heterotrophic conditions, respectively, to dissolve cell pellets. The samples were incubated for 10 minutes at 95°C in a water bath, vortexed briefly and chilled on ice with 2 minute-intervals in total 5 times and, subsequently, sonicated on ice for 30 seconds with an ultrasonic homogenizer (Bandelin Sonopuls) at output control 4 and 40% duty cycle. The lysate was centrifuged at 7,197 ×g for 1 minute at RT and the supernatant was then transferred into several 1.5 mL Eppendorf tubes and centrifuged at 20,817 ×g (Eppendorf Centrifuge 5430 with Rotor 30x1,5/2,0 mL) for 10 minutes at RT. Samples were pooled again into sterile 50 mL solvent-resistant tubes. After the 8:1 acetone:methanol precipitation and incubation overnight step, the precipitate was washed with 5 mL ice-cold 80% (v/v) acetone in water and centrifuged at 7,197 ×g for 5 minutes at 4°C. The protein pellets were air-dried at RT and later dissolved in urea buffer and stored at -20°C.

Illumina 16S rRNA amplicon sequencing

Bacterial 16S rRNA genes were amplified using universal primers, i.e., 515f: GTGYCAGCMGCCGCGGTAA (Parada *et al.*, 2016) and 806r: GGACTACNVGGGTWTCTAAT (Apprill *et al.*, 2015) fused to Illumina adapters. The PCR cycling conditions were as follows: 95°C for 3 min, 25 or 30 cycles of 95°C for 30 s, 55°C for 30 s, and 75°C for 30 s, and it was followed by a final elongation step at 72°C for 3 min. The quality of the purified amplicons was determined using agarose gel

electrophoresis. Subsequent library preparation steps, i.e., Nextera 2nd step PCR including pooling, and sequencing were performed on an Illumina MiSeq sequencing system (Illumina, San Diego, CA, USA) using the 2 × 250 bp MiSeq Reagent Kit v2 by Microsynth AG (Balgach, Switzerland). Between 68,651 and 219,333 sequencing read pairs were generated for each sample. Quality control, reconstruction of 16S rRNA gene sequences and taxonomic annotation was performed with nf-core/ampliseq v1.1.0 (Ewels *et al.*, 2020; Straub *et al.*, 2020) with Nextflow v20.04.1 (Di Tommaso *et al.*, 2017) using containerized software with singularity v3.0.3 (Kurtzer *et al.*, 2017). Primers were trimmed, and untrimmed sequences were discarded (< 8%) with Cutadapt v1.16 (Martin, 2011). Adapter and primer-free sequences were imported into QIIME2 version 2018.06 (Bolyen *et al.*, 2019), their quality was checked with demux (https://github.com/qiime2/q2-demux), and they were processed with DADA2 version 1.6.0 (Callahan *et al.*, 2016) to eliminate PhiX contamination, trim reads (position 200 in forward reads and 160 in reverse reads), correct errors, merge read pairs, and remove PCR chimeras; ultimately, 164 amplicon sequencing variants (ASVs) were obtained across all samples. Alpha rarefaction curves were produced with the QIIME2 diversity alpha-rarefaction plugin, which indicated that the richness of the samples had been fully observed. A Naive Bayes classifier was fitted with 16S rRNA gene sequences extracted with the PCR primer sequences from the QIIME compatible 99% identity clustered SILVA v132 database (Pruesse *et al.*, 2007). ASVs were classified by taxon using the fitted classifier (Bokulich *et al.*, 2018). Two ASVs that classified as chloroplasts or mitochondria were removed, totaling to < 0.1% relative abundance per sample, and the remaining ASVs had their abundances extracted by feature-table (https://github.com/qiime2/q2-feature-table).

Metagenome sequencing, assembly and annotation

Library preparation and shotgun Illumina sequencing of culture KS grown under autotrophic and heterotrophic conditions were performed by CeGaT, Tuebingen, Germany. 1 µg of DNA was used for library preparation with the TruSeq DNA PCR-Free Kit from Illumina without modifications. Libraries were sequenced on the Illumina NovaSeq 6000 platform to generate paired-end (2 × 150-bp) reads. 55.8 and 48.8 Gbp raw sequences were generated for autotrophic and heterotrophic growth conditions,

respectively. Nanopore sequencing (Oxford Nanopore Technologies; ONT) on culture KS under autotrophic conditions was performed by the NGS Competence Center Tuebingen (NCCT) in the University of Tuebingen, Germany. The DNA concentration was measured with Qubit 4.0 dsDNA BR Assay Kit and Nanodrop. The library was prepared according to the standard protocol of ONT. A PromethION flow cell (version 9.4.1) was loaded and run for 72h with standard settings (basecalling with HAC mode, bias voltage -180 mV) (Goldstein *et al.*, 2019; Moss *et al.*, 2020), producing 53 Gbp in 5 million reads.

Short and long read quality control, hybrid assembly, metagenome assembled genome binning and taxonomic annotation was performed with nf-core/mag v1.0.0 (https://nf-co.re/mag, DOI: 10.5281/zenodo.3589528) (Ewels *et al.*, 2020) with Nextflow v20.04.1 (Di Tommaso *et al.*, 2017) using containerized software with singularity v3.0.3 (Kurtzer *et al.*, 2017). Short read quality was assessed with FastQC v0.11.8 (Andrews, 2010), quality filtering and Illumina adapter removal was performed with fastp v0.20.0 (Chen *et al.*, 2018), and reads mapped with Bowtie2 v2.3.5 (Langmead and Salzberg, 2012) to the PhiX genome (Enterobacteria phage WA11, GCA_002596845.1, ASM259684v1) were removed. Long read quality was assessed with NanoPlot v1.26.3 (De Coster *et al.*, 2018), adapter trimming was done with Porechop v0.2.3_seqan2.1.1 (https://github.com/rrwick/Porechop), *Escherichia* virus Lambda (PRJNA485481, GCA_000840245.1) contamination was removed with Nanolyse v1.1.0 (De Coster *et al.*, 2018), and quality filtering was performed with Filtlong v0.2.0 (https://github.com/rrwick/Filtlong) using short reads retaining 75% of all long reads (nf-core/mag parameters “--longreads_keep_percent 75 --longreads_length_weight 1”). Finally, processed short and long reads were assembled with metaSPAdes v3.13.1 (Nurk *et al.*, 2017) and the assembly was evaluated with QUAST v5.0.2 (Gurevich *et al.*, 2013). MAGs were binned with MetaBAT2 v2.13 (Kang *et al.*, 2019) aided by the sequencing depth in libraries from autotrophic and heterotrophic conditions, checked for their completeness and contamination with BUSCO v3.0.2 (Waterhouse *et al.*, 2018) using 148 near-universal single-copy orthologs of bacteria (http://busco.ezlab.org/v3/datasets/bacteria_odb9.tar.gz) selected from OrthoDB v9 (Zdobnov *et al.*, 2017), summary statistics were obtained with QUAST for each MAG, and finally MAGs were taxonomically annotated with CAT v4.6 (von Meijenfeldt *et al.*, 2019),

using a reference database created 04 March 2020 from NCBI nr using the command "CAT prepare --fresh". Characteristics of the assembled metagenome can be found in Table 2.2. Four high-quality MAGs were obtained from the metagenome, with an estimated completeness of 95.3-99.3% and with no detectable contamination (Table 2.1).

Table 2.2. Summary of (A) metagenome, (B) metatranscriptome and (C) metaproteome data

	Culture KS Co-assembly
(A) Metagenome	
Genome size (Mbp)	18.17
No. contigs (scaffold)	117
Gene count	18082
GC (%)	66.21
No. of CDS	17832
IMG Submission ID	235566
IMG Genome ID	3300040739
GOLD Analysis Project ID	Ga0439407
rRNA	17
16S rRNA Count	6
(B) Metatranscriptome (range / average)	
Sequences [million]	21-62 / 46
% duplicates	75-94 / 85
GC%	54-61 / 56
% rRNA	4-94 / 65
% mapped to metagenome	46-95 / 78
mapped to metagenome [million]	1.7-16.8 / 11.2
Total no. of detected transcripts	17888
No. of significant higher expression level transcripts under autotrophic condition	6237
No. of significant higher expression level transcripts under heterotrophic condition	1068
(C) Metaproteome (range / average)	
Analyzed MS/MS spectra [thousand]	88-92 / 90
Identified MS/MS spectra (%)	16-37 / 28
Total no. of detected proteins	5833
No. of significant higher abundant proteins under autotrophic condition	77
No. of significant higher abundant proteins under heterotrophic condition	616

The assembled metagenome and MAGs were uploaded in June 2020 to the Joint Genome Institute's Integrated Microbial Genome and Microbiome Expert Review (IMG/MER) pipeline (IMGAP v5.0.18) for annotation (available online at https://img.jgi.doe.gov/cgi-bin/mer/main.cgi; Chen *et al.* (2019)). FeGenie (Garber *et al.*, 2020), National Center for Biotechnology Information (NCBI) basic local alignment search tool (BLAST) function (https://blast.ncbi.nlm.nih.gov/Blast.cgi) (Altschul *et al.*, 1990) and the IMG database (Chen *et al.*, 2019) were used to confirm potential Fe(II) oxidation genes. Metabolic pathways were searched by using KEGG database (https://www.genome.jp/kegg/pathway.html) (Kanehisa and Goto, 2000). GapMind was used for confirming complete gene pathways for essential amino acid biosynthesis (all with high confidence of best gene candidate) (https://papers.genomics.lbl.gov/cgi-bin/gapView.cgi) (Price *et al.*, 2020). Table S2.1 is a list of IMG accession numbers for genes of Fe(II) oxidation, carbon fixation, denitrification and complex IV of oxidative phosphorylation from four MAGs of culture KS. Supplementary text 2.6.1 described newly assembled MAG of the *Nocardioides* sp. in culture KS.

RNA sequencing, mapping and differential RNA abundance

For metatranscriptomes, DNAse treatment, library preparation including bacterial ribodepletion (with the NuGen Universal Prokaryotic RNA-Seq kit) and sequencing with 2 × 75 bp and 21 to 62 Mio clusters per sample were performed by Microsynth AG (Balgach, Switzerland) using triplicate samples of culture KS grown under autotrophic and heterotrophic conditions, respectively. For data analysis, nf-core/rnaseq v1.4.2 (https://nf-co.re/rnaseq) (Ewels *et al.*, 2020; Straub *et al.*, 2020) and its containerized software was used with singularity v3.0.3 (Kurtzer *et al.*, 2017). Firstly, an index database adjusted to small genomes (--genomeSAindexNbases 10) was created with Spliced Transcripts Alignment to a Reference (STAR) v2.6.1d (Dobin *et al.*, 2013) on the IMGAP annotation of the metagenome. Next, nf-core/rnaseq was executed with Nextflow v20.04.1 (Di Tommaso *et al.*, 2017) and performed quality checks with FastQC v0.11.8 (Andrews, 2010), removed around 1% basepairs per sample due to adapter contamination and trimming of low quality regions with Trim Galore! v0.6.4, removed 4% to 94% (average: 64%) rRNA sequences with SortMeRNA v2.1b (Kopylova *et al.*, 2012), aligned with STAR

v2.6.1d 93-95% and 46-74% reads for autotrophic and heterotrophic conditions, respectively, and finally summarized 13.2-16.8 and 1.7-16.3 million counts per sample for autotrophic and heterotrophic conditions, respectively, to genes by featureCounts v1.6.4 (Liao *et al.*, 2014). Transcripts per kilobase million (TPM) (Li and Dewey, 2011) were calculated by StringTie v2.0 (Pertea *et al.*, 2016). For the comparison of total transcript abundances under autotrophic compared to heterotrophic conditions, gene counts were used in differential abundance analysis in R v3.5.1 with DESeq2 v1.22.1 including median of ratios normalization (Love *et al.*, 2014) and a significant difference was postulated for transcripts with Benjamini and Hochberg adjusted $p \leq 0.05$. Normalized gene expression (normalized TPM) per MAG was calculated according to a previous study (McAllister *et al.*, 2020). Reference genes were selected from the list of genes validated for constitutive expression (Rocha *et al.*, 2015), but the 16S rRNA gene was excluded from consideration given that we did ribosomal RNA depletion. Further genes were excluded because either they were not detected in all MAGs or had undetectable expression (0 TPM) in all samples of at least one growth condition. Finally, the TPM values of the selected reference genes (*gapA*, *rpoA*, *rpoB*, *rpoC*, and *rpoD*) were averaged for each growth condition and MAG. Normalized TPM values for each gene were calculated by dividing its average TPM value per condition by the average TPM of the reference genes for the corresponding MAG and growth condition. For all calculations, a value of 0 TPM was treated as missing value. A summary of features of the metatranscriptome can be found in Fig. 2.2, Fig. 2.3 and Table 2.2.

Metaproteome analysis

The metaproteome analysis was conducted by the Quantitative Proteomics & Proteome Center, Tuebingen (PCT) (Schmitt *et al.*, 2019). Protein concentrations were determined via the Bradford assay (Bio-Rad) according to the user's manual. SDS PAGE short gel purification (Invitrogen) was run and in-gel digestion with Trypsin was conducted as described previously (Borchert *et al.*, 2010). Extracted peptides were desalted using C18 StageTips (Rappsilber *et al.*, 2007) and subjected to LC-MS/MS analysis. LC-MS/MS analyses were performed on an Easy-nLC 1200 UHPLC (Thermo Fisher Scientific) coupled to an QExactive HF Orbitrap mass spectrometer (Thermo Fisher Scientific) as

described elsewhere (Schmitt *et al.*, 2019). Peptides were eluted with a 127 min segmented gradient at a flow rate of 200 nl/min, selecting 12 most intensive peaks for fragmentation with HCD. The MS data was processed with MaxQuant software suite 1.6.7.0 (Cox and Mann, 2008). The iBAQ and LFQ algorithms were enabled, samples of the same treatment (autotrophic or heterotrophic conditions, respectively) were matched. Database search against protein sequences predicted by IMGAP on the metagenome assembly was performed using the Andromeda search engine (Cox *et al.*, 2011). 41,819 identified peptides by MaxQuant were loaded with R package proteus v0.2.13 (Gierlinski *et al.*, 2018) (https://github.com/bartongroup/Proteus) in R v3.6.0 (Team, 2020) (https://www.R-project.org/.) and subsequently assigned to 5,833 proteins, accumulated protein intensities were normalized by each samples median and transformed by log2. For the comparison of total protein abundances under autotrophic compared to heterotrophic conditions, differential protein abundance analysis was performed for the triplicates of autotrophic and heterotrophic conditions and the significance level for rejecting the null hypothesis was set to 0.05. Key characteristics of the metaproteomes can be found in Fig. 2.2 and Table 2.2.

Metagenome, draft genome accession numbers and data availability

The metagenome and MAGs are available through Integrated Microbial Genomes & Microbiomes (IMG) (https://img.jgi.doe.gov/), with the taxon identification (IMG Genome ID) 3300040739 for the culture KS metagenome, and IMG Genome ID 2878407288, 2878409899, 2878413433 and 2878420039 for the MAGs of the *Gallionellaceae* sp., *Rhodanobacter* sp., *Bradyrhizobium* sp. and *Nocardioides* sp., respectively.

Raw sequencing data have been deposited with links to BioProject accession number PRJNA682552 in the NCBI BioProject database (https://www.ncbi.nlm.nih.gov/bioproject/PRJNA682552). The raw mass spectrometry proteomics data have been deposited to the ProteomeXchange Consortium via the PRIDE (Perez-Riverol *et al.*, 2019) partner repository with the dataset identifier PXD023186. Accession numbers for each sample can be found in Table S2.2.

2.6. Supplementary information

2.6.1. Supplementary text

Nocardioides sp. metagenome assembled genome

In this study, a MAG of the *Nocardioides* sp. was recovered with 96.6% completeness (Table 2.1). This MAG is an addition to the MAGs retrieved in a previous metagenomic study of culture KS (He *et al.*, 2016). The closest related isolated organism to the *Nocardioides* sp. in culture KS was *Nocardioides* sp. JS614 (with 16S rRNA gene sequence identity of 99.10% and average nucleotide identity of 87.16%; Table 2.1) which utilizes vinyl chloride and ethene as carbon and energy sources (Coleman *et al.*, 2002). Moreover, another closely related organism, *Nocardioides* sp. strain in31 (with 16S rRNA gene sequence identity of 98.48%), was previously identified as mixotrophic nitrate-reducing Fe(II)-oxidizing bacterium (Benzine *et al.*, 2013).

The MAG analysis of the *Nocardioides* sp. in our study revealed the putative Fe(II) oxidation gene *mofA* (i.e., manganese oxidation gene), an *ompB* homolog, which encodes a manganese-oxidizing protein with copper domains, i.e., a multicopper oxidase (Corstjens *et al.*, 1997; Brouwers *et al.*, 2000). Transcripts of *mofA* were detected under both, autotrophic and heterotrophic conditions (Fig. 2.2). For denitrification genes and transcripts, nitrate reductase (*narGHI*), nitrite reductase (*nirK*) and nitric oxide reductase (*norB*) were detected under both conditions. In addition, NarGH, NirK and NorB proteins were detected under heterotrophic conditions (Fig. 2.2). Carbon metabolism pathway genes for the glycolysis pathway, the tricarboxylic acid cycle, and the pentose phosphate pathway were identified in the MAG of the *Nocardioides* sp. However, no essential carbon fixation genes, i.e. *rbcL* or *rbcS*, were detected in the *Nocardioides* sp. MAG. For the oxidative phosphorylation pathway, the genes for the respiratory chain complexes I (NADH quinone oxidoreductase), II (succinate dehydrogenase), III (cytochrome bc_1 complex), IV (cbb_3- and aa_3-type cytochrome c oxidases) and V (F-type ATPase) were all identified. However, only partial transcripts encoding aa_3-type cytochrome c oxidases were detected under both conditions (Fig. 2.2). For the genes of amino acid biosynthesis, most of the genes were identified in the MAG of the *Nocardioides* sp. One exemption was the gene encoding the anthranilate synthase subunit TrpE, for tryptophan biosynthesis, that was identified at low confidence, i.e. with low identity to related gene homologs.

The meta-omics findings of the *Nocardioides* sp. mostly align with the physiological data from previous studies (Tominski, 2016). An isolate of the *Nocardioides* sp. grew under oxic conditions on agar plates and showed no growth under autotrophic conditions with nitrate as electron acceptor and Fe(II) or Fe(II)-EDTA as electron donors (Tominski, 2016). The *Nocardioides* sp. only consumed substrates under mixotrophic conditions with Fe(II)-EDTA and acetate as electron donor and under heterotrophic growth conditions with acetate as electron donor (Tominski, 2016). Overall, our results suggest that the *Nocardioides* sp. in culture KS might be a facultative aerobe, which cannot proceed carbon fixation and autotrophic Fe(II) oxidation.

2.6.2. Supplementary calculation

The calculation of 1 mg/L of dissolved organic carbon in Milli-Q water producing approximately 10^6 cells/mL is as follows:

Estimated cell weight: 1 pg = 1×10^{-9} mg.

The proportion of carbon in biomass (CH_2O) = (12 g/mol)/ ((12+2×1+16) g/mol) = 40%

Therefore, in 1×10^{-9} mg cell weight, 0.4×10^{-9} mg is carbon. Assuming 100% of carbon from dissolved organic carbon goes to biomass formation, biomass can be produced from carbon: (1 mg/L)/ 0.4×10^9 mg = 2.5×10^9 cells/L = 2.5×10^6 cells/mL.

Supplementary tables

Table S2.1. List of IMG accession numbers (Locus Tag) for genes of Fe(II) oxidation, carbon fixation, denitrification and complex IV of oxidative phosphorylation

Gene Product Name	*Gallionellaceae*	*Rhodanobacter*	*Bradyrhizobium*	*Norcardioides*
Fe oxidation				
hypothetical protein (*cyc2*)	Ga0439409_05_803_2095	Ga0439410_03_678072_679457		
hypothetical protein (*cyc2*)		Ga0439410_03_1055160_1056515		
DmsE family decaheme c-type cytochrome; CXXCH motif (*mtoA*)	Ga0439409_01_391371_392324	Ga0439410_05_601238_602269		
MtrB/PioB family decaheme-associated outer membrane protein - DUF3374 (*mtoB*)	Ga0439409_01_392345_395107	Ga0439410_05_602285_604669		
FtsP/CotA-like multicopper oxidase with cupredoxin domain (*mofA*)	Ga0439409_01_575045_579349	Ga0439410_01_148354_150402	Ga0439411_01_2113509_2114609	Ga0439412_01_891723_893246
FKBP-type peptidyl-prolyl cis-trans isomerase FklB (*mofB*)	Ga0439409_01_573660_574349	Ga0439410_05_428698_429420		
CopA family copper-resistance protein (*pcoA*)		Ga0439410_01_153335_155176		
CopA family copper-resistance protein (*pcoA*)		Ga0439410_03_386483_388243		
copper resistance protein B (*pcoB*)		Ga0439410_01_152079_153338		
copper resistance protein B (*pcoB*)		Ga0439410_03_385272_386486		
Carbon fixation (RuBisCo)				
ribulose-bisphosphate carboxylase large chain (*rbcL*)	Ga0439409_02_196386_197765		Ga0439411_01_379596_381056	
ribulose-bisphosphate carboxylase large chain (*rbcL*)			Ga0439411_01_4594611_4596071	
ribulose-bisphosphate carboxylase small chain (*rbcS*)			Ga0439411_01_381068_381475	
ribulose-bisphosphate carboxylase small chain (*rbcS*)			Ga0439411_01_4594171_4594539	

Table S2.1. (continued) List of IMG accession numbers (Locus Tag) for genes of Fe(II) oxidation, carbon fixation, denitrification and complex IV of oxidative phosphorylation

Gene Product Name	*Gallionellaceae*	*Rhodanobacter*	*Bradyrhizobium*	*Norcardioides*
Denitrification				
nitrate reductase alpha subunit (*narG*)	Ga0439409_01_988048_991809	Ga0439410_05_206908_210666	Ga0439411_01_3918566_3922318	Ga0439412_02_472082_475804
nitrate reductase beta subunit (*narH*)	Ga0439409_01_986465_988012	Ga0439410_05_210666_212210	Ga0439411_01_3917025_3918569	Ga0439412_02_475885_477627
nitrate reductase gamma subunit (*narI*)	Ga0439409_01_985168_985914	Ga0439410_05_212887_213591	Ga0439411_01_3915578_3916303	Ga0439412_02_478367_479098
nitrite reductase (NO-forming) (*nirK*)	Ga0439409_02_432389_433426	Ga0439410_04_176086_178065	Ga0439411_01_6412199_6413296	Ga0439412_03_304576_307281
nitrite reductase (NO-forming) (*nirK*)		Ga0439410_05_185392_186909		
nitrite reductase (NO-forming) / hydroxylamine reductase (*nirS*)	Ga0439409_02_592761_594422		Ga0439411_01_6628345_6630063	
nitrite reductase (NO-forming) / hydroxylamine reductase (*nirS*)	Ga0439409_02_595219_596853			
nitric oxide reductase subunit B (*norB*)		Ga0439410_05_227274_229556	Ga0439411_01_1063984_1065330	Ga0439412_01_127239_129620
nitric oxide reductase subunit B (*norB*)		Ga0439410_05_233733_235430	Ga0439411_01_3808647_3810980	
nitric oxide reductase subunit B (*norB*)		Ga0439410_05_696543_698840	Ga0439411_01_3832715_3834427	
nitric oxide reductase subunit C (*norC*)			Ga0439411_01_1063489_1063941	
nitrous-oxide reductase (*nosZ*)		Ga0439410_05_268657_270606	Ga0439411_01_3826691_3828982	
nitrous-oxide reductase (*nosZ*)			Ga0439411_01_44822_46765	
Oxydative phosphorylation complex IV (cytochrome bc_1 complex)				
ubiquinol-cytochrome c reductase cytochrome b/c1 subunit (*fbcH*)		Ga0439410_05_165068_165673	Ga0439411_01_252978_255041	
ubiquinol-cytochrome c reductase iron-sulfur subunit (UQCRFS1, RIP1, *petA*)	Ga0439409_03_62071_62664	Ga0439410_05_165673_166974	Ga0439411_01_252382_252912	
ubiquinol-cytochrome c reductase iron-sulfur subunit (UQCRFS1, RIP1, *petA*)	Ga0439409_04_38335_38928			
ubiquinol-cytochrome c reductase cytochrome b subunit (CYTB, *petB*)	Ga0439409_03_60836_62074	Ga0439410_05_166967_167725		
ubiquinol-cytochrome c reductase cytochrome b subunit (CYTB, *petB*)	Ga0439409_04_37100_38338			
ubiquinol-cytochrome c reductase cytochrome c1 subunit (CYC1, CYT1, *petC*)	Ga0439409_03_60066_60818			
ubiquinol-cytochrome c reductase cytochrome c1 subunit (CYC1, CYT1, *petC*)	Ga0439409_04_36361_37077			

Table S2.1. (continued) List of IMG accession numbers (Locus Tag) for genes of Fe(II) oxidation, carbon fixation, denitrification and complex IV of oxidative phosphorylation

Gene Product Name	*Gallionellaceae*	*Rhodanobacter*	*Bradyrhizobium*	*Norcardioides*
Oxydative phosphorylation complex IV (*cbb*$_3$-type)				
cytochrome c oxidase cbb3-type subunit I (*ccoN*)	Ga0439409_04_82617_84011	Ga0439410_05_818919_820385	Ga0439411_01_510756_512414	
cytochrome c oxidase cbb3-type subunit I (*ccoN*)			Ga0439411_01_659138_660787	
cytochrome c oxidase cbb3-type subunit II (*ccoO*)	Ga0439409_04_84022_84780	Ga0439410_05_818243_818905	Ga0439411_01_512418_513149	
cytochrome c oxidase cbb3-type subunit II (*ccoO*)			Ga0439411_01_660800_661534	
cytochrome c oxidase cbb3-type subunit III (*ccoP*)	Ga0439409_04_175472_175831	Ga0439410_05_817159_818067	Ga0439411_01_513312_514190	
cytochrome c oxidase cbb3-type subunit III (*ccoP*)	Ga0439409_04_84979_85887		Ga0439411_01_661719_662591	
cytochrome c oxidase cbb3-type subunit IV (ccoQ)		Ga0439410_05_818064_818246	Ga0439411_01_513154_513321	
cytochrome c oxidase cbb3-type subunit IV (ccoQ)			Ga0439411_01_661548_661712	
Oxydative phosphorylation complex IV (*aa*$_3$-type)				
cytochrome c oxidase subunit I (*coxA*)	Ga0439409_01_25959_27665	Ga0439410_02_392830_394446	Ga0439411_01_1729373_1730995	Ga0439412_01_2213719_2215470
cytochrome c oxidase subunit I (*coxA*)	Ga0439409_01_498172_499758		Ga0439411_01_518788_520398	Ga0439412_02_747973_749649
cytochrome c oxidase subunit I (*coxA*)			Ga0439411_01_6026147_6027772	
cytochrome c oxidase subunit I (*coxA*)			Ga0439411_01_6618588_6620309	
cytochrome c oxidase subunit II (*coxB*)	Ga0439409_01_25395_25952	Ga0439410_02_391858_392757	Ga0439411_01_1730982_1731557	Ga0439412_01_2212790_2213722
cytochrome c oxidase subunit II (*coxB*)	Ga0439409_01_499768_500811		Ga0439411_01_6025226_6026065	Ga0439412_02_747386_747976
cytochrome c oxidase subunit II (*coxB*)			Ga0439411_01_6618008_6618583	
cytochrome c oxidase subunit III (*coxC*)	Ga0439409_01_496628_497482	Ga0439410_02_394759_395646	Ga0439411_01_6029668_6030564	Ga0439412_01_2221152_2221721

Table S2.2. Overview of multi-omics samples, archived in the Sequencing Read Archive (SRA, bioproject PRJNA682552) or ProteomeXchange Consortium (via the PRIDE partner repository, identifier PXD023186).

Conditions	Time-point	Replicate	Amplicon sequencing	Metagenomics	Metatranscriptomics	Metaproteomics
Autotrophic	D0	1	SRR13197605			
	D2	1	SRR13197604	SAMN17088344 (Illumina)	SRR13245408	R17
	D2	2	SRR13197593		SRR13245407	R18
	D2	3	SRR13197591		SRR13245406	R19
	D2	4	SRR13197590			
	D3	1	SRR13197589			
	D3	2	SRR13197588			
	D3	3	SRR13197587			
	D7	1	SRR13197586	SAMN17088346 (Nanopore)		
	D7	2	SRR13197585			
	D7	3	SRR13197603			
Heterotrophic	D00	1	SRR13197602			
	D05	1	SRR13197601		SRR13245405	R20
	D05	2	SRR13197600		SRR13245404	R21
	D05	3	SRR13197599		SRR13245403	R22
	D09	1	SRR13197598			
	D09	2	SRR13197597			
	D09	3	SRR13197596			
	D13	1	SRR13197595	SAMN17088345 (Illumina)		
	D13	2	SRR13197594			
	D13	3	SRR13197592			

3. A novel enrichment culture highlights core features of microbial networks contributing to autotrophic Fe(II) oxidation coupled to nitrate reduction

Yu-Ming Huang[a, b], Daniel Straub[a, c], Andreas Kappler[b, d], Nicole Smith[a], Nia Blackwell[a] and Sara Kleindienst[a]

[a] Microbial Ecology, Center for Applied Geoscience, University of Tuebingen, Germany
[b] Geomicrobiology, Center for Applied Geoscience, University of Tuebingen, Germany
[c] Quantitative Biology Center (QBiC), University of Tuebingen, Germany
[d] Cluster of Excellence: EXC 2124: Controlling Microbes to Fight Infections, University of Tübingen, Tübingen, Germany

Slightly modified version published in ***Microbial Physiology***
Special Issue "Bacterial survival strategies"
Huang, Y., Straub, D., Kappler, A., Smith, N., Blackwell, N., and Kleindienst, S. (2021) A novel enrichment culture highlights core features of microbial networks contributing to autotrophic Fe(II) oxidation coupled to nitrate reduction. *Microbial Physiol*.
https://doi.org/10.1159/000517083

3.1. Abstract

Fe(II) oxidation coupled to nitrate reduction (NRFeOx) has been described for many environments. Yet, very few autotrophic microorganisms catalysing NRFeOx have been cultivated and their diversity, as well as their mechanisms for NRFeOx *in situ*, remain unclear. A novel autotrophic NRFeOx enrichment culture, named culture BP, was obtained from a freshwater sediment. After more than 20 transfers per year from 2018, culture BP oxidized 8.22 mM of Fe(II) and reduced 2.42 mM of nitrate within 6.5 days under autotrophic conditions. We applied metagenomic, metatranscriptomic and metaproteomic analyses to culture BP to identify the microorganisms involved in autotrophic NRFeOx and to unravel their metabolism. Overall, twelve metagenome-assembled genomes (MAGs) were constructed, including a dominant *Gallionellaceae* sp. MAG (≥71% relative abundance). Genes and transcripts associated with potential Fe(II) oxidizers in culture BP, identified as a *Gallionellaceae* sp., *Noviherbaspirillum* sp., and *Thiobacillus* sp., were likely involved in metal oxidation (e.g. *cyc2*, *mtoA*), denitrification (e.g. *nirK*/*S*, *norBC*), carbon fixation (e.g. *rbcL*) and oxidative phosphorylation. The putative Fe(II)-oxidizing protein Cyc2 was detected for the *Gallionellaceae* sp. and *Noviherbaspirillum* sp., respectively. Overall, a complex network of microbial interactions among several Fe(II) oxidizers and denitrifiers was deciphered in culture BP that might resemble NRFeOx mechanisms *in situ*. Furthermore, 16S rRNA gene amplicon sequencing from environmental samples revealed 36 distinct *Gallionellaceae* taxa, including the key player of NRFeOx from culture BP (~0.13% relative abundance *in situ*). Since several of these *in situ* detected *Gallionellaceae* taxa were closely related to the key player in culture BP, this suggests that the diversity of organisms contributing to NRFeOx might be higher than currently known.

3.2. Introduction

Oxidation of ferrous iron [Fe(II)] and reduction of ferric iron [Fe(III)] contribute to biogeochemical carbon, nitrogen, oxygen and sulfur cycles and can be mediated by specific microorganisms. There are three physiological types of Fe(II)-oxidizing bacteria (FeOB), i.e. microaerophiles, photoferrotrophs and nitrate-reducing Fe(II) oxidizers. Autotrophic nitrate-reducing Fe(II) oxidizers have the ability to fix carbon dioxide (CO_2) and to oxidize Fe(II) coupled with complete or incomplete denitrification and can, thus, influence the fate of the groundwater pollutant nitrate and the greenhouse gases nitrous oxide (N_2O) and carbon dioxide (CO_2). However, detailed knowledge about the enzymatic mechanisms of autotrophic Fe(II) oxidation coupled to nitrate reduction (NRFeOx) in the environment is missing.

Based on several laboratory studies on autotrophic and mixotrophic nitrate-reducing Fe(II)-oxidizing bacteria (ZoBell, 1944; Rabus and Widdel, 1995; Straub *et al.*, 1996; Buchholz-Cleven *et al.*, 1997; Edwards *et al.*, 2003; Beller *et al.*, 2006b; Kumaraswamy *et al.*, 2006; Weber *et al.*, 2006; Su *et al.*, 2015; Zhang *et al.*, 2015; Zhou *et al.*, 2016), it was proposed that to be classified as true autotrophic nitrate-reducing Fe(II) oxidizing cultures, the cultures must (i) have no need of an additional organic carbon source, (ii) maintain Fe(II) oxidation over several (>3) transfers without organic carbon addition, (iii) have confirmed growth of cells with only Fe(II), nitrate and CO_2 provided, and (iv) show CO_2 uptake by incorporation of labelled CO_2 into biomass during Fe(II) oxidation (Bryce *et al.*, 2018). To date, there has only been one example of a stable autotrophic nitrate-reducing Fe(II)-oxidizing bacterial culture that fits all of the above criteria, enrichment culture KS (Straub *et al.*, 1996; He *et al.*, 2016; Tominski *et al.*, 2018a; Tominski *et al.*, 2018b). Culture KS was initially described in Straub *et al.* (1996), originates from Bremen, Germany, and is composed of FeOB, i.e. an unclassified *Gallionellaceae* sp., and denitrifiers, i.e. *Rhodanobacter* sp. and *Bradyrhizobium* sp. (He *et al.*, 2016). These FeOB and denitrifiers in culture KS showed that species interdependencies are used as a survival strategy under the carbon limited but Fe(II)- and nitrate-rich culture conditions (Huang *et al.*, 2021a). Yet, it remains unknown whether additional autotrophic nitrate-reducing Fe(II)-oxidizing cultures, aside from culture KS, can be cultivated to expand the diversity of known key players of autotrophic NRFeOx.

Nitrate-reducing Fe(II)-oxidizing bacteria were found in various types of environments (Straub and Buchholz-Cleven, 1998; Laufer *et al.*, 2016) and were studied as treatments for contaminated groundwater (Su *et al.*, 2016; Zhang *et al.*, 2016; Kiskira *et al.*, 2017) and constructed wetlands (i.e. wastewater treatment systems) (Song *et al.*, 2016). Furthermore, microorganisms of the family *Gallionellaceae* were widely found in a variety of natural environments (Wang *et al.*, 2009; McBeth *et al.*, 2013; Emerson *et al.*, 2016; Fabisch *et al.*, 2016; Jewell *et al.*, 2016; Li *et al.*, 2017). In addition, several observations pointed towards an involvement of *Gallionellaceae* spp. in NRFeOx processes in different habitats (Emerson *et al.*, 2016; Jewell *et al.*, 2016; Bethencourt *et al.*, 2020). However, it remained largely unknown whether these FeOB are dependent on other microbial community members, similar to the interdependencies described for culture KS (He *et al.*, 2016).

Here, we explored a novel autotrophic NRFeOx enrichment culture, named culture BP (Bremen Pond), that originated from a freshwater sediment in Bremen, Germany, and was obtained in 2015 from a pond close to the sampling site of culture KS. We studied the physiology of culture BP by analysing its geochemistry, cell numbers and microbial community composition (via 16S rRNA gene amplicon sequencing). In addition, we used metagenomic, metatranscriptomic and metaproteomic (meta-omics) analysis to (i) identify the key players of NRFeOx in culture BP, (ii) study their potential metabolism, particularly for Fe(II) oxidation, denitrification and carbon fixation, (iii) explore possible microbial interspecies interactions in culture BP, and (iv) compare the more recent culture BP that might resemble environmental NRFeOx processes more closely to the long-term established culture KS. We furthermore performed DNA- and RNA-based 16S rRNA (gene) amplicon sequencing of six sites at the original habitat of culture BP to (v) assess the *in-situ* diversity and relative abundance of potential key players involved in NRFeOx.

3.3. Results

Physiology and microbial community composition of the novel enrichment culture BP

To explore the diversity of cultivable autotrophic FeOB contributing to NRFeOx in the environment, we sampled a freshwater habitat, a pond in Bremen (Germany), which is in the vicinity of the origin of the existing NRFeOx culture KS (a connected ditch nearby). We established the novel culture BP, maintained under the same autotrophic growth conditions as culture KS (Tominski *et al.*, 2018a). Culture BP was grown under autotrophic conditions (i.e. with 10 mM Fe(II) as an electron donor and 4 mM nitrate as an electron acceptor in bicarbonate-buffered medium) and under heterotrophic conditions (i.e. with 5 mM acetate as an electron donor and 4 mM nitrate as an electron acceptor) as alternative growth condition for three successive transfers in triplicates, respectively. Samples for meta-omics analyses were collected on the 2nd day under autotrophic conditions, and at 18 hours under heterotrophic conditions; optimum sampling points were determined based on geochemical and short-read 16S rRNA gene amplicon sequencing analyses conducted in parallel.

Under autotrophic conditions, 8.22 mM of Fe(II) was oxidized in 6.5 days with an average Fe(II) oxidation rate of 1.66 mM/day during the active growth phase (i.e. between 23 and 90 hours) (Fig. 3.1A). This co-occurred with a reduction of 2.42 mM of nitrate and an average nitrate reduction rate of 0.53 mM/day, without detectable nitrite production (Fig. 3.1A). The average $Fe(II)_{oxidized}$/$nitrate_{reduced}$ stoichiometric ratio was 3.4, which was lower than theoretical ration 5, indicating incomplete denitrification, and cell numbers increased from 1.04×10^6 cells/mL to 4.31×10^6 cells/mL within 3.75 days (Fig. 3.1C).

Under heterotrophic conditions, 3.4 mM of acetate was consumed with an average acetate oxidation rate of 2.7 mM/day during the exponential growth phase (i.e. between 11 to 37 hours). This co-occurred with a reduction of 4.0 mM nitrate and an average nitrate reduction rate of 3.5 mM/day. Nitrite increased from 0.02 to 0.8 mM from 11 to 18 hours, but decreased again afterwards (Fig. 3.1B). The average ratio for $acetate_{oxidized}$/$nitrate_{reduced}$ was 0.85, which is higher than the theoretical stoichiometry value of 0.625, suggesting that acetate was oxidized not only for energy generation but also used for biomass production and nitrate was eventually reduced completely to N_2.

Throughout the experiment, cell numbers increased from 3.89 × 10^4 cells/mL to 3.68 × 10^7 cells/mL within 37 hours (Fig. 3.1D).

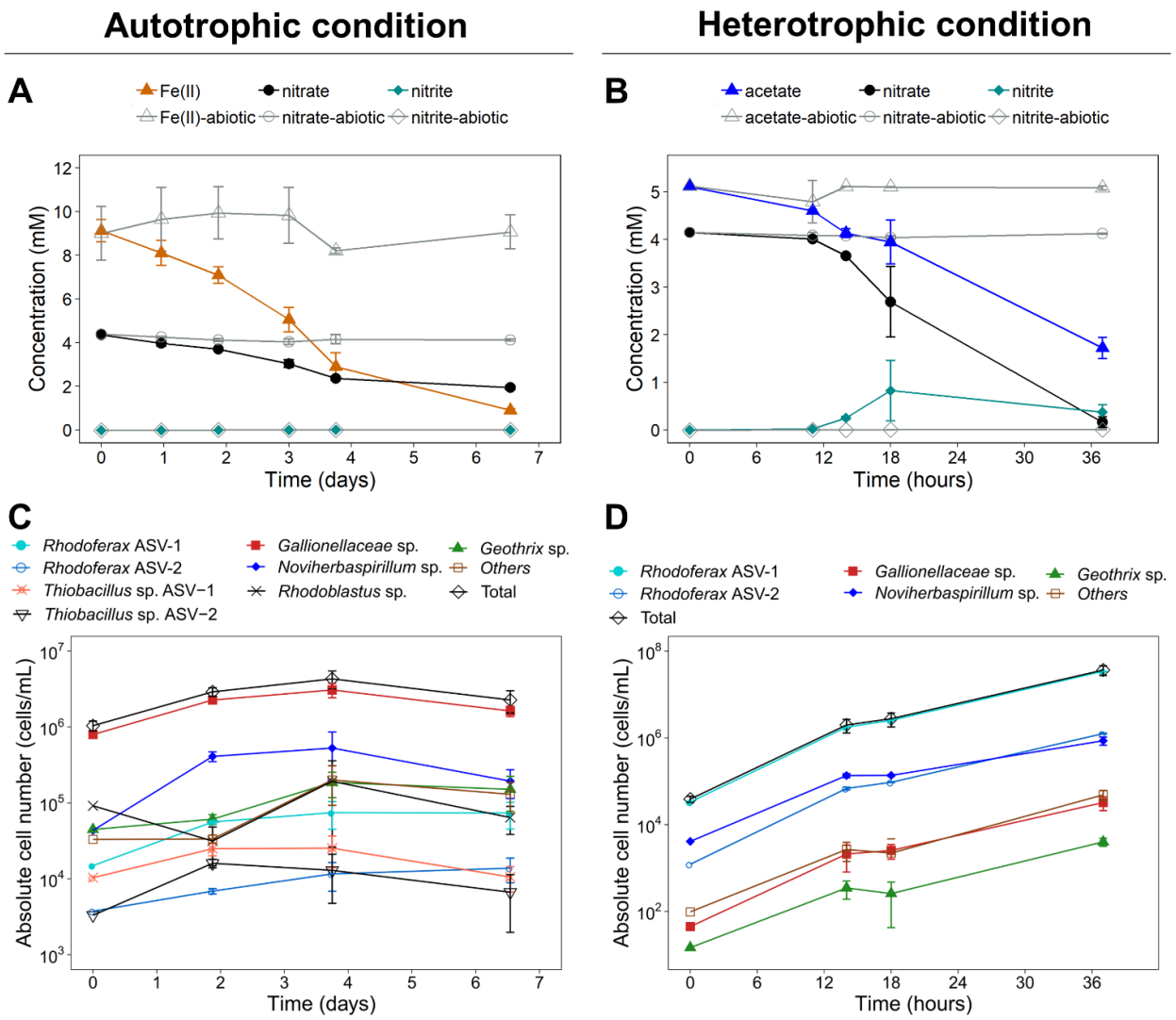

Fig. 3.1. Geochemistry of culture BP under autotrophic (left) and heterotrophic (right) conditions. Changes in (A) Fe(II), nitrate and nitrite concentrations, (B) acetate, nitrate and nitrite concentrations, (C and D) estimated absolute cell numbers (calculated using total cell numbers and short-read 16S rRNA gene amplicon sequencing relative abundance data), as monitored over time. Error bars represent the standard deviation of three biological replicates (except for T0).

Under autotrophic conditions, an amplicon sequencing variant (ASV) classified as *Gallionellaceae* sp. dominated with 71-78% relative abundance at days 1, 2, 4 and 7 (corresponding to ca. up to 3.1 × 10^6 cells/mL; Fig. 3.1C). In addition to short-reads, long-read 16S rRNA gene amplicon sequencing was performed to obtain improved taxonomic identification of the microbial populations in culture BP (long-read and short-read 16S rRNA gene sequences are presented in the supplementary data S1 and S2, respectively).

Based on long-reads, the novel unclassified *Gallionellaceae* sp. in culture BP shared 97.88% sequence identity with the unclassified *Gallionellaceae* sp. in culture KS and 96.17% with *Ferrigenium kumadai* (Table S3.1). Other abundant ASVs were classified as *Noviherbaspirillum* (9-15%; corresponding to ca. up to 5.3×10^5 cells/mL), *Geothrix* (2-7%; ca. up to 1.9×10^5 cells/mL), *Rhodoferax* (ASV-1 with 2-3%; ca. up to 7.5×10^4 cells/mL), *Thiobacillus* (two ASVs with 0.4-1.6%; ca. up to 4.1×10^4 cells/mL) and *Rhodoblastus* (1-5%; ca. up to 1.9×10^5 cells/mL) (Fig. 3.1C). Under heterotrophic growth conditions, a *Rhodoferax* sp. (ASV-1) dominated with 84-94% relative abundance (corresponding to ca. up to 3.5×10^7 cells/mL) throughout the 3rd transfer under heterotrophic conditions, while lower relative abundances were detected for ASVs classified as *Noviherbaspirillum* (2-11%; ca. up to 8.6×10^5 cells/mL), *Rhodoferax* (ASV-2, only 1 nucleotide difference to ASV-1; 2-3%; ca. up to 1.3×10^6 cells/mL), *Gallionellaceae* (up to 0.1%; ca. up to 3.2×10^4 cells/mL) and *Geothrix* (up to 0.03%; ca. up to 4.0×10^3 cells/mL) (Fig. 3.1D). The long-read 16S rRNA gene amplicon sequence of *Rhodoferax* sp. was closely related to *Curvibacter delicatus* strain NBRC 14919 (98.56% sequence identity; Table S3.1).

We identified highly similar 16S rRNA gene sequences of the *Rhodoblastus* sp. using short- and long-read 16S rRNA amplicon sequencing compared to the metagenome-assembled genome (MAG), see below. However, for the *Gallionellaceae* sp., *Noviherbaspirillum* sp., *Rhodoferax* sp., *Thiobacillus* sp., *Geothrix* sp. and *Betaproteobacteria* bacterium, only short- and long-read sequencing offered 16S rRNA gene sequences of the respective taxa. The phylogenetic relationships of the 16S rRNA gene sequences of the amplicon sequencing approach and the MAG is shown in supplementary Fig. S3.1.

General characteristics of the metagenome-assembled genomes in culture BP

In order to study the genomic potential of key players involved in NRFeOx and to use this information as reference for our meta-omics approach, twelve MAGs were retrieved from the metagenome of culture BP (supplementary data S3). Among these twelve MAGs, six had high-quality with completeness >90% (*Gallionellaceae* sp., *Noviherbaspirillum* sp., *Rhodoferax* sp., *Rhodoblastus* sp., *Thiobacillus* sp. and *Betaproteobacteria* bacterium; Table S3.1.), two had medium-quality with 88% and 64.8% completeness (*Ramlibacter*

sp. and *Geothrix* sp., respectively; Table S3.1), and four had low-quality with <50% completeness (*Geothrix* sp., *Mesorhizobium* sp. and two unclassified MAGs), according to the definition of Bowers *et al.* (2017). The four low-quality MAGs and one medium-quality MAG (*Geothrix* sp.) did not contain Fe(II) oxidation genes and showed only partial genes for denitrification. Thus, these five MAGs were not explored further. Additionally, the classification of the *Betaproteobacteria* bacterium MAG was vague, and it did not express any denitrification genes in culture BP. Therefore, we mainly focused on the remaining six MAGs, i.e. the *Gallionellaceae* sp.*, Noviherbaspirillum* sp.*, Rhodoferax* sp.*, Rhodoblastus* sp., *Thiobacillus* sp. and *Ramlibacter* sp., representing up to 98% of the microbial community during the Fe(II) oxidation phase. These MAGs harboured genes associated with key biogeochemical cycles, including carbon, nitrogen, oxygen and iron, in particular Fe(II) oxidation (Fig. 3.2). In order to add more evidence to gene level information, we conducted metatranscriptomic and metaproteomic analyses to gain additional evidence at RNA and protein levels. The detection of a protein confirmed its presence and therefore suggested that the catalysed reaction of this particular protein was likely happening. Statistical meta-omics data are presented in supplementary table S3.2.

Fe(II) oxidation

To explore the pathways of Fe(II) oxidation in culture BP, we searched for homologues of known and putative Fe(II) oxidation genes in the six MAGs, such as *cyc2*, *mtoA* and *mofA* (Corstjens *et al.*, 1997; Castelle *et al.*, 2008; El Gheriany *et al.*, 2009; Liu *et al.*, 2012; He *et al.*, 2017). Specifically, the *cyc2* gene was identified in the MAGs of the *Gallionellaceae* sp., *Rhodoblastus* sp., *Thiobacillus* sp. and *Ramlibacter* sp. At the transcript level, *cyc2* was detected for the *Gallionellaceae* sp. and *Thiobacillus* sp. with significantly higher abundance (i.e. amount of detected transcript) under autotrophic conditions compared to heterotrophic conditions. In addition, the Cyc2 protein from the *Gallionellaceae* sp. was detected under autotrophic conditions (Fig. 3.2 and Fig. 3.3). To uncover the evolutionary relationship of Cyc2 between culture BP and other studied organisms, we performed phylogenetic analysis of Cyc2 amino acids sequences, including those of the *Gallionellaceae* sp., *Rhodoblastus* sp. and *Ramlibacter* sp. (Fig. S3.2).

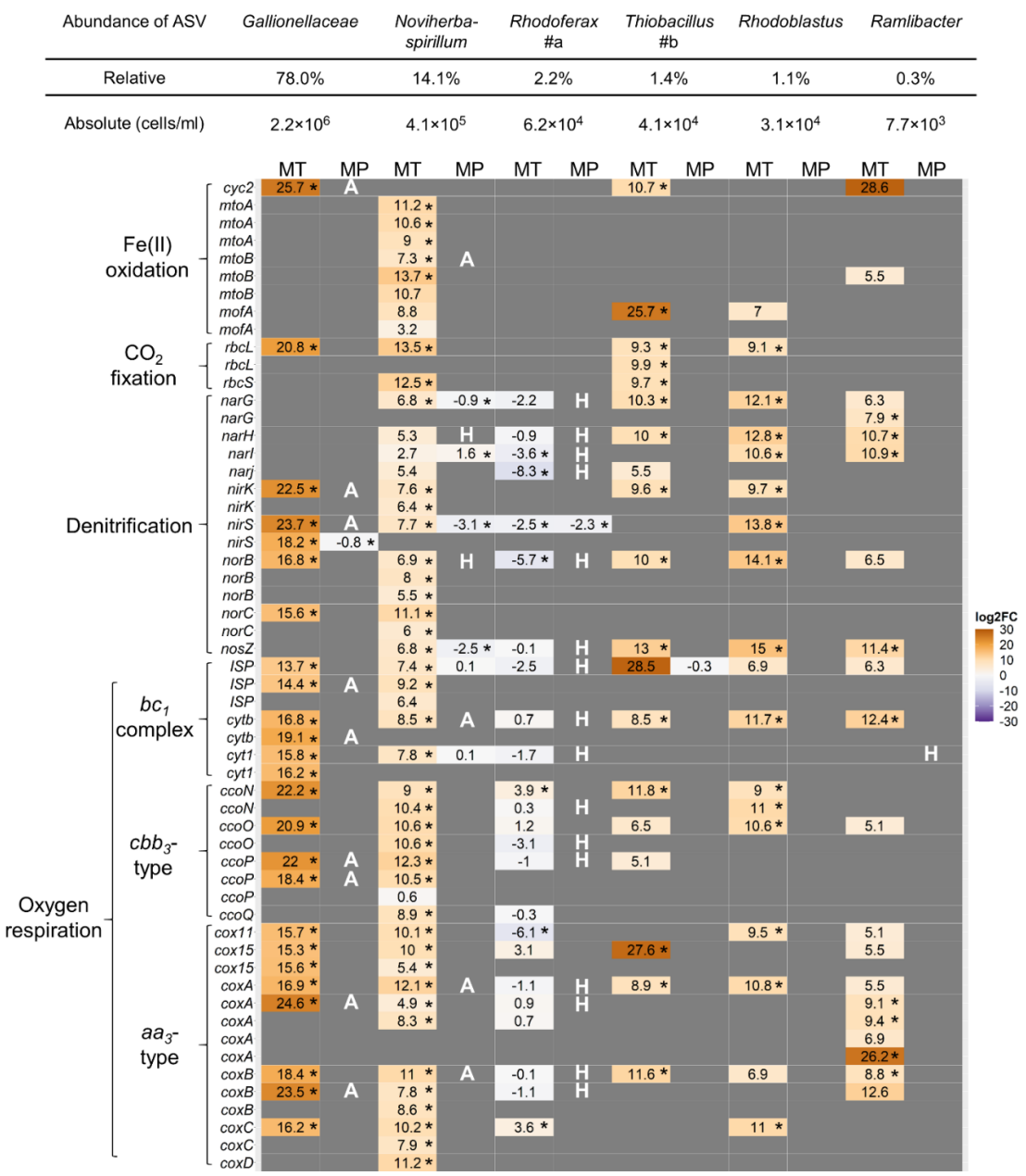

Fig. 3.2. The relative and estimated absolute abundance (calculated using total cell numbers and short-read 16S rRNA gene amplicon sequencing relative abundance data) of related ASVs under autotrophic conditions accompanied by fold changes (log2) of key transcripts and proteins involved in Fe(II) oxidation, CO_2 fixation, acetate oxidation, denitrification and potential oxygen respiration genes under autotrophic conditions compared to heterotrophic conditions. Genes with several copy numbers are listed multiple times. MT: metatranscriptomic analysis; MP: metaproteomic analysis. A star "*" indicates significant changes (adjusted $p \leq 0.05$). A white "A" indicates the protein was only detected under autotrophic conditions. A white "H" indicates the protein was only detected under heterotrophic conditions. A hashtag a "#a" means: two short-read *Rhodoferax* ASVs were combined, which had 100% and 99.6% sequence identity, respectively, to the long-read *Rhodoferax* sp. (only one nucleotide difference). A hashtag b "#b" means: two short-read *Thiobacillus* ASVs were combined, which had three nucleotides difference to each other).

The Cyc2 of the *Gallionellaceae* sp. in culture BP and of *Sideroxydans lithotrophicus* ES-1 were closely related to each other. Overall, there appeared to be distinct clusters within the Cyc2 tree, which consisted of *Gallionellaceae* spp. and *Zetaproteobacteria* spp. (related to *Mariprofundus* spp.), respectively (Fig. S3.2). In addition, *mtoAB* genes were identified for the *Noviherbaspirillum* sp. MAG and the transcripts were at a significantly higher abundance (Fig. 3.2). Phylogenetic analysis of MtoAB from *Noviherbaspirillum* sp. demonstrated that they are closely related to the MtoAB from other proposed microaerophilic FeOB (Fig. S3.3) (Liu *et al.*, 2012). Particularly for MtoB, there appeared to a be a distinct cluster for *Noviherbaspirillum* (Fig. S3.3). Furthermore, *mofA* genes were identified in the *Thiobacillus* sp. MAG and the transcripts were also significantly higher abundant under autotrophic compared to heterotrophic conditions (Fig. 3.2).

Denitrification (*nirK/S*, *norBC*)

To investigate the mechanisms of denitrification in culture BP, we identified genes encoding the nitrate reductase (*narGHI*), nitrite reductase (*nirK* or *nirS*), nitric oxide reductase (*norBC*) and nitrous oxide reductase (*nosZ*) in the MAGs of *Noviherbaspirillum* sp., *Thiobacillus* sp., *Rhodoblastus* sp. and *Ramlibacter* sp. Among these organisms, the transcripts of detected denitrification genes had significantly higher abundance under autotrophic conditions compared to heterotrophic conditions (Fig. 3.2). Although the denitrification pathway was incomplete in the *Gallionellaceae* sp., it appeared to contribute to nitrite reduction and nitric oxide reduction. Both nitrite reductase (*nirK* and *nirS*) and nitric oxide reductase (*norB* and *norC*) transcripts from the *Gallionellaceae* sp. were detected at significantly higher abundance under autotrophic conditions compared to heterotrophic conditions, and the proteins of NirK/S were detected under autotrophic conditions (Fig. 3.2). Since the transcripts and proteins of these *nirK*/*S* genes in the MAGs of the dominant *Gallionellaceae* sp. were detected under autotrophic conditions (Fig. 3.2 and 3.3), this suggests that the reduction of nitrite coupled to biotic Fe(II) oxidation in culture BP might have occurred enzymatically. However, an abiotic contribution to the reduction of nitrite and nitric oxide by Fe(II) cannot be ruled out. Alternatively, it is possible that the *Gallionellaceae* sp. was expressing nitrite reductase genes to detoxify the products derived from nitrate reduction performed by other community members.

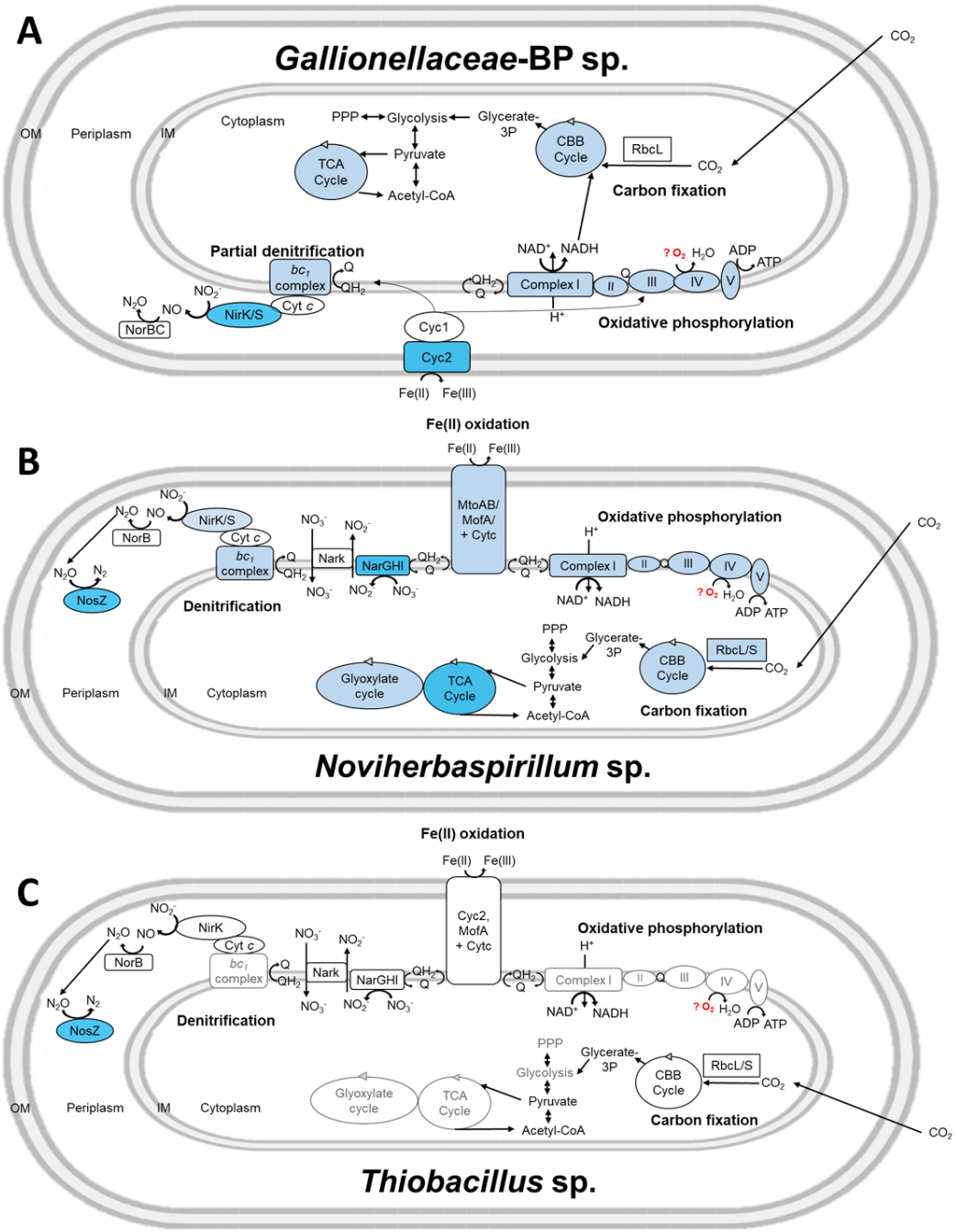

Fig. 3.3. Overview of the meta-omics results for the extracellular electron transfer system, denitrification, carbon metabolism and oxidative phosphorylation in the three proposed key players for Fe(II) oxidation, i.e. the (A) *Gallionellaceae*-BP sp., (B) *Noviherbaspirillum* sp. and (C) *Thiobacillus* sp. under autotrophic conditions. Black font and line: complete pathway of transcripts detected under autotrophic conditions; grey font and line: incomplete pathway of transcripts detected under autotrophic conditions; intense blue color filling: all proteins of the complete pathway detected under autotrophic conditions; lighter blue color filling: incomplete pathway of proteins detected under autotrophic conditions.

Carbon fixation

Carbon fixation is essential for the growth of autotrophic microorganisms; thus, we explored carbon fixation pathways in culture BP under autotrophic conditions. All six MAGs contained genes involved in carbon metabolism pathways, i.e. the reductive pentose phosphate (CBB) cycle, glycolysis, tricarboxylic acid (TCA) cycle and pentose phosphate pathway (PPP) (Table S3.3). More specifically, genes responsible for carbon fixation (*rbcL*/*S*), encoding ribulose-1,5-bisphosphate carboxylase-oxygenase (RuBisCO), were identified in the MAGs of the *Gallionellaceae* sp.*, Noviherbaspirillum* sp.*, Rhodoblastus* sp., *Thiobacillus* sp. and *Ramlibacter* sp. (Fig. 3.2, 3.3 and Fig. S3.4). The transcripts of *rbcL* were detected at a significantly higher level under autotrophic conditions compared to heterotrophic conditions for *Gallionellaceae* sp.*, Noviherbaspirillum* sp.*,* *Thiobacillus* sp. and *Rhodoblastus* sp., as well as *rbcS* for the *Noviherbaspirillum* sp. and *Thiobacillus* sp. (Fig. 3.2). However, none of the RuBisCO related proteins were detected (Fig. 3.2). Phylogenetic analysis of the large chain RuBisCO (RbcL) (Fig. S3.4A) and small chain RuBisCO (RbcS) (Fig. S3.4B) revealed that the RbcL of the *Gallionellaceae* spp. from culture BP and culture KS were closely related to each other as well as to other FeOB (Fig. S3.4A). This indicates that the RbcL of the *Gallionellaceae* sp. in culture BP might have the same function as the RbcL of the *Gallionellaceae* sp. in culture KS (Fig. S3.4A).

Amino acid biosynthesis pathways

Essential amino acids are vital for the survival of individual isolated organisms and, therefore, the biosynthesis of the essential amino acids of the bacterial community members in culture BP was analysed. Except for the *Geothrix* sp., all community members had most, if not all, essential amino acid biosynthesis pathways at least partially encoded. However, the gene encoding histidine isomerase (*hisA*) was detected at medium confidence for the MAG of the *Gallionellaceae* sp. and *Rhodoferax* sp. with the tool of GapMind (Price *et al.*, 2020). The genes encoding ribose-phosphate diphosphokinase (*prs*) for histidine biosynthesis and homoserine kinase (*thrB*) for threonine biosynthesis were missing in the MAG of the *Thiobacillus* sp. Furthermore, the gene encoding glutamine synthetase (*glnA*) for glutamine biosynthesis was missing in the MAG of the

Rhodoblastus sp. In addition, the genes encoding homoserine dehydrogenase (*hom*) and vitamin B12-dependent methionine synthase (*metH*) for methionine biosynthesis were missing in the MAG of the *Ramlibacter* sp. Almost all of the essential amino acid biosynthesis pathways in the MAGs of both *Gallionellaceae* sp. and *Noviherbaspirillum* sp. were expressed (i.e. the transcripts were detected).

Energy generation and electron transport phosphorylation

In order to identify energy generation pathways in culture BP, we explored the different levels of gene expression and proteins for terminal electron acceptors. The genes involved in oxidative phosphorylation complexes I-V, were found in the MAGs of the *Gallionellaceae* sp., *Noviherbaspirillum* sp., *Rhodoferax* sp., *Thiobacillus* sp., *Rhodoblastus* sp. and *Ramlibacter* sp. Under autotrophic conditions, the *Gallionellaceae* sp., *Noviherbaspirillum* sp. and *Rhodoblastus* sp. had significantly higher expression of these respiration genes in comparison to heterotrophic conditions (Fig. 3.2). On the protein level, partial oxidative phosphorylation proteins were detected under autotrophic conditions for the *Gallionellaceae* sp. and *Noviherbaspirillum* sp. (Fig. 3.2 and Fig. 3.3). In addition, *cbb*$_3$-type and *aa*$_3$-type cytochrome *c* oxidase-related transcripts and proteins of complex IV, that typically have high and low affinities to oxygen, were detected under both conditions (Fig. 3.2), even though culture BP was grown under anoxic conditions.

***In-situ* microbial community analysis**

In order to identify the *in-situ* distribution and relative abundance of the enriched populations in culture BP, field studies were conducted in 2017. The microbial community was investigated at the sampling site of the origin of culture BP (and culture KS). To this end, sediment cores of a pond and a ditch were obtained, and DNA- and RNA-based short-read 16S rRNA (gene) sequencing was performed from a total of 50 samples. At the sampling sites, 37 different ASVs were classified as *Gallionellaceae* (20 ASVs were detected at the pond and 23 ASVs at the ditch; Fig. S3.6); of these, eight were identified as *Gallionella* spp., eleven as *Sideroxydans* spp., three as *Candidatus* Nitrotoga spp. and fifteen as unclassified spp. (Fig. S3.5). In the environmental samples, among these ASVs assigned to the family *Gallionellaceae* (accounting for up to 3.13% relative abundance for

the whole family; Fig. S3.6), nine DNA-based and two RNA-based samples, corresponding to three sediment cores, revealed the same ASV (100% sequence identity) as the dominant *Gallionellaceae* sp. ASV in culture BP. It accounted for up to 0.13% relative abundance and was found both, at the pond and at the ditch (Fig. S3.6). Therefore, the *Gallionellaceae* sp. in culture BP (i.e. the investigated sequence) was detectable, relatively widespread and likely active at the sampling sites. The 37 different *Gallionellaceae* ASVs were furthermore quite diverse and affiliated, based on phylogenetic analysis, for instance with *Sideroxydans lithotrophicus* ES-1, *Gallionella capsiferriformans* ES-2 and *Ferrigenium kumadai* (Fig. S3.5). The other members in culture BP, i.e. the *Rhodoferax* sp., *Thiobacillus* sp. and *Rhodoblastus* sp. were also found at the pond and the ditch with up to 0.13% relative abundance for identical ASVs as in culture BP, respectively, and up to 2.0% relative abundance for the whole genus, i.e. *Rhodoblastus* (Fig. S3.6). Neither the *Noviherbaspirillum* sp. and *Ramlibacter* sp. in culture BP nor the *Gallionellaceae* sp. in culture KS were found within these sediment samples. However, our sampling procedure might just have missed them, in terms of methodological detection limit, sampling location or season.

3.4. Discussion

A novel autotrophic nitrate-reducing Fe(II)-oxidizing enrichment culture

Microbial NRFeOx is considered to be an important pathway for nitrate removal in organic-poor, Fe-abundant environments, whereby microorganisms gain electrons from Fe(II) for carbon fixation and for energy generation (by nitrate reduction) which is utilized for growth, ultimately transforming CO_2 into biomass (Weber *et al.*, 2006). The enrichment of two autotrophic NRFeOx cultures (i.e. the culture KS and in this study culture BP) from two close-by organic-rich environments (e.g. total organic carbon (TOC) in sediment: 0.16-0.45% (wt%), and dissolved organic carbon (DOC): 0.6-0.7 mg/L in pond water next to Max Plank Institute Bremen in 2017) suggests that this process might be more widespread than expected and might therefore be occurring in diverse habitats.

The physiology in growing cultures of culture BP was slightly different from the results for culture KS described in previous studies. The ratio of $Fe(II)_{oxidized}$/$nitrate_{reduced}$ was reported in the range of 4.3-4.8 in culture KS (Straub *et al.*, 1996; Tominski, 2016; Tominski *et al.*, 2018a), which was higher than the $Fe(II)_{oxidized}$/$nitrate_{reduced}$ ratio of 3.4 in

this study. Theoretically, the stoichiometry suggests that the $Fe(II)_{oxidized}$/$nitrate_{reduced}$ ratio should be around 5 or even higher than 5, when the electrons required from Fe(II) for carbon fixation are also considered, potentially indicating incomplete denitrification or an additional electron donor (i.e. traces of DOC, in the growth medium, theoretically, 1 mg/L can produce 2.5×10^6 cells/mL) (Huang *et al.*, 2021a). However, cell numbers increased from 1.04×10^6 cells/mL to 4.31×10^6 cells/mL within 4 days, and therefore the electrons must not only have derived from the DOC but also from Fe(II) oxidation.

In this study, we show that culture BP fulfils the following three criteria of autotrophic NRFeOx (Bryce *et al.*, 2018): (i) there is no need for an additional organic carbon substrate for continuous growth, (ii) the culture is able to maintain Fe(II) oxidation over several transfers without organic carbon addition, (iii) there is confirmed growth of cells with only Fe(II), nitrate and CO_2 provided. Additionally, our meta-omics data demonstrated that culture BP not only has the genetic potential but also expresses carbon fixation genes. Especially the *rbcL* gene of the *Gallionellaceae* sp. in culture BP (hereafter *Gallionellaceae*-BP sp.) was closely related to the *rbcL* gene of the *Gallionellaceae* sp. in culture KS (hereafter *Gallionellaceae*-KS sp.), which was proven to fix ^{13}C-labeld inorganic carbon (Tominski *et al.*, 2018b). Culture BP is therefore a novel autotrophic nitrate-reducing, Fe(II)-oxidizing enrichment culture that provides the opportunity to study NRFeOx under more environmentally relevant conditions, i.e. in a more complex microbial network with probably less laboratory evolutionary influence, compared to the long-term established culture KS.

Role of *Gallionellaceae* for Fe(II) oxidation in culture BP and beyond

In this study, the dominant *Gallionellaceae*-BP sp. in culture BP (51-87% relative abundance) was identified as an Fe(II) oxidizer and was shown to be closely related to known FeOB, such as the unclassified *Gallionellaceae*-KS sp. from culture KS, a nitrate-reducing Fe(II)-oxidizing culture enriched from the same freshwater habitat as culture BP (Straub *et al.*, 1996). Comparing meta-omics analysis of culture KS from previous studies (He *et al.*, 2016) with those of culture BP in this study, some interesting differences were observed for the *Gallionellaceae* spp. Although both, the *Gallionellaceae*-KS sp. and *Gallionellaceae*-BP sp., likely perform Fe(II) oxidation, partial denitrification and carbon fixation, the genes encoding these functions differed. For example, the proposed Fe(II)

oxidation genes, *cyc2*, *mtoAB* and *mofAB*, were identified in the *Gallionellaceae*-KS sp. (He *et al.*, 2016; Huang *et al.*, 2021a). In addition, the transcripts of *cyc2*, *mtoAB* and *mofAB* were all detected, and the MofA protein of the *Gallionellaceae*-KS sp. was shown to be present (Huang *et al.*, 2021a). For the *Gallionellaceae*-BP sp. *cyc2* was detected at DNA, RNA and protein levels in this study. In a previous study (Castelle *et al.*, 2008), the outer membrane-bound cytochrome c Cyc2 of acidophilic Fe(II) oxidizing bacteria, *Acidithiobacillus ferrooxidans*, was purified and shown to be responsible to perform Fe(II) oxidation. Therefore, combined with the fact that the *Gallionellaceae*-BP sp. dominates culture BP, these results indicate that the Cyc2 of the *Gallionellaceae*-BP sp. likely plays the main role for Fe(II) oxidation in culture BP under autotrophic conditions. As for denitrification, the *Gallionellaceae*-BP sp. harboured the genes encoding nitrite reductase (*nirK/S*) and nitric oxide reductase (*norBC*), whereas, the *Gallionellaceae*-KS sp. harboured the genes encoding nitrate reductase (*narGHI*) and nitrite reductase (*nirK/S*). In contrast to the *Gallionellaceae*-KS sp., the *Gallionellaceae*-BP sp. possesses an NO reductase and can reduce NO to N_2O. However, both *Gallionellaceae* spp. in culture BP and culture KS require other flanking community members to complete denitrification (i.e. they are missing the *nosZ* gene). To investigate whether nitrite or NO can serve as electron acceptors and generate energy in the *Gallionellaceae*-BP sp., further experiments are required. Moreover, we detected *coxABC* encoding for aa_3-type cytochrome *c* oxidases and belonging to the *Gallionellaceae*-BP sp. and additional community members in culture BP, both at the transcript level and some at the protein level. Interestingly, normally *coxABC* are observed under oxic conditions [Krab and Slater, 1979]. In contrast, in our cultivation system under autotrophic and heterotrophic conditions, we used N_2/CO_2 in the headspace and amended with $FeCl_2$ prior to inoculation, which would have consumed any atmosphere O_2 contamination during the preparation procedure. However, one possible scenario might be that the *coxABC* genes in the organisms in culture BP do not require oxygen to be expressed. Alternatively, there might be a so far undetected internal oxygen production pathway in at least one of the organisms in culture BP, similar to the proposed aerobic methane oxidation under anoxic conditions (Ettwig *et al.*, 2010). The latter hypothesis was already discussed for culture KS by He *et al.* (2016). Nevertheless, these possible scenarios remain highly speculative at this point and require further investigation.

Based on 16S rRNA gene sequences, the *Gallionellaceae*-BP sp. was closely related to *Ferrigenium kumadai*, and *Sideroxydans lithotrophicus* strain ES-1. While *Ferrigenium kumadai* was isolated from rice paddy soils (Khalifa *et al.*, 2018; Nakagawa *et al.*, 2020), *Sideroxydans lithotrophicus* strain ES-1 was isolated from a groundwater-fed iron seep (Emerson and Moyer, 1997). It is apparent, when combining our results with other studies, that *Gallionellaceae* spp. play important roles as FeOB within freshwater ecosystems. Furthermore, our *in-situ* survey indicated a high diversity of *Gallionellaceae* spp. at the field site, suggesting that, in addition to the microbial populations in culture KS and culture BP, there might be a higher diversity of organisms contributing to NRFeOx in freshwater environments and other habitats than currently known from cultivation approaches.

Contribution of *Noviherbaspirillum* sp. and *Thiobacillus* sp. to NRFeOx in culture BP

The second most abundant organism in culture BP under autotrophic conditions was the *Noviherbaspirillum* sp. (9-15%). Based on 16S rRNA gene sequences, the top three closest related isolates were *Noviherbaspirillum autotrophicum* strain TSA66 (Ishii *et al.*, 2017), *Noviherbaspirillum agri* K-1-15 (Chaudhary and Kim, 2017), and *Noviherbaspirillum denitrificans* TSA40 (Ishii *et al.*, 2017) (Table S3.1). Among these isolates, only *Noviherbaspirillum autotrophicum* strain TSA66 was reported to be able to grow autotrophically by using H_2 as an energy source to perform denitrification (Ishii *et al.*, 2017). However, a gene search on the Joint Genome Institute's Integrated Microbial Genome (JGI/IMG) database showed that the genome of *Noviherbaspirillum autotrophicum* strain TSA66 has genes encoding RuBisCO but does not have Fe(II) oxidation gene homologues, neither *mtoA* nor *cyc2*, which were detected in the *Noviherbaspirillum* sp. from culture BP. Therefore, the *Noviherbaspirillum* sp. from culture BP might have unique capabilities for NRFeOx within this genus.

Another potential FeOB in culture BP was the *Thiobacillus* sp., which accounted for only up to 1.6% relative abundance in culture BP and possessed the potential Fe(II) oxidation gene homologues *cyc2* and *mofA*. The top three closest related isolates based on 16S rRNA gene sequences with an available genome sequence were *Thiobacillus thioparus* strain THI 111, *Thiobacillus thioparus* DSM 505, and *Thiobacillus thioparus* strain Starkey (Boden *et al.*, 2012) (Table S3.1). Additionally, *Thiobacillus denitrificans* ATCC 25259 was

previously proposed as an autotrophic nitrate-reducing Fe(II)-oxidizing organism (Straub *et al.*, 1996; Beller *et al.*, 2006b). Interestingly, only *Thiobacillus thioparus* DSM 505 has the Fe(II) oxidation gene *cyc2*, and neither *Thiobacillus denitrificans* ATCC 25259 and *Thiobacillus denitrificans* RG nor *Thiobacillus thiophilus* DSM 19892 revealed potential Fe(II) oxidation genes. The copper resistance genes, *copAB*, i.e. the homologues of the putative Fe(II)-oxidizing genes, *pcoAB* (He *et al.*, 2017), were detected in *Thiobacillus denitrificans* ATCC 25259, *Thiobacillus denitrificans* RG, *Thiobacillus denitrificans* DSM 12475 and *Thiobacillus thiophilus* DSM 19892 (Beller *et al.*, 2006b; Beller *et al.*, 2013). We therefore suggest that the *Thiobacillus* sp. in culture BP was also actively contributing to NRFeOx.

Interestingly, in culture KS, there seems to be no community member with a similar role to that of the *Noviherbaspirillum* sp. and *Thiobacillus* sp. in culture BP. For example, the second most abundant organism in culture KS under autotrophic conditions, a *Rhodanobacter* sp., was the main organism cooperating with *Gallionellaceae*-KS, which is likely able to perform NRFeOx under autotrophic conditions (Huang *et al.*, 2021a). The *Rhodanobacter* sp. likely performs Fe(II) oxidation and complete denitrification but does not have the ability to conduct carbon fixation (He *et al.*, 2016; Huang *et al.*, 2021a). Therefore, the isolation and the study of *Noviherbaspirillum* sp. and *Thiobacillus* sp. in culture BP, which likely contribute to Fe(II) oxidation and CO_2 fixation, would be beneficial in order to broaden our knowledge of autotrophic nitrate-reducing Fe(II)-oxidizing bacteria.

Expanding the microbial network for NRFeOx in culture BP

Besides the *Gallionellaceae*-BP sp., *Noviherbaspirillum* sp. and *Thiobacillus* sp., other flanking members potentially also play a relevant role in culture BP: *Rhodoblastus* sp. (up to 5% relative abundance), *Rhodoferax* sp. (up to 3%), and *Ramlibacter* sp. (up to 1%). We identified Fe(II) oxidation gene homologues in the MAGs of the *Rhodoblastus* sp. (*cyc2* and *mofA*) and the *Ramlibacter* sp. (*cyc2* and *mtoB*), indicating that they can potentially play a role in Fe(II) oxidation, despite the fact that *cyc2* transcripts were not detected for the *Rhodoblastus* sp., and neither *cyc2* nor *mtoB* transcripts for the *Ramlibacter* sp. were detected at significant levels. Furthermore, we observed that the genes necessary to perform full denitrification were present in these three flanking members, i.e. the *Rhodoblastus* sp., *Rhodoferax* sp. and *Ramlibacter* sp., and some of

them were detected at significantly higher transcript levels. Regarding carbon fixation, there was a complete CBB reductive pentose phosphate cycle detected in both, the *Rhodoblastus* sp. and *Ramlibacter* sp., while only a partial cycle was found for the *Rhodoferax* sp. (Table S3.3). As a result, although the relative abundance of these three flanking community members accounted for less than 5% (respectively) throughout the autotrophic growth conditions, our findings suggest that they play partial roles in NRFeOx and carbon fixation (Fig. 3.4).

To summarize, there were five potential Fe(II)-oxidizing microbial key players in culture BP: the *Gallionellaceae*-BP sp., *Noviherbaspirillum* sp., *Thiobacillus* sp., *Rhodoblastus* sp. and *Ramlibacter* sp. (Fig. 3.4). Among these, the *Gallionellaceae*-BP sp., *Noviherbaspirillum* sp. and *Thiobacillus* sp., may not only perform Fe(II) oxidation but also carbon fixation (Fig. 3 and Fig. 3.4). The resulting fixed organic carbon was likely provided to other heterotrophic community members and used for their growth (Fig. 3.4). During denitrification, the nitrate may be reduced by flanking community members, while the *Gallionellaceae*-BP sp. may contribute to partial denitrification, i.e. nitrite and nitric oxide reduction, and the remaining flanking community members complete the denitrification (Fig. 3.4). Therefore, in order to survive and indeed thrive, the dominant *Gallionellaceae*-BP sp. has to cooperate with other community members under autotrophic conditions (Fig. 3.4). In turn, the heterotrophic community members may have to rely for their survival on Fe detoxification and carbon fixation likely performed by the *Gallionellaceae*-BP sp., *Noviherbaspirillum* sp. and *Thiobacillus* sp. (Fig. 3.4). In addition, our findings highlighted potential interdependencies between the microbial community members regarding amino acid biosynthesis that might be crucial for their survival as well.

Comparing the microbial network of culture BP with that of culture KS, the most active species in culture KS were the *Gallionellaceae*-KS sp. and the *Rhodanobacter* sp. under autotrophic conditions (He *et al.*, 2016; Huang *et al.*, 2021a). However, in culture BP, there were several active populations involved in NRFeOx under autotrophic conditions, i.e. the *Gallionellaceae*-BP sp., *Noviherbaspirillum* sp., *Thiobacillus* sp., *Rhodoblastus* sp., *Rhodoferax* sp. and *Ramlibacter* sp. (Fig. 3.2 and Fig. 3.3). Therefore, in contrast to culture BP, culture KS is likely characterized by a reduced microbial network, which may be due to long-term cultivation and selection of specialized organisms. The occurrence of the lower relative abundance, yet active, organisms (i.e. the *Rhodoblastus* sp.,

Rhodoferax and *Ramlibacter* sp.) in culture BP expands the microbial network contributing to NRFeOx processes which might be more similar to the complex microbial interactions in the environment.

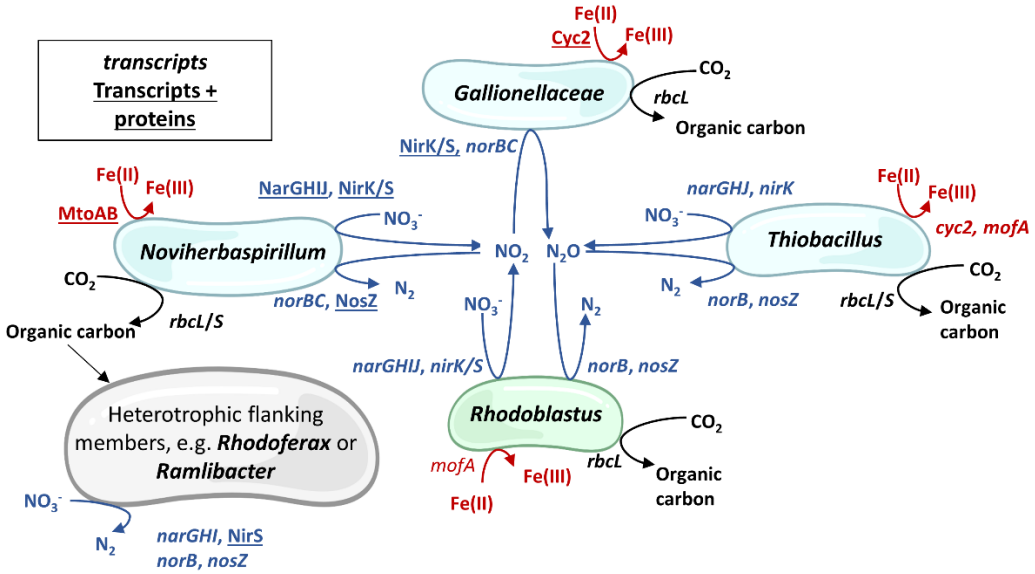

Fig. 3.4. Overview of the proposed microbial interactions in culture BP, mainly essential for the organisms' survival under autotrophic conditions. The depicted putative reactions are based on the meta-omics data for Fe(II) oxidation (red arrows and font), denitrification (blue arrows and font), and CO_2 fixation (black arrows and font), for the *Gallionellaceae*-BP sp., *Noviherbaspirillum* sp., *Thiobacillus* sp., *Rhodoblastus* sp. and *Rhodoferax* sp. The cells in blue indicate Fe(II)-oxidizing bacteria with carbon fixation ability, in grey indicate heterotrophs and in green indicate that the organism can conduct carbon fixation and potentially Fe(II) oxidation. The detected transcripts are in italic font, and a combination of both detected transcripts and proteins are with underlined font. The transcripts with significantly higher expression under autotrophic conditions compared to heterotrophic conditions are in bold font.

NRFeOx core features of complex microbial networks including *Gallionellaceae* spp.

There seems to be several core features that might be similar for autotrophic NRFeOx processes carried out by complex microbial networks including *Gallionellaceae* spp. (Fig. 3.4): (i) NRFeOx requires Fe(II) oxidation features, with several possible electron transfer pathways (i.e. different putative Fe(II)-oxidizing proteins might be used). (ii) During denitrification, the *Gallionellaceae* spp. may contribute to partial denitrification (e.g. reducing nitrate to nitric oxide or nitrite to nitrous oxide), while the flanking microbial community members complete the denitrification. (iii) Fixed organic carbon from the autotrophic lifestyle of *Gallionellaceae* spp. is provided to other heterotrophic community members and used for their growth. Therefore, the key FeOB (i.e. the *Gallionellaceae* sp.)

has to cooperate with other community members under autotrophic conditions, however, (iv) the identity of these flanking community members seems interchangeable. We suggest that these core features are relevant for NRFeOx processes in the environment as well, that nitrate-reducing FeOB is widespread including organic-rich habitats, that several microbial key players of NRFeOx *in situ* thrive in complex microbial networks and are yet-to-be discovered.

3.5. Experimental procedures

Cultivation, analytical methods and cell counts

Culture BP originated from sediments of a freshwater pond (latitude 53°06'36.7"N and longitude 8°50'48.6"E) at the Max Planck Institute for Marine Microbiology, located in Bremen, Germany, sampled in 2015. Sediments from ca. 10 cm depth were taken and stored in Schott bottles (filled up completely with half sediment and half pond water) at 4°C. The sediment was transferred into 25 mL mineral medium (Hegler *et al.*, 2008; Blöthe and Roden, 2009) growing with anoxic headspace (N_2/CO_2 ratio was 90/10), unfiltered bicarbonate-buffered medium, containing 10 mM $FeCl_2$, 4 mM $NaNO_3$, vitamins and trace elements with a final pH of 6.9 to 7.2 in 58 mL serum bottles. The culture BP was incubated at temperature 28°C in the dark starting in February 2016 and was first transferred in March 2016 with 10% (v/v) inoculum with the same medium and additives under autotrophic conditions. Since 2018, it was transferred for more than 20 times per year until 2020. Under heterotrophic conditions, 5 mM acetate was used instead of 10 mM $FeCl_2$ as the electron donor. Analytical methods of Fe(II), Fe(total), nitrate, nitrite and acetate concentrations were described in Tominski *et al.* (2018a).

For the cell counts under autotrophic growth conditions, using the protocols obtained from personal communication with Stefanie Becker, 200 µL of cell samples from the enrichment culture BP were taken and cells were fixed with 10 µL of 20% (w/v) paraformaldehyde (PFA) (Sigma-Aldrich). In addition, the sample was treated with 590 µL oxalate solution (oxic; 2.8 g ammonium oxalate, 1.5 g oxalic acid, total volume 100 mL, pH 3, filtered sterile, Sigma-Aldrich) and 200 µL ferrous ethylenediammonium sulfate (Fe-EDAS, 100 mM, anoxic, filtered into an anoxic autoclaved serum bottle, Sigma-Aldrich) to dissolve the Fe minerals prior to the cell counts (personal communication with Stefanie Becker). For the heterotrophic conditions, 1 mL of sample of the enrichment culture BP was taken

and the cells were fixed with 50 µL of 20% PFA. The cell samples of heterotrophic conditions were diluted to the range of 100-1,300 cells/µL prior to the measurement. For flow cytometry, cells were stained with BacLight Green stain (Thermo Fisher Scientific, 1 mM stain/1mL sample). Cell numbers were determined with an Attune NxT Flow Cytometer (Thermo Fisher Scientific) with the setting adapted from Schmidt *et al.* (2020). The results were reported as average from the measurements conducted in triplicates. Estimated absolute cell numbers were calculated by multiplying flow cytometer-based total cell numbers with short-read 16S rRNA gene amplicon sequencing relative abundance data (described below).

Experimental setup and biomass sampling of culture BP

The metagenome sample was obtained in 2019, at the 2nd day of incubation under autotrophic conditions with 10 mM of Fe(II) and 4 mM of nitrate in a 22 mM bicarbonate-buffered medium. For the metatranscriptomics and metaproteomics analysis, conducted in 2020, both autotrophic and heterotrophic conditions were used with biological triplicates, respectively. Under autotrophic conditions, within 4 days on average 80% of Fe(II) was oxidized and 50% of nitrate was reduced. Therefore, samples under autotrophic conditions were taken at the 2nd day (remaining Fe(II) and NO_3^- was 7.1 mM and 3.7 mM, respectively; 2.91 × 10^6 cells/mL, Fig. 3.1A, 3.1C). Under heterotrophic conditions, in a first step a pre-culture was grown for two transfers with 10% and 1% (vol/vol) inoculum for 24 hours each, allowing more than seven generations under pre-culture conditions, considering an average doubling time of 3 hours, to avoid carryover of signals from gene and protein expression under autotrophic conditions. In a second step, the 3rd transfer under heterotrophic conditions with 1% (vol/vol) inoculum was used for the experimental setup: within 37 hours, 66% of acetate was oxidized and 96% of nitrate was reduced. Therefore, samples of the cultures grown under heterotrophic conditions were taken after approximately 18 hours (remaining acetate, NO_3^- and NO_2^- was 3.94 mM, 2.69 mM and 0.82 mM, respectively; 2.78 × 10^6 cells/mL, 3.1B, 3.1D). At the sampling time points, biomass of culture BP with total cell numbers ranging from 10^8 (for DNA/RNA extraction) to 10^9 cells (for protein extraction) was collected under sterile conditions on cellulose filters (EMD Millipore S-Pak mixed cellulose ester sterile filter membrane, 0.22 µm pore size, 47mm filter diameter; Millipore) using vacuum filtration. The filters were cut into pieces

under sterile conditions and either stored in 15 mL falcon tubes at -80°C before proceeding with DNA and RNA extractions or stored in 50 mL falcon tubes at -80°C before proceeding with the protein extractions.

DNA/RNA co-extraction for metagenomics and metatranscriptomics

DNA/RNA co-extraction was done according to the protocol of Lueders *et al.* (2004) with the following modifications: two tubes of "MP Bio Lysis Matrix E" beads were added into a 15 mL falcon tube, including the filter pieces with the collected biomass. To disrupt the cells, 3.75 mL PB buffer (with 112.87 mM Na_2HPO_4 and 7.12 mM NaH_2PO_4) and 1.25 mL TNS buffer (with 500 mM Tris-HCL, 100 mM NaCl and 10% w/v SDS) were added, followed by bead beating for 4 minutes on the vortex adapter (maximum power) at room temperature (RT). The following centrifugation steps were all at maximum speed (7,197 ×g; Eppendorf Centrifuge 5430 with Rotor F35-6-30) at 4°C. All transfer steps were done on ice. The samples were centrifuged twice for 15 minutes and transferred to a new 15 mL falcon tube in between centrifugation steps, to obtain a clear supernatant. Then, the supernatant was split into new sterile 2 mL tubes (1 mL per tube) to proceed with phenol-chloroform-isoamyl alcohol and chloroform-isoamyl alcohol extractions according to Lueders *et al.* (2004). Subsequently, all aqueous phases were pooled again into a new 15 mL tube for polyethylene glycol (with 30% w/v polyethylene glycol 6000 and 1.6 M NaCl) precipitation overnight. From the ethanol-washing step on, the extraction was done under a clean bench. The ethanol was removed carefully with a pipette with filter tips and the pellet was dried at RT for ca. 10 minutes. The DNA/RNA pellet was dissolved in 20-50 µl DEPC-treated water with Invitrogen™ Ambion™ RNase inhibitor (40 Unit/µl, 1 µl RNase inhibitor/ 40 µl), at RT for 30 min. All samples were stored at -80°C before sequencing.

Protein extraction for metaproteomics

Protein extraction was performed according to the "Protein extraction method B" from Spät *et al.* (2015) with the following modifications: 5 mL and 2 mL lysis buffer were added to the samples from autotrophic and heterotrophic conditions, respectively, to dissolve cell pellets. The samples were incubated for 10 minutes at 95°C in a water bath, vortexed briefly and chilled on ice with 2 minute-intervals in total 5 times and, subsequently,

sonicated on ice for 30 seconds with an ultrasonic homogenizer (Bandelin Sonopuls) at output control 4 and 40% duty cycle. The lysate was centrifuged at 7,197 ×g for 1 minute at RT and the supernatant was then transferred into several 1.5 mL Eppendorf tubes and centrifuged at 20,817 ×g (Eppendorf Centrifuge 5430 with Rotor 30x1,5/2,0 mL) for 10 minutes at RT. Samples were pooled again into sterile 50 mL solvent-resistant tubes. After the 8:1 acetone:methanol precipitation and incubation step, the precipitate was washed with 5 mL ice-cold 80% (v/v) acetone in water and centrifuged at 7,197 ×g for 5 minutes at 4°C. The protein pellets were air-dried at RT and later dissolved in urea buffer and stored at -20°C.

Sampling, DNA/RNA co-extraction and cDNA synthesis for *in situ* analysis

In order to investigate the relative abundance of microorganisms in environmental samples, six cores were obtained in 2017. The three cores were from a pond and other three cores from a ditch near the Max Planck Institute for Marine Microbiology in Bremen. The sediment cores were separated into six different depths: 0-0.5 cm, 0.5-1 cm, 1-2 cm, 2-4 cm, 4-7 cm, and 7-10 cm. DNA and RNA were co-extracted using the method published by Griffiths *et al.* (2000) with the following modifications. At the first step, we used 1 g of sediment wet sample in the tubes of “MP Bio Lysis Matrix E” beads, followed by bead beating for 10 minutes on the vortex adapter (maximum power) at RT. At precipitation step, we used 2 volumes of 10% (w/v) polyethylene glycol 8000 with 1.2 M NaCl. To synthesize cDNA from the extracted RNA samples, DNA digestion was proceeded by following a rigorous DNase treatment of the TURBO DNA-free™ kit (Invitrogen, Thermo Fisher Scientific) and reverse transcription was conducted following the user manual of SuperScript™ III Reverse Transcriptase (Invitrogen, Thermo Fisher Scientific). All centrifugation steps were performed with 16,100 ×g in an Eppendorf Centrifuge 5430 with Rotor FA-45-30.

Short-read 16S rRNA (gene) amplicon sequencing

PCR on DNA and cDNA with universal primers 515f: GTGYCAGCMGCCGCGGTAA (Parada *et al.*, 2016) and 806r: GGACTACNVGGGTWTCTAAT (Apprill *et al.*, 2015) fused to Illumina adapters was performed with cycling conditions as follows: 95°C for 3 min, 24 or 30 cycles of 95°C for 30 s, 55°C for 30 s, and 75°C for 30 s, and it was followed by a

final elongation step at 72°C for 3 min. The quality of the purified amplicons was determined using agarose gel electrophoresis. Subsequent library preparation steps and sequencing steps of the 16S rRNA (gene) amplicons were performed on an Illumina MiSeq sequencing system (Illumina, San Diego, CA, USA) using the 2 × 250 bp MiSeq Reagent Kit v2 by Microsynth AG (Balgach, Switzerland). From 9,852 to 224,723 (average 95,455) read pairs were generated per sample in two separate sequencing runs on the same MiSeq machine, resulting in total in 6.7 million read pairs. Quality control, reconstruction of 16S rRNA (gene) sequences and taxonomic annotation was performed with nf-core/ampliseq v1.1.0 (Ewels *et al.*, 2020; Straub *et al.*, 2020) with Nextflow v20.10.0 (Di Tommaso *et al.*, 2017) using containerized software with singularity v3.4.2 (Kurtzer *et al.*, 2017). Data from the two sequencing runs were treated initially separately by the pipeline using the option “mulipleSequencingRuns” and ASV tables were merged. Primers were trimmed, and untrimmed sequences were discarded (one sample 71%, others < 30%, on average 8.6%) with Cutadapt v1.16 (Martin, 2011). Adapter and primer-free sequences were imported into QIIME2 version 2018.06 (Bolyen *et al.*, 2019), their quality was checked with demux (https://github.com/qiime2/q2-demux), and they were processed with DADA2 version 1.6.0 (Callahan *et al.*, 2016) to eliminate PhiX contamination, trim reads (position 230 in forward reads and 170 in reverse reads), correct errors, merge read pairs, and remove PCR chimeras; ultimately, 30,936 amplicon sequencing variants (ASVs) were obtained across all samples. Alpha rarefaction curves were produced with the QIIME2 diversity alpha-rarefaction plugin, which indicated that the richness of the samples had been fully observed. A Naive Bayes classifier was fitted with 16S rRNA (gene) sequences extracted with the PCR primer sequences from the QIIME compatible, 99%-identity clustered SILVA v132 database (Pruesse *et al.*, 2007). ASVs were classified by taxon using the fitted classifier (Bokulich *et al.*, 2018). 273 ASVs that classified as chloroplasts or mitochondria were removed, totalling to < 21% (average 1.2%) relative abundance per sample, and the remaining ASVs had their abundances extracted by feature-table (https://github.com/qiime2/q2-feature-table).

Long-read 16S rRNA gene amplicon sequencing

DNA for long-read 16S rRNA gene amplicon sequencing was extracted using the DNEasy UltraClean Microbial Kit (QIAGEN, Hilden, Germany), according to the user's manual.

DNA from culture BP was amplified in two rounds and sequenced at the Helmholtz Zentrum München, Germany. At the first round, the KAPA HiFi Hot Start ReadyMix PCR Kit (KAPA BioSystems, Cape Town, South Africa) was used with primers universal for bacterial 16S rRNA gene, tailed with PacBio universal sequencing adapters (universal tags) and 5' amino modifiers (27F gcagtcgaacatgtagctgactcaggtcacAGRGTTYGATYMTGGCTCAG,1492R tggatcacttgtgcaagcatcacatcgtagRGYTACCTTGTTACGACTT) (Biomers.net, Ulm, Germany) to amplify the long-read 16S rRNA gene from the genomic DNA extracted for culture BP. The first PCR amplification program was performed with 26 cycles: initial denaturation at 95°C for 3 minutes, denaturation at 95°C for 30 seconds, annealing at 57°C for 30 seconds and extension at 72°C for 60 seconds. Amplicons were purified with the QIAquick PCR purification kit (QIAGEN, Hilden, Germany) according to the user's manual. The second PCR was performed using the PacBio Barcoded Universal F/R Primers Plate – 96 (Pacific Biosciences, California, USA) with KAPA HiFi ReadyMix PCR Kit, followed by AMPure PB bead kit (Pacific biosciences, California, USA) purification according to the user manual. The second PCR amplification program was performed with 20 cycles: denaturation at 95°C for 30 seconds, annealing at 57°C for 30 seconds and extension at 72°C for 60 seconds. The quality and quantity of PCR products were checked using an Agilent 2100 Bioanalyzer System (Agilent, California, USA) after both PCR rounds. SMRTbell Template Prep Kit (PacBio biosciences, California, USA) with user manual instructions was used for SMRTbell library preparation (Franzén *et al.*, 2015). Subsequently, 20,635 circular consensus sequencing reads were analyzed with DADA2 v1.10.0 (Callahan *et al.*, 2016; Callahan *et al.*, 2019) in R v 3.5.1 (Team, 2018) by sequentially orienting reads and removing primers, filtering (no ambiguous nucleotides and maximum 2 expected errors) and trimming (1000 bp to 1600 bp read length; leading to 11,978 sequences), dereplicating sequences (7,161 unique sequences), learning error rates, removing bimera de novo and finally assigning taxonomy to the detected sequences based on SILVA v132 (Callahan, 2018). Lastly, 25 ASVs with 7,831 total counts were obtained.

Metagenome analysis and draft genome recovery

Approximately 1 µg of DNA was used for library preparation with the TruSeq DNA PCR-Free Kit from Illumina without modifications and libraries were sequenced on the Illumina NovaSeq 6000 platform to generate 91,056,140 paired-end (2 × 150-bp) reads (27.48 giga base pairs) by CeGaT, Tuebingen, Germany. Raw read quality control, assembly, metagenome assembled genome binning and taxonomic annotation was performed with nf-core/mag v1.0.0 (https://nf-co.re/mag, DOI: 10.5281/zenodo.3589528) (Ewels *et al.*, 2020) with Nextflow v20.04.1 (Di Tommaso *et al.*, 2017) using containerized software with singularity v3.0.3 (Kurtzer *et al.*, 2017). Read quality was assessed with FastQC v0.11.8 (Andrews, 2010), quality filtering and Illumina adapter removal was performed with fastp v0.20.0 (Chen *et al.*, 2018), and reads mapped with Bowtie2 v2.3.5 (Langmead and Salzberg, 2012) to the PhiX genome (Enterobacteria phage WA11, GCA_002596845.1, ASM259684v1) were removed. Finally, 90,303,622 processed read pairs (27.25 giga base pairs) were assembled with MEGAHIT v1.2.7 (Li *et al.*, 2015) and the assembly was evaluated with QUAST v5.0.2 (Gurevich *et al.*, 2013), 99.35% reads were represented in the assembly. Metagenome assembled genomes (MAGs) were binned with MetaBAT2 v2.13 (Kang *et al.*, 2019) aided by the sequencing depth, checked for their completeness and contamination with BUSCO v3.0.2 (Waterhouse *et al.*, 2018) using 148 near-universal single-copy orthologues (http://busco.ezlab.org/v3/datasets/bacteria_odb9.tar.gz) selected from OrthoDB v9 (Zdobnov *et al.*, 2017), and summary statistics were obtained with QUAST for each MAG.

Characteristics of the assembled metagenome can be found in Table S3.2. Twelve MAGs were obtained from the metagenome, of which eleven had ≤2% estimated contamination, of these, seven had ≥88% estimated completeness and four had from 11% to 45% completeness. Selected MAGs are presented in Table S3.1. The assembled metagenome and MAGs were uploaded to the Joint Genome Institute's Integrated Microbial Genome and Microbiome Expert Review (IMG/MER) pipeline (IMGAP v5.0.8) for annotation (available online at https://img.jgi.doe.gov/cgi-bin/mer/main.cgi; (Chen *et al.*, 2019)).

FeGenie (Garber *et al.*, 2020) and the IMG database (Chen *et al.*, 2019) were used to search for potential Fe(II) oxidation genes, i.e. *cyc2, mtoAB, pcoAB, mofA* (He *et al.*, 2017), for the closely related species of the community in culture BP.

Metatranscriptome analysis.

For RNA analysis, DNAse treatment, library preparation including bacterial ribodepletion (with Illumina Stranded Total RNA Prep with Ribo-Zero Plus kit) and sequencing with 2 × 75 bp and 6 to 53 Mio clusters per sample were performed by Microsynth AG (Balgach, Switzerland) using triplicate samples of culture BP grown under autotrophic and heterotrophic conditions, respectively. Nf-core/rnaseq v1.4.2 (https://nf-co.re/rnaseq, DOI: 10.5281/zenodo.3503887) (Ewels *et al.*, 2020) and its containerized software was used with singularity v3.0.3 (Kurtzer *et al.*, 2017) and executed with Nextflow v20.04.1 (Di Tommaso *et al.*, 2017). The pipeline performed quality checks with FastQC v0.11.8 (Andrews, 2010), removed 0.1% to 3.7% base pairs per sample due to adapter contamination and trimming of low quality regions with Trim Galore! v0.6.4, removed 35% to 76% (average: 54%) rRNA sequences with SortMeRNA v2.1b (Kopylova *et al.*, 2012), aligned with STAR v2.6.1d 88-91% and 9-92% (9%, 90%, 92%) reads for autotrophic and heterotrophic conditions, respectively, to the metagenome and finally summarized 2.7-16.8 and 0.3-27.1 million counts per sample for autotrophic and heterotrophic conditions, respectively, to genes based on the IMGAP annotation by featureCounts v1.6.4 (Liao *et al.*, 2014). The definition of a significant difference was postulated for transcripts with Benjamini and Hochberg adjusted $p \leq 0.05$. A summary of features of the metatranscriptome is described in Table S3.2.

Metaproteome analysis

The metaproteome measurement with LC-MS/MS and MaxQuant software suite 1.6.7.0 (Cox and Mann, 2008) was conducted by the Quantitative Proteomics & Proteome Center, Tuebingen (PCT) as described in Schmitt *et al.* (2019). Protein concentrations were determined via the Bradford assay (Bio-Rad) according to the user's manual. As for autotrophic samples, the entire protein extract was used for digestion. SDS PAGE short gel purification (Invitrogen) was run and in-gel digestion with Trypsin was conducted as described previously (Borchert *et al.*, 2010). Extracted peptides were desalted using C18 StageTips (Rappsilber *et al.*, 2007). The entire sample for autotrophic samples and calculated 4 µg of peptides for heterotrophic samples were subjected to LC-MS/MS analysis. Peptides were separated on a 20 cm analytical column packed in house with ReprosSil-Pur C18-AQ 1.9 µm resin (Dr. Maisch GmbH (Ltd.), Ammerbuch, Germany)

using Easy-nLC 1200 UHPLC (Thermo Fisher Scientific). It was coupled to an QExactive HF-X Orbitrap mass spectrometer (Thermo Fisher Scientific) with nano-electrospray source. The peptides were injected in HPLC solvent A (0.1% formic acid) and subsequently eluted with a 127 min segmented gradient of 10-33-50-90% of HPLC solvent B (80% acetonitrile in 0.1% formic acid) at a flow rate of 200 nl/min. The 12 most intense precursor ions were selected for fragmentation with HCD, sequenced mass precursors were excluded from further fragmentation for 30 s. Target values were 3,000,000 charges for the MS scan with a resolution of 60,000 and 100,000 charges for the MS/MS fragmentation scan with a resolution of 30,000. The MS data was processed with MaxQuant software suite v.1.6.7.0. (Cox and Mann, 2008). The iBAQ and LFQ algorithms were enabled, and samples of the same treatment were matched. Database search against provided database (IMG metagenome ID: 3300036710) was performed using the Andromeda search engine (Cox *et al.*, 2011). 23,626 identified peptides by MaxQuant were loaded with R package proteus v0.2.13 (https://github.com/bartongroup/Proteus) (Gierlinski *et al.*, 2018) in R v3.6.0 (https://www.R-project.org/) (Team, 2018) and subsequently assigned to 3,792 proteins, accumulated protein intensities were normalized by each samples median, transformed by log2, and finally differential protein abundance analysis was performed for the two conditions with three samples each. Key characteristics of the metaproteomes are described in Fig. 3.2 and Fig. 3.3 as well as in Tables S1 and S2. The definition of a significant difference was postulated for proteins with Benjamini and Hochberg adjusted $p \leq 0.05$.

Phylogenetic analysis, figure illustration and data availability

Phylogenetic analysis of Cyc2, MtoA/B, RbcL/S protein sequences of culture BP and related Fe(II)-oxidizing bacteria (FeOB), as well as 16S rRNA genes of culture BP, *Gallionellaceae* spp. identified in environmental samples and isolated *Gallionellaceae* spp. were conducted (Fig. S3.1, S3.2, S3.3, S3.4 and S3.5). Analyses were conducted in MEGA X using the Maximum Likelihood method and the Tamura-Nei model with bootstrap values of 1000 for each tree (Felsenstein, 1985; Tamura and Nei, 1993; Kumar *et al.*, 2018). The tree with the highest log likelihood and the percentage of trees in which the associated taxa clustered together was indicated next to the branches. Initial trees for the

heuristic search were obtained automatically by applying Neighbor-Join and BioNJ algorithms to a matrix of pairwise distances estimated using the Tamura-Nei model, and then selecting the topology with superior log likelihood value. The tree was drawn to scale, with branch lengths measured in the number of substitutions per site. These analyses involved 68 16S rRNA nucleotide sequences (Fig. S3.1), 38 RbcL, 23 RbcS, 38 Cyc2, 7 MtoA, 16 MtoB amino acid sequences, respectively (Fig. S3.2, S3.3, and S3.4) and 49 nucleotide sequences (Fig. S3.5).

The amino acid biosynthesis pathways were determined by using the tool: GapMind: Automated annotation of Amino acid biosynthesis (https://papers.genomics.lbl.gov/cgi-bin/gapView.cgi) (Price *et al.*, 2020). The physiological growth plots, cell count plots, heat map and bubble plots (Fig. 3.1, Fig. 3.2 and Fig. S3.6) were constructed via R v.3.6.1 and its working interface RStudio (https://www.R-project.org/ and http://www.rstudio.com/) (Team, 2019; Team, 2020). Figure illustrations of cell shapes (Fig. 3.3 and Fig. 3.4) were adapted from “Icons > Cell Membranes > Simplified Bilayer Membranes” and “Icons > Cell Structures > Organelles”, respectively, by using BioRender.com (2021, https://app.biorender.com/biorender-templates).

The datasets presented in this study can be found in online repositories. The names of the repositories and accession numbers are described below and in Table S3.4. Raw sequencing data and metagenome assembly were deposited at the Sequence Reads Archive (SRA, https://www.ncbi.nlm.nih.gov/bioproject/PRJNA693457). The mass spectrometry proteomics data have been deposited to the ProteomeXchange Consortium via the PRIDE (Perez-Riverol *et al.*, 2019) partner repository with the dataset identifier PXD023710. The IMG metagenome ID for BP culture is 3300036710 and the corresponding accession numbers of MAGs are: *Gallionellaceae* sp.: 2831290873, *Noviherbaspirillum* sp.: 2831285802, *Rhodoferax* sp.: 2840079448, *Thiobacillus* sp.: 2840071692, *Rhodoblastus* sp.: 2840074988, *Ramlibacter* sp.: 2840082686, *Geothrix* sp.: 2840087968 and *Betaproteobacteria* bacterium: 2840090052 (Table S3.1 and S3.2) (Chen *et al.*, 2019). The other four MAGs did not reach the quality criteria for submission to IMG; therefore, these MAGs were deposited in SRA database.

3.6. Supplementary information

Supplementary Tables

Table S3.1. Metagenome assembled genome (MAG) quality and data statistics with mapped number of significantly changed (adjusted $p \leq 0.05$) transcripts and proteins under autotrophic conditions compared to heterotrophic conditions.

	Gallionellaceae	*Noviherbaspirillum*	*Rhodoferax*	*Thiobacillus*	*Rhodoblastus*	*Ramlibacter*
Information of genome bins						
Estimated completeness (%)	93.2	90.5	98	90.6	94.6	88.5
Estimated contamination (%)	0	2	0.7	1.4	0	2
No. contigs (scaffold)	42	41	14	15	88	458
Largest contig	241555	621421	1452120	926960	324380	78674
Gene count	2374	5070	3237	3295	4459	5281
Genome size (bp)	2,408,093	5,429,401	3,368,592	3,249,831	4,511,103	5,100,867
Sequencing depth	6757	1506	121	24	17	9
GC (%)	59.05	59.52	63.91	62.7	62.96	66.61
No. of CDS	2325	5002	3177	3241	4376	5222
Taxonomy ID	96	1344552	28065	919	168658	174951
IMG Submission ID	215615	215613	221513	221511	221512	221514
IMG Genome ID	2831290873	2831285802	2840079448	2840071692	2840074988	2840082686
GOLD Analysis Project ID	Ga0394452	Ga0394450	Ga0401103	Ga0401101	Ga0401102	Ga0401104
16S rRNA gene similarity (%) of closest related isolated species*	*Ferrigenium kumadai* (96.17)	*Noviherbaspirillum autotrophicum* strain TSA66 (98.97)	*Curvibacter delicatus* strain NBRC 14919 (98.56)	*Thiobacillus thioparus strain* THI 111 (99.66)	*Rhodoblastus sphagnicola* strain RS (97.94)	*Xenophilus aerolatus* strain 5516S-2 (97.68)
Community composition (exponential phase) (%)						
Autotrophic	77.11	14.76	2.24	1.42	1.11	0.27
Heterotrophic	0.08	4.93	94.87	0	0	0
Number of significantly changed (adjusted $p \leq 0.05$) transcripts under autotrophic conditions compared to heterotrophic conditions						
Total	2396	4546	216	696	747	532
Significant-up	2396	4546	59	696	747	532
Significant-down	0	0	157	0	0	0
Number of significantly changed proteins (adjusted $p \leq 0.05$) under autotrophic conditions compared to heterotrophic conditions						
Total	12	122	103	0	1	2
Significant-up	3	96	5	0	0	1
Significant-down	9	26	98	0	1	1

*16S rRNA gene similarities are based on PacBio long-read amplicon sequencing

Table S3.2. Metagenome (A), metatranscriptome (B) and metaproteome (C) data statistics.

	Culture BP
(A) Metagenome	
Raw read pairs	91,056,140 (27.48×10^9 base pairs)
Read pairs that passed QC	90,303,622 (27.25×10^9 base pairs)
Genome size (10^6 base pairs, Mbp)	57,442,683
Proportion of reads assembled (%)	99.35
No. contigs (scaffold)	25083
Gene count	75943
GC (%)	64.01
No. of CDS	75105
IMG Submission ID	221510
IMG Genome ID	3300036710
GOLD Analysis Project ID	Ga0394449
rRNA	103
16S rRNA Count	34
(B) Metatranscriptome (range / average)	
Sequences [million]	6.3 – 53.3 / 25
% duplicates	94 – 99 / 98
GC%	52 - 54 / 53
% rRNA	35 – 76 / 54
% mapped to metagenome	9.5 – 92.6 / 77
mapped to metagenome [million]	0.3 – 30.2 / 10
Total no. of detected transcripts	17,471
No. of significant higher expression level transcripts under autotrophic condition	10,503
No. of significant higher expression level transcripts under heterotrophic condition	157
(C) Metaproteome (range / average)	
Analyzed MS/MS spectra [thousand]	85 – 89 / 87
Identified MS/MS spectra (%)	3.7 – 27.8 / 16
Total no. of detected proteins	3792
No. of significant higher abundant proteins under autotrophic condition	126
No. of significant higher abundant proteins under heterotrophic condition	150

Table S3.3. Summary of key metabolic pathways in selected NRFeOx-related metagenome assembled genomes (MAGs).

Function	*Gallionellaceae* -KS	*Gallionellaceae* -BP	*Noviherbaspirillum*	*Rhodoblastus*	*Thiobacillus*	*Rhodoferax*	*Ramlibacter*
Carbon Metabolism							
CBB reductive pentose phosphate cycle	+	+	+	+	+	(+)	+
Glycolysis (Embden-Meyerhof pathway)	+	+	+	+	+	+	+
Pyruvate oxidation to acetyl-CoA through pyruvate dehydrogenase	+	+	+	+	+	+	+
Citrate cycle (TCA cycle, Krebs cycle)	+	+	+	+	(+)	+	+
Pentose phosphate pathway	+	+	(+)	(+)	+	(+)	(+)
Glyoxylate cycle	-	(+)	+	(+)	(+)	(+)	+
Nitrogen Metabolism							
Nitrogen fixation, nitrogen → ammonia	-	-	-	(+)	-	-	-
Dissimilatory nitrate reduction	-	(+)	+	+	+	+	+
Assimilatory Nitrate reduction	-	-	(+)	(+)	(+)	(+)	(+)
Nitrification, ammonia → nitrite	-	-	-	-	-	-	-

Table S3.3. (Continued) Summary of key metabolic pathways in selected NRFeOx-related metagenome assembled genomes (MAGs).

Denitrification							
Nitrate → nitrite	+	-	+	+	+	+	+
Nitrite → nitric oxide	+	+	+	+	+	+	+
Nitric oxide → nitrous oxide	-	+	+	+	+	+	+
Nitrous oxide → nitrogen gas	-	-	+	+	+	+	+
Complete denitrification	No	No	Yes	Yes	Yes	Yes	Yes
Oxidative Phosphorylation							
Complex I, NADH: quinone oxidoreductase	+	+	+	+	+	+	(+)
Complex II, succinate dehydrogenase	+	+	+	+	+	+	+
Complex III, cytochrome bc_1 complex	+	+	+	+	+	+	+
Alternative complex III (ACIII)	-	-	-	-	-	-	-
***aa*$_3$-type cytochrome *c* oxidase**	+	+	+	+	+	+	+
Cytochrome *bd* ubiquinol oxidase	-	-	(+)	(+)	(+)	-	(+)
cbb$_3$-type cytochrome *c* oxidase	+	+	+	+	+	+	+
F-type ATPase	+	+	+	+	+	+	+
V-type ATPase	-	-	-	-	-	-	-

Table S3.4. Overview of meta-omics samples from culture BP, archived in the Sequencing Read Archive (SRA, bioproject PRJNA693457) or ProteomeXchange Consortium (via the PRIDE partner repository, identifier PXD023710). All amplicon sequencing was performed with primers 515f and 805r, except SRR13504099, that was amplified with primers 27F and 1492R.

Conditions	Time-points	Replicate	Amplicon sequencing	Metagenomics	Metatranscriptomics	Metaproteomics
Autotrophic	T3	1	SRR13504099			
Autotrophic	T1	1		SRR13494970		
Autotrophic	T0	1	SRR13489090			
	T1	1	SRR13489089		SRR13494978	R23
	T1	2	SRR13489148		SRR13494977	R24
	T1	3	SRR13489137		SRR13494976	R25
	T2	1	SRR13489126			
	T2	2	SRR13489115			
	T2	3	SRR13489104			
	T3	1	SRR13489093			
	T3	2	SRR13489092			
	T3	3	SRR13489091			
Heterotrophic	T0	1	SRR13489088			
	T1	1	SRR13489087			
	T1	2	SRR13489156			
	T1	3	SRR13489155			
	T2	1	SRR13489154		SRR13494975	R26
	T2	2	SRR13489153		SRR13494974	R27
	T2	3	SRR13489152		SRR13494973	R28
	T3	1	SRR13489151			
	T3	2	SRR13489150			
	T3	3	SRR13489149			

Supplementary Figures

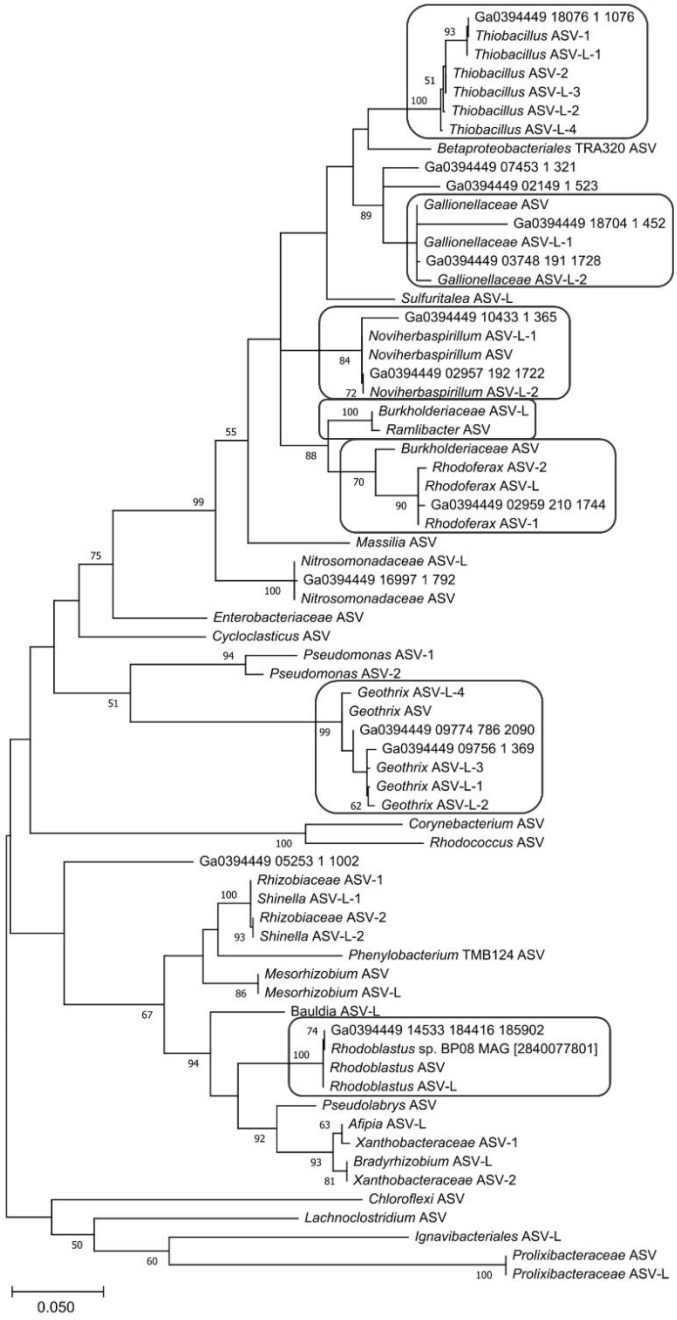

Fig. S3.1. Phylogenetic tree showing the relationships between 68 16S rRNA nucleotide sequences obtained by different methods. 1. Long-read ASVs ("ASV-L-x"), 2. short-read ASVs ("ASV-x"), 3. MAG sequence ("MAG"), and 4. metagenome sequences ("Ga0394449"). If there were more ASVs, the number "x" was added right after the "ASV-L-" or "ASV-". 16S rRNA sequences retrieved from the MAG and metagenome were only included if their length was ≥300 bp and if they overlapped with the V4 region of the 16S rRNA gene (i.e. with the short-read amplicons). The taxa related to the organisms mentioned in this study are marked with boxes. Evolutionary analyses were conducted in MEGA-X and the bootstrap values were calculated on 100 replicates using the Maximum Likelihood method.

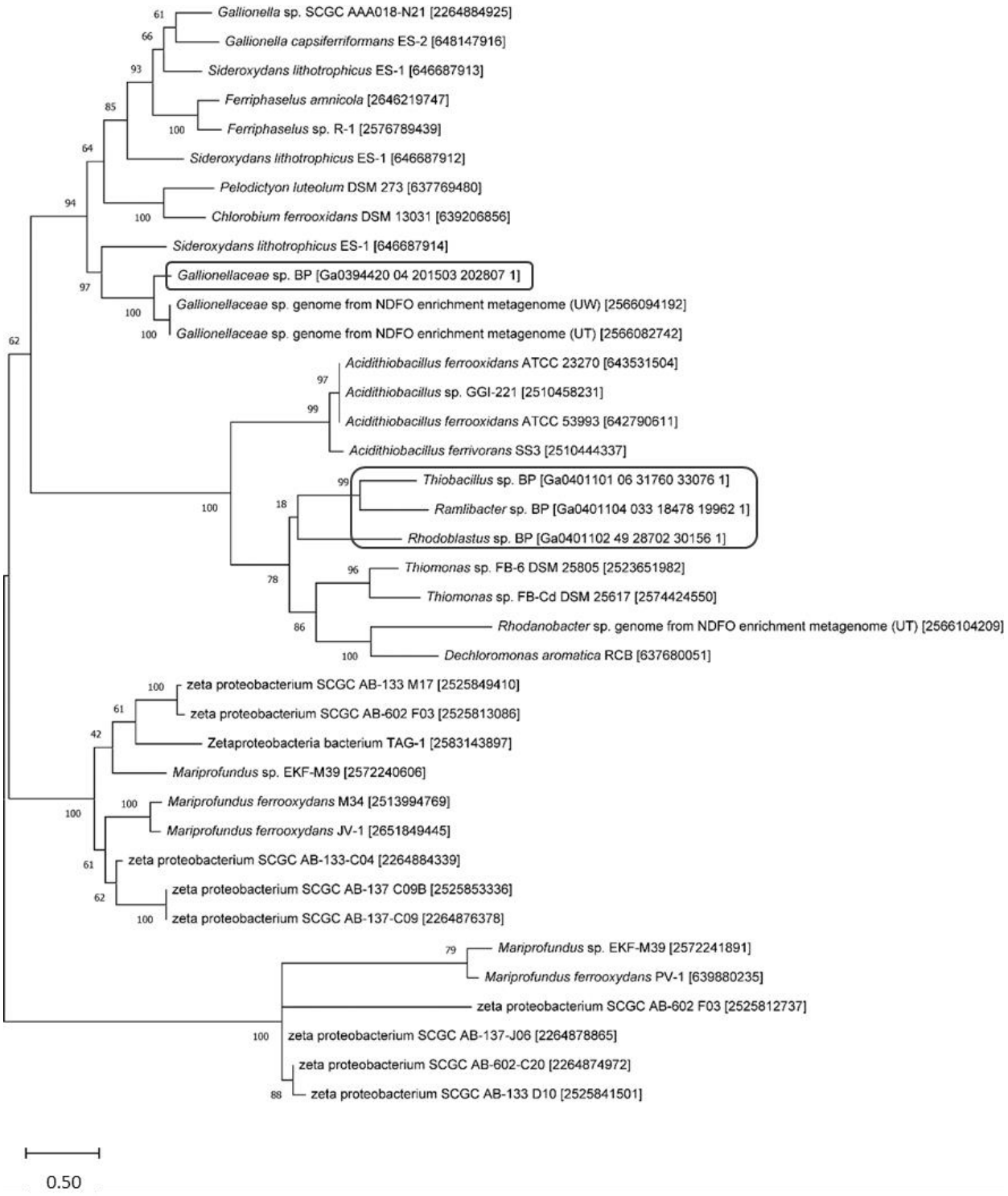

Fig. S3.2. Phylogenetic tree of Cyc2 from the organisms in culture BP and other Fe(II)-oxidizing bacteria based on amino acid sequences with bootstrap values, calculated on 1000 replicates using the Maximum Likelihood method. The organisms in culture BP are marked with boxes. The scale bar indicates branch lengths measured by the number of substitutions per site. Numbers in brackets show the identifier of each gene in IMG.

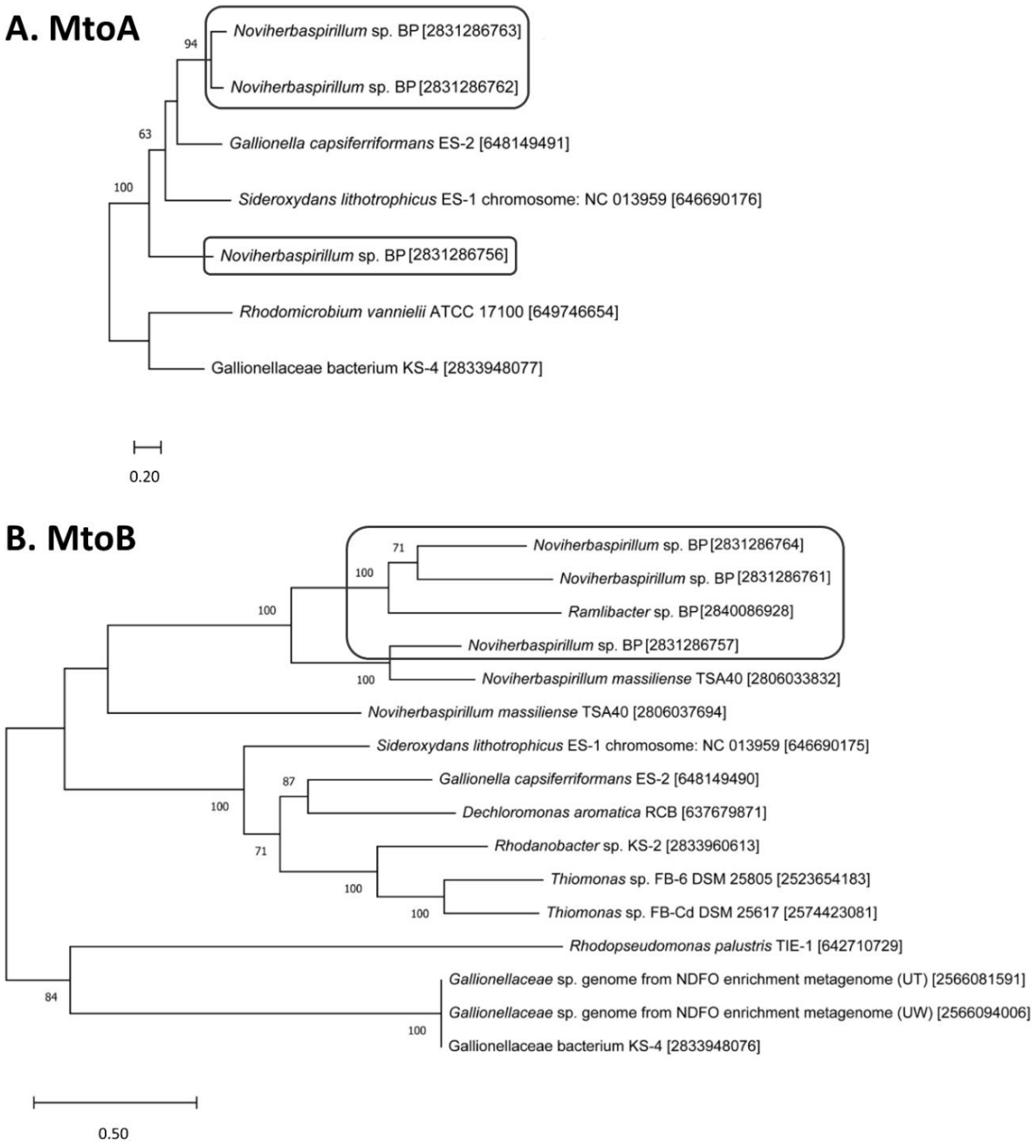

Fig. S3.3. Phylogenetic trees of MtoA (A) and MtoB (B) of *Noviherbaspirillum* sp. and other Fe(II)-oxidizing bacteria based on amino acid sequences with bootstrap values, calculated on 1000 replicates using the Maximum Likelihood method. The organisms in culture BP are marked with boxes. The scale bar indicates branch lengths measured by the number of substitutions per site. Numbers in brackets show the identifier of each gene in IMG.

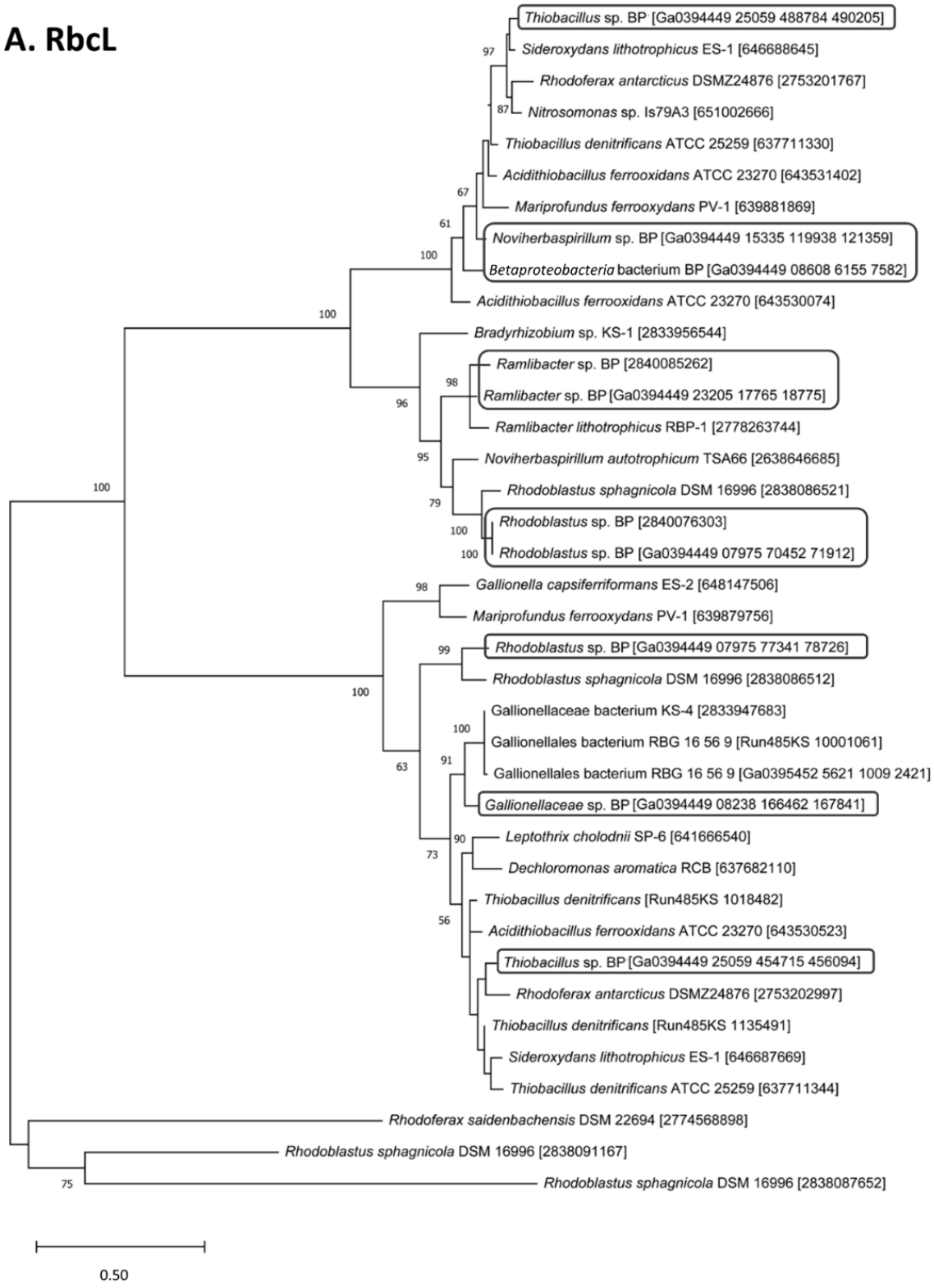
A. RbcL
Thiobacillus sp. BP [Ga0394449 25059 488784 490205]
Sideroxydans lithotrophicus ES-1 [646688645]
Rhodoferax antarcticus DSMZ24876 [2753201767]
Nitrosomonas sp. Is79A3 [651002666]
Thiobacillus denitrificans ATCC 25259 [637711330]
Acidithiobacillus ferrooxidans ATCC 23270 [643531402]
Mariprofundus ferrooxydans PV-1 [639881869]
Noviherbaspirillum sp. BP [Ga0394449 15335 119938 121359]
Betaproteobacteria bacterium BP [Ga0394449 08608 6155 7582]
Acidithiobacillus ferrooxidans ATCC 23270 [643530074]
Bradyrhizobium sp. KS-1 [2833956544]
Ramlibacter sp. BP [2840085262]
Ramlibacter sp. BP [Ga0394449 23205 17765 18775]
Ramlibacter lithotrophicus RBP-1 [2778263744]
Noviherbaspirillum autotrophicum TSA66 [2638646685]
Rhodoblastus sphagnicola DSM 16996 [2838086521]
Rhodoblastus sp. BP [2840076303]
Rhodoblastus sp. BP [Ga0394449 07975 70452 71912]
Gallionella capsiferriformans ES-2 [648147506]
Mariprofundus ferrooxydans PV-1 [639879756]
Rhodoblastus sp. BP [Ga0394449 07975 77341 78726]
Rhodoblastus sphagnicola DSM 16996 [2838086512]
Gallionellaceae bacterium KS-4 [2833947683]
Gallionellales bacterium RBG 16 56 9 [Run485KS 10001061]
Gallionellales bacterium RBG 16 56 9 [Ga0395452 5621 1009 2421]
Gallionellaceae sp. BP [Ga0394449 08238 166462 167841]
Leptothrix cholodnii SP-6 [641666540]
Dechloromonas aromatica RCB [637682110]
Thiobacillus denitrificans [Run485KS 1018482]
Acidithiobacillus ferrooxidans ATCC 23270 [643530523]
Thiobacillus sp. BP [Ga0394449 25059 454715 456094]
Rhodoferax antarcticus DSMZ24876 [2753202997]
Thiobacillus denitrificans [Run485KS 1135491]
Sideroxydans lithotrophicus ES-1 [646687669]
Thiobacillus denitrificans ATCC 25259 [637711344]
Rhodoferax saidenbachensis DSM 22694 [2774568898]
Rhodoblastus sphagnicola DSM 16996 [2838091167]
Rhodoblastus sphagnicola DSM 16996 [2838087652]
0.50

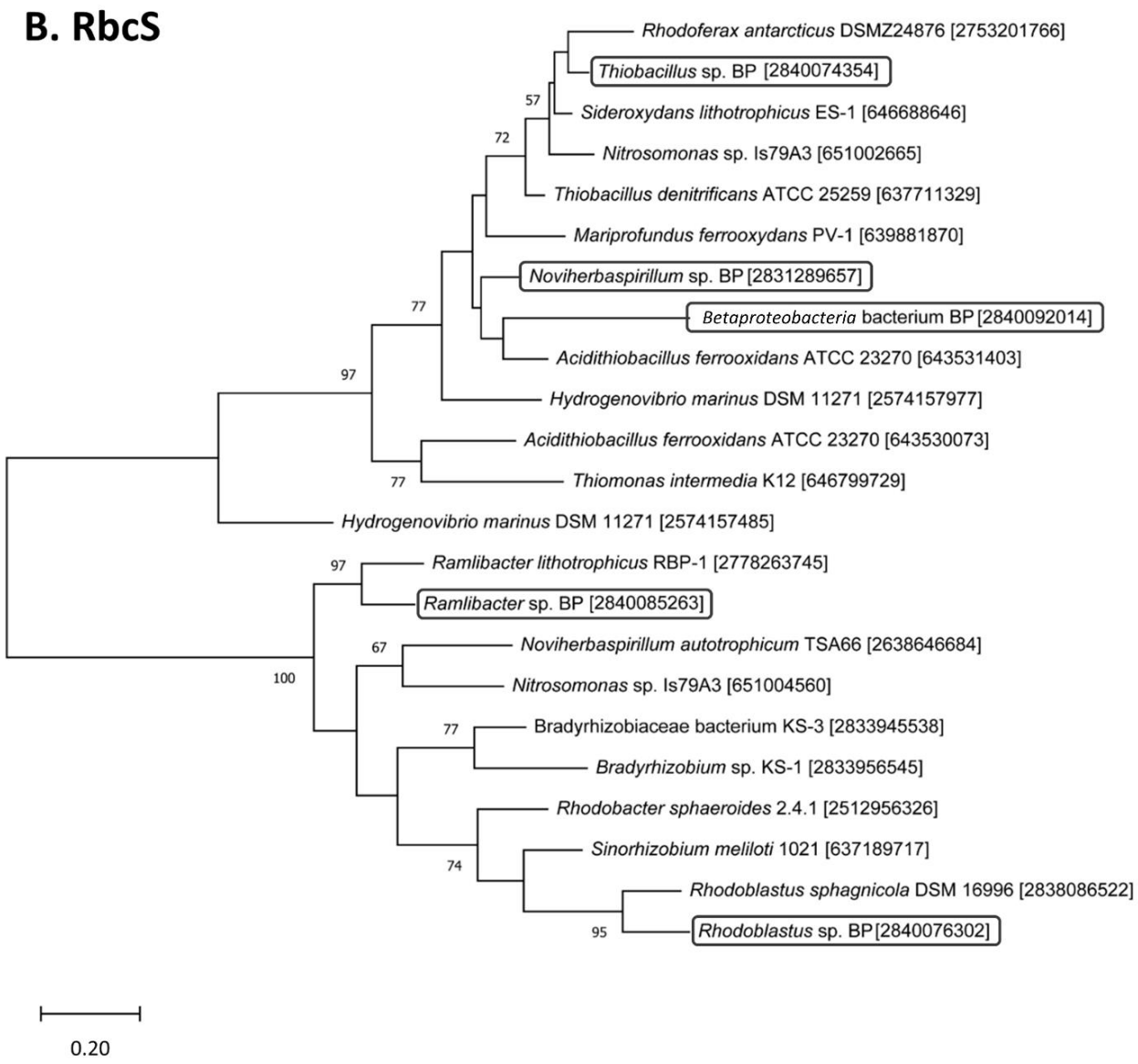

Fig. S3.4. Phylogenetic trees of RuBisCO from culture BP, flanking members and other Fe(II)-oxidizing bacteria: RbcL (A) and RbcS (B) based on amino acid sequences with bootstrap values, calculated on 1000 replicates using the Maximum Likelihood method. The organisms in culture BP are marked with boxes. The scale bar indicates branch lengths measured by the number of substitutions per site. Numbers in brackets show the identifier of each gene in IMG.

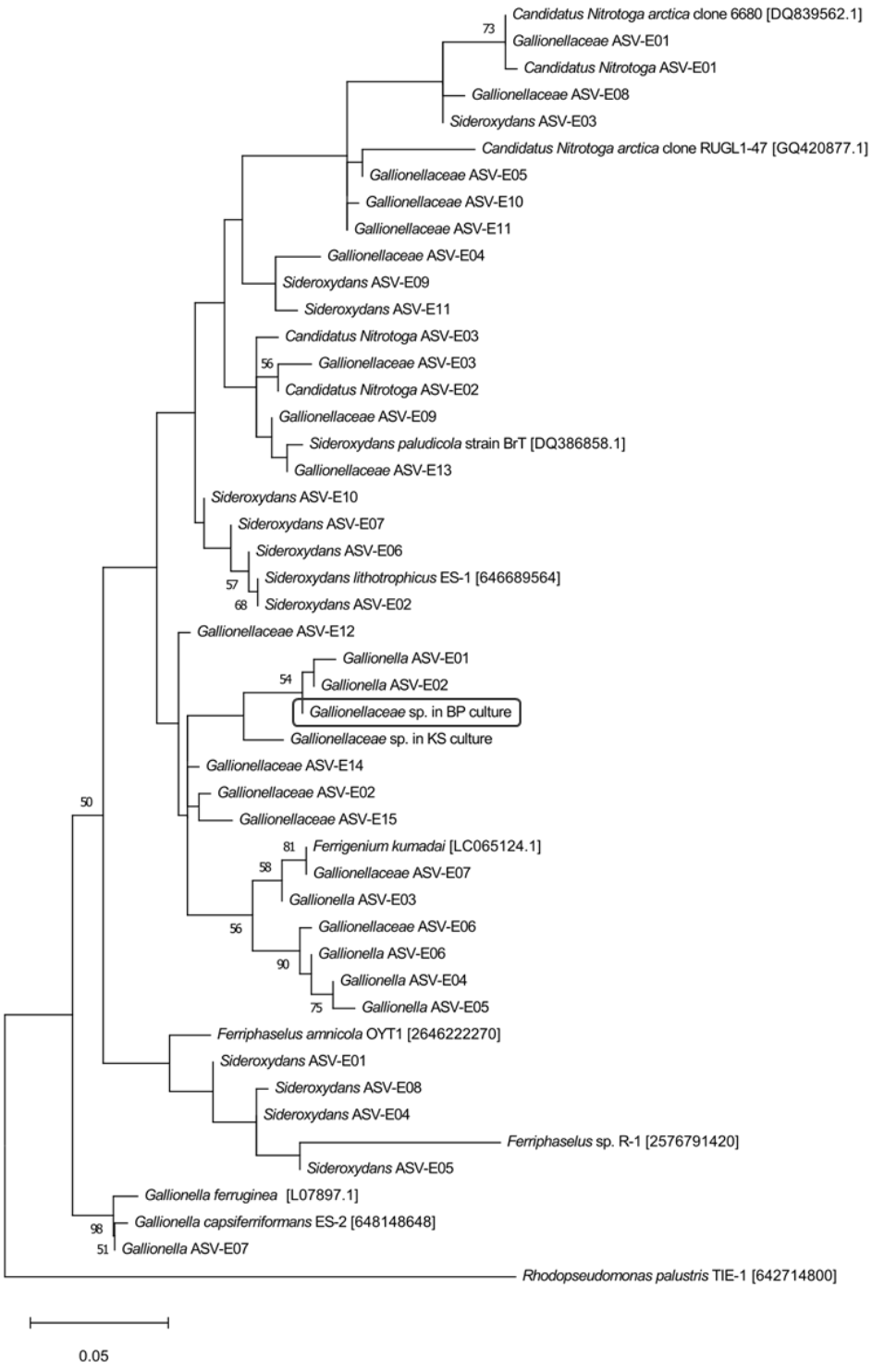

Fig. S3.5. Phylogenetic tree of the *Gallionellaceae* spp. ASVs detected in the environmental sediments compared to isolated *Gallionellaceae* spp. and Fe(II)-oxidizing bacteria based on nucleotide sequences with bootstrap values, calculated on 1000 replicates using the Maximum Likelihood method. The *Gallionellaceae* sp. in culture BP is marked with a box. The scale bar indicates branch lengths measured by the number of substitutions per site. Numbers in brackets show accession numbers.

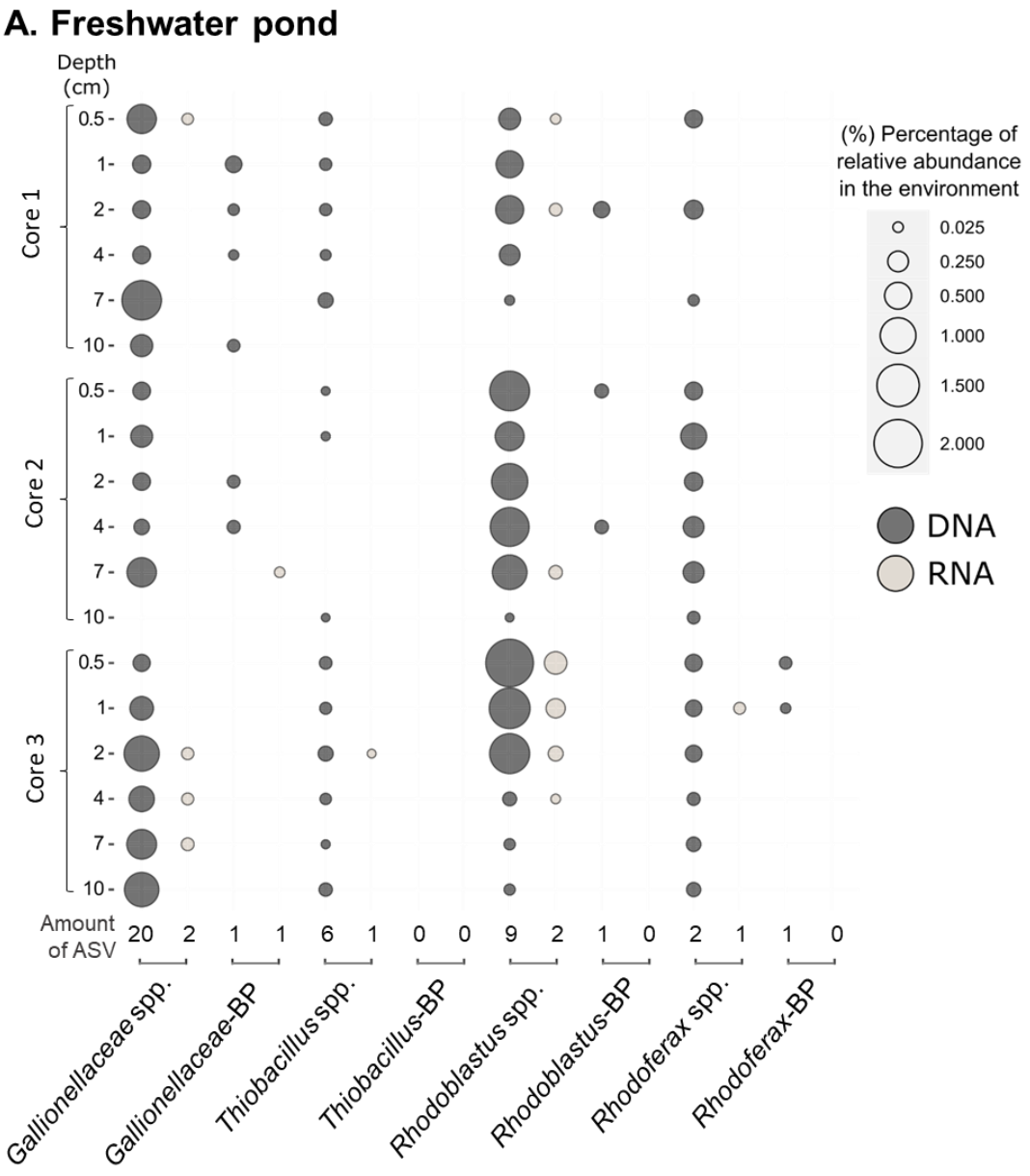
A. Freshwater pond
Depth (cm)
Core 1
Core 2
Core 3
0.5
1
2
4
7
10
Amount of ASV
20 2 1 1 6 1 0 0 9 2 1 0 2 1 1 0
(%) Percentage of relative abundance in the environment
0.025
0.250
0.500
1.000
1.500
2.000
DNA
RNA
Gallionellaceae spp.
Gallionellaceae-BP
Thiobacillus spp.
Thiobacillus-BP
Rhodoblastus spp.
Rhodoblastus-BP
Rhodoferax spp.
Rhodoferax-BP

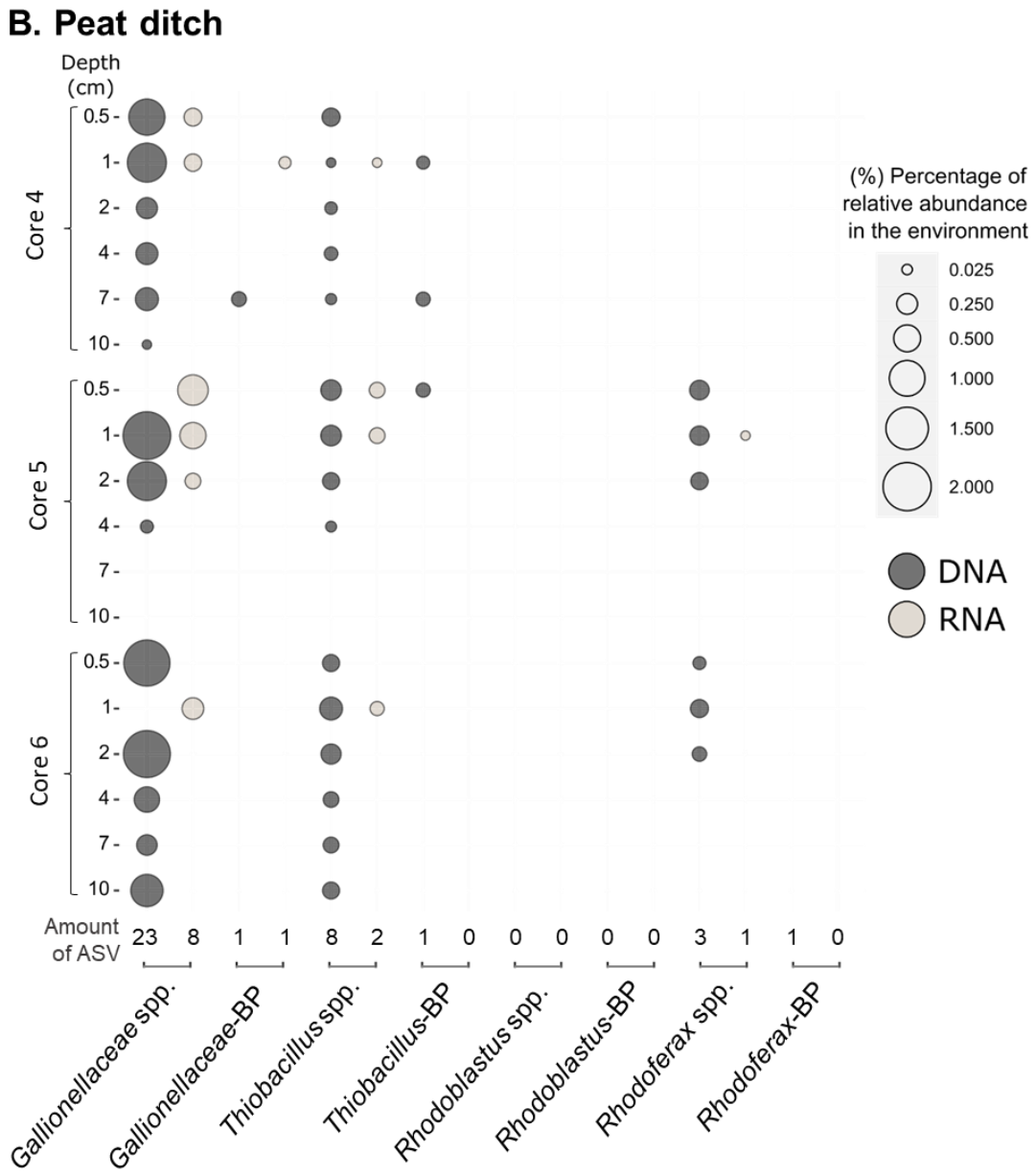

Fig. S3.6. Bubble plot showing the relative abundance of amplicon sequence variants (ASVs) of microbial populations from culture BP (identical ASV and genus or family level, respectively), detected in environmental sediments. Samples were taken (A) at an organic-rich freshwater pond and (B) at an organic-rich peat ditch in Bremen, Germany. Sediments were taken from three different cores per site and from 0-10 cm depth. Dark and light grey bubbles demonstrate DNA- and RNA-based short-read 16S rRNA (gene) amplicon sequencing data, respectively.

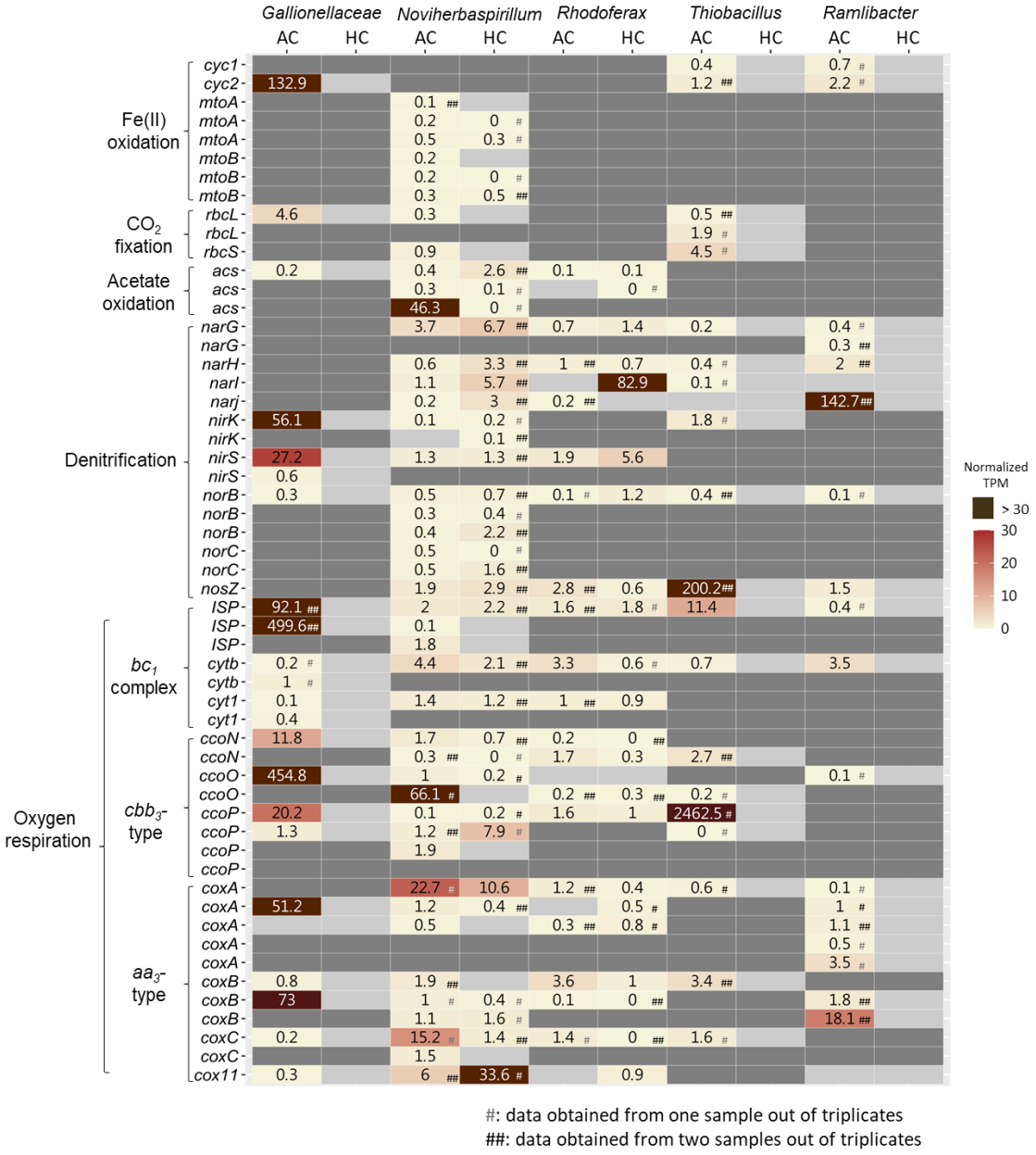

Fig. S3.7. Heatmap of normalized transcripts per kilobase million (TPM) of the *Gallionellaceae* sp., *Noviherbaspirillum* sp., *Thiobacillus* sp., *Rhodoferax* sp. and *Ramlibacter* sp. metagenome-assembled genomes. Visualized are normalized TPM values for the pathways of Fe(II) oxidation, carbon fixation, denitrification and oxygen respiration. AC: autotrophic conditions; HC: heterotrophic conditions; #: data obtained from one sample out of triplicates (i.e. two data points out of three were 0 TPM and treated as missing data, therefore data have to be interpreted with caution also indicated by the gray font of these data); ##: data obtained from two samples out of triplicates; numbers without #: data obtained from all three triplicates; light gray-colored cell: no transcript of the identified gene detected among triplicate samples; dark gray-colored cell: no gene and no transcript detected.

4. '*Candidatus* Ferrigenium straubiae' sp. nov., '*Candidatus* Ferrigenium bremense' sp. nov., '*Candidatus* Ferrigenium altingense' sp. nov., are autotrophic Fe(II)-oxidizing bacteria of the family *Gallionellaceae*.

Yu-Ming Huang[a, b], Natalia Jakus[a, b], Daniel Straub[a, c], Andreas Kappler[b, d], Konstantinos T. Konstantinidisd[e], Nia Blackwell[a] and Sara Kleindienst[a]

[a] Microbial Ecology, Center for Applied Geoscience, University of Tuebingen, Germany
[b] Geomicrobiology, Center for Applied Geoscience, University of Tuebingen, Germany
[c] Quantitative Biology Center (QBiC), University of Tuebingen, Germany
[d] Cluster of Excellence: EXC 2124: Controlling Microbes to Fight Infections, Tübingen, Germany
[e] School of Civil and Environmental Engineering, School of Biological Sciences, and Center for Bioinformatics and Computational Genomics, Georgia Institute of Technology, Atlanta, GA, 30332, USA

Unpublished manuscript

Abstract

Iron(II) [Fe(II)] oxidation coupled to denitrification is recognized as an environmentally important process in many ecosystems. However, the autotrophic denitrifying Fe(II)-oxidizing bacteria (FeOB) dominating these enrichment cultures, affiliated with the family *Gallionellaceae*, remain poorly taxonomically defined due to lack of representative isolates. We describe the taxonomic classification of three novel FeOB based on metagenome-assembled genomes (MAGs) acquired from the autotrophic nitrate-reducing enrichment cultures KS, BP and AG, originating from freshwater sediments in Bremen, Northern Germany (cultures KS and BP), and groundwater in Altingen, Ammerbuch, Southern Germany (culture AG). Phylogenetic analysis of nearly full-length 16S rRNA gene sequences demonstrated that these three FeOB were most closely affiliated to the genera *Ferrigenium*, *Sideroxydans* and *Gallionella*, with up to 96.5%, 95.4% and 96.2% 16S rRNA gene sequence identities to representative isolates of these genera, respectively. In addition, average amino acid identities (AAI) of the genomes compared to the most closely related genera revealed highest AAI with *Ferrigenium kumadai* An22 (76.35-76.74%), suggesting that the three FeOB are members of this genus. Phylogenetic analysis of conserved functional genes further supported that these FeOB represent three novel species of the genus *Ferrigenium*. Physiological observations of the FeOB revealed unique features, such as the ability to perform partial denitrification coupled to Fe(II) oxidation and carbon fixation. Scanning electron microscopy of the enrichment cultures showed slightly curved rod-shaped cells, ranging from 0.2-0.7 µm in width and 0.5-2.3 µm in length. Based on the phylogenetic, genomic, and physiological characteristics, we propose that these FeOB represent three novel species, '*Candidatus* Ferrigenium straubiae' sp. nov., '*Candidatus* Ferrigenium bremense' sp. nov. and '*Candidatus* Ferrigenium altingense' sp. nov. that might have unique metabolic features among the genus *Ferrigenium*.

Introduction

Ferrous iron [Fe(II)] oxidation can be mediated by specific microorganisms and plays a crucial role in biogeochemical nitrogen, carbon, oxygen and sulfur cycles of natural and engineered ecosystems (Kappler *et al.*, 2021), such as freshwater sediment (Straub *et al.*, 1996; Straub and Buchholz-Cleven, 1998; Straub *et al.*, 2004), marine coastal sediment (Laufer *et al.*, 2015; Laufer *et al.*, 2016) and constructed wetlands (Zhimiao *et al.*, 2020). Fe(II)-oxidizing bacteria (FeOB) are capable of oxidizing both solid and dissolved Fe(II) as electron donors. Studies of FeOB living at circumneutral pH have demonstrated that these organisms flourish within the zone in which ferrous ions are stable, i.e. at microoxic to anoxic conditions at which abiotic Fe(II) oxidation is limited enough for microorganisms to compete (Rentz *et al.*, 2007; Jewell *et al.*, 2016). Most known FeOB are members of *Proteobacteria* and are grouped into three physiological types, depending on the electron acceptor and energy source used for Fe(II) oxidation: light-dependent (photoferrotrophs), O_2-dependent (microaerophiles), and nitrate-reducing (Ehrenberg, 1838; Widdel *et al.*, 1993; Straub *et al.*, 1996).

Many of the common neutrophilic Fe(II)-oxidizing bacteria belong to the family *Gallionellaceae*, which are divided into eight defined genera. Four of these are represented entirely by FeOB: *Ferrigenium, Ferriphaselus, Gallionella* and *Sideroxydans.* These bacteria typically oxidize Fe(II) under microoxic conditions (Hallbeck and Pedersen, 1991; Emerson and Moyer, 1997; Emerson and Merrill Floyd, 2005; Weiss *et al.*, 2007; Krepski *et al.*, 2012; Emerson *et al.*, 2013; Kato *et al.*, 2013; Kato *et al.*, 2015; Kadnikov *et al.*, 2016; Khalifa *et al.*, 2018) and a few of them, unclassified *Gallionellaceae* spp., were suggested to coupled Fe(II) oxidation to partial denitrification under anoxic conditions (Straub *et al.*, 1996; He *et al.*, 2016; Jewell *et al.*, 2016; Huang *et al.*, 2021a; Huang *et al.*, 2021b; Jakus *et al.*, 2021). Additionally, some of the FeOB in the *Gallionellaceae* family were reported to perform carbon fixation (Hallbeck and Pedersen, 1991; Emerson and Moyer, 1997; Emerson and Merrill Floyd, 2005; Weiss *et al.*, 2007; Krepski *et al.*, 2012; Emerson *et al.*, 2013; Kato *et al.*, 2013; Kato *et al.*, 2015; Jewell *et al.*, 2016; Kadnikov *et al.*, 2016; Khalifa *et al.*, 2018), as they are very often inhabiting organic carbon depleted environments such as aquifers (Jewell *et al.*, 2016), geysers and high-CO_2 subsurface wetland soils (Emerson *et al.*, 2016), inactive seafloor hydrothermal sulfide chimneys (Li *et al.*, 2017), as well as mine water discharges (Fabisch *et al.*, 2016).

Despite the genetic potential of these bacteria and the broad variety of habitats that members of the family *Gallionellaceae* occupy, there is no reported isolate of neutrophilic autotrophic nitrate-reducing Fe(II)-oxidizing (NRFeOx) bacteria. However, members of the family *Gallionellaceae* were found to dominate microbial communities of known neutrophilic autotrophic NRFeOx enrichment cultures (Straub *et al.*, 1996; Huang *et al.*, 2021b; Jakus *et al.*, 2021).

So far there are only three published examples of stable autotrophic NRFeOx enrichment cultures. Two of the cultures were obtained from freshwater sediments in Bremen, northern Germany (cultures KS and BP) (Straub *et al.*, 1996; Huang *et al.*, 2021b), and one was obtained from an anoxic groundwater monitoring well in Altingen, southern Germany (culture AG) (Jakus *et al.*, 2021). Recent metagenomic analysis revealed that all of these unclassified *Gallionellaceae* spp. in the three enrichment cultures share many common features. They possess the genes encoding putative Fe(II) oxidases such as Cyc2 and/or MtoAB, and genes involved in denitrification such as nitrate reductase (*narGHI*), nitrite reductase (*nirK/S*) and/or nitric oxide reductase (*norBC*) (He *et al.*, 2016; Huang *et al.*, 2021a; Huang *et al.*, 2021b; Jakus *et al.*, under review; and provided to the reviewers with this submission). The bacteria were also found to possess the large subunit ribulose-1,5-bisphosphate carboxylase-oxygenase gene (*rbcL*), a key gene for carbon dioxide fixation during the Calvin–Benson–Bassham (CBB) cycle (He *et al.*, 2016; Tominski *et al.*, 2018a; Huang *et al.*, 2021a; Huang *et al.*, 2021b; Jakus *et al.*, under review; and provided to the reviewers with this submission). Thus, they likely have the ability to perform autotrophic Fe(II) oxidation coupled to partial denitrification. Based on nearly full-length 16S rRNA gene sequence (~1460 bp) analysis, most closely related isolated species of the dominating *Gallionellaceae* spp. present in these cultures are *Ferrigenium kumadai* An22, *Sideroxydans lithotrophicus* ES-1 and *Gallionella capsiferriformans* ES-2. Despite elaborate cultivation attempts, these three FeOB *Gallionellaceae* spp. have so far not been isolated (He *et al.*, 2016; Tominski *et al.*, 2018a; Huang *et al.*, 2021b; Jakus *et al.*, 2021). Furthermore, the exact phylogenetic placement and taxonomic description for these FeOB in the *Gallionellaceae* family remains unresolved.

An increasing number of available genomes derived from metagenomics studies of so far uncultured members of the family *Gallionellaceae*, sharing the potential of coupling Fe(II)

oxidation to partial denitrification, shows the importance of classifying these new taxa of FeOB (Jewell *et al.*, 2016; Kadnikov *et al.*, 2016; Bethencourt *et al.*, 2020). In addition, the key FeOB of the only stable NRFeOx cultures that exist to date (i.e. cultures KS, BP and AG) and that are currently frequently used as model systems to study autotrophic nitrate reduction coupled to Fe(II) oxidation remain to be classified. Moreover, the advancement of methods in (meta)genomics complement traditional approaches and promote the assessment of the existing taxonomic system (Konstantinidis and Tiedje, 2007; Murray *et al.*, 2020). For example, a widely applied approach is to use the category of '*Candidatus*' to propose putative taxa (Stackebrandt *et al.*, 2002). These yet-to-be isolated microorganisms do not meet all requirements of the International Code of Nomenclature of Prokaryotes (2019); however, there is sufficient evidence to justify their classification through (meta)genomic data (Murray and Stackebrandt, 1995; Konstantinidis and Rosselló-Móra, 2015; Konstantinidis *et al.*, 2017; 2019; Murray *et al.*, 2020). Here, we describe phylogenetic, genomic, and phenotypic analyses to suggest the designation of the three novel FeOB species within the family *Gallionellaceae*.

Experimental procedures

Cultivation and isolation strategies

Culture KS, named after Kristina Straub who reported the first study on this culture (Straub *et al.*, 1996) (dominated by '*Ca.* Ferrigenium straubiae' strain KS) originated from a freshwater ditch in Bremen, Germany. Since then, culture KS has been transferred for more than 20 years under autotrophic conditions with 1-10% (v/v) inoculum (He *et al.*, 2016; Tominski *et al.*, 2018a; Huang *et al.*, 2021a). Several cultivation and isolation techniques have been used, e.g. cultivation under microoxic conditions in gradient tubes and zero-valent iron (ZVI) plates (Tominski *et al.*, 2018a), or growth with different substrates under anoxic conditions in serum bottles, such as $FeCl_2$, Fe(II)-EDTA, and $FeSO_4$ as the electron donor with nitrate as the electron acceptor (Straub *et al.*, 1996; Blöthe and Roden, 2009; Tominski *et al.*, 2018a).

Culture BP, named after Bremen Pond, (dominated by '*Ca.* Ferrigenium bremense' strain BP) originated from a freshwater pond in the backyard of the Max Planck Institute for Marine Microbiology, Bremen, Germany in 2015 (Huang *et al.*, 2021b). Since then, culture BP has been transferred for more than 2 years (>20 times/year since 2018) under autotrophic conditions with 4-10% (v/v) inoculum. Both culture KS and BP were stored and transferred continuously in 25 mL mineral medium (Hegler *et al.*, 2008; Blöthe and Roden, 2009), pH 6.9-7.2, with 10 mM $FeCl_2$ and 4 mM $NaNO_3$ in 58 mL serum bottles and incubated in the dark at 28°C.

Culture AG, named after Altingen Groundwater, (dominated by '*Ca.* Ferrigenium altingense' strain AG) originated from an anoxic groundwater monitoring well in Altingen, southern Germany (Jakus *et al.*, 2021). Since then, culture AG has been transferred for more than 3 years (>20 times/year since 2018) under autotrophic conditions with 2 mM $FeCl_2$ and 2 mM $NaNO_3$ in 58 mL serum bottles containing 25 mL of medium and with 10% (v/v) inoculum (Jakus *et al.*, 2021).

PacBio 16S rRNA gene amplicon sequencing

DNA extraction for culture KS, culture BP and culture AG was reported previously (Huang *et al.*, 2021b; Jakus *et al.*, 2021). PacBio Sequel SMRT long-read amplicon sequencing was performed at the Helmholtz Zentrum München, Germany. DNA amplification was conducted twice using two rounds of PCR with primers universal for bacterial 16S rRNA,

tailed with PacBio universal sequencing adapters (universal tags) and 5' amino modifiers (27F gcagtcgaacatgtagctgactcaggtcacAGRGTTYGATYMTGGCTCAG, 1492R tggatcacttgtgcaagcatcacatcgtagRGYTACCTTGTTACGACTT) (Biomers.net, Ulm, Germany) to amplify the nearly full-length 16S rRNA genes from the genomic DNA extracted of all three cultures, respectively (Huang *et al.*, 2021b; Jakus *et al.*, 2021). The PCR amplification protocol was described in detail previously (Huang *et al.*, 2021b; Jakus *et al.*, 2021). For the SMRTbell library preparation (Franzen *et al.*, 2015), the SMRTbell Template Prep Kit (PacBio biosciences, California, USA) was applied according to the user's manual instructions.

Subsequently, 11,688 circular consensus sequencing reads were analyzed with DADA2 v1.10.0 (Callahan *et al.*, 2016; Callahan *et al.*, 2019) in R v3.5.1 (Team, 2018) by sequentially orienting reads and removing primers, filtering (no ambiguous nucleotides and maximum 2 expected errors) and trimming (1000 bp to 1600 bp read length; leading to 7,475 sequences), dereplicating sequences (4,138 unique sequences), learning error rates, removing bimera de novo and finally assigning taxonomy to the detected sequences based on SILVA v132 (Callahan, 2018). Lastly, 8 ASVs with 5,543 total counts were obtained.

Phylogenetic tree construction

The evolutionary history was inferred by using the Maximum Likelihood method and the Tamura-Nei model (Tamura and Nei, 1993). This analysis involved 14 nearly full-length 16S rRNA gene nucleotide sequences and 9 concatenated house-keeping, protein-coding, amino acid gene sequences. There were a total of 1622 and 4529 positions in the final dataset, respectively. The tree with the highest log likelihood was selected with 1000 bootstraps of nucleotide and amino acid sequences. The percentage of trees in which the associated taxa clustered together was indicated next to the branches. Initial trees for the heuristic search were obtained automatically by applying Neighbor-Join and BioNJ algorithms to a matrix of pairwise distances estimated using the Tamura-Nei model, and then selecting the topology with superior log likelihood value. The tree was drawn to scale, with branch lengths measured in the number of substitutions per site. Evolutionary analyses were conducted in MEGA X (Kumar *et al.*, 2018). The house-keeping genes, i.e. RNA polymerase α subunit (*rpoA*), DNA gyrase α subunit (*gyrA*), protein translocase

subunit (*secA*), isoleucyl-tRNA synthetase (*ileS*), rho termination factor (*rho*) and translation initiation factor IF-2 (*infB*), were selected via the gene sequence availability of the top three closest related isolated genomes and other physiological related species (i.e. FeOB of the family *Gallionellaceae* and nitrate-reducing FeOB), to generate a concatenated maximum likelihood phylogenetic tree (Holmes *et al.*, 2004; Emerson *et al.*, 2013; Glaeser and Kämpfer, 2015; Rocha *et al.*, 2015).

Average nucleotide identity (ANI) and Average amino acid identity (AAI)

The average nucleotide identity (ANI) and alignment fraction (AF) was analyzed via the online tool IMG/MER Pairwise ANI (https://img.jgi.doe.gov/cgi-bin/mer/main.cgi?section=ANI&page=pairwise) (Varghese *et al.*, 2015; Chen *et al.*, 2017; Chen *et al.*, 2019). Average amino acid identity (AAI) was conducted via the online tool AAI calculator, developed by the Environmental Microbial Genomics Laboratory (enve-omics lab) at the Georgia Institute of Technology (Kostas lab) (http://enve-omics.ce.gatech.edu/) (Rodriguez-R and Konstantinidis, 2016).

Metagenome assembly genome (MAGs) analysis

Three metagenome-assembled genomes (MAGs) of strain KS, strain BP and strain AG were obtained from the Joint Genome Institute's Integrated Microbial Genome and Microbiome Expert Review (IMG/MER) database (https://img.jgi.doe.gov/; (Chen *et al.*, 2019)). FeGenie (Garber *et al.*, 2020) was used to search for potential Fe(II) oxidation genes, e.g. *cyc2, mtoAB, mofA* (He *et al.*, 2017), and the IMG (Chen *et al.*, 2019) and the National Center for Biotechnology Information (NCBI) (https://www.ncbi.nlm.nih.gov/; (Coordinators, 2016; Schoch *et al.*, 2020) databases were used for obtaining genomes and 16S rRNA gene sequences of closely related taxa. The basic local alignment search tool (BLAST) (Altschul *et al.*, 1990) was used to compare the nearly full-length 16S rRNA gene sequences of the *Gallionellaceae* spp. of cultures KS, BP and AG to those gene sequences of *Gallionellaceae* spp. that were isolated or identified in environmental samples.

Scanning electron microscopy

For scanning electron microscopy (SEM) analysis, samples of the enrichment cultures KS, BP and AG were taken during the mid Fe(II)-oxidizing phase (after 3 days of incubation under autotrophic conditions) and at the end of the Fe(II) oxidation phase (after

6 days of incubation under autotrophic conditions). SEM samples were fixed in 2.5% glutaraldehyde for three hours on ice, by adding 100 µl of a 25% glutaraldehyde solution directly to 900 µl of centrifuged cell suspension in culture medium. After fixation, the samples were centrifuged (1 min, 2348x g) to concentrate the cells and approximately 900 µl of supernatant was removed and replaced by MQ H_2O to wash out the glutaraldehyde from the sample. This procedure was repeated twice. 25 µl of each sample was dropped onto Poly-l-Lysine coated cover glass slides [coated each with 75 µl 0.1% Poly-L-Lysine solution (PLANO, Wetzlar, item number 18026) and air dried over night before usage], placed in a 12-well plate. The plate was then covered with the plate lid and left for 15 minutes for the samples to settle. In the following, the samples were dehydrated by a graded ethanol series (30%, 70%, 95% for 5 min each; 2 x 100% for 30 min). In a final step, the samples were dipped into hexamethyldisilazane (HMDS) in two separated continuous-flow analysis vials in sequence for 30 seconds each and left to dry on filter paper afterwards. The cover glass slides were then fixed onto aluminum stubs with carbon tape (PLANO, Wetzlar, item numbers G301 & G3347) and sputter-coated with ~ 8 nm Pt by use of a BAL-TEC SCD 005. The SEM examination was performed at a Crossbeam 550L FIB-SEM (Zeiss, Oberkochen, Germany) using the InLens detector at an acceleration voltage of 2 kV and working distances of 4–5 mm.

Data availability and figure illustration

The heat maps were constructed via R v3.6.1 and its graphical user interface RStudio (https://www.R-project.org/ and http://www.rstudio.com/) (Team, 2019; Team, 2020).

The datasets presented in this study can be found in online repositories: SRR13504099 for culture BP including '*Ca*. Ferrigenium bremense' strain BP, and SRR10568922 for culture AG including '*Ca.* Ferrigenium altingense' strain AG (Table 4.1). The three nearly full-length 16S rRNA sequences of strain KS, strain BP and strain AG are provided in the supplementary file. The IMG metagenome IDs for cultures KS, BP and AG are 3300040739, 3300036710, and 3300041015 and the corresponding accession numbers of the MAGs of '*Ca.* Ferrigenium straubiae', '*Ca.* Ferrigenium bremense', and '*Ca.* Ferrigenium altingense' in IMG are 2878407288, 2831290873, and 2860363623, respectively (Table 4.1).

Table 4.1. Description table of '*Candidatus* Ferrigenium straubiae' sp. nov., '*Candidatus* Ferrigenium bremense' sp. nov. and '*Candidatus* Ferrigenium altingense' sp. nov.

Genus name	***Candidatus* Ferrigenium**	***Candidatus* Ferrigenium**	***Candidatus* Ferrigenium**
Species name	*straubiae*	*bremense*	*altingense*
Type species of the genus	*Ferrigenium kumadai* An22	*Ferrigenium kumadai* An22	*Ferrigenium kumadai* An22
Specific epithet	*straubiae*	*bremense*	*altingense*
Species status	sp. nov.	sp. nov.	sp. nov.
Species etymology	strau'bi.ae. N.L. gen. n. *straubiae*, of Straub, honouring Dr. Kristina Straub who enriched, cultured and studied the culture KS in 1993-1996.	bre.men'se. M.L. neut. adj. *bremense*, the enrichment sample originating from Bremen, Germany.	al.tin.gen'se. N.L. neut. adj. *altingense*, the enrichment sample originating from Altingen, Germany.
Description of the new taxon and diagnostic traits	Found in freshwater habitats. Cells are rod shaped. Fimbriae and flagella were not observed. Cells are 0.8–2.2 µm long and 0.2–0.7 µm wide. *In silico* genome analysis indicated that the species possesses potential Fe(II) oxidation genes: *cyc2, mtoAB, mofABC*; denitrification genes: *narGHIJ, nirK/S*; and the carbon fixation gene: *rbcL*.	Found in freshwater habitats. Cells are rod shaped. Fimbriae and flagella were not observed. Cells are 1.1–2.3 µm long and 0.2–0.6 µm wide. *In silico* genome analysis indicated that the species possesses potential Fe(II) oxidation genes: *cyc2*; denitrification genes: *narGHIJ, nirK/S*; and the carbon fixation gene: *rbcL*.	Found in freshwater habitats. Cells are rod shaped. Fimbriae and flagella were not observed. Cells are 0.5–1.8 µm long and 0.2–0.6 µm wide. *In silico* genome analysis indicated that the species possesses potential Fe(II) oxidation genes: *cyc2, mofAB (distant homologs)*; denitrification genes: *narGHIJ, nirK/S, norBC*; and the carbon fixation gene: *rbcL*.
Country of origin	Germany	Germany	Germany
Region of origin	Bremen, Bremen	Bremen, Bremen	Altingen, Baden-Wuerttemberg
Source of isolation	freshwater sediment	freshwater sediment	aquifer, groundwater monitoring well
Sampling date (dd/mm/yyyy)	1993	25/09/2015	12/09/2017
Latitude	-	53°06'36.7"N	48° 33' 47.52"N
Longitude	-	8°50'48.6"E	8° 53' 59.28"W
16S rRNA gene accession nr.	IMG gene ID: 2878408845	Sequence listed in supplementary file	IMG gene ID: 2860363887
IMG Genome ID	2878407288	2831290873	2860363623
Genome status	incomplete (MAG) completeness: 99.3%	incomplete (MAG) completeness: 93.2%	incomplete (MAG) completeness: 89.9%

Results and discussion

The novel strains represent dominant taxa of autotrophic NRFeOx enrichment cultures

Based on the near full-length 16S rRNA gene sequences analysis all three *Gallionellaceae* spp., strain KS, strain BP and strain AG, dominated the autotrophic NRFeOx enrichment cultures KS, BP and AG, with ≥95%, ≥71% and ≥50% relative sequence abundance, respectively (He *et al.*, 2016; Huang *et al.*, 2021a; Huang *et al.*, 2021b; Jakus *et al.*, 2021). Highest abundance of these strains was observed during the exponential phase of growth, i.e. during the most active Fe(II) oxidation and nitrate reduction phase. All three NRFeOx cultures were cultivated under anoxic autotrophic conditions with $FeCl_2$ and $NaNO_3$ (Straub *et al.*, 1996; Huang *et al.*, 2021b; Jakus *et al.*, 2021) as electron donor and acceptor, respectively. The average $Fe(II)_{oxidized}$/$nitrate_{reduced}$ stoichiometric ratio was 4.28 in culture KS, 3.4 in culture BP and 5.0 in culture AG. (Tominski *et al.*, 2018a; Huang *et al.*, 2021a; Huang *et al.*, 2021b; Jakus *et al.*, 2021).

Both culture KS and culture BP originate from freshwater sediments collected in Bremen from a ditch (Straub *et al.*, 1996) and a pond (Huang *et al.*, 2021b), respectively, while culture AG was obtained from an aquifer (Jakus *et al.*, 2021). The geochemistry at the habitat of enrichment culture KS's origin was neither stated in the first publication (Straub *et al.*, 1996) nor in subsequent publications. However, since the ditch of culture KS's origin is close by and connected to the pond of culture BP's origin, the geochemistry might be similar. The physiochemical conditions at the area of the sampling site, where culture BP was obtained, were measured in 2017 as follows; temperature: 11.7-11.9°C, pH: 6.0-6.3, oxygen saturation: 8.5-74.3%, conductivity: 32.5-36.8 µS/m, $Fe(II)_{pore\ water}$: 0.324-4.85 µM, $Fe(III)_{pore\ water}$: 2.51-1 µM, nitrate: 0.714 µM, total organic carbon (TOC) in sediment: 0.16-0.45% (wt%), and dissolved organic carbon (DOC) in pond water: 0.6-0.7 mg/L (Sauter, 2018). The physico-chemical parameters of the groundwater accessed via the monitoring well in Altingen were continuously monitored during observation periods (2004-2018) and the average values were calculated as follows; temperature: 12.5±1.6°C, pH: 7.1±0.1, dissolved O_2: 0.1±0.1 mg/L, conductivity: 885.1±75.1 µS/cm, nitrate concentration: 0.02±0.01 mM and DOC: 1.2±0.3 mg/L (Jakus *et al.*, 2021).

Despite the different isolation habitats of the three cultures, all three FeOB unite a unique feature within the family *Gallionellaceae*, i.e. the ability to grow under autotrophic anoxic conditions and perform partial nitrate reduction coupled to Fe(II) oxidation (Straub *et al.*, 1996; Huang *et al.*, 2021b; Jakus *et al.*, 2021). This unique capability differentiates them from all the isolated strains of the family *Gallionellaceae*, which typically perform microaerophilic Fe(II) oxidation using oxygen as electron acceptor (Kucera and Wolfe, 1957; Straub *et al.*, 1996; Emerson and Moyer, 1997; Krepski *et al.*, 2012; Kato *et al.*, 2014; Khalifa *et al.*, 2018; Huang *et al.*, 2021b; Jakus *et al.*, 2021).

Phylogenetic and genome (MAG) identity analysis of FeOB within the *Gallionellaceae*

In order to classify the three *Gallionellaceae* spp., strain KS, strain BP and strain AG, we performed phylogenetic analysis, using nearly full-length 16S rRNA gene sequences and available MAGs in the family *Gallionellaceae* (Fig. 4.1 and Fig. 4.2). Strain KS, strain BP and strain AG were closely related to each other and formed a novel clade within the phylogenetic tree (Fig. 4.1).

The most closely related isolated species was *Ferrigenium kumadai*, which is a microaerophilic Fe(II)-oxidizing bacterium and was cultivated using gradient tubes (Khalifa *et al.*, 2018). *Ferrigenium kumadai* has 96.45%, 96.17% and 96.24% of nearly full-length 16S rRNA gene sequence identity with strain KS, strain BP and strain AG, respectively (Fig. 4.2A) (Huang *et al.*, 2021a; Huang *et al.*, 2021b; Jakus *et al.*, 2021). The second most closely related isolated species of strain KS and strain BP was *Sideroxydans lithotrophicus* ES-1, with 95.9% and 95.30% identity of nearly full-length 16S rRNA gene sequences, respectively (Fig. 4.2A) (Huang *et al.*, 2021a; Huang *et al.*, 2021b). The second most closely related isolated species of strain AG was *Gallionella capsiferriformans* ES-2, sharing 96.17% of nearly full-length 16S rRNA gene sequence identity (Fig. 4.2A) (Jakus *et al.*, 2021).

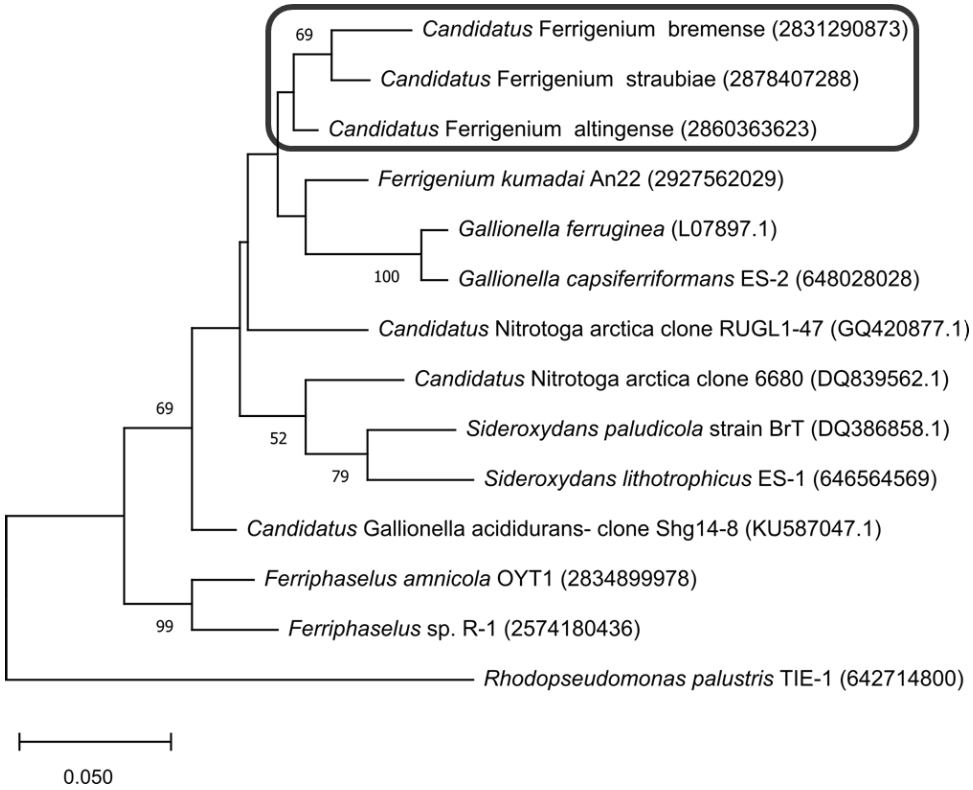

Figure 4.1. Phylogenetic tree of seven isolated *Gallionellaceae* spp. and six metagenome assembled genomes (*Candidatus* species), using available full or nearly full-length 16S rRNA gene sequences and calculated on 1000 replicates using the Maximum Likelihood method. The box highlights the species classified in this study. The scale bar represents branch lengths measured by the number of substitutions per site. The numbers in brackets show the identifier of each gene in the IMG or NCBI databases.

As with *Ferrigenium kumadai*, both *Sideroxydans lithotrophicus* ES-1 and *Gallionella capsiferriformans* ES-2 are microaerophilic Fe(II)-oxidizing bacteria (Emerson and Moyer, 1997) and have been cultivated using gradient tubes. While *Ferrigenium kumadai* An22 originated from rice paddy soil (Khalifa *et al.*, 2018), *Sideroxydans lithotrophicus* ES-1 and *Gallionella capsiferriformans* ES-2 were both from a groundwater-fed iron seep (Emerson and Moyer, 1997). The three *Gallionellaceae* spp., strain KS, strain BP and strain AG, revealed 16S rRNA gene similarities of 97.06-97.88% among each other indicating that they represent distinct species within the same genus (Fig. 4.2).

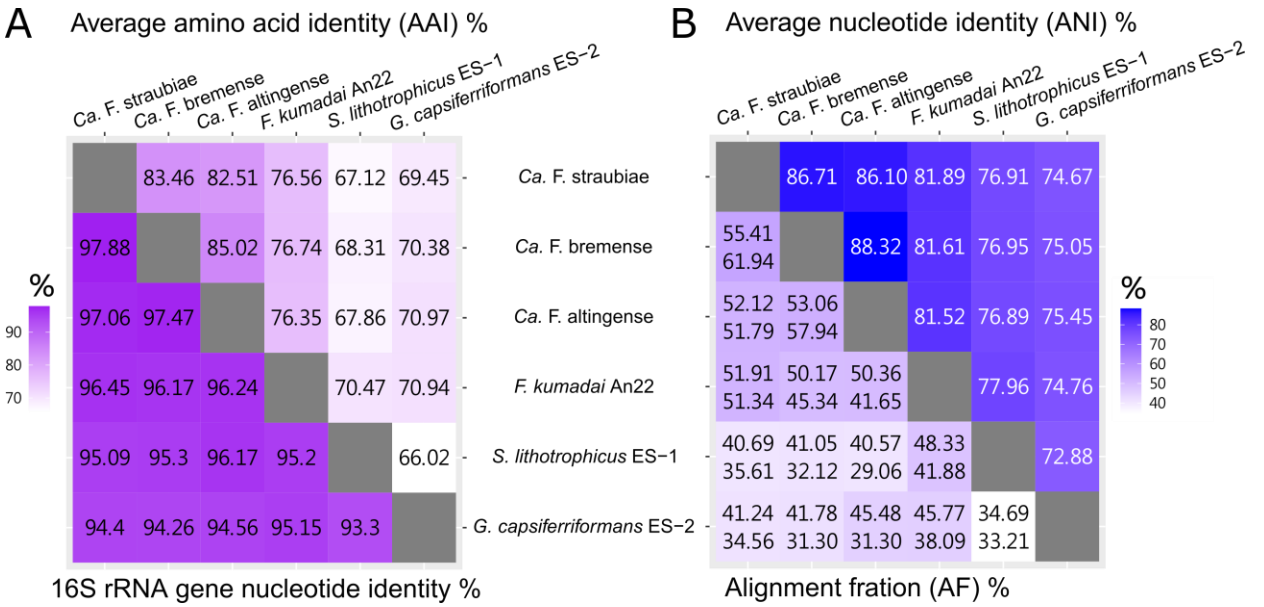

Figure 4.2. Nearly full-length 16S rRNA gene identity, average amino acid identity (AAI), average nucleotide identity (ANI), alignment fraction (AF; genome x aligned to genome y [upper no.], genome y aligned to genome x [lower no.]) of strains from '*Candidatus* Ferrigenium straubiae' (strain KS) sp. nov., '*Candidatus* Ferrigenium bremense' (strain BP) sp. nov. and '*Candidatus* Ferrigenium altingense' (strain AG) sp. nov. compared to their top three closely related isolated strains affiliating with the genera *Ferrigenium*, *Sideroxydans* and *Gallionella*. Recommended thresholds: nearly full-length 16S rRNA gene sequence identity: genus >95%, species >98.6%; AAI: genus 65–95%, species ≥95% (Konstantinidis *et al.*, 2017); ANI: species >96.5%; AF: species ≥60% (Varghese *et al.*, 2015; Barco *et al.*, 2020).

In addition, using metagenome binning methods, nearly complete and high-quality genomes (MAGs) were obtained for the *Gallionellaceae* spp. strain KS, strain BP and strain AG, with a completeness of 99.3%, 93.2% and 89.9%, respectively (Table 4.1) (Huang *et al.*, 2021a; Huang *et al.*, 2021b; Jakus *et al.*, 2021). Further, we compared the AAI and ANI of all five isolated *Gallionellaceae* spp. to the MAGs of strain KS, strain BP and strain AG. Based on the AAI and ANI results, the closest related, isolated strains affiliated with the genera *Ferrigenium*, *Sideroxydans* and *Gallionella* (Fig. 4.2A, 4.2B). All three of the novel *Gallionellaceae* spp., i.e. strain KS, strain BP and strain AG, displayed AAI values in the range between 76.35% to 76.74% for *Ferrigenium kumadai* and 67.12% to 70.97% for *Sideroxydans lithotrophicus* ES-1 and *Gallionella capsiferriformans* ES-2 (Fig. 4.2A). As the AAI of the three novel *Gallionellaceae* spp. compared to *Ferrigenium kumadai* were higher in comparison to *Sideroxydans lithotrophicus* ES-1 and *Gallionella capsiferriformans* ES-2, this indicates that all three strains (i.e. strain KS, strain BP and strain AG) belong to the same genus (AAI threshold >65%), postulated as genus

Ferrigenium, but represent different species (AAI threshold <95%) (Rodriguez-R and Konstantinidis, 2016). Notably, these results are consistent with the 16S rRNA gene-based results mentioned above. Moreover, these novel species, i.e. strain KS, strain BP and strain AG, have AAI values in the range of 82.51% to 85.02% compared to each other (Fig. 4.2A), suggesting that they are more closely related to each other than to any described isolate. This result suggests that they should be probably consisted as distinct species of the same genus. As for ANI, a threshold of ANI ≥ 96.5% (alignment fraction: AF ≥ 60%) was proposed for the same species (Varghese *et al.*, 2015; Barco *et al.*, 2020). Our results showed that the ANI values between the three novel *Gallionellaceae* spp. and the most closely related isolate, *Ferrigenium kumadai*, range between 81.12% to 81.38% (Fig. 4.2B), while the ANI to *Sideroxydans lithotrophicus* ES-1 and *Gallionella capsiferriformans* ES-2 are in the range of 75.05% to 79.47% (Fig. 4.2B).

For more evidence of the genealogical position, the amino acid sequences of house-keeping genes, which encode the RNA polymerase α subunit (*rpoA*), DNA gyrase α subunit (*gyrA*), protein translocase subunit (*secA*), isoleucyl-tRNA synthetase (*ileS*), rho termination factor (*rho*), and translation initiation factor IF-2 (*infB*), were selected to generate a concatenated maximum likelihood phylogenetic tree (Fig. 4.3) (Holmes *et al.*, 2004; Emerson *et al.*, 2013; Glaeser and Kämpfer, 2015; Rocha *et al.*, 2015). The phylogenetic analysis of concatenated house-keeping genes indicated that strain KS, strain BP and strain AG were closely affiliated to *Ferrigenium kumadai* An22, and were more distantly related to other isolated members of *Gallionellaceae* genera, a proposed neutrophilic mixotrophic nitrate-reducing FeOB, i.e. *Thiobacillus denitrificans* (Beller *et al.*, 2006b) and an acidophilic aerobic FeOB, i.e. *Acidithiobacillus ferrooxidans* (Fig. 4.3) (Valdés *et al.*, 2008). Taken together the results of nearly full-length 16S rRNA gene identity and phylogeny as well as AAI, ANI and house-keeping gene phylogenetic analyses indicated strain KS, strain BP and strain AG, belong to the same genus, postulated as *Ferrigenium*, but represent different species.

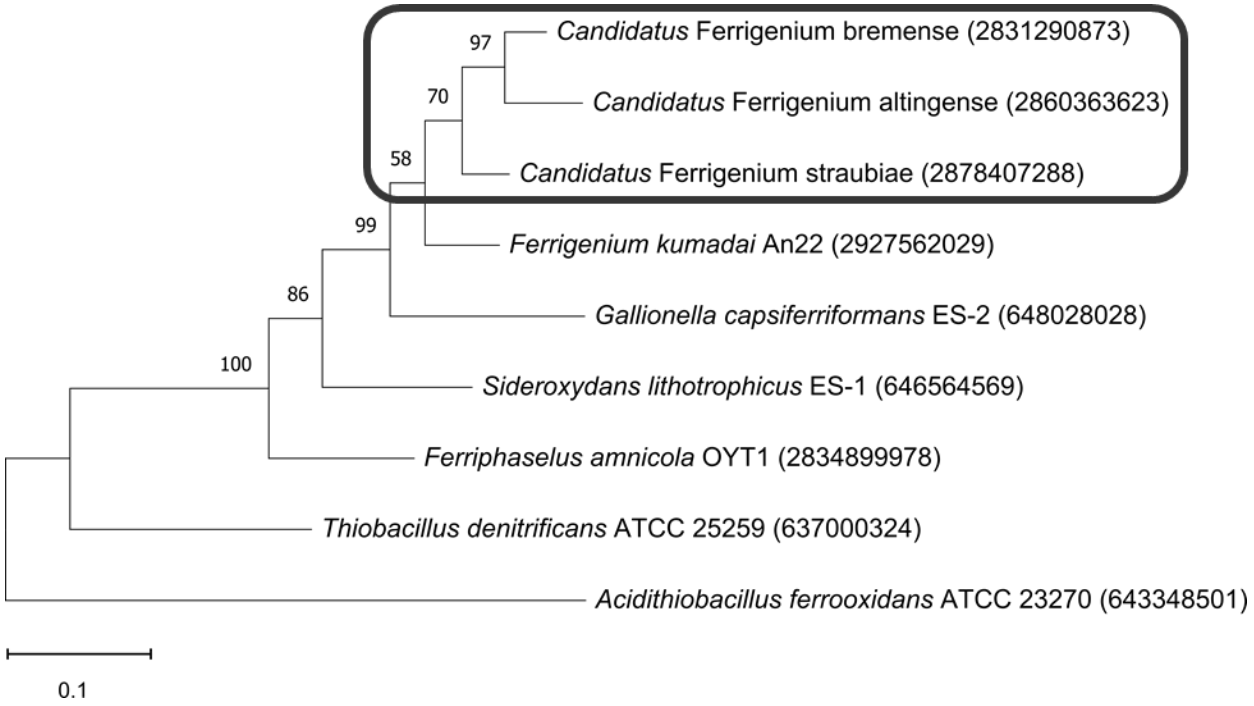

Figure 4.3. Phylogenetic tree of nine concatenated house-keeping genes amino acid sequences of *rpoA, gyrA, secA, ileS, rho* and *infB* of isolated and *Candidatus* members of the *Gallionellaceae* family and other FeOB, calculated on 1000 replicates using the Maximum Likelihood method. The box highlights the species classified in this study. The scale bar represents branch lengths measured by the number of substitutions per site. The numbers in brackets show the identifier of each gene in IMG.

Putative metabolic and physiological features

The metagenomic results showed that all three *Gallionellaceae* MAGs of strain KS, strain BP and strain AG have at least one putative Fe(II) oxidation gene, which could accept the electrons from the Fe(II) substrate, i.e. *cyc2* and *mofA* for all three MAGs and *mtoA* in the MAG of strain KS (Fig. 4.4) (He *et al.*, 2016; He *et al.*, 2017; Huang *et al.*, 2021b; Jakus *et al.*, under review; and provided to the reviewers with this submission). Among these genes, *cyc2*, *mtoA* and *mofA* were detected at transcript level and MofA was detected at protein level in culture KS (Huang *et al.*, 2021a). On the other hand, both transcript and protein of *cyc2* were detected in culture BP (Huang *et al.*, 2021b). To date, a metagenome was constructed and analyzed for culture AG (Jakus *et al.*, under review; and provided to the reviewers with this submission), while metatranscriptomic and metaproteomic analysis for culture AG have not yet been done.

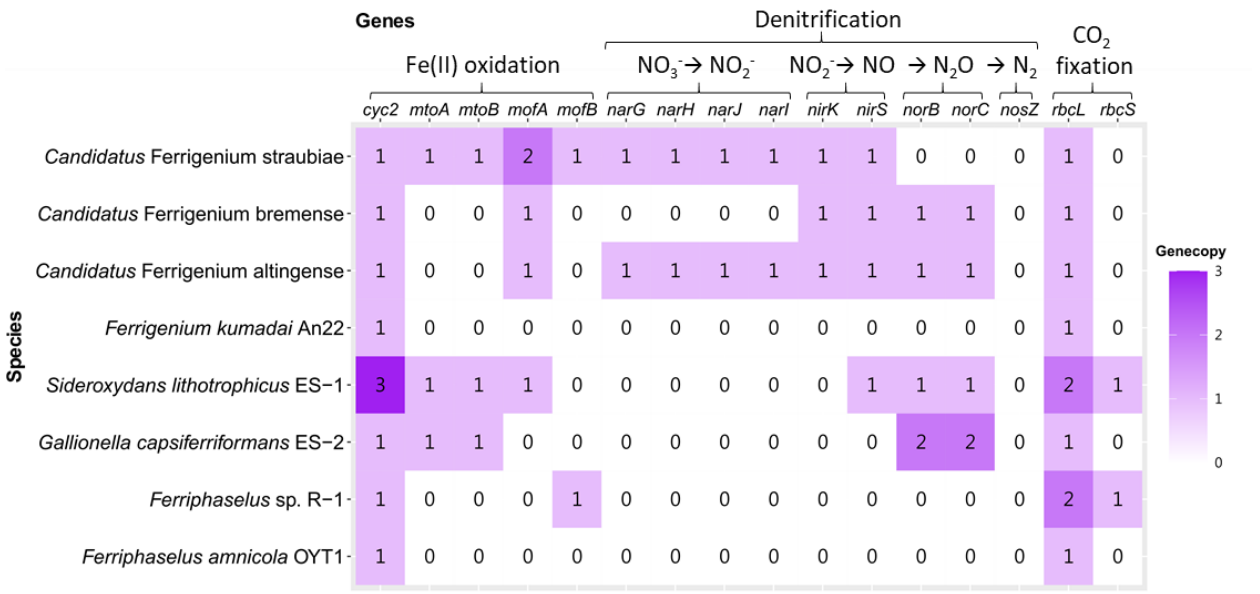

Figure 4.4. Summary of key gene copy numbers involved in putative Fe(II)-oxidation, denitrification and carbon fixation of '*Ca.* Ferrigenium straubiae', '*Ca.* Ferrigenium bremense' and '*Ca.* Ferrigenium altingense', *Ferrigenium kumadai* An22, *Sideroxydans lithotrophicus* ES-1, *Gallionella capsiferriformans* ES-2, *Ferriphaselus* sp. R-1, *Ferriphaselus amnicola* OYT1.

As for the electron acceptor, the genes for a partial denitrification pathway detected in MAGs of the strain KS, strain BP and strain AG were different. For strain KS, the genes, transcripts and proteins encoding nitrate reductase (NarGHI) and nitrite reductase (NirK/S) were detected under autotrophic conditions (Fig. 4.4) (Huang *et al.*, 2021a). For strain BP, the genes, transcripts and proteins encoding NirK/S were detected and the genes and transcripts encoding nitric oxide reductase (NorBC) were detected under autotrophic conditions (Fig. 4.4) (Huang *et al.*, 2021b). The genes encoding NarGHI, NirK/S and NorBC were all detected in strain AG (Fig. 4.4) (Jakus *et al.*, under review; and provided to the reviewers with this submission). These results indicated that strain KS, strain BP and strain AG have the ability to perform only partial denitrification. As previously suggested (Huang *et al.*, 2021a; Huang *et al.*, 2021b; Jakus *et al.*, under review; and provided to the reviewers with this submission), they might require other denitrifiers to complete the denitrification pathways.

An alternative electron accepting pathway was speculated to be oxidative phosphorylation (e.g., via respiratory chain complexes I-V) (Mitchell, 1961; Kalckar, 1991; He *et al.*, 2016). The genetic potential for energy generation via respiratory chain complexes I-V were detected in strain KS, strain BP and strain AG (He *et al.*, 2016; Huang *et al.*, 2021b; Jakus *et al.*, under review; and provided to the reviewers with this submission). Interestingly, the

detection of homologous genes encoding the *cbb*$_3$- and *aa*$_3$- type cytochrome *c* oxidases of complex IV indicates that strain KS, strain BP and strain AG could have the ability to respire oxygen (Huang *et al.*, 2021a; Huang *et al.*, 2021b; Jakus *et al.*, under review; and provided to the reviewers with this submission). Some microoxic growth conditions were tested for culture KS (Tominski *et al.*, 2018a), as well as culture AG (Jakus *et al.*, 2021), i.e. in gradient tubes or zero valent iron plates, but a stable growth was not yet observed. Moreover, due to the detection of the essential gene of carbon fixation, i.e. the large subunit ribulose-1,5-bisphosphate carboxylase-oxygenase gene (*rbcL*), it was proposed that strain KS, strain BP and strain AG have the ability to fix carbon to grow under autotrophic conditions (He *et al.*, 2016; Tominski *et al.*, 2018b; Huang *et al.*, 2021a; Huang *et al.*, 2021b; Jakus *et al.*, under review; and provided to the reviewers with this submission). The dominance of strain KS, strain BP and strain AG in the different NRFeOx enrichment cultures, i.e. culture KS, culture BP and culture AG, respectively, was likely caused by the ability to fix carbon by these three strains. In culture KS, carbon fixation by strain KS was additionally reported using nanoscale secondary ion mass spectrometry (NanoSIMS) to monitor the fate of ^{13}C-labeled bicarbonate (Tominski *et al.*, 2018b) and the transcript and protein encoding the essential carbon fixation enzyme, RbcL, were detected for strain KS under autotrophic conditions (Huang *et al.*, 2021a). For strain BP, the transcript of *rbcL* was also detected (Huang *et al.*, 2021b), while there are currently no transcript and protein data available for culture AG .

Morphology of the three *Gallionellaceae* spp.

In this study, we analyzed the cell morphology by scanning electron microscopy (SEM) (Fig. 4.5). It should be noted, however, that the timepoint for SEM sampling was determined based on relative nearly full-length 16S rRNA gene sequence abundance to capture the most dominant strains (i.e. Fe(II) oxidizers); the relative abundance of strain KS, strain BP, and strain AG in the three cultures KS, BP and AG were ≥95%, ≥71% and ≥50% (Huang *et al.*, 2021b; Jakus *et al.*, 2021). For strain KS, the cell sizes (averaged for 17 cells) ranged from 0.8-2.2 µm in length and 0.2-0.7 µm in width (Table 4.2). For strain BP, the cell sizes (averaged for 27 cells) ranged from 1.1-2.3 µm in length and 0.2-0.6 µm in width (Table 4.2). As for strain AG, the cell sizes (averaged for 15 cells) ranged from 0.5-1.8 µm in length and 0.2-0.6 µm in width (Table 4.2). In the SEM images of the three

enrichment cultures, the observed cells were either rod shaped or they revealed a slightly curved rod shape (Fig. 4.5). Given the fact that strain KS, strain BP and strain AG dominate the enrichment cultures KS, BP and AG, respectively, we estimated the morphology of strain KS, strain BP and strain AG based on the dominating morphological type of the culture, i.e. the rod or slightly curved rod-shaped cells. For culture KS, there were in addition several different imaging analyses performed in previous studies: 4',6-diamidino-2-phenylindole (DAPI) staining (Tominski *et al.*, 2018a; Tominski *et al.*, 2018b) and fluorescence *in situ* hybridization (FISH) in combination with fluorescence microscopy, and helium ion microscopy (HIM) (Nordhoff *et al.*, 2017). The results for cell sizes and cell morphology of these imaging analyses corresponded to the SEM observations for strain KS in this study. No diagnostic stalks or capsules were observed for the three cultures using SEM. Most of the cells we observed in all three cultures (i.e. 16 out of 17 cells analyzed for culture KS, 25 out of 27 cells for culture BP and 15 out of 15 cells for culture AG) were closely associated with minerals and in a few cases, cells even seemed to be partly or completely encrusted in Fe minerals, although it remains unknown whether these cells were still alive or whether such encrustation only happened with dead or inactive cells. Additionally, although the genes for flagellar assembly were detected in the three MAGs of strain KS, strain BP and strain AG, the fimbriae and flagella were not observed under SEM. However, during the chemical preparation, the fimbriae and flagella might have been destroyed and, thus, we cannot rule out the existence of fimbriae and flagella. Motility was furthermore not observed for cells of cultures KS, BP and AG using light microscopy.

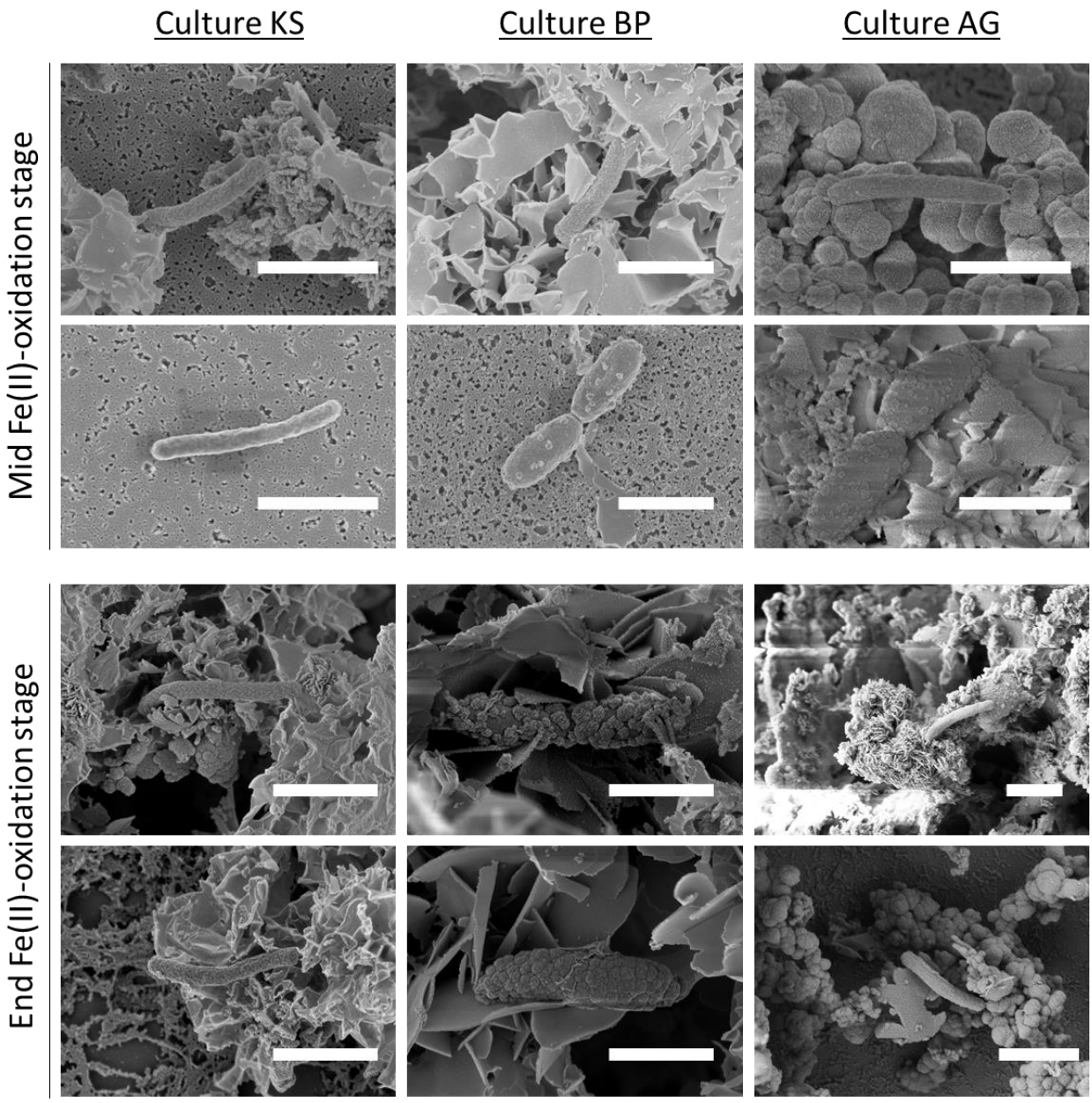

Figure 5. Scanning electron microscopy (SEM) pictures of culture KS, culture BP and culture AG during the mid Fe(II)-oxidation stage (exponential growth phase) and at the end of the Fe(II)-oxidation stage (lag phase). The scale bars represent 1 µm. Cells were slightly curved rod shaped and partly encrusted with putative Fe(III) minerals in cultures BP and AG (and to a minor extent in culture KS; not shown), especially at end of the Fe(II)-oxidation stage.

Table 4.2. Phenotypic and genotypic information of '*Candidatus* Ferrigenium straubiae' sp. nov., '*Candidatus* Ferrigenium bremense' sp. nov. and '*Candidatus* Ferrigenium altingense' sp. nov. compared with closely related strains of different genera in the family *Gallionellaceae.*

Characteris-tics	***Candidatus* Ferrigenium straubiae**	***Candidatus* Ferrigenium bremense**	***Candidatus* Ferrigenium altingense**	***Ferrigenium kumadai* An22**	***Sideroxydans lithotrophicus* ES-1**	***Gallionella capsiferriformans* ES-2**
Isolation source	Sediment	Sediment	Aquifer	Rice paddy soil	Groundwater	Groundwater
Geographic location	Bremen, Germany	Bremen, Germany	Altingen, Germany	Anjo, Japan	Michigan, USA	Michigan, USA
Cell morphology	curved rod	curved rod	curved rod	curved rod	helical rod	curved rod
Cell size (LxW, in µm)	0.8–2.2 x 0.2–0.7†	1.1–2.3 x 0.2–0.6†	0.5–1.8 x 0.2–0.6†	0.9–2.0 x 0.2–0.4	0.3 diameter	0.7 diameter
Stalk formation	N/O	N/O	N/O	-	-	-
Motile/Flagella	N/O	N/O	N/O	+	+	+
Doubling time (h)	9.4±2.9	46.11#	34.98#	6.2	8	12.5
highest relative abundance in the culture	98%	86%	68%	N/A	N/A	N/A
Genome size (bp)	2,659,708	2,446,084	2,180,025	2,572,603	3,003,656	3,162,471
G + C content (mol %)	60.13	58.92	57.97	61.4	57.5	52.8
16S rRNA gene copies	2	1	1	2	2	3
Fe(II) oxidation	+	+	+	+	+	+
Carbon fixation	+	+	+	+	+	+
Growth temperature	28°C*	28°C*	25°C*	12 - 37°C	10 - 35°C	4 - 30°C
Growth pH	6.8-7.2*	6.9-7.2*	6.0-7.0*	5.2–6.8	5.5-7.0	5.5-7.0
Reference	(Straub *et al.*, 1996; He *et al.*, 2016; Tominski *et al.*, 2018b; Huang *et al.*, 2021a)	(Huang *et al.*, 2021b)	(Jakus *et al.*, 2021; Jakus *et al.*, under review; and provided to the reviewers with this submission)	(Khalifa *et al.*, 2018)	(Emerson *et al.*, 2013)	(Emerson *et al.*, 2013)

† Cell size was estimated using SEM analysis of enrichment culture at a time point where the strain dominated the culture
N/A: not applicable; N/O: not observed
Doubling time of '*Ca.* Ferrigenium bremense' and '*Ca.* Ferrigenium altingense' was estimated by multiplying total cell counts of the enrichment culture obtained by flow cytometry with relative abundance data determined by V4 region 16S rRNA gene amplicon sequencing, respectively, as reported previously (Huang *et al.*, 2021b; Jakus *et al.*, 2021).
* Temperature and pH of the whole enrichment culture KS, BP and AG was measured.

Environmental occurrence

To estimate the environmental occurrence, i.e. potential niches and preferred habitats, of the three FeOB and closely related organisms that affiliate with the same species (and the same strain), nearly full-length 16S rRNA gene sequences that showed a similarity >98.6% (and >99.5%) compared to strain KS, strain BP or strain AG were identified using the BLAST function and the NCBI database. For strain KS, the highest similarity (nearly full-length 16S rRNA gene identity 99.52-99.93%) was found for sequences originating from a parallel culture to culture KS cultivated at the University of Wisconsin - Madison and identified as uncultured betaproteobacterium sp. (acc. nos. FN430662.1, FN430666.1, FN430669.1, FN430668.1, FN430670.1, FN430663.1 and FN430659.1; clones F25F63, F29F67, F32F70, F31F69, F33F71, F26F64 and F21F59) (Blöthe and Roden, 2009). In addition, an uncultured bacterial sequence from an iron-rich microbial mat revealed 99.43% nearly full-length 16S rRNA gene identity (acc. no. LN870688.1; clone Hoffnungsstollen_#4-1A_D09) (Zeitvogel et al., unpublished). For strain BP, the most closely related sequence (nearly full-length 16S rRNA gene identity of 99.26%) was identified as an uncultured bacterium from a polycyclic aromatic hydrocarbon (PAH) degrading bacterial community of a PAH-contaminated soil (acc. no. FQ659636.1; clone I1AB101) (Martin *et al.*, 2012). For strain AG, closely related sequences (nearly full-length 16S rRNA gene identity of 100% and 99.93%) were retrieved from a stratified freshwater lake, Lake Mizugaki, in Japan (acc. nos. AB754138.1 and AB754154.1; clones rS43m_43 and rS43m_63) (Kojima *et al.*, 2014). Additional closely related sequences were identified as an uncultured *Gallionella* sp. (99.93% nearly full-length 16S rRNA gene sequence identity; acc. no. AM167950.1; clone BB03) from spring water consisting mostly of groundwater (Wagner *et al.*, 2007), an uncultured betaproteobacterium sp. (99.80%, 99.53% and 99.53% nearly full-length 16S rRNA gene sequence identity; acc. nos. JQ278897.1, JQ278948.1 and JQ279049.1; clones hmx-114, sf-34 and sz-131) from groundwater (Guan *et al.*, 2013), and an uncultured bacterium sp. (99.67% nearly full-length 16S rRNA gene sequence identity; acc. no. AY662038.1; clone 015C-C11) from nitric acid-bearing uranium waste contaminated groundwater (Fields *et al.*, 2005). The uncultured bacterial sequence from the iron-rich microbial mat (acc. no. LN870688.1; clone Hoffnungsstollen_#4-1A_D09) had 99.79% nearly full-length 16S rRNA gene

identity compared to strain AG (Zeitvogel et al., unpublished). From previous studies, it was reported that strain BP has ca. 0.13% relative abundance *in situ* at the origin (i.e. the freshwater pond) (Huang *et al.*, 2021b) and strain AG has ca. 14% relative abundance *in situ* at the origin (i.e. in groundwater samples from the Ammer catchment; Blackwell et al, unpublished), while no *in situ* abundance data were reported for strain KS. In summary, closely related sequences of strain KS, strain BP and strain AG were mainly identified in freshwater ecosystems, e.g. groundwater, pond or ditch sediments, as well as aquifer and wetland soils.

Table 4.3. Standard nucleotide BLAST search results to NCBI nucleotide collection (nr/nt) (June 8, 2021) of closely related sequences (>98.6% nearly full-length 16S rRNA gene identity) of strain KS, strain BP and strain AG.

Description	Query Cover	Identity (%)	Length (bp)	Accession No.	Habitat	Location	Refernce
Sequences >98.6% identical to strain KS							
Uncultured beta proteobacterium 16S rRNA gene, clone F25F63	100%	100	1464	FN430662.1	autotrophic Fe(II)-oxidizing, nitrate-reducing enrichment culture KS	Bremen, Germany	(Blöthe and Roden, 2009)
Uncultured beta proteobacterium 16S rRNA gene, clone F29F67	100%	99.93	1464	FN430666.1	autotrophic Fe(II)-oxidizing, nitrate-reducing enrichment culture KS	Bremen, Germany	(Blöthe and Roden, 2009)
Uncultured beta proteobacterium 16S rRNA gene, clone F32F70	100%	99.86	1464	FN430669.1	autotrophic Fe(II)-oxidizing, nitrate-reducing enrichment culture KS	Bremen, Germany	(Blöthe and Roden, 2009)
Uncultured beta proteobacterium 16S rRNA gene, clone F31F69	100%	99.73	1464	FN430668.1	autotrophic Fe(II)-oxidizing, nitrate-reducing enrichment culture KS	Bremen, Germany	(Blöthe and Roden, 2009)
Uncultured beta proteobacterium 16S rRNA gene, clone F33F71	100%	99.59	1464	FN430670.1	autotrophic Fe(II)-oxidizing, nitrate-reducing enrichment culture KS	Bremen, Germany	(Blöthe and Roden, 2009)
Uncultured beta proteobacterium 16S rRNA gene, clone F26F64	100%	99.59	1464	FN430663.1	autotrophic Fe(II)-oxidizing, nitrate-reducing enrichment culture KS	Bremen, Germany	(Blöthe and Roden, 2009)
Uncultured bacterium partial 16S rRNA gene, clone Iron-rich microbial mat clone Hoffnungsstollen_#4-1A_D09	94%	99.56	1396	LN870688.1	environmental Fe-rich microbial mats, abandoned pyrrhotite mine Hoffnungsstollen	Black Forest, Germany	(Zeitvogel et al, unpublished)
Uncultured beta proteobacterium 16S rRNA gene, clone F21F59	100%	99.52	1464	FN430659.1	autotrophic Fe(II)-oxidizing, nitrate-reducing enrichment culture KS	Bremen, Germany	(Blöthe and Roden, 2009)
Uncultured beta proteobacterium 16S rRNA gene, clone F28F66	100%	99.38	1464	FN430665.1	autotrophic Fe(II)-oxidizing, nitrate-reducing enrichment culture KS	Bremen, Germany	(Blöthe and Roden, 2009)
Uncultured beta proteobacterium 16S rRNA gene, clone F22F60	100%	99.38	1464	FN430660.1	autotrophic Fe(II)-oxidizing, nitrate-reducing enrichment culture KS	Bremen, Germany	(Blöthe and Roden, 2009)

Table 4.3. (continued) Standard nucleotide BLAST search results to NCBI nucleotide collection (nr/nt) (June 8, 2021) of closely related sequences (>98.6% nearly full-length 16S rRNA gene identity) of strain KS, strain BP and strain AG.

Description	Query Cover	Identity (%)	Length (bp)	Accession No.	Habitat	Location	Refernce
Sequences >98.6% identical to strain BP							
Uncultured bacterium 16S ribosomal RNA gene clone I1AB101, partial sequence	93%	99.26	1359	FQ659636.1	PAH degrading bacterial community of a contaminate soil	Chambéry, France	(Martin *et al.*, 2012)
Uncultured bacterium clone VE08-104-BAC 16S ribosomal RNA gene, partial sequence	94%	98.77	1398	GQ340331.1	Drinking water reservoir	Marathonas, Greece	(Lymperopoulou *et al.*, 2012)
Uncultured bacterium gene for 16S rRNA, partial sequence, clone: RB112	97%	98.74	1444	AB240306.1	rhizosphere of Phragmites	Sapporo, Japan	(Okabe et al, unpublished)
Sequences >98.6% identical to strain AG							
Uncultured bacterium gene for 16S ribosomal RNA, partial sequence, clone: rS43m_43	94%	100	1460	AB754138.1	stratified freshwater lake	Yamanashi, Japan	(Kojima *et al.*, 2014)
Uncultured Gallionella sp. partial 16S rRNA gene, clone BB03	96%	99.93	1491	AM167950.1	deep igneous rock aquifers	Bad Brambach, Germany	(Wagner *et al.*, 2007)
Uncultured bacterium gene for 16S ribosomal RNA, partial sequence, clone: rS43m_63	94%	99.93	1460	AB754154.1	stratified freshwater lake	Yamanashi, Japan	(Kojima *et al.*, 2014)
Uncultured beta proteobacterium clone hmx-114 16S ribosomal RNA gene, partial sequence	97%	99.8	1497	JQ278897.1	groundwater	China	(Guan *et al.*, 2013)
Uncultured bacterium partial 16S rRNA gene, clone Iron-rich microbial mat clone Hoffnungsstollen_#5-1B_E10	90%	99.79	1396	LN870871.1	environmental Fe-rich microbial mats	Black Forest, Germany	(Zeitvogel et al, unpublished)
Uncultured bacterium clone 015C-C11 small subunit ribosomal RNA gene, partial sequence	99%	99.67	1529	AY662038.1	groundwater	USA	(Fields *et al.*, 2005)

Table 4.3. (continued) Standard nucleotide BLAST search results to NCBI nucleotide collection (nr/nt) (June 8, 2021) of closely related sequences (>98.6% nearly full-length 16S rRNA gene identity) of strain KS, strain BP and strain AG.

Description	Query Cover	Identity (%)	Length (bp)	Accession No.	Habitat	Location	Refernce
Sequences >98.6% identical to strain AG							
Uncultured beta proteobacterium clone sf-34 16S ribosomal RNA gene, partial sequence	97%	99.53	1498	JQ278948.1	groundwater	China	(Guan *et al.*, 2013)
Uncultured beta proteobacterium clone sz-131 16S ribosomal RNA gene, partial sequence	97%	99.53	1497	JQ279049.1	groundwater	China	(Guan *et al.*, 2013)
Uncultured Gallionella sp. partial 16S rRNA gene, clone BB49	99%	99.22	1529	AM167944.1	deep igneous rock aquifers	Bad Brambach, Germany	(Wagner *et al.*, 2007)
Uncultured Gallionella sp. partial 16S rRNA gene, clone BB28	96%	99.13	1491	AM167970.1	deep igneous rock aquifers	Bad Brambach, Germany	(Wagner *et al.*, 2007)
Uncultured beta proteobacterium clone sf-73 16S ribosomal RNA gene, partial sequence	97%	99.06	1494	JQ278969.1	groundwater	China	(Guan *et al.*, 2013)
Uncultured bacterium clone EMIRGE_OTU_s5t4a_5708 16S ribosomal RNA gene, partial sequence	97%	99.06	1499	JX223560.1	subsurface aquifer sediment	Rifle, USA	(Handley et al, unpublished)
Uncultured beta proteobacterium clone fjc-85 16S ribosomal RNA gene, partial sequence	97%	99	1495	JQ278828.1	groundwater	China	(Guan *et al.*, 2013)
Uncultured bacterium clone EMIRGE_OTU_s3t2d_3118 16S ribosomal RNA gene, partial sequence	97%	99	1500	JX222776.1	subsurface aquifer sediment	Rifle, USA	(Handley et al, unpublished)
Uncultured Gallionella sp. partial 16S rRNA gene, clone BB46	99%	98.95	1528	AM167953.1	deep igneous rock aquifers	Bad Brambach, Germany	(Wagner *et al.*, 2007)
Uncultured Gallionella sp. partial 16S rRNA gene, clone BB59	99%	98.89	1530	AM167946.1	deep igneous rock aquifers	Bad Brambach, Germany	(Wagner *et al.*, 2007)

Conclusion

Overall, from the ecological traits, unique metabolic and physiological features, phylogenetic and MAG identity analyses, we propose the name of these three FeOB species as '*Candidatus* Ferrigenium straubiae' sp. nov., '*Candidatus* Ferrigenium bremense' sp. nov. and '*Candidatus* Ferrigenium altingense' sp. nov., named after 'Kristina Straub' who originally isolated culture KS, 'Bremen Pond' the location of culture BP's isolation and 'Altingen Groundwater' the location of culture AG's isolation. The detailed description of the proposed species is shown in table 4.1 and the phenotypic and genotypic information compared to closely related isolates of the proposed species are described in table 4.2.

5. Microbial anaerobic Fe(II) oxidation – ecology, mechanisms and environmental implications

environmental microbiology

Environmental Microbiology (2018) **20**(10), 3462–3483 doi:10.1111/1462-2920.14328

Minireview

Microbial anaerobic Fe(II) oxidation – Ecology, mechanisms and environmental implications

Casey Bryce,[1*] Nia Blackwell,[1] Caroline Schmidt,[1] Julia Otte,[1] Yu-Ming Huang,[1] Sara Kleindienst,[1] Elizabeth Tomaszewski,[1] Manuel Schad,[1] Viola Warter,[1] Chao Peng,[1] James M. Byrne[1] and Andreas Kappler[1,2]

[1]*Geomicrobiology, University of Tübingen, Tübingen, Germany.*

[2]*Center for Geomicrobiology, Department of Bioscience, Aarhus University, Aarhus, Denmark.*

Summary

Iron is the most abundant redox-active metal in the Earth's crust. The one electron transfer between the two most common redox states, Fe(II) and Fe(III), plays a role in a huge range of environmental processes from mineral formation and dissolution to contaminant remediation and global biogeochemical cycling. It has been appreciated for more than a century that microorganisms can harness the energy of this Fe redox transformation for their metabolic benefit. However, this is most widely understood for anaerobic Fe(III)-reducing or aerobic and microaerophilic Fe(II)-oxidizing bacteria. Only in the past few decades have we come to appreciate that bacteria also play a role in the anaerobic oxidation of ferrous iron, Fe(II), and thus can act to form Fe(III) minerals in anoxic settings. Since this discovery, our understanding of the ecology of these organisms, their mechanisms of Fe(II) oxidation and their role in environmental processes has been increasing rapidly. In this article, we bring these new discoveries together to review the current knowledge on these environmentally important bacteria, and reveal knowledge gaps for future research.

Biogeochemistry of iron

A substantial amount of iron (Fe) is present in soils, as well as freshwater, marine and subsurface sediments. Under oxidizing conditions, iron is found mainly in Fe(III) (oxyhydr) oxide minerals such as ferrihydrite ($Fe(OH)_3$), goethite (α-FeOOH) and haematite (α-Fe_2O_3), as well as, to a lesser extent, in dissolved Fe(III)-natural-organic-matter complexes (Fe(III)-NOM complexes) (Carlson and Schwertmann, 1981; Schwertmann and Murad, 1988; Kostka and Luther, 1994). Under reducing conditions iron is mostly found in mixed-valent Fe minerals such as magnetite and green rust, or in Fe(II) minerals such as vivianite ($Fe_3(PO_4)_2 \cdot 8H_2O$) and siderite ($FeCO_3$), or even as dissolved Fe^{2+} ions (Thompson *et al*., 2011; Daugherty *et al*., 2017; Ginn *et al*., 2017; Herndon *et al*., 2017). Under both oxidizing and reducing conditions, iron can be found as structural components of silicate minerals such as clays (Pentráková *et al*., 2013) and in iron sulfide minerals. It has also been suggested that dissolved Fe(III)- and Fe(II)-complexes and colloids are important for iron biogeochemical processes (Luther *et al*., 1992; Taillefert *et al*., 2000). The fate of iron in the environment is controlled by a series of abiotic and microbially catalysed redox reactions that lead to Fe mineral formation, transformation and dissolution (Melton *et al*., 2014a). Abiotic reactions include the oxidation of Fe(II) by manganese oxides, by oxygen and nitrogen species, or by reactive radicals from natural organic matter (NOM). Additionally, Fe(II) can be formed by photochemical reduction of Fe(III), particularly in water columns, as well as by reduction of Fe(III) by sulfide and reduced NOM (Melton *et al*., 2014a).

Microbial Fe(III) reduction can reduce Fe(III) minerals, and in turn provide Fe(II) as either a dissolved or solid phase electron donor for Fe(II)-oxidizing bacteria. Under acidic and pH-neutral conditions, aerobic and microaerophilic Fe(II)-oxidizing bacteria can use O_2 as an electron acceptor for oxidation of Fe(II) to Fe(III). Almost 200 years ago, Ehrenberg (1836) described microbially-produced stalk-like iron oxide structures reminiscent of those now known to be produced by microaerophilic Fe(II)-oxidizing bacteria. However, in the last two decades, two other metabolic types of Fe(II)-oxidizers were discovered which require anoxic conditions and oxidize Fe(II) coupled to either nitrate reduction (NRFeOx, Eq. 1) or to photosynthesis (pFeOx, Eq. 2) (Widdel *et al*., 1993; Straub *et al*., 1996).

Received 30 January, 2018; revised 15 June, 2018; accepted 16 June, 2018. *For correspondence. E-mail casey.bryce@uni-tuebingen.de; Tel. +49-7071-2974708; Fax +49-7071-29-295059.

$$10Fe^{2+} + 2NO_3^- + 24H_2O \rightarrow 10Fe(OH)_3 + N_2 + 18H^+ \quad (1)$$

$$HCO_3^- + 4Fe^{2+} + 10H_2O \rightarrow (CH_2O) + 4Fe(OH)_3 + 7H^+ \quad (2)$$

Oxygen is not abundant in all habitats on Earth: for example, vast regions of oceans and lakes are either seasonally or permanently anoxic. Oxygen can only be measured down to a few millimetres depth in soils and sediments, particularly if they are waterlogged and organic-rich. Similarly, the deep sea and the deep continental crust are oxygen-poor. Thus, the discovery of these anaerobic Fe(II)-oxidizers revealed that microorganisms could contribute to Fe(II) oxidation in environments which had previously been overlooked, rapidly broadening our appreciation of the importance of Fe(II)-oxidizing bacteria in the environment. Several strains of NRFeOx and pFeOx have been isolated and more and more data from genomic, metagenomic and metatranscriptomic studies are available (He *et al*., 2016; Jewell *et al*., 2016), yet our understanding of the ecological contribution, the physiology and of the enzymatic mechanism(s) of anaerobic Fe(II) oxidation is still very limited compared with our understanding of microbial Fe(III) reduction or microaerophilic Fe(II) oxidation. The physiology of these organisms is very different from those known from oxic environments and, since oxygen is one of the primary factors controlling biogeochemical cycling, their interaction with the surrounding environment is markedly different (Melton *et al*., 2014a). Thus, specific focus on this anoxic part of the iron cycle is required to fully appreciate the role of these bacteria in the earth system. In this review article, we compile the current knowledge on these anaerobic Fe(II)-oxidizing bacteria, highlight existing open research questions and discuss the potential environmental importance and biotechnological applications of these microorganisms.

Nitrate-reducing Fe(II) oxidation

Links between nitrate-reducers and Fe(II)

The reduction of nitrate coupled to Fe(II) oxidation was first observed more than 20 years ago (Brons *et al*., 1997; Hafenbradl *et al*., 1996; Straub *et al*., 1996). Since then we have come to appreciate that nitrate-reducing bacteria can interact with Fe(II) in three distinct ways (Fig. 1). Firstly, autotrophic nitrate-reducing Fe(II)-oxidizing bacteria (NRFeOx) use Fe(II) as an electron donor for energy generation and fixation of CO_2, from which they build biomass. These organisms do not need organic carbon in addition to the Fe(II). In contrast to autotrophic NRFeOx, most other nitrate-reducing bacteria which have been shown to oxidize Fe(II) require addition of an organic substrate such as acetate to continually oxidize Fe(II) (Straub *et al*., 2004; Kappler *et al*., 2005b). Such organisms are often referred to in the literature as 'mixotrophs'. In order to be a true mixotroph, these organisms must utilize Fe(II) as an electron donor (by an enzymatic oxidation of the Fe(II)) in addition to the organic C source. Alternatively, some of the organisms described in the literature to catalyse Fe(II) oxidation do so as a result of abiotic reactions with reactive nitrogen-containing by-products of heterotrophic denitrification, such as nitrite and nitric oxide. For our purposes, we will refer to all organisms described to simultaneously oxidize Fe(II) and reduce nitrate, but for which no enzymatic component has been proven, as 'chemodenitrifiers', but will not consider them true nitrate-reducing Fe(II)-oxidizers. Given that these reactions, as discussed in subsequent sections, seem to be common to typical denitrifiers such as *Escherichia coli* (Brons *et al*., 1997), we expect that such a classification would apply to any heterotrophic denitrifier grown with high concentrations of Fe(II).

Deciphering which mechanism is applicable to which strains is a subject of significant debate in the literature. In the following sections we will highlight this debate, which centres around two key issues. Firstly, there have been many strains proposed to be autotrophic NRFeOx yet evidence for continued Fe(II) oxidation in the absence of additional carbon sources is often lacking. Secondly, for a number of strains which do require additional organic carbon, there is much debate regarding whether or not there is an enzymatic component of Fe(II) oxidation, that is, whether or not these strains are 'mixotrophs' or simply 'chemodenitrifiers'.

Autotrophic NRFeOx

While Fe(II) oxidation coupled to nitrate reduction is thermodynamically favourable ($\Delta G^{\circ\prime}$ = –96.23 kJ mol^{-1} Fe), large quantities of Fe(II) would be required by autotrophic NRFeOx bacteria to grow (ca., 26 mol Fe(II) to fix 1 mol carbon) (Laufer *et al*., 2016a). Despite this, several studies claim to have identified autotrophic NRFeOx organisms. In Table 1 we have listed all the isolates which, to our knowledge, have been proposed to be autotrophic NRFeOx. We suggest that a true autotrophic culture would (i) require no organic carbon source, (ii) show growth of cells with only Fe(II), nitrate and CO_2 provided, (iii) maintain Fe(II) oxidation over several transfers without organic carbon addition and (iv) demonstrate CO_2 uptake during Fe(II) oxidation by incorporation of labelled CO_2 into biomass. As can be seen in Table 1, only one enrichment culture, the so-called 'KS Culture', fulfils all of these criteria while the other strains either do not fulfil these criteria, or the necessary supporting information is not described.

The chemolithoautotrophic co-culture known as Culture KS, enriched in the mid-1990s (Straub *et al*., 1996; Blöthe and Roden, 2009; Nordhoff *et al*., 2017), is therefore the most robust example of a purely autotrophic NRFeOx

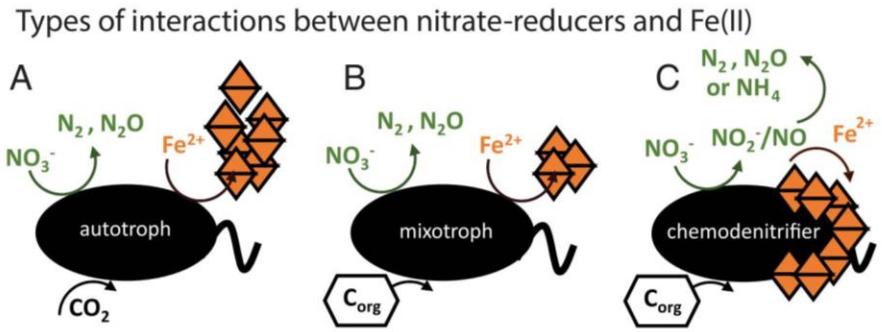

Fig. 1. Overview of the three different types of interaction between nitrate-reducing bacteria and Fe(II). (A) Autotrophic NRFeOx obtain carbon from CO_2 and oxidize Fe(II) enzymatically. (B) Mixotrophic NRFeOx require additional organic carbon as a carbon source, and Fe(II) oxidation has some enzymatic component (although there may also be some abiotic component). (C) Chemodenitrifiers require organic carbon and have no enzymatic component of Fe(II) oxidation. The position of the minerals (orange) relative to cells (black) indicates whether or not encrustation is expected.

system to date. It has been cultivated continuously for over 20 years with Fe(II) as the sole electron donor, nitrate as the sole electron acceptor, and CO_2 as the only carbon source in at least two different laboratories (Blöthe and Roden, 2009; He *et al*., 2016; Nordhoff *et al*., 2017; Tominski *et al*., 2018a). In this culture, complete oxidation of aqueous Fe(II) is observed and is coupled to denitrification to produce N_2. The dominant strain in 'Culture KS' belongs to the family *Gallionellaceae*, with a flanking community including species of *Rhizobium/Agrobacterium, Bradyrhizobium, Comamonadaceae, Nocardioides, Rhodanobacter, Polaromonas* and *Thiobacillus* which are chemodenitrifiers (Tominski *et al*., 2018a). The *Gallionellaceae* is designated as the autotrophic Fe(II)-oxidizer. The relative abundance and composition of the flanking community and the Fe(II)-oxidizer is dependent on the laboratory in which the culture is cultivated. It is hypothesized that the autotroph fixes CO_2 for the heterotrophic community members while the heterotrophic organisms detoxify nitric oxide which the autotroph does not have the genetic machinery to reduce (He *et al*., 2016; Tominski *et al*., 2018a, 2018b). The contribution of the *Gallionellaceae* strain varies between 42% and 96%, apparently as a result of different inoculum concentrations in different laboratories with lower inoculum concentrations (1%) favouring higher abundance of the Fe(II)-oxidizer (He *et al*., 2016; Nordhoff *et al*., 2017). The effect of the different community composition on the rate of Fe(II) oxidation has not been directly compared.

Mixotrophic NRFeOx and chemodenitrification

Many studies have also been conducted with bacteria which reduce nitrate and oxidize Fe(II) only in the presence of an additional carbon source, yet there is much debate over whether these organisms are mixotrophs or chemodenitrifiers (defined in Fig. 1). Some studies have shown an energetic benefit and increase in cell number when such bacteria are grown on acetate and nitrate with Fe(II) compared with setups without Fe(II) which could be seen as evidence of an enzymatic component (Muehe *et al*., 2009; Chakraborty *et al*., 2011). However, it was later suggested that this effect is probably a response to the nutritional benefit of iron addition, and not due to enzymatic Fe(II) oxidation (Klueglein and Kappler, 2013). Determination of an enzymatic component in potential mixotrophs is technically challenging to decipher and requires intricate analysis of all reactive intermediates (see most recently Jamieson *et al*., 2018). These authors claimed to have shown a requirement for an enzymatic component of oxidation in *Acidovorax* sp. strains BoFeN1 and 2AN, as well as *A. ebreus* strain TPSY, *Paracoccus denitrificans* Pd 1222 and *Pseudogulbenkiania* sp. strain 2002 by compilation and model-based interpretation of previously published experimental data. However, while this study is extensive and makes an impressive attempt at accounting for all potential abiotic processes, all previous studies on which these models were based on only account for extracellular substrate concentrations, that is, those substrates which were exported out of the cell. In the case of all of these strains, significant reactive nitrogen species production and Fe(II) oxidation occurs in the periplasm. We would argue that until these intracellular processes can be fully considered, we do not have concrete evidence that an enzymatic component is required to explain observed Fe(II) oxidation in any of the strains commonly studied as NRFeOx. As such, we will include all bacteria which have been shown to require an additional organic substrate together under 'chemodenitrifiers', of which some of the most well studied are listed in Table S1 (although this is not intended to be an exhaustive list).

Ecology of nitrate-reducing Fe(II)-oxidizers

A map displaying all isolated strains of anaerobic Fe(II)-oxidizing bacteria is shown in Fig. 2. Chemodenitrifiers have been isolated from a range of habitats including freshwater sediments (Straub *et al*., 1996), soils (Shelobolina *et al*., 2012a), hypersaline sediments (Emmerich *et al*., 2012), marine sediments (Laufer *et al*., 2016b) and hydrothermal vents (Hafenbradl *et al*., 1996; Edwards *et al*.,

Table 1. Summary of isolates/enrichment cultures of NRFeOx proposed in previous studies to be capable of autotrophic growth on Fe(II) and an indication of whether or not they meet the criteria for autotrophy proposed here. Number represents position in the map in Figure 2. This shows that all except one of the strains/cultures published as an 'autotroph' do not meet this criteria. Strain marked '*' required H_2 for Fe(II) oxidation.

No.	Culture/strain name	Class Order Family	Origin of sample	Identity of iron(III) minerals	Met criteria for autotrophy: *growth*	*Fe(II) oxidation over several generations*	*Absence of organic C source*	*Uptake of labelled CO_2 during Fe(II) oxidation*	Reference
Stable enrichment cultures									
1	Enrichment culture KS	Fe(II)-oxidizer: Betaproteobacteria Gallionellales Gallionellaceae	Freshwater sediment, Bremen, Germany	Goethite, magnetite	+	+	+	+	(Straub *et al*., 1996; He *et al*., 2016; Nordhoff *et al*., 2017; Tominski *et al*., 2018a)
Isolated strains									
2	Azoarcus Strain ToN1	Betaproteobacteria; Rhodocyclales; Zoogloeaceae	Weser river sediment, Bremen, Germany	n.a.	n.a.	n.a.	+	n.a.	(Rabus and Widdel, 1995; Straub *et al*., 1996)
3	*Pseudomonas stutzeri*	Gammaproteobacteria, Pseudomonadales; Pseudomonadaceae	Marine sample off the Californian Coast	n.a.	n.a.	n.a.	+	n.a.	(ZoBell and Upham, 1944; Straub *et al*., 1996; Peña *et al*., 2012)
4	*Ferroglobus placidus* (hyperthermophilic archaea)	Archaeoglobi; Archaeoglobales; Archaeoglobaceae	Shallow submarine hydrothermal system, Vulcano, Italy	Rusty ferric precipitates	+	–	–	n.a.	(Hafenbradl *et al*., 1996)
5	Aquabacterium Strain BrG2	Betaproteobacteria, Burkholderiales, Comamonadaceae	Freshwater sediment, Bremen, Germany	Rusty ferric precipitates	n.a.	n.a.	+	n.a.	(Straub *et al*., 1996; Buchholz-Cleven *et al*., 1991)
6	*Thiobacillus denitrificans* ATCC 25259*	Betaproteobacteria; Nitrosomonadales; Thiobacillaceae;	Sewage sludge, The United Kingdom	n.a.	–	+	+	n.a	(Straub *et al*., 1996; Beller *et al*., 2006)
7	*Geobacter metallireducens* strain GS-15	Deltaproteobacteria; Desulfuromonadales; Geobacteraceae	U-contaminated aquifer sediments, San Juan River, Shiprock	n.a.	n.a.	n.a.	+	n.a.	(Lovley, 1997; Finneran *et al*., 2002; Weber *et al*., 2006)
8	*Marinobacter* related species	Gammaproteobacteria; Alteromonadales; Alteromonadaceae	Deep sea hydrothermal system, Juan de Fuca ridge	n.a.	–	n.a.	+	n.a.	(Edwards *et al*., 2003)
9	*Hyphomonas* related species	Alphaproteobacteria; Rhodobacterales; Hyphomonadaceae;	Deep sea hydrothermal system, Juan de Fuca ridge	n.a.	–	n.a.	+	n.a.	(Edwards *et al*., 2003)
10	*Paracoccus ferrooxidans* strain BDN-1	Alphaproteobacteria, Rhodobacterales, Rhodobacteraceae	Sewage sludge from bioreactor system	Ferric iron precipitates	+	–	–	n.a.	(Kumaraswamy *et al*., 2006)
11	*Pseudogulbenkiania* sp. strain 2002	Betaproteobacteria; Neisseriales; Chromobacteriaceae	Freshwater lake sediment, Illinois University	n.a.	+	–	+	+	(Weber *et al*., 2006)
12	*Azospira* bacterium TR1	Betaproteobacteria; Rhodocyclales; Rhodocyclaceae	Bioremediation site, BC, Canada	Very fine ferric iron oxides	–	–	–	n.a.	(Mattes *et al*., 2013)

(Continues)

Table 1. Continued

No.	Culture/strain name	Class Order Family	Origin of sample	Identity of iron(III) minerals	Met criteria for autotrophy: growth	Fe(II) oxidation over several generations	Absence of organic C source	Uptake of labelled CO_2 during Fe(II) oxidation	Reference
13	*Citrobacter freundii* PXL1	Gammaproteobacteria; Enterobacterales; Enterobacteriaceae	Sewage sludge, China	Amorphous to poorly crystalline ferric iron oxides	n.a.	n.a.	–	n.a.	(Li *et al*., 2014)
14	*Pseudomonas* sp. SZF15	Gammaproteobacteria; Pseudomonadales; Pseudomonadaceae	Freshwater sediment, Tang Yu reservoir, China	n.a.	+	–	+	n.a.	(Su *et al*., 2015)
15	*Microbacterium* sp. strain W3	Actinobacteria; Micrococcales; Microbacteriaceae	Deep freshwater sediment, Lake Wuhan, China	Yellow-brown to orange rusty precipiates (assumed to be Fe(III) oxyhydroxide)	+	–	+	n.a.	(Zhang *et al*., 2015)
16	Strain W5	Actinobacteria; Micrococcales; Microbacteriaceae	Deep freshwater sediment, Lake Wuhan, China	n.a.	–	–	+	n.a.	(Zhou *et al*., 2016)

2003). Simultaneous Fe(II) oxidation and nitrate reduction has been demonstrated in enrichment cultures and natural sediment samples from freshwater (Melton *et al*., 2012), marine (Laufer *et al*., 2016c), estuarine (Robertson *et al*., 2016), fluvial (Coby *et al*., 2011) and subsurface (Benzine *et al*., 2013) environments as well as sewage sludge (Oshiki *et al*., 2013) and aquifers (Lovley *et al*., 1987). As shown in Table 1, isolation of NRFeOx organisms which fulfil all the criteria for autotrophy has proven to be more difficult. However, cultivation-independent techniques have been used to identify potentially active autotrophic NRFeOx microbes in the environment. A recent study by Laufer *et al*. (2016c) using coastal marine sediment in ^{14}C-labelled incubations provided, for the first-time, unequivocal evidence for the existence of autotrophic NRFeOx organisms in the environment. Using metagenomics and metatranscriptomics, Jewell *et al*. (2016) showed an increase in members belonging to the Fe(II)-oxidizing *Gallionellaceae* (accounting for up to 80% of the transcriptome) when nitrate was pumped into a groundwater aquifer. Another study showed that chemolithoautotrophy was dominant in an organic poor aquifer and that high fractions of the denitrifying communities were represented by OTUs closely related to the Fe(II)-oxidizer *Sideroxydans lithotrophicus* ES-1 (Herrmann *et al*., 2017). Recent studies have investigated the abundance and distribution of NRFeOx bacteria in freshwater lake sediments (Melton *et al*., 2012, 2014c) and in coastal marine sediments (Laufer *et al*., 2016b). In the freshwater lake sediments, the results indicate that NRFeOx bacteria are likely to be in competition for Fe(II) with phototrophic Fe(II)-oxidizers in the presence of light (Melton *et al*., 2012). Furthermore, while the distribution of these microbes is expected to adhere to the thermodynamically controlled geochemical stratification of substrates, this is not always the case. In marine sediments, autotrophic NRFeOx and denitrifiers which abiotically catalyse Fe(II) oxidation (as well as photoferrotrophs) may exist together in the sediment layers (Laufer *et al*., 2016b).

Mechanisms of oxidation

Mechanisms used by anaerobic NRFeOx bacteria to oxidize Fe(II) are still unclear, but appear to be different depending on whether the bacteria are autotrophs, mixotrophs or chemodenitrifiers (see Fig. 1). For autotrophic NRFeOx, three mechanisms have been proposed for Fe(II) oxidation whereby: (i) there is a dedicated Fe(II) oxidoreductase, (ii) there is an unspecific activity of the nitrate reductase or (iii) the bc1 complex accepts electrons from Fe(II) and reduces the quinone pool (Ilbert and Bonnefoy, 2012).

In recent years much research has focused on the first scenario and attempted to identify a possible dedicated outer membrane Fe(II) oxidoreductase present in autotrophic NRFeOx microorganisms (Beller *et al*.,

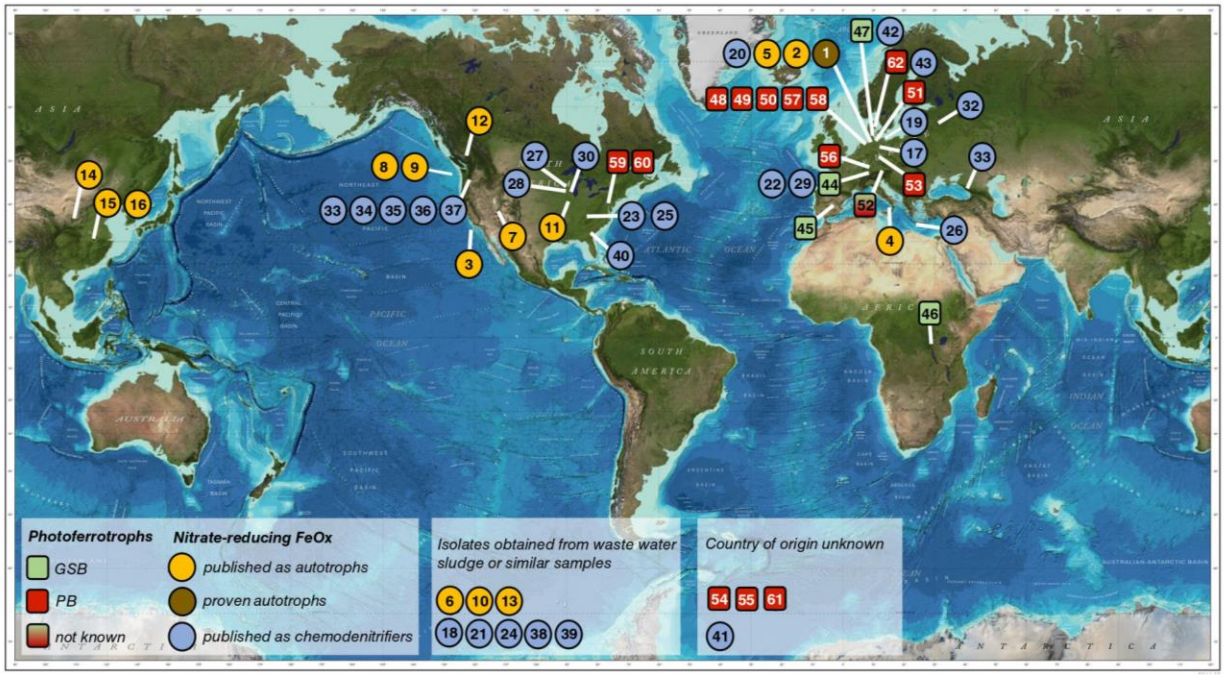

Fig. 2. Map displaying isolated strains (or stable enrichment cultures) of photoferrotrophs or nitrate-reducing bacteria implicated in Fe(II)-oxidation, as well as their source of origin. Further detail on each strain can be found in Tables 1 and 2; Supporting Information Table S1. 'Proven' autotrophs were designated based on their ability to meet the four criteria for autotrophy proposed in Table 1. Red squares include both purple sulfur bacteria and purple non-sulfur bacteria (PB). GSB represents Green Sulfur Bacteria. Map obtained from the GEBCO world map 2014 (www.gebco.net).

2013; He *et al*., 2017). A metagenomics analysis of the NRFeOx Culture KS identified homologues of the cytochrome c putative Fe(II) oxidase Cyc2 (found in other known Fe(II)-oxidizers) in the draft genomes of the *Gallionellaceae* sp. and in the *Rhodanobacter* sp. present within Culture KS (He *et al*., 2016). Homologues of the porin cytochrome c porin complex MtoAB were also found in the *Gallionellaceae* sp. in Culture KS and as well as in *D. aromatica* RCB (which was proposed to be autotrophic but has not been confirmed) (He *et al*., 2017). Figure 3A displays a potential mechanism by which the proposed autotrophic Fe(II)-oxidizer in the KS culture could oxidize Fe(II) in which an electron is obtained via Fe(II) oxidation and passed along the electron transport chain where nitrate is reduced stepwise to NO. Outside the cell, there is potential for NO to be either consumed by the flanking community or react with aqueous Fe(II).

As already discussed, there is continuing controversy as to whether some NRFeOx bacteria make use of an enzymatic machinery to oxidize Fe(II), making them true mixotrophs. Many hypothesize that Fe(II) oxidation is driven by an abiotic chemical side reaction of denitrification (Brons *et al*., 1997; Klueglein and Kappler, 2013; Klueglein *et al*., 2014). It has been proposed that nitrate-dependent Fe(II) oxidation can be promoted by all heterotrophic denitrifiers (Carlson *et al*., 2013). This is evidenced by the fact that many nitrate-reducers can oxidize Fe(II) when an organic compound is provided in combination with Fe(II), even *E. coli* (Brons *et al*., 1997). The abiotic reduction of nitrate by dissolved Fe(II) is slow (Buresh and Moraghan, 1978; Colman *et al*., 2008), but nitrite reduction by Fe(II) to N_2O is kinetically favourable under environmental conditions and likely to occur if reactive chemical substrates are present as catalysts (Zhu-Barker *et al*., 2015). For example, the reduction of nitrogen species by Fe(II) can occur via heterogeneous surface catalysis where viable surfaces include crystalline Fe(III) oxyhydroxides, green rust, pyrite (FeS_2) and cell surfaces (Moraghan and Buresh, 1977; Ottley *et al*., 1997; Kampschreur *et al*., 2011; Bosch *et al*., 2012; Dhakal *et al*., 2013; Jones *et al*., 2015; Buchwald *et al*., 2016; Grabb *et al*., 2017). Microbially driven NRFeOx, Fe-ammox (Fe(III)-coupled ammonium oxidation) and heterotrophic nitrate-reduction (denitrification) can lead to the formation of reactive nitrogen species as a metabolic intermediate (nitrite, NO_2^- or nitric oxide, NO) (Weber *et al*., 2001; Picardal, 2012; Klueglein and Kappler, 2013; Oshiki *et al*., 2013), providing ample supply of compounds which could react quickly with Fe(II).

A summary of the proposed mechanism for Fe(II) oxidation by chemodenitrification is shown in Fig. 3B. This represents an end-member mechanism for NRFeOx where there is no enzymatic component to

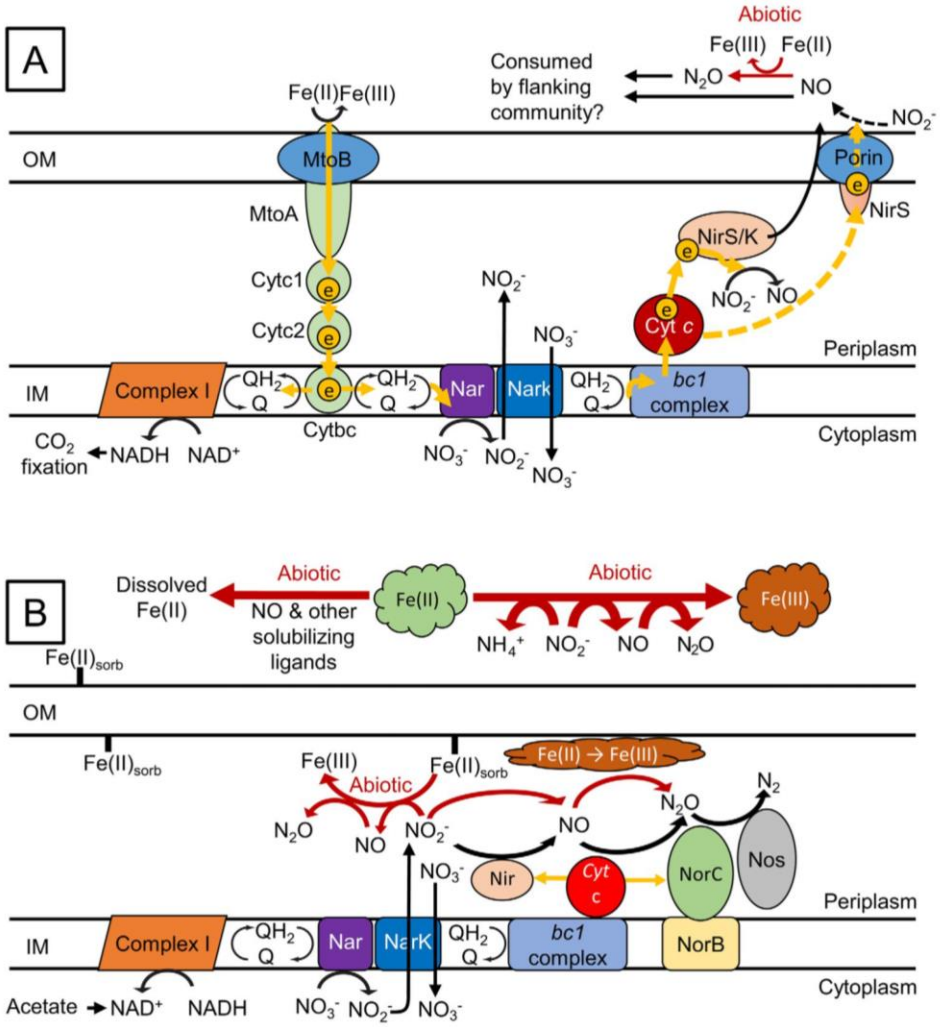

Fig. 3. Schematics of the current hypotheses on the mechanism of Fe(II) oxidation in (A) the Gallionellaceae species proposed to be the autotrophic nitrate-reducing Fe(II)-oxidizer in the KS culture (modified from He *et al*., 2016) and (B) the proposed mechanism of Fe(II) oxidation by chemodenitrification (modified from Carlson *et al*., 2013). In (B), nitrate reduction may also be catalysed by Nap instead of Nar, and nitric oxide reduction may be facilitated by NorZ instead of NorC, which accepts electrons from quinols rather than cytochrome c.

Fe(II) oxidation. In this case electrons are obtained from organic carbon oxidation, leading to stepwise reduction of nitrate to nitrogen. Intermediates may leak out at any of the steps and react with Fe(II) either inside or outside of the cell. While some Fe(II)-oxidizing bacteria such as photoferrotrophs and the autotrophic Culture KS have developed strategies for avoiding cell encrustation by Fe(III) minerals (Hegler *et al*., 2010), no such strategies have been demonstrated by chemodenitrifying bacteria (Schaedler *et al*., 2009; Klueglein *et al*., 2014). Cell encrustation inhibits respiratory complexes and other periplasmic sites which leads to decreased nitrate-dependent Fe(II) oxidation (Carlson *et al*., 2013) and eventually results in cell death (though not always for all community members, e.g., Miot *et al*., 2015).

Fe(II) sources and Fe(III) minerology

Different sources of Fe(II) species including dissolved Fe^{2+}, complexed Fe(II) [e.g., Fe(II)-EDTA] and mineral bound Fe(II) can undergo oxidation as a result of NRFeOx. Fe(II)-OM complexes such as Fe(II)-EDTA and Fe(II)-NTA were shown to be oxidized by several different species including *Dechloromonas* sp. strain UWNR4, *Paracoccus ferrooxidans* sp. nov., BDN-1, *Pseudogulbenkiania* sp. 2002 (Kumaraswamy *et al*., 2006) and *Desulfitobacterium frappieri* (Shelobolina *et al*., 2003). *Acidovorax* sp. BoFeN1 is able to promote oxidation of Fe(II)-citrate, Fe(II)-EDTA, Fe(II)-humic-acid, and Fe(II)-fulvic-acid, but only in the presence of aqueous Fe(II) (Peng *et al*., 2018). Potential toxicity of ligands may also be a controlling factor in these processes.

In addition to dissolved Fe(II), different microbial species are also able to oxidize Fe(II) mineral phases via NRFeOx. The autotrophic enrichment Culture KS, can oxidize Fe(II) in the form of microbially reduced goethite, biogenic magnetite (Fe_3O_4) and chemically precipitated siderite ($FeCO_3$) but only a small amount of biogenic siderite (Weber *et al*., 2001). Oxidation of biogenically reduced goethite, chemically precipitated siderite, biogenic magnetite and magnetite nanoparticles by a chemodenitrifier has also been observed (Chakraborty *et al*., 2011; Byrne *et al*., 2015). Sulfide minerals, such as ferrous sulfide (FeS), was observed to be oxidized by an enriched nitrate-reducing culture from marine sediment although pyrite (FeS_2) was not bioavailable for oxidation by the same culture (Schippers and Jorgensen, 2002). Vivianite can be oxidized by *Acidovorax* sp. BoFeN1 in the presence of dissolved free Fe^{2+} (Miot *et al*., 2009a), or also in cell suspension experiments with *Acidovorax ebreus* (Carlson *et al*., 2013); however, vivianite cannot be oxidized by *Acidovorax* sp. Strain BoFeN1 in the absence of dissolved Fe^{2+} (Kappler *et al*., 2005b; Miot *et al*., 2009b). Fe(II)-containing phyllosilicates, such as biotite, can be oxidized by the autotrophic enrichment Culture KS (Shelobolina *et al*., 2012b). Clay minerals such as illite, smectite and nontronite, are also available for Fe(II) oxidation by *Desulfitobacterium frappieri* (Shelobolina *et al*., 2003) and by *Pseudogulbenkiania* sp. strain 2002 (Zhao *et al*., 2017). Culturing of microbes on solid mineral substrates has, however, proved difficult. Poised electrodes could provide an alternative strategy for enrichment of mineral transforming bacteria as demonstrated by Rowe *et al*. (2015) in sediment microcosms.

The oxidation of Fe(II) species coupled to microbial nitrate reduction can lead to the precipitation of a variety of Fe(III) minerals and/or mixed-valent Fe(II)–Fe(III) mineral phases. These phases can precipitate either on the surface of the bacteria or in close association between bacteria and minerals as cell mineral aggregates. For many chemodenitrifiers, precipitation occurs in the periplasm, as shells which completely enclose the cell, or in extracellular globules or as Fe filaments on extracellular polymeric substances (EPS) (Kappler *et al*., 2005b; Miot *et al*., 2009b; Schaedler *et al*., 2009; Schmid *et al*., 2014). The extent of encrustation increasingly limits the metabolic capabilities of these bacteria until encrustation is so severe that they are killed (Miot *et al*., 2015). The extent to which encrustation is an artefact caused by high Fe(II) concentrations in lab conditions is unclear, but such structures have been observed in the environment (Miot *et al*., 2016). In addition to goethite, mineral encrustation of the bacterial periplasm may also be comprised of Fe(III) phosphate minerals, which accumulate on proteins within the periplasm of cells (Miot *et al*., 2009b). *Acidovorax* sp. strain BoFeN1 can also form extracellular magnetite when green rust is provided as an Fe(II) source (Miot *et al*., 2014).

The mineralogy of biogenic Fe(III) minerals is dependent on a myriad of variables ranging from the microbial species, growth medium (i.e., phosphate or buffer concentrations), substrate availability, as well as geochemical and physical conditions such as pH and temperature (Posth *et al*., 2014; Miot and Etique, 2016). Because solution chemistry is such a strong driver in biogenic mineral precipitation, the same strain of bacteria, *Acidovorax* sp. Strain BoFeN1 for example, is capable of forming multiple Fe(III) mineral phases (Kappler and Newman, 2004; Kappler *et al*., 2005a; Hohmann *et al*., 2009; Miot *et al*., 2009b; Posth *et al*., 2010). For instance, lepidocrocite (γ-FeOOH) can be formed directly via NRFeOx by *Acidovorax* sp. strain BoFeN1 (Larese-Casanova *et al*., 2010). However, in the presence of strong complexing ligands such as carbonate, Fe(III) mineral precipitation is directed toward goethite (α-FeOOH) (Carlson and Schwertmann, 1981; Larese-Casanova *et al*., 2010). Similarly, when phosphate concentration is high, the precipitation of both poorly crystalline or crystalline Fe(III)-phosphate minerals is favoured. In addition to Fe(III) minerals, mixed-valent minerals such as green rust (as an intermediate phase) or magnetite can also result from microbial Fe(II) oxidation coupled to nitrate reduction, by species such as *Dechlorosoma sullium* strain PS (this species is capable of using perchlorate or nitrate as an electron acceptor) (Achenbach *et al*., 2001; Chaudhuri *et al*., 2001) or by *Acidovorax* sp. strain BoFeN1 (Pantke *et al*., 2012; Klueglein and Kappler, 2013; Miot *et al*., 2014). Magnetite formation by NRFeOx has been shown in the presence of magnetite nucleation sites which function as seeds for further magnetite formation (Dippon *et al*., 2012). Green rust has also been shown to form as an intermediate phase during the oxidation of Fe^{2+} to Fe(III) minerals by *Acidovorax* sp. BoFeN1 (Pantke *et al*., 2012), *Klebsiella mobilis* (Etique *et al*., 2014) and Culture KS (Nordhoff *et al*., 2017). The formation of this metastable mineral gives an indication of the mineralization pathway, that is, via precipitation of green rust by NRFeOx followed by solid-state transformation into Fe(III) or Fe(II)–Fe(III) mineral phases.

Environmental implications

The proposed stoichiometric reaction for NRFeOx organisms is presented in Eq. 1 whereby the stepwise reduction of nitrate via denitrification coupled to Fe(II) oxidation results in the formation of N_2. While some studies have shown nitrate reduction to N_2 without the accumulation of intermediates (Chaudhuri *et al*., 2001; Straub *et al*., 2004;

Blöthe and Roden, 2009), a smaller number of studies using sediment enrichments have shown that ammonium accumulation can also occur during NRFeOx (Weber *et al*., 2006; Coby *et al*., 2011). More recent studies using sediment incubations have identified the concentration of dissolved Fe(II) to be the controlling factor on the relative contribution of denitrification and dissimilatory nitrate reduction to ammonium (DNRA) in nitrate removal (Roberts *et al*., 2014; Robertson *et al*., 2016; Robertson and Thamdrup, 2017). In addition to contributing to the accumulation of ammonium, anaerobic ammonium oxidizing (annamox) bacteria can also mediate nitrate-reducing Fe(II) oxidation (Oshiki *et al*., 2013). The role of NRFeOx in the transformation of ammonium can have important implications for wastewater treatment processes.

The abiotic reduction of nitrite by Fe(II) can produce N_2O (Eq. 3) which is not quickly reduced by Fe(II).

$$4\,Fe^{2+} + 2\,NO_2^- + 5\,H_2O \rightarrow 4\,FeOOH + N_2O + 6\,H^+ \quad (3)$$

Thus, the abiotic reduction of nitrite by Fe(II) (Eq. 3) has the potential to be a crucial source of nitrous oxide (N_2O) (Burgin and Hamilton, 2007; Picardal, 2012; Zhu-Barker *et al*., 2015). N_2O belongs to the group of greenhouse gases (Wuebbles, 2009), has 300 times the global warming potential of CO_2 on a time scale of 100 years (IPCC, 2013) and contributes to stratospheric ozone depletion (Crutzen, 1974; Ravishankara *et al*., 2009). It is known that abiotic nitrite reduction by redox-active Fe(II) has the potential to be an important source of N_2O in Fe- and carbon-rich habitats (Burgin and Hamilton, 2007; Picardal, 2012; Zhu-Barker *et al*., 2015). Chemodenitrification occurs in forest, grassland and cropland soils (van Cleemput and Samater, 1995; Zhu *et al*., 2013; Heil *et al*., 2015), paddy soils (Liu *et al*., 2012; Wang *et al*., 2016b), activated sludge (Wang et al., 2016a), hypersaline ponds and brines in Antarctica (Samarkin *et al*., 2010; Peters *et al*., 2014; Zhu-Barker *et al*., 2015; Ostrom *et al*., 2016), and marine coastal sediments (Wankel *et al*., 2017). However, the contribution of this process to the global N_2O budget is currently unknown.

The identity and morphology of iron minerals formed by NRFeOx can be influenced by the presence of metal species, such as arsenic (As) or silicon (Si) (Kleinert *et al*., 2011; Picard *et al*., 2016). For example, during initial formation, the presence of As can direct mineral formation toward the poorly crystalline Fe(III) mineral ferrihydrite as opposed to more crystalline Fe(III) mineral goethite (Kleinert *et al*., 2011). Arsenic co-precipitated with ferrihydrite could potentially be mobilized upon microbial Fe(III) reduction whereas As-goethite co-precipitates would likely be more stable (Hohmann *et al*., 2009). This transformation process may be inhibited if minerals are co-precipitated with Si, which has been shown to stabilize phases such as ferrihydrite and goethite (Picard *et al*., 2016). Repeated redox cycling between oxidizing and reducing conditions can influence the products which form as a result of nitrate-reducing Fe(II) oxidation (Mejia *et al*., 2016) which may influence the interactions between the minerals and other environmental factors. Immobilization of iron by oxidation is itself an important environmental process. For example, it has been shown that NRFeOx processes can act to limit iron transport from oceanic oxygen minimum zones (Scholz *et al*., 2016). Since iron is a major limiting nutrient in the world's oceans (Moore *et al*., 2013), the limitation of iron transport from zones where dissolved iron is higher than average seawater can thus have an influence on global oceanic productivity.

It should be noted that the concentrations of nitrate in an environment do not need to be high to lead to Fe(II) oxidation, because nitrate production and nitrate consumption can proceed simultaneously. Therefore the net concentrations which are measured (e.g., in porewater) do not necessarily reflect the amount of nitrate that is available to interact with NRFeOx bacteria. Additionally, the abiotic oxidation of Fe(II) is primarily driven by reaction with reactive nitrogen intermediates (NO, NO_2^-) which are unstable and rapidly react, such that they would not be detected in bulk measurements of porewater substrate concentrations.

Anoxygenic phototrophic Fe(II)-oxidizers

Physiology, existing isolates/cultures and ecology

The second group of anoxygenic bacteria which can oxidize Fe(II) are anoxygenic phototrophs. These bacteria harvest energy from light and oxidize Fe(II) in order to produce reducing equivalents for CO_2 fixation. The existence of phototrophic organisms which could oxidize Fe(II) was first proposed as an explanation for the formation of vast, economically important iron-rich rock formations by Hartman (1984) who disagreed with the geologist Preston Cloud that these were formed as a result of cyanobacterial oxygenic photosynthesis (Cloud, 1973). Hartman suggested that anoxygenic photosynthetic microorganisms thrived in Earth's ancient, oxygen-poor and iron-rich oceans, and utilized the abundant Fe(II) as an electron donor. Nevertheless, it took almost a decade for the first anoxygenic phototrophic Fe(II)-oxidizer, described as a purple non-sulfur bacteria, to be isolated (Widdel *et al*., 1993).

Anoxygenic phototrophic Fe(II)-oxidizers have since been isolated from both the purple sulfur (Gammaproteobacteria) and non-sulfur bacteria (Alphaproteobacteria), and from the green sulfur bacteria (see Table 2). Isolated purple non-sulfur bacteria include *Rhodobacter ferrooxidans* strain

Table 2. Summary of isolated phototrophic Fe(II)-oxidizers (pFeOx) which all oxidize Fe(II) for CO_2 fixation and gain energy from light with the exception of *R. capsulatus* (*). Number represents position in the map in Figure 2.

No.	Strain	Class, Order, Family	Origin of sample	Identity of iron(III) minerals	Reference
Green sulfur bacteria (Chlorobiaceae)					
44	*Chlorobium ferrooxidans* KoFox [co-culture with KoFum (*Geospirillum arsenophilum*)]	Chlorobia Chlorobiales Chlorobiaceae	Freshwater sediment, Lake Constance, Germany	bulbous, spiky and needle like amorphous Fe(III) hydroxides, ferrihydrite; encrustation mainly on KoFum; no encrustation of KoFox	(Heising *et al*., 1999; Gauger *et al*., 2016)
45	*Chlorobium* sp. [co-culture: *Chlorobium* sp. (80%) and *Acidobacteria* sp. (20%)]	Chlorobia Chlorobiales Chlorobiaceae	Water column of Lake La Cruz, Spain	Fe(III) oxides	(Walter *et al*., 2014)
46	*Chlorobium phaeoferrooxidans*	Chlorobia Chlorobiales Chlorobiaceae	Water column of Lake Kivu, Rep. Congo	Fe(III) oxides	(Llirós *et al*., 2015; Crowe *et al*., 2017)
47	*Chlorobium* sp. strain N1	Chlorobia Chlorobiales Chlorobiaceae	Marine sediment, Aarhus, Denmark	Fe(III) oxyhydroxides, amorphous to poorly crystalline Fe(III) phase, ferrihydrite, akageneite and/ or lepidocrocite; no encrustation of cells	(Laufer *et al*., 2017)
Purple sulfur and non-sulfur bacteria					
48	*Rhodomicrobium* isolate	Alphaproteobacteria Rhizobiales Hyphomicrobiaceae	Marine sediment Jadebusen, North Sea, Germany	Fe(III) oxides, cells covered with Fe(III) precipitates	(Widdel *et al*., 1993)
49	*Rhodopseudomonas palustris*	Alphaproteobacteria Rhizobiales Bradyrhizobiaceae	Marine sediment Jadebusen, North Sea, Germany	Fe(III) oxides	(Widdel *et al*., 1993)
50	*Thiodyction* sp.	Gammaproteobacteria	Marine sediment Jadebusen, North Sea, Germany	Fe(III) oxides	(Widdel *et al*., 1993)
51	Strain L7 (closest relative *Chromatium* sp.)	NA	Freshwater sediment, Lübeck, Germany	Ochre to light brown, rusty ferric precipitates; cells are only loosely associated with precipitates	(Ehrenreich and Widdel, 1994)
52	Strain SF4	NA	Forest soil, Munich, Germany	Orange-brown precipitates with fluffy appearance; cells mainly free of encrustation	(Ehrenreich and Widdel, 1994)
53	*Rhodobacter ferrooxidans* SW2	Alphaproteobacteria Rhodobacterales Rhodobacteraceae	Freshwater sediment, Hanover, Germany	Ferrihydrite, lepidocrocite, goethite, poorly crystalline Fe-carbonates; encrustation away from cell on EPS	(Ehrenreich and Widdel, 1994; Kappler and Newman, 2004; Miot *et al*., 2009)
54	*Rhodobacter capsulatus* DSM 1710 *(photoheterotrophic)*	Alphaproteobacteria Rhodobacterales Rhodobacteraceae	n.a.	Green to dark green Fe(II)/Fe(III) minerals	(Ehrenreich and Widdel, 1994)
55	*Rhodopseudomonas palustris* DSM 123	Alphaproteobacteria Rhizobiales Bradyrhizobiaceae	Surface water or mud, country of origin unknown	Green to dark green Fe(II)/Fe(III) minerals	(Ehrenreich and Widdel, 1994)
56	*Rhodomicrobium vannielii* BS-1	Alphaproteobacteria Rhizobiales Hyphomicrobiaceae	Freshwater sediment, Tübingen, Germany	Cell encrustation by ferric minerals	(Heising and Schink, 1998)
57	*Rhodovulum iodosum*	Alphaproteobacteria Rhodobacterales Rhodobacteraceae	Marine sediment Jadebusen, North Sea, Germany	No cell encrustation, ferric mineral precipitation on EPS	(Straub *et al*., 1999)

(Continues)

Table 2. Continued

No.	Strain	Class, Order, Family	Origin of sample	Identity of iron(III) minerals	Reference
58	*Rhodovulum robiginosum*	Alphaproteobacteria Rhodobacterales Rhodobacteraceae	Marine sediment Jadebusen, North Sea, Germany	Green to dark green Fe(II)/Fe(III) minerals	(Straub *et al*., 1999)
59	*Thiodictyon* sp. strain F4	Gammaproteobacteria	Marsh sediment, Woods Hole, US	Rusty Fe(III) precipitates, two-line ferrihydrite, potential trace amounts of goethite, vivianite and siderite	(Croal *et al*., 2004; Hegler *et al*., 2008, 2010)
60	*Rhodopseudomonas palustris* TIE-1	Alphaproteobacteria Rhizobiales Bradyrhizobiaceae	Marsh sediment, Woods Hole, US	Poorly crystalline iron(oxy)hydroxides, goethite, magnetite	(Jiao *et al*., 2005)
61	*Rhodobacter capsulatus* SB 1003*	Alphaproteobacteria Rhodobacterales Rhodobacteraceae	n.a.	n.a.	(Poulain and Newman, 2009; Kopf and Newman, 2012)
62	*Rhodobacter* sp.	Alphaproteobacteria Rhodobacterales Rhodobacteraceae	Marine sediment, Kalo Vig, Denmark	Cells closely associated with rusty-orange Fe(III) minerals	(Laufer *et al*., 2016b)

**Rhodobacter capsulatus* SB1003 can catalyse Fe(II) oxidation but does not appear to be able to grow from this metabolism.

SW2 (Ehrenreich and Widdel, 1994), *Rhodopseudomonas palustris* strain TIE-1 (Jiao *et al*., 2005), *Rhodovulum iodosum* and *Rhodovulum robiginosum* (Straub *et al*., 1999; Wu *et al*., 2014). The only purple sulfur bacteria isolate available is *Thiodycton* sp. strain F4 (Croal *et al*., 2004). All isolated photoferrotrophs from the green sulfur bacteria belong to the genus Chlorobium. These include *Chlorobium ferrooxidans* strain KoFox (Heising *et al*., 1999) and two recently isolated species: *Chlorobium phaeoferrooxidans* (Crowe *et al*., 2017; Thompson *et al*., 2017) and *Chlorobium* sp. strain N1 which is closely related to *Chlorobium luteolum* (Laufer *et al*., 2017). These organisms typically oxidize aqueous Fe(II) completely under normal culture conditions, similarly to Culture KS and in contrast to most other NRFeOx bacteria. *Rhodobacter capsulatus* can also oxidize Fe(II) but does not appear to use this process to support growth (Poulain and Newman, 2009). This organism instead utilizes Fe(II) oxidation as a detoxification mechanism. Fe(II) can also be oxidized by purple non-sulfur bacteria *Rhodomicrobium vannielli* strain BS-1, however, the physiological role of Fe(II) oxidation by this organism seems to be somewhat of an enigma. Heising and Schink (1998) showed that while this strain could oxidize Fe(II), this process is significantly aided by the presence of an organic substrate and can only be maintained for two to three generations. This led them to suggest that Fe(II) oxidation was of minor physiological importance and was merely a side-reaction of normal metabolism. However, *Rhodomicrobium vannielli* strain BS-1 does have the same set of genes for Fe(II) oxidation as *Rhodopseudomonas palustris* strain TIE-1 (He *et al*., 2017) and, thus, it is unclear why this strain does not use Fe(II) as the sole electron donor whereas *Rhodopseudomonas palustris* TIE-1 does.

Purple non-sulfur bacteria and green sulfur bacteria that oxidize Fe(II) live in both high and low salinity environments. Marine strains include *Chlorobium* sp. strain N1, *Rhodovulum iodosum* and *Rhodovulum robiginosum* while all other isolates stem from freshwater habitats. Phototrophic Fe(II)-oxidizers from the green sulfur bacteria can utilize lower light intensities than the purple sulfur bacteria due to differences in their pigments such as bacteriochlorphylls and carotenoids (Kappler *et al*., 2005a). Some green sulfur bacteria utilize extremely low light intensities (down to > 0.005% of surface irradiance; Manske *et al*., 2005) and have a light saturation much lower than that of purple bacteria (< 50 lux for *Chlorobium ferrooxidans* strain KoFox compared with 400 lux for *Rhodobacter ferrooxidans* strain SW2 or 800 lux for *Thiodycton* sp. strain F4) (Hegler *et al*., 2008). Green sulfur bacteria such as *Chlorobium* sp. strain N1, however, utilize higher light intensities (saturation at 400 lux) thus they are not limited to very low light environments (Laufer *et al*., 2017). All isolated anoxygenic phototrophic Fe(II)-oxidizers are metabolically flexible and have the ability to

utilize multiple electron donors for CO_2 fixation instead of Fe(II), such as H_2 and H_2S (Croal *et al*., 2009). Alternatively, they are able to use organic carbon compounds instead of CO_2 (Melton *et al*., 2014b).

Possibly as a result of their metabolic flexibility, anoxygenic phototrophs are widespread in both aquatic and terrestrial habitats. Most of the isolated species were obtained from either freshwater or marine sediments with the exception of *Chlorobium phaeoferrooxidans* which was isolated from the water column of ferruginous Lake Kivu, East Africa (Crowe *et al*., 2017). However, despite the lack of pelagic isolates, these bacteria have been shown (using microcosms and in situ observations) to substantially contribute to Fe(II) oxidation in numerous stratified lakes. For example, in ferruginous Lake La Cruz, Spain, an anoxygenic phototrophic Fe(II)-oxidizer closely related to *Chlorobium ferrooxidans* strain KoFox was enriched from the water column and shown to contribute to Fe(III) mineral formation in situ (Walter *et al*., 2014). These bacteria even thrive in low iron environments like mermomictic Lake Cadagno, where they are thought to account for up to 10% of total carbon fixation (Berg *et al*., 2016). Given the metabolic flexibility of anoxygenic phototrophic Fe(II)-oxidizers, it is challenging to determine whether or not they contribute to Fe(II) oxidation in their environment of origin simply from the analysis of in situ DNA or RNA.

Mechanisms of Fe(II) oxidation by photoferrotrophs

The mechanisms involved in Fe(II) oxidation by anoxygenic phototrophic Fe(II)-oxidizing bacteria are still not fully understood. Questions remain about how these bacteria can oxidize different forms of Fe(II) at circumneutral pH including dissolved Fe^{2+}aq, ligand bound Fe(II) and solid phase minerals (Byrne *et al*., 2015, 2016) as well as poised electrodes (Bose *et al*., 2014). Furthermore, it is not clear exactly how these bacteria are able to deal with the solid phase mineral precipitates (e.g., ferrihydrite) that are formed as a result.

The mechanism of phototrophic microbial Fe(II) oxidation has been most widely studied in *Rhodopseudomonas palustris* TIE-1. In this organism, electron transfer by Fe(II) oxidation is thought to require the *pioABC* operon, where *pio* stands for 'photosynthetic Fe(II)-oxidation' (Jiao and Newman, 2007). This is a 3 gene operon containing genes encoding for the proteins PioA (a periplasmic decaheme c-type cytochrome), PioB (an outer membrane beta-barrel protein) and PioC (a periplasmic high potential iron–sulfur cluster protein) (Jiao and Newman, 2007). PioA and PioB are homologous with MtrA and MtrB, respectively, that are for instance expressed by the Fe(III)-reducer *Shewanella oneidensis* MR-1 (Jiao and Newman, 2007). PioC is similar to the putative Fe(II) oxidoreductase Iro in *Acidothiobacillus ferrooxidans*. *Rhodopseudomonas palustris* TIE-1 most likely transfers electrons from PioA to PioC, which then donates electrons to the bc1 complex. Some authors have also suggested that the electrons could be passed to the inner membrane phototrophic reaction centre (Bird *et al*., 2014) (Fig. 4A). A *pioABC* operon was also found in *Rhodomicrobium vannielii* that probably functions similarly to that of *Rhodopseudomonas palustris* TIE-1 (He *et al*., 2017).

Deletion of PioA in *Rhodopseudomonas palustris* TIE-1 results in almost complete loss of Fe(II)-oxidizing ability whereas PioB and PioC deletions only result in partial loss compared with the wild type (Bose and Newman, 2011). The *pio* genes show highest expression with Fe(II) as an electron donor, but are transcribed and translated under all anoxic growth conditions (Bose and Newman, 2011). Expression of the *pio* operon is regulated by the global regulator FixK (Bose and Newman, 2011). Transcriptome-level insights have generated additional information on how Fe(II) shapes cellular processes in *Rhodopseudomonas palustris* TIE-1. These show that high levels of Fe(II) induce stress responses even under anoxic conditions where classical Fe(II) toxicity via oxidative stress induced by the Fenton reaction should not be an issue. The cellular response is primarily characterized by the induction of numerous metal efflux mechanisms (Bird *et al*., 2013).

To date, evidence relating to the location of PioA in the cell is somewhat contradictory. On one hand, based on sequence information, PioA is predicted to be a periplasmic protein (Jiao and Newman, 2007). Recent findings, however, show that *Rhodopseudomonas palustris* TIE-1 can oxidize the solid phase mixed-valent Fe(II)–Fe(III) mineral magnetite Fe_3O_4 (Byrne *et al*., 2015), and utilized electrons directly from poised electrodes (Bose *et al*., 2014). This suggests that PioA, with its electron transport mechanism and thus the ability to oxidize Fe(II), must be present on the outer membrane of the cell. Furthermore, it was shown that *Rhodopseudomonas palustris* TIE-1 is only able to access surface bound Fe(II) in the magnetite which further suggests a direct surface-mineral contact mechanism might be required (Byrne *et al*., 2016).

The other widely studied mechanism of anoxygenic phototrophic Fe(II) oxidation is that of *Rhodobacter ferrooxidans* SW2. This organism oxidizes Fe(II) via the *foxEYZ* operon (Croal *et al*., 2007). *foxE* encodes a c-type cytochrome with no significant similarity to other known Fe(II)-oxidizing or Fe(III)-reducing proteins. *foxE* and *foxY* are co-transcribed in the presence of Fe(II) and/or hydrogen, whereas *foxZ* is only transcribed in the presence of Fe(II) (Croal *et al*., 2007). It is thought that FoxE is positioned in the periplasm (Saraiva *et al*., 2012). It has further been proposed that electrons from Fe(II) are transferred to FoxE, then to FoxY and from there to the bc1 complex or,

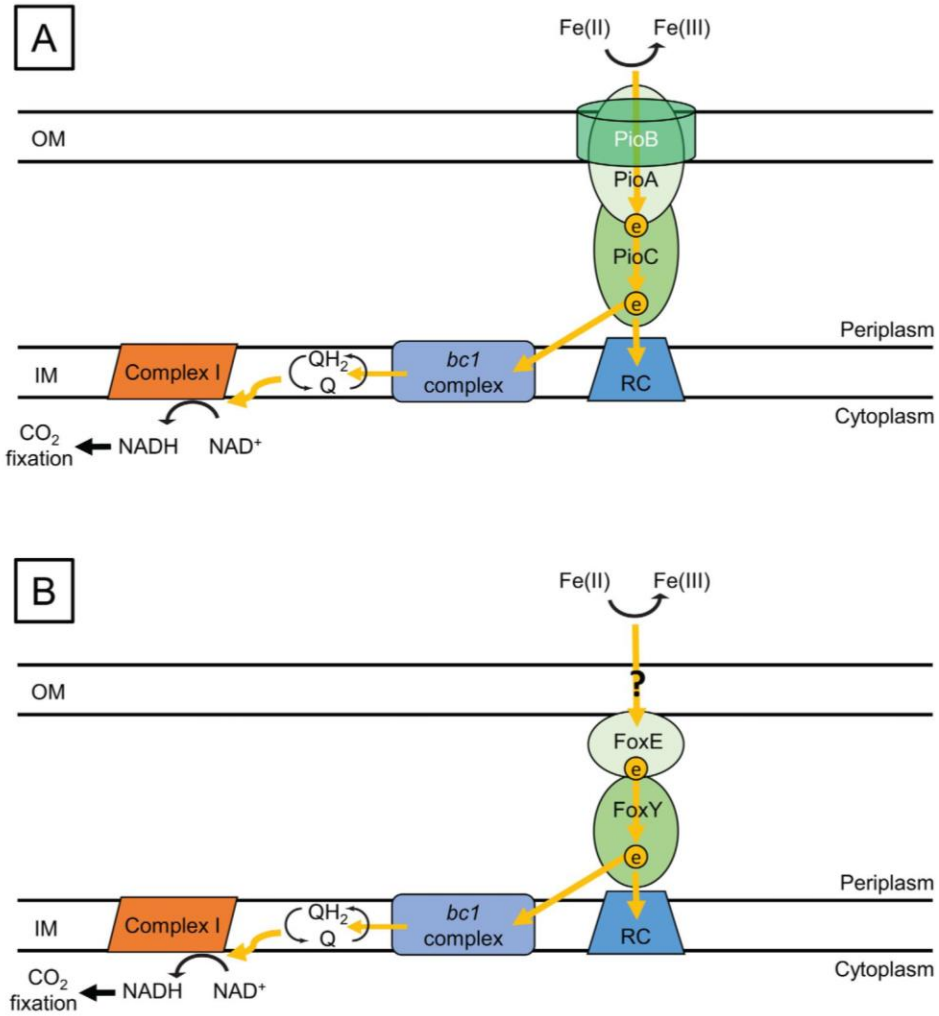

Fig. 4. Schematics of the current hypotheses on the mechanism of Fe(II) oxidation: (**A**) proposed Fe(II) oxidation mechanism in *Rhodopseudomonas palustris* TIE-1 and (**B**) proposed Fe(II) oxidation mechanism for *Rhodobacter ferrooxidans* SW2 (modified from Bird *et al*., 2011).

possibly, to the reaction centre (Bird *et al*., 2011) (Fig. 4A). To date, there is no evidence which shows the ability for *Rhodobacter ferrooxidans* SW2 to oxidize solid phase Fe(II) mineral phases.

The recently sequenced genome of *Chlorobium phaeoferrooxidans* suggests that yet another mechanism exists in these green sulfur bacteria. This genome encodes for an outer membrane cytochrome ($cyc2_{PV\text{-}1}$), which is known to be responsible for Fe(II) oxidation in the microaerophilic Fe(II)-oxidizer *Mariprofundus ferrooxidans* PV-1 (Crowe *et al*., 2008). $Cyc2_{PV\text{-}1}$ is a distant homologue of Cyc2, which is widely present in many known obligate lithotrophic Fe(II)-oxidizing bacteria (He *et al*., 2017). Cyc2 is also encoded in the genome of *Chlorobium ferrooxidans* DSM13031 (He *et al*., 2017).

The electron transfer mechanisms and proteins responsible for Fe(II) oxidation are probably diverse and one single mechanism is neither universally present among all physiological types of Fe(II)-oxidizers nor within one group of Fe(II)-oxidizers such as the phototrophs.

Mineral formation by photoferrotrophs

Phototrophic Fe(II)-oxidizing bacteria are able to oxidize a variety of Fe(II) species (see previous paragraph) resulting in the formation of poorly soluble Fe(III) (oxyhydr)oxides (Ehrenreich and Widdel, 1994; Straub *et al*., 1999; Kappler and Newman, 2004; Jiao *et al*., 2005; Gauger *et al*., 2015). Several studies observed the transformation of these amorphous to low crystalline initial precipitates to higher crystalline and thermodynamically more stable Fe mineral phases, such as goethite, lepidocrocite and magnetite over time (Straub *et al*., 1999; Kappler and Newman, 2004; Jiao *et al*., 2005; Miot *et al*., 2009c; Schaedler *et al*., 2009; Wu *et al*., 2014). Partial

dissolution and re-precipitation processes in combination with mineral transformation by sorption of residual Fe(II) represent potential transformation pathways (Posth *et al*., 2014). Laufer *et al*. (2016c) suggested that a close association between minerals and organics might constrain mineral growth and subsequent transformation, thus preserving the poorly crystalline ferrihydrite. The final mineral product of the Fe(II) oxidation therefore depends on various factors such as the geochemical conditions and/or the microbial community in the surrounding environment, and the Fe(II) concentration (e.g., Schaedler *et al*., 2009; Posth *et al*., 2010, 2013). In the case of strain *R. palustris* TIE-1 the pH seemed to be of particular importance, since at low pH conditions, poorly crystalline Fe(III) oxyhydroxides and goethite were formed while at pH conditions above 7.2, the formation of magnetite was observed (Jiao *et al*., 2005).

It has been suggested that Fe(II) oxidation occurs at different, strain specific localities, such as the cell surface or the periplasm. In close proximity to bacteria, freshly formed Fe(III) minerals, are expected to strongly adsorb to the negatively charged cell surface (Kappler and Newman, 2004; Schaedler *et al*., 2009). However, in contrast to nitrate-reducing Fe(II)-oxidizing bacteria, a lack of encrustation seems characteristic for photoferrotrophs (Schaedler *et al*., 2009; Wu *et al*., 2014). Yet, the extent to which cells and minerals are associated seems to be strain-specific. Furthermore, varying cell-mineral aggregate morphologies, ranging from irregular and bulbous to more symmetric (e.g., flower- and star-like shapes) have been reported and seem to depend on the mineralogy and age of culture (Ehrenreich and Widdel, 1994; Kappler and Newman, 2004; Jiao *et al*., 2005; Posth *et al*., 2010; Wu *et al*., 2014; Gauger *et al*., 2015; Laufer *et al*., 2017).

Much research has focused on the question as to why mineral precipitates and cells are closely associated while the cell surface itself remains (mostly) free of mineral precipitates and no encrustation occurs in the case of most photoferrotroph strains. Miot *et al*. (2009c) demonstrated an occurrence of goethite only outside of the cell and along organic fibres produced by *Rhodobacter ferrooxidans* sp. SW2. Likewise, Wu *et al*. (2014) found that in the case of *Rhodovulum iodosum*, the final precipitation product was mainly localized at the exopolysaccharides (EPS) and suggested the excretion of EPS as a strategy to prevent mineral encrustation on the cell surface. Another potential mechanism was presented by Hegler *et al*. (2010), who suggested that a low-pH environment around the cell would prevent Fe(III) mineral precipitation on the cell surface, probably in combination with the presence of EPS structures that direct the precipitation away from the cell surface. Avoidance of encrustation may also be a result of the location of the Fe(II) oxidase in the outer membrane and not in the periplasm as is likely to be the case in *Rhodopseudomonas palustris* TIE-1. This process may also be aided by the location of the Fe(II) oxidase within an outer membrane porin (Fig. 4A), which could facilitate the extrusion of Fe(III) from the cell before it has time to precipitate (Bird *et al*., 2011). The precipitation of Fe(III) outside of the cell on organic fibres in *Rhodobacter ferrooxidans* SW2 (Miot *et al*., 2009c) is consistent with either extracellular oxidation or rapid removal of Fe(III) from the cell. Alternatively, the structure of the Fe(II) oxidation protein itself may aid in the avoidance of encrustation as proposed by Pereira et al. (2017) who suggested that the structure of FoxE in *Rhodobacter ferrooxidans* SW2 discourages precipitation of Fe(III) within the periplasm following Fe(II) oxidation. A comparison between the iron oxidation mechanisms in these two strains is shown in Fig. 4.

A clear exception among the phototrophic Fe(II)-oxidizing bacteria is the strain *R. vannielii* BSI, which has been shown to produce Fe(III) oxyhydroxides that precipitated directly on the cell surface, forming crusts, which hindered further metabolic activity and hence, impeded Fe(II) oxidation after prolonged cultivation (Heising and Schink, 1998). The authors suggest that, other than during a laboratory cultivation, in a natural environment, this strain is likely able to re-dissolve the crusts of Fe(III) minerals and hence, maintain microbial activity and cell growth. In co-cultures of the green sulfur bacteria *Chlorobium ferrooxidans* KoFox and *Geospirillum* sp. KoFum, mineral encrustations are also observed but only prominently on KoFum cells (Schaedler *et al*., 2009). This suggests photoferrotrophs have active mechanisms to avoid encrustation.

Photoferrotrophs and their interactions with metals

Similar to biogenic Fe minerals produced by NRFeOx bacteria, biogenic Fe minerals produced by phototrophs react with and can even remove heavy metals from solution through sorption and/or co-precipitation processes. This association is mediated by forming Fe-metal bonds, rather than metal bonds with organic carbon. For example, when nickel (Ni) is reacted with biogenic phases produced by phototrophic bacteria, this heavy metal demonstrates a clear preference for associations with Fe on EPS, rather than with carbon (Eickhoff *et al*., 2014). Similarly, when the association of Ni with Si in biogenic Fe minerals produced by either *Rhodobacter ferrooxidans* SW2 or *Rhodovulum iodosum* is examined using scanning transmission X-ray microscopy (STXM), it is clear that Ni preferentially is associated with Fe rather than with Si (Eickhoff *et al*., 2014).

The preferential association of trace metals with Fe in biogenic Fe(III) minerals produced via phototrophic bacteria does not necessarily ensure decreased mobility of the

trace metal. For example, biogenic ferrihydrite produced by *Rhodobacter ferrooxidans* SW2 removes 99% of both As(V) and As(III) added (Hohmann *et al*., 2009). While this poorly crystalline phase adsorbs and incorporates As to a greater extent compared with more crystalline phases, ferrihydrite is also more susceptible to microbial Fe(III) reduction. Microbial Fe(III) reduction may induce dissolution of the solid and potentially release of As back into solution. Phosphate, which behaves similarly to arsenic in the environment, will also bind to Fe(III) minerals thus dissolution of Fe(III) minerals can release P and lead to eutrophication (Orihel *et al*., 2015). This effect may be enhanced in biogenic Fe minerals compared with abiogenic minerals due to the presence of organic carbon on the mineral surface and within the mineral structure itself due to co-precipitation with organics. In addition to organic carbon content, abiogenic and biogenic minerals produced by phototrophic bacteria differ in the extent of metal sorption and/or incorporation into the mineral structure. For example, a two to three-fold lower Ni/Fe ratio is observed for biogenic phases than for abiogenic phases. This decrease is likely due to surface site blockage by organic carbon (Eickhoff *et al*., 2014).

Co-existence of anaerobic Fe(II)-oxidizers in sediments

One of the key recent discoveries in the field of sedimentary Fe(II) oxidation is that anaerobic Fe-transforming metabolisms (NRFeOx, pFeOx, Fe(III)-reduction) are found to co-exist in both freshwater and marine sediments (Melton *et al*., 2012; Laufer *et al*., 2016b; Otte *et al*., 2018). Based on the thermodynamically-controlled stratification of redox-active compounds in sediments, it was previously suggested that Fe(II)-oxidizing microorganisms would be spatially separated over very short distances based on where the optimum geochemical conditions are found (Schmidt *et al*., 2010). The distribution of these metabolisms in shallow water sediments from Aarhus Bay (marine) shows that none of the physiological groups of Fe(II)-oxidizing bacteria in these sediments showed strong correlations with geochemical gradients (Laufer *et al*., 2016b; Otte *et al*., 2018), however some correlation with the abundance of cable bacteria was observed (Otte *et al*., 2018). It should be noted however, that these groups did show some correlation with geochemical gradients in deeper, profundal sediments in Lake Constance (Melton *et al*., 2012). Of the three physiological types, MPN studies showed microaerophilic Fe(II)-oxidizers were the most dominant, followed by nitrate-reducing Fe(II) oxidizers, with anoxygenic phototrophic iron oxidizers being the least abundant.

Possible applications in biotechnology

These anaerobic Fe(II)-oxidizing bacteria are not only environmentally important, but may have some useful biotechnological applications. Firstly, the ability of Fe(II)-oxidizers to remove nitrate may be harnessed for the improvement of drinking water, waste water and sludge in sewage treatment plants (Davidson *et al*., 2003; Zhang *et al*., 2015; Wang *et al*., 2016a; Kiskira *et al*., 2017). This may already occur naturally in aquifers where Fe(II)-oxidizing bacteria could couple nitrate reduction to oxidation of Fe(II)-rich clays or Fe(II)-containing minerals such as pyrite (Haaijer *et al*., 2007; Vaclavkova *et al*., 2015; Jessen *et al*., 2017). There is also potential to use minerals produced by these anaerobic Fe(II)-oxidizers, particularly reactive Fe(II)–Fe(III) phases like green rust or magnetite in remediation of metals and contaminants (reviewed in Usman *et al*., 2018). The importance of (biogenic) iron minerals in controlling As mobility has already been well documented (Hohmann *et al*., 2010). In anoxic Fe- and As-rich systems such as rice paddy soil or As-contaminated aquifers, the formation of iron minerals can act to bind arsenic and limit its dispersal in the environment (Seyfferth *et al*., 2010; Yamaguchi *et al*., 2014; Smith *et al*., 2017; Vega *et al*., 2017), although nothing is yet known about the importance of biogenic Fe(III) minerals in As-contaminated aquifers. The As-binding properties of iron are also harnessed in drinking water filters in arsenic-rich areas to provide low cost filtration solutions for contaminated water in developing counties (Nitzsche *et al*., 2015). On the one hand, Fe(II)-oxidizing bacteria could help remove As by co-precipitation (Hohmann *et al*., 2010). On the other hand, it has been shown that less As binds to biogenic Fe(III) minerals in such filter systems than to abiogenic Fe(II) minerals, probably due to surface sorption competition with the organic material stemming from the bacteria (Kleinert *et al*., 2011).

Conclusions

The extensive research conducted on these two distinct groups of anaerobic Fe(II)-oxidizing bacteria has provided a fundamental understanding of their physiology, Fe(II) oxidation mechanisms and role in the environment. However, there is much work still to be done. Regarding their physiology, there is still an important need to further test the proposed models for Fe(II) oxidation mechanisms for both types of anaerobic Fe(II) oxidation and establish how universal or variable these mechanisms are. Many of the proposed autotrophic NRFeOx bacteria also need to be re-tested to establish whether they are indeed autotrophic. We suggest that the four criteria used in Table 1 all need to be demonstrated in order to make this claim. There also remains some doubt as to whether organisms which require additional organic C for NRFeOx have

some enzymatic component of Fe(II) oxidation or whether it is all abiotic. We suggest that the role of intracellular reactions needs to be considered before this can be proven. Further understanding of how some Fe(II)-oxidizers avoid encrustation by minerals whereas some do not, and why some anoxygenic phototrophs can grow using Fe(II) as an electron donor and others cannot, is also needed. Another key knowledge gap is in the role of solid substrates as an electron donor for such bacteria which can often prove challenging. A promising avenue of research in this regard is the use of poised electrodes to simulate soil mineral substrates.

In terms of the environmental implications of these metabolisms, while bacteria have been isolated from many different environments (Fig. 2), we are still lacking a complete overview of the abundance and environmental distribution of these metabolisms. For example, almost all isolates of anaerobic Fe(II)-oxidizing bacteria have come from freshwater or marine sedimentary environments in Europe and North America (Table 1 and Supporting Information Table S1). However, their demonstrated ubiquity in these environments, as well as in freshwater stratified lakes, suggests that these bacteria are widespread. NRFeOx processes in particular are likely to play a key role in agricultural soils and aquifers where nitrate contamination is high and iron is generally plentiful. There is also a distinct European and North American bias in our knowledge of the environmental role of these organisms. Future work should focus on determining the role of these organisms in more tropical settings, or in more extreme climatic conditions such as arid or cold regions.

We also still need to better understand how our chosen growth conditions influence the minerals which are formed by Fe(II)-oxidizers, and why only some isolates can oxidize solid substrates. The knowledge of what minerals form under environmentally relevant conditions, for example, under low iron concentrations or in the presence of competing (organic or inorganic) substrates, has been barely studied yet is critical for transferring our knowledge of these processes out of the lab. A focus on this may also aid in our understanding of the distribution of these organisms within redox gradients in the environment by determining if their even distribution can be explained by metabolic flexibility.

It is an exciting time to work on the anoxic side of the microbial iron cycle. Our appreciation of the role of these bacteria in many different environments is increasing rapidly, and we are beginning to establish the fundamental mechanisms underpinning these metabolisms, and the effects they have on mineral formation and element cycling under environmental conditions. Over the coming years, we hope that more and more researchers will begin to look for these types of organisms in their own anoxic systems and consider their potential biotechnological usage when faced with an environmental problem.

Acknowledgements

The authors would like to thank three anonymous reviewers for their role in the improvement of this manuscript. Additionally, we are grateful to the German Research Foundation (DFG)-funded research training group RTG 1708 'Molecular principles of bacterial survival strategies' (grant # 174858087; Y.H.), a DFG-funded Emmy-Noether fellowship (grant # 326028733 to S.K) and to the European Union's Seventh Framework Programme (FP/2007-2013) (ERC grant, Agreement # 307320 – MICROFOX to A.K).

References

Achenbach, L. A., Michaelidou, U., Bruce, R. A., Fryman, J., and Coates, J. D. (2001) Dechloromonas agitata gen. nov., sp. nov. and Dechlorosoma suillum gen. Nov., sp. nov., two novel environmentally dominant (per) chlorate-reducing bacteria and their phylogenetic position Laurie. *Int J Syst Evol Microbiol* **51**: 527–533.

Beller, H. R., Chain, P. S. G., Letain, T. E., Chakicherla, A., Larimer, F. W., Richardson, P. M., *et al*. (2006) The genome sequence of the obligately chemolithoautotrophic, facultatively anaerobic bacterium Thiobacillus denitrificans. *J Bacteriol* **188**: 1473–1488.

Beller, H. R., Zhou, P., Legler, T. C., Chakicherla, A., Kane, S., Letain, T. E., and O'Day, P. A. (2013) Genome-enabled studies of anaerobic, nitrate-dependent oxidation in the chemolithoautotrophic bacterium Thiobacillus denitrificans. *Front Microbiol* **4**: 1–16.

Benzine, J., Shelobolina, E., Xiong, M. Y., Kennedy, D. W., McKinley, J. P., Lin, X., and Roden, E. E. (2013) Fe-phyllosilicate redox cycling organisms from a redox transition zone in Hanford 300 area sediments. *Front Microbiol* **4**: 1–13.

Berg, J., Michellod, D., Pjevac, P., Martinez-Perez, C., Buckner, C., Hach, P., *et al*. (2016) Intensive cryptic microbial iron cycling in the low iron water column of the meromictic Lake Cadagno. *Environ Microbiol* **18**: 5288–5302.

Bird, L. J., Bonnefoy, V., and Newman, D. K. (2011) Bioenergetic challenges of microbial iron metabolisms. *Trends Microbiol* **19**: 330–340.

Bird, L. J., Coleman, M. L., and Newman, D. K. (2013) Iron and copper act synergistically to delay anaerobic growth of bacteria. *Appl Environ Microbiol* **79**: 3619–3627.

Bird, L., Saraiva, I., Park, S., Calcada, E., Salgueiro, C., Nitschke, W., *et al*. (2014) Nonredundant roles for cytochrome c2 and two high-potential iron-sulfur proteins in the Photoferrotroph Rhodopseudomonas palustris TIE-1. *J Bacteriol* **196**: 850–858.

Blöthe, M., and Roden, E. E. (2009) Composition and activity of an autotrophic Fe(II)-oxidizing, nitrate-reducing enrichment culture. *Appl Environ Microbiol* **75**: 6937–6940.

Bosch, J., Lee, K. Y., Jordan, G., Kim, K. W., and Meckenstock, R. U. (2012) Anaerobic, nitrate-dependent oxidation of pyrite nanoparticles by thiobacillus denitrificans. *Environ Sci Technol* **46**: 2095–2101.

Bose, A., and Newman, D. K. (2011) Regulation of the phototrophic iron oxidation (pio) genes in Rhodopseudomonas palustris TIE-1 is mediated by the global regulator, FixK. *Mol Microbiol* **79**: 63–75.

Bose, A., Gardel, E. J., Vidoudez, C., Parra, E. A., and Girguis, P. R. (2014) Electron uptake by iron-oxidizing phototrophic bacteria. *Nat Commun* **5**: 3391.

Brons, H. J., Hagen, W. R., and Zehnder, A. J. B. (1991) Ferrous iron dependent nitric oxide production in nitrate reducing cultures of Escherichia coli. *Arch Microbiol* **155**: 341–347.

Buchholz-Cleven, B. E. E., Rattunde, B., and Straub, K. L. (1997) Screening for genetic diversity of isolates of anaerobic Fe(II)-oxidizing bacteria using DGGE and whole-cell hybridization. *Syst Appl Microbiol* **20**: 301–309.

Buchwald, C., Grabb, K., Hansel, C. M., and Wankel, S. D. (2016) Constraining the role of iron in environmental nitrogen transformations: dual stable isotope systematics of abiotic NO^{2-} reduction by Fe(II) and its production of N_2O. *Geochim Cosmochim Acta* **186**: 1–12.

Buresh, R. J., and Moraghan, J. T. (1978) Chemical reduction of nitrate by ferrous iron. *J Environ Qual* **5**: 320–325.

Burgin, A. J., and Hamilton, S. K. (2007) Have we overemphasized the role of denitrification in aquatic ecosystems? A review of nitrate removal pathways. *Front Ecol Environ* **5**: 89–96.

Byrne-Bailey, K. G., Weber, K. A., Chair, A. H., Bose, S., Knox, T., Spanbauer, T. L., *et al*. (2010) Completed genome sequence of the anaerobic iron-oxidizing bacterium Acidovorax ebreus strain TPSY. *J Bacteriol* **192**: 1475–1476.

Byrne, J., Klueglein, N., Pearce, C., Rosse, K., Appel, E., and Kappler, A. (2015) Redox cycling of Fe(II) and Fe(III) in magnetite by Fe-metabolizing bacteria. *Science* **347**: 1473–1476.

Byrne, J. M., Van Der Laan, G., Figueroa, A. I., Qafoku, O., Wang, C., Pearce, C. I., *et al*. (2016) Size dependent microbial oxidation and reduction of magnetite nano- and micro-particles. *Sci Rep* **6**: 30969.

Carlson, L., and Schwertmann, U. (1981) Natural ferrihydrites in surface deposits from Finland and their association with silica. *Geochim Cosmochim Acta* **45**: 421–429.

Carlson, L., and Schwertmann, U. (1990) The effect of CO_2 and oxidation rate on the formation of goethite versus lepidocrocite from an Fe(II) system at pH 6 and 7. *Clay Miner* **25**: 65–71.

Carlson, H. K., Clark, I. C., Blazewicz, S. J., Iavarone, A. T., and Coates, J. D. (2013) Fe(II) oxidation is an innate capability of nitrate-reducing bacteria that involves abiotic and biotic reactions. *J Bacteriol* **195**: 3260–3268.

Chakraborty, A., Roden, E. E., Schieber, J., and Picardal, F. (2011) Enhanced growth of Acidovorax sp . Strain 2AN during nitrate-dependent Fe(II) oxidation in batch and continuous-flow systems. *Appl Environ Microbiol* **77**: 8548–8556.

Chaudhuri, S. K., Lack, J. G., and Coates, J. D. (2001) Biogenic magnetite formation through anaerobic biooxidation of Fe(II) biogenic magnetite formation through anaerobic biooxidation of Fe(II). *Appl Environ Microbiol* **67**: 2844–2948.

van Cleemput, O., and Samater, A. H. (1995) Nitrite in soils: accumulation and role in the formation of gaseous N compounds. *Fert Res* **45**: 81–89.

Cloud, P. (1973) Paleoecological significance of the banded iron-formation. *Econ Geol* **68**: 1135–1143.

Coby, A. J., Picardal, F., Shelobolina, E., Xu, H., and Roden, E. E. (2011) Repeated anaerobic microbial redox cycling of iron. *Appl Environ Microbiol* **77**: 6036–6042.

Colman, B. P., Fierer, N., and Schimel, J. P. (2008) Abiotic nitrate incorporation, anaerobic microsites, and the ferrous wheel. *Biogeochemistry* **91**: 223–227.

Croal, L., Johnson, C., Beard, B., and Newman, D. (2004) Iron isotope fractionation by Fe(II)-oxidizing photoautotrophic bacteria. *Geochim Cosmochim Acta* **68**: 1227–1242.

Croal, L. R., Jiao, Y., and Newman, D. K. (2007) The fox operon from Rhodobacter strain SW2 promotes phototrophic Fe (II) oxidation in Rhodobacter capsulatus SB1003. *J Bacteriol* **189**: 1774–1782.

Croal, L. R., Jiao, Y., Kappler, A., and Newman, D. K. (2009) Phototrophic Fe(II) oxidation in an atmosphere of H_2: implications for Archean banded iron formations. *Geobiology* **7**: 21–24.

Crowe, S. A., Jones, C., Katsev, S., Magen, C., O'Neill, A. H., Sturm, A., *et al*. (2008) Photoferrotrophs thrive in an Archean Ocean analogue. *Proc Natl Acad Sci* **105**: 15938–15943.

Crowe, S., Hahn, A., Morgan-Lang, C., Thompson, K., Simister, R., Lliros, M., *et al*. (2017) Draft genome sequence of the pelagic Photoferrotroph Chlorobium phaeoferrooxidans. *Am Soc Microbiol* **5**: 13–14.

Crutzen, P. J. (1974) Photochemical reactions initiated by and influencing ozone in unpolluted tropospheric air. *Tellus* **26**: 47–57.

Daugherty, E. E., Gilbert, B., Nico, P. S., and Borch, T. (2017) Complexation and redox buffering of iron(II) by dissolved organic matter. *Environ Sci Technol* **51**: 11096–11104.

Davidson, E. A., Chorover, J., and Dail, D. B. (2003) A mechanism of abiotic immobilization of nitrate in forest ecosystems: the ferrous wheel hypothesis. *Glob Chang Biol* **9**: 228–236.

Dhakal, P., Matocha, C. J., Huggins, F. E., and Vandiviere, M. M. (2013) Nitrite reactivity with magnetite. *Environ Sci Technol* **47**: 6206–6213.

Dippon, U., Pantke, C., Porsch, K., Larese-casanova, P., and Kappler, A. (2012) Potential function of added minerals as nucleation sites and E ff ect of humic substances on mineral formation by the nitrate-reducing Fe(II)-oxidizer Acidovorax sp. BoFeN1. *Environ Sci Technol* **46**: 6556–6565.

Edwards, K., Rogers, D., Wirsen, C., and McCollom, T. (2003) Isolation and characterization of novel psychrophilic, neutrophilic, Fe-oxidizing, chemolithoautotrophic α- and γ-proteobacteria from the deep sea. *Nature* **69**: 2906–2913.

Ehrenberg, C. (1836) Vorlaufige Mittheilung uber das wirkliche Vorkommen fossiler Infusorien und ihre grosse Verbreitung. *Ann Phys* **38**: 13–227.

Ehrenreich, A., and Widdel, F. (1994) Anaerobic oxidation of ferrous iron by purple bacteria, a new type of phototrophic metabolism. *Appl Environ Microbiol* **60**: 4517–4526.

Eickhoff, M., Obst, M., Schröder, C., Hitchcock, A. P., Tyliszczak, T., Martinez, R. E., *et al*. (2014) Nickel partitioning in biogenic and abiogenic ferrihydrite: the influence of silica and implications for ancient environments. *Geochim Cosmochim Acta* **140**: 65–79.

Emmerich, M., Bhansali, A., Kappler, A., and Behrens, S. (2012) Reducing microorganisms in hypersaline sediments of Lake Kasin. *Appl Environ Microbiol* **78**: 4386–4399.

Etique, M., Jorand, F. P. A., Zegeye, A., Grégoire, B., Despas, C., and Ruby, C. (2014) Abiotic process for Fe(II) oxidation and green rust mineralization driven by a heterotrophic nitrate reducing bacteria (Klebsiella mobilis). *Environ Sci Technol* **48**: 3742–3751.

Finneran, K. T., Housewright, M. E., and Lovley, D. R. (2002) Multiple influences of nitrate on uranium solubility during bioremediation of uranium-contaminated subsurface sediments. *Environ Microbiol* **4**: 510–516.

Gallus, C., and Schink, B. (1994) Anaerobic degradation of pimelate by newly isolated denitrifying bacteria. *Microbiology* **140**: 409–416.

Gauger, T., Konhauser, K., and Kappler, A. (2015) Protection of phototrophic iron(II)-oxidizing bacteria from UV irradiation by biogenic iron(III) minerals: implications for early archean banded iron formation. *Geology* **43**: 1067–1070.

Gauger, T., Byrne, J. M., Konhauser, K. O., Obst, M., Crowe, S., and Kappler, A. (2016) Influence of organics and silica on Fe(II) oxidation rates and cell-mineral aggregate formation by the green-sulfur Fe(II)-oxidizing bacterium Chlorobium ferrooxidans KoFox - implications for Fe(II) oxidation in ancient oceans. *Earth Planet Sci Lett* **443**: 81–89.

Ginn, B., Meile, C., Wilmoth, J., Tang, Y., and Thompson, A. (2017) Rapid iron reduction rates are stimulated by high-amplitude redox fluctuations in a tropical Forest soil. *Environ Sci Technol* **51**: 3250–3259.

Grabb, K. C., Buchwald, C., Hansel, C. M., and Wankel, S. D. (2017) A dual nitrite isotopic investigation of chemodenitrification by mineral-associated Fe(II) and its production of nitrous oxide. *Geochim Cosmochim Acta* **196**: 388–402.

Haaijer, S. C. M., Lamers, L. P. M., Smolders, A. J. P., Jetten, M. S. M., and Op den Camp, H. J. M. (2007) Iron sulfide and pyrite as potential electron donors for microbial nitrate reduction in freshwater wetlands. *Geomicrobiol J* **24**: 391–401.

Hafenbradl, D., Keller, M., Dirmeier, R., Rachel, R., Roßnagel, P., Burggraf, S., *et al*. (1996) Ferroglobus placidus gen. Nov., sp. nov., a novel hyperthermophilic archaeum that oxidizes Fe2+ at neutral pH under anoxic conditions. *Arch Microbiol* **166**: 308–314.

Handley, K. M., Héry, M., and Lloyd, J. R. (2009) Marinobacter santoriniensis sp. nov., an arsenate respiring and arsenite-oxidizing bacterium isolated from hydrothermal sediment. *Int J Syst Evol Microbiol* **59**: 886–892.

Hartman, H. (1984)The evolution of photosynthesis and microbial mats: a speculation on banded iron formations . In *Microbial Mats: Stromatolites*, Cohen, Y., Castenholz, R. W., and Halverson, H. O. (eds). New York, NY: Alan R. Liss, Inc., pp. 449–453.

He, S., Tominski, C., Kappler, A., Behrens, S., and Roden, E. E. (2016) Metagenomic analyses of the autotrophic Fe(II)-oxidizing, nitrate-reducing enrichment culture KS. *Appl Environ Microbiol* **82**: 2656–2668.

He, S., Barco, R. A., Emerson, D., and Roden, E. E. (2017) Comparative genomic analysis of neutrophilic iron (II) oxidizer genomes for candidate genes in extracellular electron transfer. *Front Microbiol* **8**: 1–17.

Hegler, F., Posth, N. R., Jiang, J., and Kappler, A. (2008) Physiology of phototrophic iron(II)-oxidizing bacteria: implications for modern and ancient environments. *FEMS Microbiol Ecol* **66**: 250–260.

Hegler, F., Schmidt, C., Schwarz, H., and Kappler, A. (2010) Does a low-pH microenvironment around phototrophic FeII-oxidizing bacteria prevent cell encrustation by FeIII minerals? *FEMS Microbiol Ecol* **74**: 592–600.

Heil, J., Liu, S., Vereecken, H., and Brüggemann, N. (2015) Abiotic nitrous oxide production from hydroxylamine in soils and their dependence on soil properties. *Soil Biol Biochem* **84**: 107–115.

Heising, S., and Schink, B. (1998) Phototrophic oxidation of ferrous iron by a Rhodomicrobium vannielii strain. *Microbiology* **144**: 2263–2269.

Heising, S., Richter, L., Ludwig, W., and Schink, B. (1999) Chlorobium ferrooxidans sp. nov., a phototrophic green sulfur bacterium that oxidizes ferrous iron in coculture with a 'Geospirillum' sp. strain. *Arch Microbiol* **172**: 116–124.

Herndon, E., Albashaireh, A., Singer, D., Roy, T., Gu, B., and Graham, D. (2017) Influence of iron redox cycling on organo-mineral associations in Arctic tundra soil. *Geochim Cosmochim Acta* **207**: 210–231.

Herrmann, M., Opitz, S., Harzer, R., Totsche, K., and Küsel, K. (2017) Attached and suspended denitrifier communities in pristine limestone Aquifers Harbor high fractions of potential autotrophs oxidizing reduced iron and sulfur compounds. *Microb Ecol* **74**: 264–277.

Hohmann, C., Winkler, E., Morin, G., and Kappler, A. (2009) Anaerobic Fe(II)-oxidizing bacteria show as resistance and immobilize as during Fe (III) mineral precipitation. *Environ Sci Technol* **44**: 94–101.

Hohmann, C., Winkler, E., Morin, G., and Kappler, A. (2010) Anaerobic Fe(II)-oxidizing bacteria show as resistance and immobilize as during Fe(III) mineral precipitation. *Environ Sci Technol* **44**: 94–101.

Ilbert, M., and Bonnefoy, V. (2012) Insight into the evolution of the iron oxidation pathways. *BBA-Bioenergetics* **1827**: 161–175.

IPCC. (2013)Summary for policymakers . In *Climate Change 2013: The Physical Science Basis. Contribution of Working Group I to the Fifth Assessment Report of the Intergovernmental Panel on Climate Change*, Stocker, T. F., Qin, D., Plattner, G. K., Tignor, M. M. B., Allen, S. K., Boschung, J., *et al*. (eds). Cambridge, UK: Cambridge University Press.

Jamieson, J., Prommer, H., Kaksonen, A., Siade, A., Yusov, A., and Bostick, B. C. (2018) Identifying and quantifying the intermediate processes during nitrate dependent iron (II) oxidation. *Environ Sci Technol* **52**: 5771–5781.

Jessen, S., Postma, D., Thorling, L., Müller, S., Leskelä, J., and Engesgaard, P. (2017) Decadal variations in groundwater quality: a legacy from nitrate leaching and denitrification by pyrite in a sandy aquifer. *Water Resour Res* **53**: 184–198.

Jewell, T. N. M., Karaoz, U., Brodie, E. L., Williams, K. H., and Beller, H. R. (2016) Metatranscriptomic evidence of

pervasive and diverse chemolithoautotrophy relevant to C, S, N and Fe cycling in a shallow alluvial aquifer. *ISME J* **10**: 2106–2117.

Jiao, Y., and Newman, D. K. (2007) The pio operon is essential for phototrophic Fe(II) oxidation in Rhodopseudomonas palustris TIE-1. *J Bacteriol* **189**: 1765–1773.

Jiao, Y., Kappler, A., Croal, L. R., Newman, K., and Newman, D. K. (2005) Isolation and characterization of a genetically tractable photoautotrophic isolation and characterization of a genetically tractable photoautotrophic Fe(II)-oxidizing bacterium, Rhodopseudomonas palustris strain TIE-1. *Appl Environ Microbiol* **71**: 4487–4496.

Jones, L. C., Peters, B., Lezama Pacheco, J. S., Casciotti, K. L., and Fendorf, S. (2015) Stable isotopes and iron oxide mineral products as markers of chemodenitrification. *Environ Sci Technol* **49**: 3444–3452.

Kalmbach, S., Manz, W., Wecke, J., and Szewzyk, U. (1999) Aquabacterium gen. nov., with description of Aquabacterium citratiphilum sp. nov., Aquabacterium parvum sp. nov. and Aquabacterium commune sp. nov., three in situ dominant bacterial species from the berlin drinking water system. *Int J Syst Bacteriol* **49**: 769–777.

Kampschreur, M. J., Kleerebezem, R., de Vet, W. W. J. M., and Van Loosdrecht, M. C. M. (2011) Reduced iron induced nitric oxide and nitrous oxide emission. *Water Res* **45**: 5945–5952.

Kappler, A., and Newman, D. (2004) Formation of Fe (III) minerals by Fe(II)-oxidizing photoautotrophic bacteria. *Geochim Cosmochim Acta* **68**: 1217–1226.

Kappler, A., Pasquero, C., Konhauser, K. O., and Newman, D. K. (2005a) Deposition of banded iron formations by anoxygenic phototrophic Fe(II)-oxidizing bacteria. *Geology* **33**: 865–868.

Kappler, A., Schink, B., and Newman, D. (2005b) Fe(III) mineral formation and cell encrustation by the nitrate-dependent Fe(II)-oxidizer strain BoFeN1. *Geobiology* **3**: 235–245.

Kiskira, K., Papirio, S., van Hullebusch, E. D., and Esposito, G. (2017) Fe(II)-mediated autotrophic denitrification: a new bioprocess for iron bioprecipitation/biorecovery and simultaneous treatment of nitrate-containing wastewaters. *Int Biodeterior Biodegradation* **119**: 631–648.

Kleinert, S., Muehe, E. M., Posth, N. R., Dippon, U., Daus, B., and Kappler, A. (2011) Biogenic Fe(III) minerals lower the efficiency of iron-mineral-based commercial filter Systems for Arsenic Removal. *Environ Sci Technol* **45**: 7533–7541.

Klueglein, N., and Kappler, A. (2013) Abiotic oxidation of Fe(II) by reactive nitrogen species in cultures of the nitrate-reducing Fe(II) oxidizer Acidovorax sp . BoFeN1 – questioning the existence of enzymatic Fe(II) oxidation. *Geobiology* **11**: 180–190.

Klueglein, N., Zeitvogel, F., Stierhof, Y.-D., Floetenmeyer, M., Konhauser, K. O., and Kappler, A. (2014) Potential role of nitrite for abiotic Fe (II) oxidation and cell encrustation during nitrate reduction by denitrifying bacteria. *Appl Environ Microbiol* **80**: 1051–1061.

Kopf, S. H., and Newman, D. K. (2012) Photomixotrophic growth of Rhodobacter capsulatus SB1003 on ferrous iron. *Geobiology* **10**: 216–222.

Kostka, J. E., and Luther, G. W. (1994) Partitioning and speciation of solid-phase iron in salt- marsh sediments. *Geochim Cosmochim Acta* **58**: 1701–1710.

Kumaraswamy, R., Sjollema, K., Kuenen, G., van Loosdrecht, M., and Muyzer, G. (2006) Nitrate-dependent [Fe(II)EDTA]2-oxidation by Paracoccus ferrooxidans sp. nov., isolated from a denitrifying bioreactor. *Syst Appl Microbiol* **29**: 276–286.

Lack, J. G., Chaudhuri, S. K., Chakraborty, R., Achenbach, L. A., and Coates, J. D. (2002) Anaerobic biooxidation of Fe(II) by Dechlorosoma suillum. *Microb Ecol* **43**: 424–431.

Larese-Casanova, P., Haderlein, S. B., and Kappler, A. (2010) Biomineralization of lepidocrocite and goethite by nitrate-reducing Fe(II)-oxidizing bacteria: effect of pH, bicarbonate, phosphate, and humic acids. *Geochim Cosmochim Acta* **74**: 3721–3734.

Laufer, K., Røy, H., and Jørgensen, B. (2016a) Evidence for the existence of autotrophic nitrate-reducing Fe (II)-oxidizing bacteria in marine coastal sediment. *Appl Environ Microbiol* **82**: 6120–6131.

Laufer, K., Nordhoff, M., Schmidt, C., Behrens, S., Jørgensen, B. B., and Kappler, A. (2016b) Co-existence of microaerophilic, nitrate-reducing, and phototrophic Fe(II)-oxidizers and Fe(III)-reducers in coastal marine sediment. *Appl Environ Microbiol* **82**: 1433–1447.

Laufer, K., Byrne, J. M., Glombitza, C., Schmidt, C., Jørgensen, B. B., and Kappler, A. (2016c) Anaerobic microbial Fe(II) oxidation and Fe(III) reduction in coastal marine sediments controlled by organic carbon content. *Environ Microbiol* **18**: 3159–3174.

Laufer, K., Niemeyer, A., Nikeleit, V., Halama, M., Byrne, J. M., and Kappler, A. (2017) Physiological characterization of a halotolerant anoxygenic phototrophic Fe(II)-oxidizing green-sulfur bacterium isolated from a marine sediment. *FEMS Microbiol Ecol* **93**: 1–13.

Li, B., Tian, C., Zhang, D., and Pan, X. (2014) Anaerobic nitrate-dependent iron(II) oxidation by a novel autotrophic bacterium, Citrobacter freundii strain PXL1. *Geomicrobiol J* **31**: 138–144.

Liu, S., Zhang, L., Liu, Q., and Zou, J. (2012) Fe(III) fertilization mitigating net global warming potential and greenhouse gas intensity in paddy rice-wheat rotation systems in China. *Environ Pollut* **164**: 73–80.

Llirós, M., Garcia-Armisen, T., Darchambeau, F., Morana, C., Triadó-Margarit, X., Inceoğlu, Ö., *et al*. (2015) Pelagic photoferrotrophy and iron cycling in a modern ferruginous basin. *Sci Rep* **5**: 13803.

Lovley, D. R. (1997) Microbial Fe(III) reduction in subsurface environments. *FEMS Microbiol Rev* **20**: 305–313.

Lovley, D. R., Stolz, J. F., Nord, G. L., Jr., and Phillips, E. J. P. (1987) Anaerobic production of magnetite by a dissimilatory iron-reducing microorganism. *Nature* **330**: 252–254.

Luther, G. W., Kostka, J. E., Church, T. M., Sulzberger, B., and Stumm, W. (1992) Seasonal iron cycling in the salt-marsh sedimentary environment: the importance of ligand complexes with Fe(II) and Fe(III) in the dissolution of Fe(III) minerals and pyrite, respectively. *Mar Chem* **40**: 81–103.

Manske, A. K., Glaeser, J., Kuypers, M. M. M., and Overmann, J. (2005) Physiology and phylogeny of green sulfur bacteria forming a monospecific phototrophic assemblage at a depth of 100 meters in the Black Sea. *Appl Environ Microbiol* **71**: 8049–8060.

Mattes, A., Gould, D., Taupp, M., and Glasauer, S. (2013) A novel autotrophic bacterium isolated from an engineered wetland system links nitrate-coupled iron oxidation to the removal of as, Zn and S. *Water Air Soil Pollut* **224**: 1490.

Mejia, J., Roden, E. E., and Ginder-Vogel, M. (2016) Influence of oxygen and nitrate on Fe (Hydr)oxide mineral transformation and soil microbial communities during redox cycling. *Environ Sci Technol* **50**: 3580–3588.

Melton, E. D., Schmidt, C., and Kappler, A. (2012) Microbial iron(II) oxidation in littoral freshwater lake sediment: the potential for competition between phototrophic vs. nitrate-reducing iron(II)-oxidizers. *Front Microbiol* **3**: 1–12.

Melton, E. D., Swanner, E. D., Behrens, S., Schmidt, C., and Kappler, A. (2014a) The interplay of microbially mediated and abiotic reactions in the biogeochemical Fe cycle. *Nat Rev Microbiol* **12**: 797–809.

Melton, E. D., Schmidt, C., Behrens, S., Schink, B., and Kappler, A. (2014b) Metabolic flexibility and substrate preference by the Fe(II)-oxidizing purple non-Sulphur bacterium Rhodopseudomonas palustris strain TIE-1. *Geomicrobiol J* **31**: 37–41.

Melton, E. D., Stief, P., Behrens, S., Kappler, A., and Schmidt, C. (2014c) High spatial resolution of distribution and interconnections between Fe- and N-redox processes in profundal lake sediments. *Environ Microbiol* **16**: 3287–3303.

Miot, J., and Etique, M. (2016)Formation and transformation of iron-bearing minerals by iron(II)-oxidizing and iron(III)-reducing bacteria . In *Iron Oxides*, Faivre, D. (ed). Weinheim, Germany: Wiley-VCH Verlag GmbH & Co KGaA, pp. 53–98.

Miot, J., Benzerara, K., Morin, G., Bernard, S., Beyssac, O., Larquet, E., *et al*. (2009a) Transformation of vivianite by anaerobic nitrate-reducing iron-oxidizing bacteria. *Geobiology* **7**: 373–384.

Miot, J., Benzerara, K., Morin, G., Kappler, A., Bernard, S., Guigner, J., *et al*. (2009b) Iron biomineralization by anaerobic neutrophilic iron-oxidizing bacteria. *Geochim Cosmochim Acta* **73**: 696–711.

Miot, J., Benzerara, K., Obst, M., Kappler, A., Hegler, F., Schädler, S., *et al*. (2009c) Extracellular iron biomineralization by photoautotrophic iron-oxidizing bacteria. *Appl Environ Microbiol* **75**: 5586–5591.

Miot, J., Li, J., Benzerara, K., Sougrati, M. T., Ona-Nguema, G., Bernard, S., *et al*. (2014) Formation of single domain magnetite by green rust oxidation promoted by microbial anaerobic nitrate-dependent iron oxidation. *Geochim Cosmochim Acta* **139**: 327–343.

Miot, J., Remusat, L., Duprat, E., Gonzalez, A., Pont, S., and Poinsot, M. (2015) Fe biomineralization mirrors individual metabolic activity in a nitrate-dependent Fe(II)-oxidizer. *Front Microbiol* **6**: 1–13.

Miot, J., Jézéquel, D., Benzerara, K., Cordier, L., Rivas-Lamelo, S., Skouri-Panet, F., *et al*. (2016) Mineralogical diversity in Lake Pavin: connections with water column chemistry and biomineralization processes. *Minerals* **6**: 24.

Moore, C. M., Mills, M. M., Arrigo, K. R., Berman-Frank, I., Bopp, L., Boyd, P. W., *et al*. (2013) Processes and patterns of oceanic nutrient limitation. *Nat Geosci* **6**: 701–710.

Moraghan, J. T., and Buresh, R. J. (1977) Chemical reduction of nitrite and nitrous oxide by ferrous iron. *Soil Sci Soc Am* **41**: 47–50.

Muehe, E. M., Gerhardt, S., Schink, B., and Kappler, A. (2009) Ecophysiology and the energetic benefit of mixotrophic Fe(II) oxidation by various strains of nitrate-reducing bacteria. *FEMS Microbiol Ecol* **70**: 335–343.

Nitzsche, K. S., Weigold, P., Lösekann-Behrens, T., Kappler, A., and Behrens, S. (2015) Microbial community composition of a household sand filter used for arsenic, iron, and manganese removal from groundwater in Vietnam. *Chemosphere* **138**: 47–59.

Nordhoff, M., Tominski, C., Halama, M., Byrne, J. M., Obst, M., Kleindienst, S., *et al*. (2017) Insights into nitrate-reducing Fe(II) oxidation mechanisms through analysis of cell-mineral associations, cell encrustation, and mineralogy in the chemolithoautotrophic enrichment culture KS. *Appl Environ Microbiol* **83**: e00752–e00717.

Orihel, D. M., Schindler, D. W., Ballard, N. C., Graham, M. D., O'Connell, D. W., Wilson, L. R., and Vinebrooke, R. D. (2015) The 'nutrient pump:' iron-poor sediments fuel low nitrogen-to-phosphorus ratios and cyanobacterial blooms in polymictic lakes. *Limnol Oceanogr* **60**: 856–871.

Oshiki, M., Ishii, S., Yoshida, K., Fujii, N., Ishiguro, M., Satoh, H., and Okabe, S. (2013) Nitrate-dependent ferrous iron oxidation by anaerobic ammonium oxidation (anammox) bacteria. *Appl Environ Microbiol* **79**: 4087–4093.

Ostrom, N. E., Gandhi, H., Trubl, G., and Murray, A. E. (2016) Chemodenitrification in the cryoecosystem of Lake Vida, Victoria Valley, Antarctica. *Geobiology* **14**: 575–587.

Otte, J. M., Harter, J., Laufer, K., Blackwell, N., Kappler, A., and Kleindienst, S. (2018) The distribution of active iron cycling bacteria in marine and freshwater sediments is decoupled from geochemical gradients. *Environ Microbiol* doi:10.1111/1462-2920.14260

Ottley, C. J., Davison, W., and Edmunds, W. M. (1997) Chemical catalysis of nitrate reduction by iron (II). *Geochim Cosmochim Acta* **61**: 1819–1828.

Pantke, C., Obst, M., Benzerara, K., Morin, G., Ona-Nguema, G., Dippon, U., and Kappler, A. (2012) Green rust formation during Fe(II) oxidation by the nitrate-reducing acidovorax sp. strain BoFeN1. *Environ Sci Technol* **46**: 1439–1446.

Park, S., Kim, D. H., Lee, J. H., and Hur, H. G. (2014) Sphaerotilus natans encrusted with nanoball-shaped Fe(III) oxide minerals formed by nitrate-reducing mixotrophic Fe(II) oxidation. *FEMS Microbiol Ecol* **90**: 68–77.

Peña, A., Busquets, A., Gomila, M., Bosch, R., Nogales, B., Elena, G. V., *et al*. (2012) Draft genome of pseudomonas stutzeri strain ZoBell (CCUG 16156), a marine isolate and model organism for denitrification studies. *J Bacteriol* **194**: 1277–1278.

Peng, C., Sundman, A., Catrouillet, C., Bryce, C., Borch, T., and Kappler, A. (2018) Oxidation of Fe(II)-organic-matter complexes in the presence of the mixotrophic nitrate-reducing Fe(II)-oxidizing bacterium Acidovorax sp. BoFeN1. *Environ Sci Technol* **52**: 5753–5763.

Pentráková, L., Su, K., Pentrák, M., and Stucki, J. W. (2013) A review of microbial redox interactions with structural Fe in clay minerals. *Clay Miner* **48**: 543–560.

Pereira, L., Saraiva, I. H., So, A., Oliveira, F., Soares, C. M., Louro, R. O., and Frazão, C. (2017) Molecular structure of

FoxE, the putative iron oxidase of Rhodobacter ferrooxidans SW2. *BBA-Bioenergetics* **1858**: 847–853.

Peters, B., Casciotti, K. L., Samarkin, V. A., Madigan, M. T., Schutte, C. A., and Joye, S. B. (2014) Stable isotope analyses of NO^{2-}, NO^{3-}, and N_2O in the hypersaline ponds and soils of the McMurdo dry valleys, Antarctica. *Geochim Cosmochim Acta* **135**: 87–101.

Picard, A., Obst, M., Schmid, G., Zeitvogel, F., and Kappler, A. (2016) Limited influence of Si on the preservation of Fe mineral-encrusted microbial cells during experimental diagenesis. *Geobiology* **14**: 276–292.

Picardal, F. (2012) Abiotic and microbial interactions during anaerobic transformations of Fe(II) and NOx. *Front Microbiol* **3**: 1–7.

Posth, N. R., Huelin, S., Konhauser, K. O., and Kappler, A. (2010) Size, density and composition of cell – mineral aggregates formed during anoxygenic phototrophic Fe(II) oxidation : impact on modern and ancient environments. *Geochim Cosmochim Acta* **74**: 3476–3493.

Posth, N. R., Konhauser, K. O., and Kappler, A. (2013) Microbiological processes in banded iron formation deposition. *Sedimentology* **60**: 1733–1754.

Posth, N. R., Canfield, D. E., and Kappler, A. (2014) Biogenic Fe(III) minerals: from formation to diagenesis and preservation in the rock record. *Earth Sci Rev* **135**: 103–121.

Poulain, A. J., and Newman, D. K. (2009) Rhodobacter capsulatus catalyzes light-dependent Fe(II) oxidation under anaerobic conditions as a potential detoxification mechanism. *Appl Environ Microbiol* **75**: 6639–6646.

Rabus, R., and Widdel, F. (1995) Anaerobic degradation of ethylbenzene and other aromatic hydrocarbons by new denitrifying bacteria. *Arch Microbiol* **163**: 96–103.

Ravishankara, A. R., Daniel, J. S., and Portmann, R. W. (2009) Nitrous oxide (N_2O): the dominant ozone-depleting substance emitted in the 21st century. *Science* **326**: 123–125.

Roberts, K. L., Kessler, A. J., Grace, M. R., and Cook, P. L. M. (2014) Increased rates of dissimilatory nitrate reduction to ammonium (DNRA) under oxic conditions in a periodically hypoxic estuary. *Geochim Cosmochim Acta* **133**: 313–324.

Robertson, E. K., and Thamdrup, B. (2017) The fate of nitrogen is linked to iron(II) availability in a freshwater lake sediment. *Geochim Cosmochim Acta* **205**: 84–99.

Robertson, E. K., Roberts, K. L., Burdorf, L. D. W., Cook, P., and Thamdrup, B. (2016) Dissimilatory nitrate reduction to ammonium coupled to Fe(II) oxidation in sediments of a periodically hypoxic estuary. *Limnol Oceanogr* **61**: 365–381.

Rowe, A. R., Chellamuthu, P., Lam, B., Okamoto, A., and Nealson, K. H. (2015) Marine sediments microbes capable of electrode oxidation as a surrogate for lithotrophic insoluble substrate metabolism. *Front Microbiol* **6**: 1–15.

Samarkin, V. A., Madigan, M. T., Bowles, M. W., Casciotti, K. L., Priscu, J. C., McKay, C. P., and Joye, S. B. (2010) Abiotic nitrous oxide emission from the hypersaline don Juan pond in Antarctica. *Nat Geosci* **3**: 341.

Saraiva, I. H., Newman, D. K., and Louro, R. O. (2012) Functional characterization of the FoxE iron oxidoreductase from the Photoferrotroph Rhodobacter ferrooxidans SW2. *J Biol Chem* **287**: 25541–25548.

Schaedler, S., Burkhart, C., Hegler, F., Straub, K., Miot, J., Benzerara, K., and Kappler, A. (2009) Formation of cell-iron-mineral aggregates by phototrophic and nitrate-reducing anaerobic Fe(II)-oxidizing bacteria. *Geomicrobiol J* **26**: 96–103.

Schippers, A., and Jorgensen, B. B. (2002) Biogeochemistry of pyrite and iron sulfide oxidation in marine sediments. *Geochim Cosmochim Acta* **66**: 85–92.

Schmid, G., Zeitvogel, F., Hao, L., Ingino, P., and Floetenmeyer, M. (2014) 3-D analysis of bacterial cell-(iron) mineral aggregates formed during Fe(II) oxidation by the nitrate-reducing Acidovorax sp. strain BoFeN1 using complementary microscopy tomography approaches. *Geobiology* **12**: 340–361.

Scholz, F., Löscher, C. R., Fiskal, A., Sommer, S., Hensen, C., Lomnitz, U., *et al*. (2016) Nitrate-dependent iron oxidation limits iron transport in anoxic ocean regions. *Earth Planet Sci Lett* **454**: 272–281.

Schwertmann, U., and Murad, E. (1988) The nature of an iron oxide-organic iron association in a peaty environment. *Clay Miner* **23**: 291–299.

Senko, J. M., Dewers, T. A., and Krumholz, L. R. (2005) Effect of oxidation rate and Fe (II) state on microbial nitrate-dependent Fe (III) mineral formation. *Appl Environ Microbiol* **71**: 7172–7177.

Seyfferth, A. L., Webb, S. M., Andrews, J. C., and Fendorf, S. (2010) Arsenic localization, speciation, and co-occurrence with iron on Rice (Oryza sativa L.) roots having variable Fe coatings. *Environ Sci Technol* **44**: 8108–8113.

Shelobolina, E. S., Vanpraagh, C. G., and Lovley, D. R. (2003) Use of ferric and ferrous iron containing minerals for respiration by Desulfitobacterium frappieri. *Geomicrobiol J* **20**: 143–156.

Shelobolina, E., Konishi, H., Xu, H., Benzine, J., Xiong, M. Y., Wu, T., *et al*. (2012a) Isolation of phyllosilicate-iron redox cycling microorganisms from an illite-smectite rich hydromorphic soil. *Front Microbiol* **3**: 1–10.

Shelobolina, E., Xu, H., Konishi, H., Kukkadapu, R., Wu, T., Blöthe, M., and Roden, E. (2012b) Microbial lithotrophic oxidation of structural Fe(II) in biotite. *Appl Environ Microbiol* **78**: 5746–5752.

Smith, R. L., Kent, D. B., Repert, D. A., and Böhlke, J. K. (2017) Anoxic nitrate reduction coupled with iron oxidation and attenuation of dissolved arsenic and phosphate in a sand and gravel aquifer. *Geochim Cosmochim Acta* **196**: 102–120.

Sorokina, A. Y., Chernousova, E. Y., and Dubinina, G. A. (2012a) Ferrovibrio denitrificans gen. Nov., sp. nov., a novel neutrophilic facultative anaerobic Fe(II)-oxidizing bacterium. *FEMS Microbiol Lett* **335**: 19–25.

Sorokina, A. Y., Chernousova, E. Y., and Dubinina, G. A. (2012b) Hoeflea siderophila sp. nov., a new neutrophilic iron-oxidizing bacterium. *Microbiology* **81**: 59–66.

Straub, K. L., Benz, M., Schink, B., and Widdel, F. (1996) Anaerobic, nitrate-dependent microbial oxidation of ferrous iron. *Appl Environ Microbiol* **62**: 1458–1460.

Straub, K. L., Raineyr, F. A., and Widdell, F. (1999) Rhodovulum iodosum sp. nov. and Rhodovulum robiginosum sp. nov., two new marine phototrophic ferrous-iron-oxidizing purple bacteria. *Int J Syst Biotechnol* **49**: 729–735.

Straub, K. L., Schönhuber, W. A., Buchholz-Cleven, B. E. E., and Schink, B. (2004) Diversity of ferrous iron-oxidizing,

nitrate-reducing bacteria and their involvement in oxygen-independent iron cycling. *Geomicrobiol J* **21**: 371–378.
Strous, M., Pelletier, E., Mangenot, S., Rattei, T., Lehner, A., Taylor, M. W., *et al*. (2006) Deciphering the evolution and metabolism of an anammox bacterium from a community genome. *Nature* **440**: 790.
Su, J. F., Shao, S. C., Huang, T. L., Ma, F., Yang, S. F., Zhou, Z. M., and Zheng, S. C. (2015) Anaerobic nitrate-dependent iron(II) oxidation by a novel autotrophic bacterium, pseudomonas sp. SZF15. *J Environ Chem Eng* **3**: 2187–2193.
Taillefert, M., Bono, A. B., and Luther, G. W. (2000) Reactivity of freshly formed Fe(III) in synthetic solutions and (pore)waters: Voltammetric evidence of an aging process. *Environ Sci Technol* **34**: 2169–2177.
Thompson, A., Rancourt, D. G., Chadwick, O. A., and Chorover, J. (2011) Iron solid-phase differentiation along a redox gradient in basaltic soils. *Geochim Cosmochim Acta* **75**: 119–133.
Thompson, K. J., Simister, R. L., Hahn, A. S., Hallam, S. J., and Crowe, S. A. (2017) Nutrient acquisition and the metabolic potential of Photoferrotrophic Chlorobi. *Front Microbiol* **8**: 1212.
Tominski, C., Heyer, H., Lösekann-Behrens, T., Behrens, S., and Kappler, A. (2018a) Growth and population dynamics of the anaerobic Fe(II)-oxidizing and nitrate-reducing enrichment culture KS. *Appl Environ Microbiol* **84**: 1–15.
Tominski, C., Lösekann-Behrens, T., Ruecker, A., Hagemann, N., Kleindienst, S., Mueller, C. W., *et al*. (2018b) FISH-SIMS imaging of an autotrophic, nitrate-reducing, Fe(II)-oxidizing enrichment culture provides insights into carbon metabolism. *Appl Environ Microbiol* In Press **84**: 9.
Usman, M., Byrne, J. M., Chaudhary, A., Orsetti, S., Hanna, K., Ruby, C., *et al*. (2018) Magnetite and green rust: synthesis, properties, and environmental applications of mixed-valent iron minerals. *Chem Rev* **118**: 3251–3304.
Vaclavkova, S., Schultz-Jensen, N., Jacobsen, O. S., Elberling, B., and Aamand, J. (2015) Nitrate-controlled anaerobic oxidation of pyrite by Thiobacillus cultures. *Geomicrobiol J* **32**: 412–419.
Vega, M. A., Kulkarni, H. V., Mladenov, N., Johannesson, K., Hettiarachchi, G. M., Bhattacharya, P., *et al*. (2017) Biogeochemical controls on the release and accumulation of Mn and as in shallow aquifers, West Bengal, India. *Front Environ Sci* **5**: 1–16.
Walter, X. A., Picazo, A., Miracle, M. R., Vicente, E., Camacho, A., Aragno, M., *et al*. (2014) Phototrophic Fe(II)-oxidation in the chemocline of a ferruginous meromictic lake. *Front Microbiol* **5**: 1–9.
Wang, H., Ye, Y., Sai, J., Chen, D., Yang, K., Zhou, J., and He, Q. (2016a) Characteristics of nitrate reduction using Fe(II) as electron donor in activated sludge. *Geomicrobiol J* **33**: 505–512.
Wang, M., Hu, R., Zhao, J., Kuzyakov, Y., and Liu, S. (2016b) Iron oxidation affects nitrous oxide emissions via donating electrons to denitrification in paddy soils. *Geoderma* **271**: 173–180.
Wankel, S. D., Ziebis, W., Buchwald, C., Charoenpong, C., Beer, D., Di Dentinger, J., *et al*. (2017) Evidence for fungal and chemodenitrification based N_2O flux from nitrogen impacted coastal sediments. *Nat Commun* **8**: 1–11.
Weber, K. A., Picardal, F. W., and Roden, E. E. (2001) Microbially catalyzed nitrate-dependent oxidation of biogenic solid-phase Fe(II) compounds. *Environ Sci Technol* **35**: 1644–1650.
Weber, K. A., Urrutia, M. M., Churchill, P. F., Kukkadapu, R. K., and Roden, E. E. (2006) Anaerobic redox cycling of iron by freshwater sediment microorganisms. *Environ Microbiol* **8**: 100–113.
Widdel, F., Schnell, S., Heising, S., Ehrenreich, A., Assmus, B., and Schink, B. (1993) Ferrous iron oxidation by anoxygenic phototrophic bacteria. *Nature* **362**: 834–836.
Wu, W., Swanner, E. D., Hao, L., Zeitvogel, F., Obst, M., Pan, Y., and Kappler, A. (2014) Characterization of the physiology and cell-mineral interactions of the marine anoxygenic phototrophic Fe(II) oxidizer Rhodovulum iodosum - implications for Precambrian Fe(II) oxidation. *FEMS Microbiol Ecol* **88**: 503–515.
Wuebbles, D. J. (2009) Nitrous oxide: no laughing matter. *Science* **326**: 56–57.
Yamaguchi, N., Ohkura, T., Takahashi, Y., Maejima, Y., and Arao, T. (2014) Arsenic distribution and speciation near Rice roots influenced by iron plaques and redox conditions of the soil matrix. *Environ Sci Technol* **48**: 1549–1556.
Zhang, H., Wang, H., Yang, K., Sun, Y., Tian, J., and Lv, B. (2015) Nitrate removal by a novel autotrophic denitrifier (microbacterium sp.) using Fe(II) as electron donor. *Ann Microbiol* **65**: 1069–1078.
Zhang, X., Ma, F., and Szewzyk, U. (2016) Draft genome sequence of a potential nitrate-dependent Fe (II)-oxidizing bacterium, Aquabacterium parvum B6. *Genome Announc* **4**: e01651–e01615.
Zhao, L., Dong, H., Edelmann, R. E., Zeng, Q., and Agrawal, A. (2017) Coupling of Fe(II) oxidation in illite with nitrate reduction and its role in clay mineral transformation. *Geochim Cosmochim Acta* **200**: 353–366.
Zhou, J., Wang, H., Yang, K., Ji, B., Chen, D., Zhang, H., *et al*. (2016) Autotrophic denitrification by nitrate-dependent Fe(II) oxidation in a continuous up-flow biofilter. *Bioprocess Biosyst Eng* **39**: 277–284.
Zhu-Barker, X., Cavazos, A. R., Ostrom, N. E., Horwath, W. R., and Glass, J. B. (2015) The importance of abiotic reactions for nitrous oxide production. *Biogeochemistry* **126**: 251–267.
Zhu, X., Silva, L. C. R., Doane, T. A., and Horwath, W. R. (2013) Iron: the forgotten driver of nitrous oxide production in agricultural soil. *PLoS One* **8**: 1–6.
ZoBell, C. E., and Upham, H. C. (1944) *A List of Marine Bacteria Including Descriptions of Sixty New Species*. Berkeley, CA, USA: University of California Press, pp. 239–292.

Supporting Information

Additional Supporting Information may be found in the online version of this article at the publisher's web-site:

Appendix S1. SUPPORTING INFORMATION

Table S1. Selection of the more well-studied bacteria which are thought to be chemodenitrifiers (i.e., an enzymatic contribution to Fe(II) oxidation is not confirmed), displaying their genetic diversity, point of origin and minerals which can be formed.

6. Discussion, conclusion and outlook

Microbial Fe redox transformations coupled to carbon, nitrogen and oxygen biogeochemical cycles play vital roles in the natural environment (Kappler *et al.*, 2021). Many studies have increased knowledge regarding microbial Fe redox transformation, for example, microbial Fe(II) oxidation coupled to the reduction of nitrate (NRFeOx) has been studied for more than two decades (Straub *et al.*, 1996; Tominski *et al.*, 2018b; Huang *et al.*, 2021a). One of the most commonly used models for studying this process is culture KS consisting of several key microorganisms such as *Gallionellaceae* sp. and *Rhodanobacter* sp. (He *et al.*, 2016; Tominski *et al.*, 2018b). This dissertation further elucidates the role of individual culture KS community members in Fe(II) oxidation, reduction of the nitrogen species, and potential oxygen respiration in chapter 2 (Huang *et al.*, 2021a). In addition to culture KS, the metabolic functions and microbial physiology of a novel autotrophic nitrate-reducing Fe(II)-oxidizing enrichment, culture BP, is reported in chapter 3 (Huang *et al.*, 2021b). In particularly, this dissertation reports (i) the genes expressed and proteins produced by Fe(II)-oxidizing bacteria (FeOB) and other community members of cultures KS and BP under autotrophic and heterotrophic conditions (chapters 2 and 3), (ii) the potential mechanisms for Fe(II) oxidation, denitrification, carbon fixation, and oxidative phosphorylation in each key player of cultures KS and BP (chapters 2 and 3), (iii) the potential interspecies interactions that enables FeOB to survive under autotrophic NRFeOx conditions in cultures KS and BP (chapters 2 and 3), (iv) the microbial diversity and relative abundance of potential key players involved in NRFeOx at the original habitat of culture BP (chapter 3), and (v) the classification and comparison of the three unclassified *Gallionellaceae* spp. in enrichment cultures KS, BP and AG (chapter 4).

6.1. Meta-omics and microbial interaction in the enrichment cultures

This dissertation presents new knowledge on metabolic mechanisms, which occur in the neutrophilic autotrophic NRFeOx enrichment cultures KS (chapter 2) and BP (chapter 3) at the gene, transcript, and protein level (Huang *et al.*, 2021a; Huang *et al.*, 2021b). Both cultures contain different species affiliated with the genus *Ferrigenium* in the family *Gallionellaceae*, i.e. '*Candidatus* Ferrigenium straubiae' in culture KS and '*Candidatus*

Ferrigenium bremense' in culture BP, and both of them are able to perform Fe(II) oxidation and carbon fixation. However, they require other flanking members to complete denitrification, i.e. syntrophic interaction between '*Ca.* Ferrigenium straubiae' and *Rhodanobacter* sp. (Huang *et al.*, 2021a) or '*Ca.* Ferrigenium bremense' and any of the *Noviherbaspirillum* sp., *Thiobacillus* sp. or other flanking members (Huang *et al.*, 2021b). Tight couplings between the key microorganisms in both culture KS and BP enhance the growth of the dominant microbial taxa. Chapter 2 results suggest that both the '*Ca.* Ferrigenium straubiae' and *Rhodanobacter* sp. in culture KS are likely involved in the processes of Fe(II) oxidation and partial or full denitrification. While the *Rhodanobacter* sp. likely requires organic carbon fixed by the '*Ca.* Ferrigenium straubiae' for survival, in return, likely removes NO, the toxic product of incomplete denitrification produced by '*Ca.* Ferrigenium straubiae'. This indicates that '*Ca.* Ferrigenium straubiae' and the *Rhodanobacter* sp. use a syntrophic relationship to survive in culture KS under autotrophic conditions in Fe(II)- and nitrate-rich environment (Huang *et al.*, 2021a). Based on the results of chapter 3, '*Ca.* Ferrigenium bremense', the *Noviherbaspirillum* sp., *Thiobacillus* sp., and *Rhodoblastus* sp. could be involved in partial or full denitrification, coupled to Fe(II) oxidation and carbon fixation (Huang *et al.*, 2021b). The most probable denitrifiers, *Rhodoferax* sp. and *Ramlibacter* sp., appear to rely on an organic carbon source fixed by '*Ca.* Ferrigenium bremense', the *Noviherbaspirillum* sp., *Thiobacillus* sp. or *Rhodoblastus* sp. Thus, NRFeOx seems to be performed by a consortium of microorganisms. These data, the community complexity combined with the low abundance of dominant microbial taxa of culture BP in the origin environment, e.g. 0.13% of '*Ca.* Ferrigenium bremense' and 0.08% of the *Thiobacillus* sp., demonstrate that culture BP might better emulate the complex microbial interactions in the environment when compared to culture KS. Additional environmental studies, isolation of each species into pure culture, and subsequent physiological experiments with these purified cultures are required to test this hypothesis. Despite the fact that we cannot prove direct enzymatic NRFeOx and NO detoxification, our meta-omics analyses strengthen the evidence of these mechanisms and reveals the metabolic interdependencies of the microbial key players in cultures KS and BP.

6.2. Comparison and nomenclature of the three *Gallionellaceae* spp.

The increasing number of available genomes derived from meta-omics studies of still uncultured members of the family *Gallionellaceae*, demonstrates the potential for coupled Fe(II)-oxidation and partial denitrification. Therefore, it is important to classify new taxa of FeOB (Jewell *et al.*, 2016; Kadnikov *et al.*, 2016; Bethencourt *et al.*, 2020). In addition, the key FeOB of the only stable NRFeOx cultures that exist to date, i.e. *Gallionellaceae* spp. strains in cultures KS, BP and AG, are currently frequently used as model systems to study autotrophic NRFeOx. These strains remain unclassified. Therefore, based on the ecological, phylogenetic, genomic, and physiological traits, we suggested the designation of three novel FeOB species within the family *Gallionellaceae*. These three *Gallionellaceae* spp. are part of the genus *Ferrigenium* in cultures KS, BP and AG and were classified as '*Candidatus* Ferrigenium straubiae' sp. nov., '*Candidatus* Ferrigenium bremense' sp. nov. and '*Candidatus* Ferrigenium altingense' sp. nov. respectively.

6.3. Future implications and environmental relevance

This dissertation revealed transcripts and proteins in cultures KS and BP via the meta-omics analysis that are a vital baseline for follow-up studies (chapters 2 and 3). For instance, chapter 2 results could provide insights into a method to isolate the NRFeOx microorganism, '*Ca.* Ferrigenium straubiae' from NRFeOx enrichment cultures by using a growth chamber with a permeable membrane, e.g. a diffusion growth chamber (Kaeberlein *et al.*, 2002; Steinert *et al.*, 2014). One side of the growth chamber could be used to grow '*Ca.* Ferrigenium straubiae' via serial dilution from culture KS and the other side of the growth chamber, separated by a permeable membrane, could be used to grow isolated *Rhodanobacter* sp. to detoxify the NO produced from '*Ca.* Ferrigenium straubiae'. This method would allow chemicals (e.g. organic carbon and NO) to permeate through the permeable membrane, creating a spatially separated co-culture with complete pathways of NRFeOx and carbon metabolism (Kaeberlein *et al.*, 2002; Steinert *et al.*, 2014). Furthermore, the *Noviherbaspirillum* sp. and *Thiobacillus* sp. seem to be new strains of potential autotrophic NRFeOx microorganisms (chapter 3). The meta-omic results indicated that the *Noviherbaspirillum* sp. and *Thiobacillus* sp. have the ability to conduct full NRFeOx, carbon fixation and oxygen respiration. Thus, they could be isolated

under oxic or anoxic, autotrophic NRFeOx conditions (chapter 3). So far, the only true autotrophic NRFeOx microorganisms are enrichment cultures with several different microorganisms (chapters 3 and 5) (Laufer *et al.*, 2016; Tominski, 2016; Bryce *et al.*, 2018; Tominski *et al.*, 2018a; Huang *et al.*, 2021b; Jakus *et al.*, 2021). Therefore, the isolation of true autotrophic NRFeOx microorganism isolates is of primary interest. The isolation of the *Noviherbaspirillum* sp. or *Thiobacillus* sp., and their subsequent cultivation in a diffusion growth chamber can contribute to obtaining isolates of '*Ca.* Ferrigenium bremense' and '*Ca.* Ferrigenium altingense'. Ultimately, these isolates would facilitate a more detailed study of their metabolic capabilities.

To confirm whether '*Ca.* Ferrigenium bremense', *Noviherbaspirillum* sp. and *Thiobacillus* sp. can perform carbon fixation, the experiment of fixing ^{13}C-labelld inorganic carbon, i.e. nanoscale secondary ion mass spectrometry (NanoSIMS) combining with fluorescence *in situ* hybridization (CARD-FISH) can be used in culture BP by referencing the methods in Tominski *et al.* (2018b).

Additionally, in both cultures KS and BP, we found genes and transcripts homologs encoding the cbb_3- and aa_3- type cytochrome *c* oxidases of complex IV, which have high and low affinity to oxygen, respectively. Additionally, the potential homolog of nitric oxide dismutase (*nod*) genes were identified in both cultures. Nitric oxide dismutase can possibly produce oxygen and dinitrogen and is wide spread in the environments (Ettwig *et al.*, 2010; Zhu *et al.*, 2017). Even though the oxygen affinity genes could be constitutively expressed, and the most similar gene to the published *nod* genes has only 34% amino acid identity in the *Rhodanobacter* sp. in culture KS and 36% amino acid identity in the *Geothrix* sp. in culture BP, an enzyme similar to Nod producing O_2 or reactive oxygen species, e.g. hydroxyl radicals, superoxide, and hydrogen peroxide, might occur in the cultures KS and BP system (Mumford *et al.*, 2016). Therefore, to understand the energy generation process in these anoxic enrichment cultures, optical, electrochemical and isotope methods or knock-out mutants of the specific expressed genes (e.g. cytochrome cbb_3- and aa_3- type oxidases, or *bd* quinol oxidase) could be performed to detect and quantify the potential internal oxygen production and respiration in enrichment cultures KS and BP.

Considering the environmental influence of NRFeOx microorganisms, e.g. turnover of nitrate in the pyrite-rich nitrate-contaminated groundwater (Jakus *et al.*, 2021), the

exploration of the physiology and the metabolism of members of the cultures KS and BP will add new knowledge to the role of NRFeOx in the natural habitats, such as Fe(II)- and nitrate-containing but organic carbon-limited aquifers. The knowledge about operation of NRFeOx in oligotrophic aquifers may furthermore be used for development of treatment strategies of contaminated groundwater (Su *et al.*, 2016; Zhang *et al.*, 2016; Kiskira *et al.*, 2017). In addition, determination of the survival limits of NRFeOx microorganisms is especially interesting for astrobiology. Thus, the detection of Fe- (Hoefen *et al.*, 2003) and nitrate-containing minerals (Stern *et al.*, 2015), water (Michalski *et al.*, 2013), organic (Ming *et al.*, 2014) and inorganic carbon (Mahaffy *et al.*, 2013) on Mars, suggests that NRFeOx microorganisms could potentially exist and participate in primary production in subsurface environments on Mars (Price *et al.*, 2018). Therefore, our research results could also serve as a foundation for knowledge about the potential mechanism of microbial interactions on Mars.

7. References

(2019) International code of nomenclature of prokaryotes. *Int J Syst Evol Microbiol* 69: S1-S111.

Altschul, S.F., Gish, W., Miller, W., Myers, E.W., and Lipman, D.J. (1990) Basic local alignment search tool. *J Mol Biol* 215: 403-410.

Andrews, S. (2010) FastQC: A quality control tool for high throughput sequence data

Apprill, A., McNally, S., Parsons, R., and Weber, L. (2015) Minor revision to V4 region SSU rRNA 806R gene primer greatly increases detection of SAR11 bacterioplankton. *Aquat Microb Ecol* 75: 129-137.

Arai, H., Kawakami, T., Osamura, T., Hirai, T., Sakai, Y., and Ishii, M. (2014) Enzymatic characterization and *in vivo* function of five terminal oxidases in *Pseudomonas aeruginosa*. *J Bacteriol* 196: 4206-4215.

Badger, M.R., and Bek, E.J. (2008) Multiple rubisco forms in proteobacteria: their functional significance in relation to CO_2 acquisition by the CBB cycle. *J Exp Bot* 59: 1525-1541.

Barco, R.A., Garrity, G.M., Scott, J.J., Amend, J.P., Nealson, K.H., and Emerson, D. (2020) A genus definition for *Bacteria* and *Archaea* based on a standard genome relatedness Index. *mBio* 11.

Beller, H., Zhou, P., Legler, T., Chakicherla, A., Kane, S., Letain, T., and O'Day, P. (2013) Genome-enabled studies of anaerobic, nitrate-dependent iron oxidation in the chemolithoautotrophic bacterium *Thiobacillus denitrificans*. *Front Microbiol* 4.

Beller, H.R., Letain, T.E., Chakicherla, A., Kane, S.R., Legler, T.C., and Coleman, M.A. (2006a) Whole-genome transcriptional analysis of chemolithoautotrophic thiosulfate ixidation by *Thiobacillus denitrificans* under aerobic versus denitrifying conditions. *J Bacteriol* 188: 7005-7015.

Beller, H.R., Chain, P.S., Letain, T.E., Chakicherla, A., Larimer, F.W., Richardson, P.M. *et al.* (2006b) The genome sequence of the obligately chemolithoautotrophic, facultatively anaerobic bacterium *Thiobacillus denitrificans*. *J Bacteriol* 188: 1473-1488.

Benz, M., Brune, A., and Schink, B. (1998) Anaerobic and aerobic oxidation of ferrous iron at neutral pH by chemoheterotrophic nitrate-reducing bacteria. *Arch Microbiol* 169: 159-165.

Benzine, J., Shelobolina, E., Xiong, M.Y., Kennedy, D., McKinley, J., Lin, X., and Roden, E. (2013) Fe-phyllosilicate redox cycling organisms from a redox transition zone in Hanford 300 Area sediments. *Front Microbiol* 4.

Bethencourt, L., Bochet, O., Farasin, J., Aquilina, L., Borgne, T.L., Quaiser, A. *et al.* (2020) Genome reconstruction reveals distinct assemblages of *Gallionellaceae* in surface and subsurface redox transition zones. *FEMS Microbiol Ecol* 96.

Bird, L.J., Bonnefoy, V., and Newman, D.K. (2011) Bioenergetic challenges of microbial iron metabolisms. *Trends Microbiol* 19: 330-340.

Blöthe, M., and Roden, E.E. (2009) Composition and activity of an autotrophic Fe(II)-oxidizing, nitrate-reducing enrichment culture. *Appl Environ Microbiol* 75: 6937-6940.

Boden, R., Cleland, D., Green, P.N., Katayama, Y., Uchino, Y., Murrell, J.C., and Kelly, D.P. (2012) Phylogenetic assessment of culture collection strains of *Thiobacillus thioparus*, and definitive 16S rRNA gene sequences for *T. thioparus*, *T. denitrificans*, and *Halothiobacillus neapolitanus*. *Arch Microbiol* 194: 187-195.

Bokulich, N.A., Kaehler, B.D., Rideout, J.R., Dillon, M., Bolyen, E., Knight, R. *et al.* (2018) Optimizing taxonomic classification of marker-gene amplicon sequences with QIIME 2's q2-feature-classifier plugin. *Microbiome* 6: 90.

Bolyen, E., Rideout, J.R., Dillon, M.R., Bokulich, N.A., Abnet, C.C., Al-Ghalith, G.A. *et al.* (2019) Reproducible, interactive, scalable and extensible microbiome data science using QIIME 2. *Nat Biotechnol* 37: 852-857.

Borchert, N., Dieterich, C., Krug, K., Schutz, W., Jung, S., Nordheim, A. *et al.* (2010) Proteogenomics of *Pristionchus pacificus* reveals distinct proteome structure of nematode models. *Genome Res* 20: 837-846.

Bowers, R.M., Kyrpides, N.C., Stepanauskas, R., Harmon-Smith, M., Doud, D., Reddy, T.B.K. *et al.* (2017) Minimum information about a single amplified genome (MISAG) and a metagenome-assembled genome (MIMAG) of bacteria and archaea. *Nat Biotechnol* 35: 725-731.

Brouwers, G.J., Corstjens, P.L.A.M., de Vrind, A., Verkamman, J.P.M., de Kuyper, M., and W., d.V.-d.J.E. (2000) Stimulation of Mn^{2+} oxidation in *Leptothrix discophora* SS-1 by Cu^{2+} and sequence analysis of the region flanking the gene encoding putative multicopper oxidase MofA. *Geomicrobiol J* 17: 25-33.

Bryce, C., Blackwell, N., Schmidt, C., Otte, J., Huang, Y.M., Kleindienst, S. *et al.* (2018) Microbial anaerobic Fe(II) oxidation - Ecology, mechanisms and environmental implications. *Environ Microbiol* 20: 3462-3483.

Buchholz-Cleven, B.E.E., Rattunde, B., and Straub, K.L. (1997) Screening for genetic diversity of isolates of anaerobic Fe(II)-oxidizing bacteria using DGGE and whole-cell hybridization. *Syst Appl Microbiol* 20: 301-309.

Callahan, B. (2018) *Silva taxonomic training data formatted for DADA2 (Silva version 132)*.

Callahan, B.J., McMurdie, P.J., Rosen, M.J., Han, A.W., Johnson, A.J., and Holmes, S.P. (2016) DADA2: High-resolution sample inference from Illumina amplicon data. *Nat Methods* 13: 581-583.

Callahan, B.J., Wong, J., Heiner, C., Oh, S., Theriot, C.M., Gulati, A.S. *et al.* (2019) High-throughput amplicon sequencing of the full-length 16S rRNA gene with single-nucleotide resolution. *Nucleic Acids Res* 47: e103.

Carlson, H.K., Clark, I.C., Melnyk, R.A., and Coates, J.D. (2012) Toward a mechanistic understanding of anaerobic nitrate-dependent iron oxidation: balancing electron uptake and detoxification. *Front Microbiol* 3: 57.

Carlson, H.K., Clark, I.C., Blazewicz, S.J., Iavarone, A.T., and Coates, J.D. (2013) Fe(II) oxidation is an innate capability of nitrate-reducing bacteria that involves abiotic and biotic reactions. *J Bacteriol* 195: 3260-3268.

Castelle, C., Guiral, M., Malarte, G., Ledgham, F., Leroy, G., Brugna, M., and Giudici-Orticoni, M.T. (2008) A new iron-oxidizing/O_2-reducing supercomplex spanning both inner and outer membranes, isolated from the extreme acidophile *Acidithiobacillus ferrooxidans*. *J Biol Chem* 283: 25803-25811.

Chakraborty, A., Roden, E.E., Schieber, J., and Picardal, F. (2011) Enhanced growth of *Acidovorax* sp. strain 2AN during nitrate-dependent Fe(II) oxidation in batch and continuous-flow systems. *Appl Environ Microbiol* 77: 8548-8556.

Chan, C.S., Emerson, D., and Luther III, G.W. (2016) The role of microaerophilic Fe-oxidizing micro-organisms in producing banded iron formations. *Geobiology* 14: 509-528.

Chaudhary, D.K., and Kim, J. (2017) *Noviherbaspirillum agri* sp. nov., isolated from reclaimed grassland soil, and reclassification of *Herbaspirillum massiliense* (Lagier et al., 2014) as *Noviherbaspirillum massiliense* comb. nov. *Int J Syst Evol Microbiol* 67: 1508-1515.

Chen, I.A., Markowitz, V.M., Chu, K., Palaniappan, K., Szeto, E., Pillay, M. *et al.* (2017) IMG/M: integrated genome and metagenome comparative data analysis system. *Nucleic Acids Res* 45: D507-D516.

Chen, I.A., Chu, K., Palaniappan, K., Pillay, M., Ratner, A., Huang, J. *et al.* (2019) IMG/M v.5.0: an integrated data management and comparative analysis system for microbial genomes and microbiomes. *Nucleic Acids Res* 47: D666-D677.

Chen, S., Zhou, Y., Chen, Y., and Gu, J. (2018) fastp: an ultra-fast all-in-one FASTQ preprocessor. *Bioinformatics* 34: i884-i890.

Clarke, F.W., and Washington, H.S. (1924) The composition of the Earth's crust. In *Professional Paper*.

Coleman, N.V., Mattes, T.E., Gossett, J.M., and Spain, J.C. (2002) Phylogenetic and kinetic diversity of aerobic vinyl chloride-assimilating bacteria from contaminated sites. *Appl Environ Microbiol* 68: 6162-6171.

Coleman, N.V., Wilson, N.L., Barry, K., Brettin, T.S., Bruce, D.C., Copeland, A. *et al.* (2011) Genome sequence of the ethene- and vinyl chloride-oxidizing actinomycete *Nocardioides* sp. strain JS614. *J Bacteriol* 193: 3399-3400.

Coordinators, N.R. (2016) Database resources of the National Center for Biotechnology Information. *Nucleic acids research* 44: D7-D19.

Coram, N.J., and Rawlings, D.E. (2002) Molecular relationship between two groups of the genus *Leptospirillum* and the finding that *Leptospirillum ferriphilum* sp. nov. dominates South African commercial biooxidation tanks that operate at 40 degrees C. *Appl Environ Microbiol* 68: 838-845.

Cornell, R., and Schwertmann, U. (1996) The iron oxides-structure. In.

Corstjens, P.L., de Vrind, J.P., Westbroek, P., and de Vrind-de Jong, E.W. (1992) Enzymatic iron oxidation by *Leptothrix discophora*: identification of an iron-oxidizing protein. *Appl Environ Microbiol* 58: 450-454.

Corstjens, P.L.A.M., de Vrind, J.P.M., Goosen, T., and Jong, E.W.d.V.d. (1997) Identification and molecular analysis of the *Leptothrix discophora* SS-1 *mofA* gene, a gene putatively encoding a manganese-oxidizing protein with copper domains. *Geomicrobiol J* 14: 91-108.

Cox, J., and Mann, M. (2008) MaxQuant enables high peptide identification rates, individualized p.p.b.-range mass accuracies and proteome-wide protein quantification. *Nat Biotechnol* 26: 1367-1372.

Cox, J., Neuhauser, N., Michalski, A., Scheltema, R.A., Olsen, J.V., and Mann, M. (2011) Andromeda: a peptide search engine integrated into the MaxQuant environment. *J Proteome Res* 10: 1794-1805.

Davison, W., and Seed, G. (1983) The kinetics of the oxidation of ferrous iron in synthetic and natural waters. *Geochimica et Cosmochimica Acta* 47: 67-79.

De Coster, W., D'Hert, S., Schultz, D.T., Cruts, M., and Van Broeckhoven, C. (2018) NanoPack: visualizing and processing long-read sequencing data. *Bioinformatics* 34: 2666-2669.

Di Tommaso, P., Chatzou, M., Floden, E.W., Barja, P.P., Palumbo, E., and Notredame, C. (2017) Nextflow enables reproducible computational workflows. *Nat Biotechnol* 35: 316-319.

Dobin, A., Davis, C.A., Schlesinger, F., Drenkow, J., Zaleski, C., Jha, S. *et al.* (2013) STAR: ultrafast universal RNA-seq aligner. *Bioinformatics* 29: 15-21.

Edwards, K.J., Rogers, D.R., Wirsen, C.O., and McCollom, T.M. (2003) Isolation and characterization of novel psychrophilic, neutrophilic, Fe-oxidizing, chemolithoautotrophic alpha- and gamma-proteobacteria from the deep sea. *Appl Environ Microbiol* 69: 2906-2913.

Ehrenberg, C.G. (1838) *Die infusionsthierchen als vollkommene organismen: Ein blick in das tiefere organische leben der natur*: L. Voss.

Ehrenreich, A., and Widdel, F. (1994) Anaerobic oxidation of ferrous iron by purple bacteria, a new type of phototrophic metabolism. *Appl Environ Microbiol* 60: 4517-4526.

Ehrlich, H., Newman, D., and Kappler, A. (2015) *Ehrlich's Geomicrobiology*.

El Gheriany, I.A., Bocioaga, D., Hay, A.G., Ghiorse, W.C., Shuler, M.L., and Lion, L.W. (2009) Iron requirement for Mn(II) oxidation by *Leptothrix discophora* SS-1. *Appl Environ Microbiol* 75: 1229-1235.

Emerson, D. (2012) Biogeochemistry and microbiology of microaerobic Fe(II) oxidation. *Biochem Soc Trans* 40: 1211-1216.

Emerson, D., and Moyer, C. (1997) Isolation and characterization of novel iron-oxidizing bacteria that grow at circumneutral pH. *Appl Environ Microbiol* 63: 4784-4792.

Emerson, D., and Merrill Floyd, M. (2005) Enrichment and isolation of iron-oxidizing bacteria at neutral pH. In *Environ Microbiol*, pp. 112-123.

Emerson, D., Fleming, E.J., and McBeth, J.M. (2010) Iron-oxidizing bacteria: an environmental and genomic perspective. *Annu Rev Microbiol* 64: 561-583.

Emerson, D., Field, E.K., Chertkov, O., Davenport, K.W., Goodwin, L., Munk, C. *et al.* (2013) Comparative genomics of freshwater Fe-oxidizing bacteria: implications for physiology, ecology, and systematics. *Front Microbiol* 4: 254.

Emerson, J.B., Thomas, B.C., Alvarez, W., and Banfield, J.F. (2016) Metagenomic analysis of a high carbon dioxide subsurface microbial community populated by chemolithoautotrophs and bacteria and archaea from candidate phyla. *Environ Microbiol* 18: 1686-1703.

Ettwig, K.F., Butler, M.K., Le Paslier, D., Pelletier, E., Mangenot, S., Kuypers, M.M. *et al.* (2010) Nitrite-driven anaerobic methane oxidation by oxygenic bacteria. *Nature* 464: 543-548.

Ewels, P.A., Peltzer, A., Fillinger, S., Patel, H., Alneberg, J., Wilm, A. *et al.* (2020) The nf-core framework for community-curated bioinformatics pipelines. *Nat Biotechnol* 38: 276-278.

Fabisch, M., Freyer, G., Johnson, C.A., Büchel, G., Akob, D.M., Neu, T.R., and Küsel, K. (2016) Dominance of '*Gallionella capsiferriformans*' and heavy metal association with *Gallionella*-like stalks in metal-rich pH 6 mine water discharge. *Geobiology* 14: 68-90.

Felsenstein, J. (1985) Confidence limits on phylogenies: an approach using the bootstrap. *Evolution* 39: 783-791.

Fields, M.W., Yan, T., Rhee, S.K., Carroll, S.L., Jardine, P.M., Watson, D.B. *et al.* (2005) Impacts on microbial communities and cultivable isolates from groundwater contaminated with high levels of nitric acid-uranium waste. *FEMS Microbiol Ecol* 53: 417-428.

Franzén, O., Hu, J., Bao, X., Itzkowitz, S.H., Peter, I., and Bashir, A. (2015) Improved OTU-picking using long-read 16S rRNA gene amplicon sequencing and generic hierarchical clustering. *Microbiome* 3: 43.

Franzen, O., Hu, J., Bao, X., Itzkowitz, S.H., Peter, I., and Bashir, A. (2015) Improved OTU-picking using long-read 16S rRNA gene amplicon sequencing and generic hierarchical clustering. *Microbiome* 3: 43.

Garber, A.I., Nealson, K.H., Okamoto, A., McAllister, S.M., Chan, C.S., Barco, R.A., and Merino, N. (2020) FeGenie: A comprehensive tool for the identification of iron genes and iron gene neighborhoods in genome and metagenome assemblies. *Front Microbiol* 11: 37.

Gierlinski, M., Gastaldello, F., Cole, C., and Barton, G.J. (2018) *Proteus*: an R package for downstream analysis of *MaxQuant* output. *bioRxiv*: 416511.

Glaeser, S.P., and Kämpfer, P. (2015) Multilocus sequence analysis (MLSA) in prokaryotic taxonomy. *Syst Appl Microbiol* 38: 237-245.

Goldstein, S., Beka, L., Graf, J., and Klassen, J.L. (2019) Evaluation of strategies for the assembly of diverse bacterial genomes using MinION long-read sequencing. *BMC Genomics* 20: 23.

Griffiths, R.I., Whiteley, A.S., O'Donnell, A.G., and Bailey, M.J. (2000) Rapid method for coextraction of DNA and RNA from natural environments for analysis of ribosomal DNA- and rRNA-based microbial community composition. *Appl Environ Microbiol* 66: 5488-5491.

Guan, X., Liu, F., Xie, Y., Zhu, L., and Han, B. (2013) Microbiota associated with the migration and transformation of chlorinated aliphatic hydrocarbons in groundwater. *Environ Geochem Health* 35: 535-549.

Gurevich, A., Saveliev, V., Vyahhi, N., and Tesler, G. (2013) QUAST: quality assessment tool for genome assemblies. *Bioinformatics* 29: 1072-1075.

Hafenbradl, D., Keller, M., Dirmeier, R., Rachel, R., Roßnagel, P., Burggraf, S. *et al.* (1996) *Ferroglobus placidus* gen. nov., sp. nov., a novel hyperthermophilic archaeum that oxidizes Fe^{2+} at neutral pH under anoxic conditions. *Arch Microbiol* 166: 308-314.

Hallbeck, L., and Pedersen, K. (1991) Autotrophic and mixotrophic growth of *Gallionella ferruginea*. *Microbiology* 137: 2657-2661.

Hau, H.H., and Gralnick, J.A. (2007) Ecology and biotechnology of the genus *Shewanella*. *Annu Rev Microbiol* 61: 237-258.

He, S., Barco, R.A., Emerson, D., and Roden, E.E. (2017) Comparative genomic analysis of neutrophilic iron(II) oxidizer genomes for candidate genes in extracellular electron transfer. *Front Microbiol* 8: 1584.

He, S., Tominski, C., Kappler, A., Behrens, S., and Roden, E.E. (2016) Metagenomic analyses of the autotrophic Fe(II)-oxidizing, nitrate-reducing enrichment culture KS. *Appl Environ Microbiol* 82: 2656-2668.

Hedrich, S., Schlömann, M., and Johnson, D.B. (2011) The iron-oxidizing proteobacteria. *Microbiology* 157: 1551-1564.

Hegler, F., Posth, N.R., Jiang, J., and Kappler, A. (2008) Physiology of phototrophic iron(II)-oxidizing bacteria: implications for modern and ancient environments. *FEMS Microbiol Ecol* 66: 250-260.

Heising, S., Richter, L., Ludwig, W., and Schink, B. (1999) *Chlorobium ferrooxidans* sp. nov., a phototrophic green sulfur bacterium that oxidizes ferrous iron in coculture with a "*Geospirillum*" sp. strain. *Archives of Microbiology* 172: 116-124.

Hoefen, T.M., Clark, R.N., Bandfield, J.L., Smith, M.D., Pearl, J.C., and Christensen, P.R. (2003) Discovery of olivine in the Nili Fossae region of Mars. *Science* 302: 627-630.

Holmes, D.E., Nevin, K.P., and Lovley, D.R. (2004) Comparison of 16S rRNA, *nifD*, *recA*, *gyrB*, *rpoB* and *fusA* genes within the family *Geobacteraceae* fam. nov. *Int J Syst Evol Microbiol* 54: 1591-1599.

Hu, Q.-Q., Zhou, Z.-C., Liu, Y.-F., Zhou, L., Mbadinga, S.M., Liu, J.-F. *et al.* (2019) High microbial diversity of the nitric oxide dismutation reaction revealed by PCR amplification and analysis of the nod gene. *Int Biodeterior Biodegradation* 143: 104708.

Huang, Y., Straub, D., Blackwell, N., Kappler, A., and Kleindienst, S. (2021a) Meta-omics reveal *Gallionellaceae* and *Rhodanobacter* as interdependent key players for Fe(II) oxidation and nitrate reduction in the autotrophic enrichment culture KS. *Appl Environ Microbiol*: AEM.00496-00421.

Huang, Y., Straub, D., Kappler, A., Smith, N., Blackwell, N., and Kleindienst, S. (2021b) A novel enrichment culture highlights core features of microbial networks contributing to autotrophic Fe(II) oxidation coupled to nitrate reduction. *Microb Physiol*: 1-16.

Huston, W.M., Jennings, M.P., and McEwan, A.G. (2002) The multicopper oxidase of *Pseudomonas aeruginosa* is a ferroxidase with a central role in iron acquisition. *Mol Microbiol* 45: 1741-1750.

Ilbert, M., and Bonnefoy, V. (2013) Insight into the evolution of the iron oxidation pathways. *Biochimica et Biophysica Acta (BBA) - Bioenergetics* 1827: 161-175.

Intergovernmental Panel on Climate Change (2015) *Climate Change 2014: Mitigation of climate change: working group III contribution to the IPCC fifth assessment report*. Cambridge: Cambridge University Press.

Ishii, S., Ashida, N., Ohno, H., Segawa, T., Yabe, S., Otsuka, S. *et al.* (2017) *Noviherbaspirillum denitrificans* sp. nov., a denitrifying bacterium isolated from rice paddy soil and *Noviherbaspirillum autotrophicum* sp. nov., a denitrifying, facultatively autotrophic bacterium isolated from rice paddy soil and proposal to reclassify *Herbaspirillum massiliense* as *Noviherbaspirillum massiliense* comb. nov. *Int J Syst Evol Microbiol* 67: 1841-1848.

Jakus, N., Blackwell, N., Straub, D., Kappler, A., and Kleindienst, S. (under review; and provided to the reviewers with this submission) Metagenomics reveal the potential role of *Gallionellaceae* sp. to perform near-complete denitrification coupled to Fe(II) oxidation under autotrophic conditions. *FEMS Microbiol Ecol*.

Jakus, N., Blackwell, N., Osenbrück, K., Straub, D., Byrne, J.M., Wang, Z. *et al.* (2021) Nitrate removal by a novel lithoautotrophic nitrate-reducing iron(II)-oxidizing culture enriched from a pyrite-rich limestone aquifer. *Appl Environ Microbiol* 87: e00460-00421.

Jewell, T.N.M., Karaoz, U., Brodie, E.L., Williams, K.H., and Beller, H.R. (2016) Metatranscriptomic evidence of pervasive and diverse chemolithoautotrophy relevant to C, S, N and Fe cycling in a shallow alluvial aquifer. *ISME J* 10: 2106-2117.

Jiao, Y., Kappler, A., Croal, L.R., and Newman, D.K. (2005) Isolation and characterization of a genetically tractable photoautotrophic Fe(II)-oxidizing bacterium, *Rhodopseudomonas palustris* strain TIE-1. *Appl Environ Microbiol* 71: 4487-4496.

Kadnikov, V.V., Ivasenko, D.A., Beletskii, A.V., Mardanov, A.V., Danilova, E.V., Pimenov, N.V. *et al.* (2016) A novel uncultured bacterium of the family *Gallionellaceae*: description and genome reconstruction based on metagenomic analysis of microbial community in acid mine drainage. *Microbiology* 85: 449-461.

Kaeberlein, T., Lewis, K., and Epstein, S.S. (2002) Isolating "uncultivable" microorganisms in pure culture in a simulated natural environment. *Science* 296: 1127-1129.

Kalckar, H.M. (1991) 50 years of biological research--from oxidative phosphorylation to energy requiring transport regulation. *Annu Rev Biochem* 60: 1-38.

Kanehisa, M., and Goto, S. (2000) KEGG: kyoto encyclopedia of genes and genomes. *Nucleic Acids Res* 28: 27-30.

Kang, D.D., Li, F., Kirton, E., Thomas, A., Egan, R., An, H., and Wang, Z. (2019) MetaBAT 2: an adaptive binning algorithm for robust and efficient genome reconstruction from metagenome assemblies. *PeerJ* 7: e7359.

Kappler, A., Schink, B., and Newman, D.K. (2005) Fe(III) mineral formation and cell encrustation by the nitrate-dependent Fe(II)-oxidizer strain BoFeN1. *Geobiology* 3: 235-245.

Kappler, A., Bryce, C., Mansor, M., Lueder, U., Byrne, J.M., and Swanner, E.D. (2021) An evolving view on biogeochemical cycling of iron. *Nat Rev Microbiol* 19: 360-374.

Kato, S., Chan, C., Itoh, T., and Ohkuma, M. (2013) Functional gene analysis of freshwater iron-rich flocs at circumneutral pH and isolation of a stalk-forming microaerophilic iron-oxidizing bacterium. *Appl Environ Microbiol* 79: 5283-5290.

Kato, S., Krepski, S., Chan, C., Itoh, T., and Ohkuma, M. (2014) *Ferriphaselus amnicola* gen. nov., sp. nov., a neutrophilic, stalk-forming, iron-oxidizing bacterium isolated from an iron-rich groundwater seep. *Int J Syst Evol Microbiol* 64: 921-925.

Kato, S., Ohkuma, M., Powell, D.H., Krepski, S.T., Oshima, K., Hattori, M. *et al.* (2015) Comparative genomic insights into ecophysiology of neutrophilic, microaerophilic iron oxidizing bacteria. *Front Microbiol* 6: 1265.

Keffer, J.L., McAllister, S.M., Garber, A., Hallahan, B.J., Sutherland, M.C., Rozovsky, S., and Chan, C.S. (2021) Iron oxidation by a fused cytochrome-porin common to diverse iron-oxidizing bacteria. *bioRxiv*: 228056.

Khalifa, A., Nakasuji, Y., Saka, N., Honjo, H., Asakawa, S., and Watanabe, T. (2018) *Ferrigenium kumadai* gen. nov., sp. nov., a microaerophilic iron-oxidizing bacterium isolated from a paddy field soil. *Int J Syst Evol Microbiol* 68: 2587-2592.

Kiskira, K., Papirio, S., van Hullebusch, E.D., and Esposito, G. (2017) Fe(II)-mediated autotrophic denitrification: A new bioprocess for iron bioprecipitation/biorecovery and simultaneous treatment of nitrate-containing wastewaters. *Int Biodeterior Biodegradation* 119: 631-648.

Kojima, H., Watanabe, T., Iwata, T., and Fukui, M. (2014) Identification of major planktonic sulfur oxidizers in stratified freshwater lake. *PLoS One* 9: e93877.

Konstantinidis, K.T., and Tiedje, J.M. (2007) Prokaryotic taxonomy and phylogeny in the genomic era: advancements and challenges ahead. *Curr Opin Microbiol* 10: 504-509.

Konstantinidis, K.T., and Rosselló-Móra, R. (2015) Classifying the uncultivated microbial majority: A place for metagenomic data in the *Candidatus* proposal. *Syst Appl Microbiol* 38: 223-230.

Konstantinidis, K.T., Rosselló-Móra, R., and Amann, R. (2017) Uncultivated microbes in need of their own taxonomy. *ISME J* 11: 2399-2406.

Kopylova, E., Noe, L., and Touzet, H. (2012) SortMeRNA: fast and accurate filtering of ribosomal RNAs in metatranscriptomic data. *Bioinformatics* 28: 3211-3217.

Krepski, S.T., Hanson, T.E., and Chan, C.S. (2012) Isolation and characterization of a novel biomineral stalk-forming iron-oxidizing bacterium from a circumneutral groundwater seep. *Environ Microbiol* 14: 1671-1680.

Kucera, S., and Wolfe, R.S. (1957) A selective enrichment method for *Gallionella ferruginea*. *J Bacteriol* 74: 344-349.

Kumar, S., Stecher, G., Li, M., Knyaz, C., and Tamura, K. (2018) MEGA X: molecular evolutionary genetics analysis across computing platforms. *Mol Biol Evol* 35: 1547-1549.

Kumaraswamy, R., Sjollema, K., Kuenen, G., van Loosdrecht, M., and Muyzer, G. (2006) Nitrate-dependent [Fe(II)EDTA]$^{2-}$ oxidation by *Paracoccus ferrooxidans* sp. nov., isolated from a denitrifying bioreactor. *Syst Appl Microbiol* 29: 276-286.

Kurtzer, G.M., Sochat, V., and Bauer, M.W. (2017) Singularity: Scientific containers for mobility of compute. *PLoS One* 12: e0177459.

Langmead, B., and Salzberg, S.L. (2012) Fast gapped-read alignment with Bowtie 2. *Nat Methods* 9: 357-359.

Laufer, K., Røy, H., Jørgensen, B.B., and Kappler, A. (2016) Evidence for the existence of autotrophic nitrate-reducing Fe(II)-oxidizing bacteria in marine coastal sediment. *Appl Environ Microbiol* 82: 6120-6131.

Laufer, K., Nordhoff, M., Røy, H., Schmidt, C., Behrens, S., Jørgensen, B.B., and Kappler, A. (2015) Coexistence of microaerophilic, nitrate-reducing, and phototrophic Fe(II) Oxidizers and Fe(III) reducers in coastal marine sediment. *Appl Environ Microbiol* 82: 1433-1447.

Li, B., and Dewey, C.N. (2011) RSEM: accurate transcript quantification from RNA-Seq data with or without a reference genome. *BMC Bioinformatics* 12: 323.

Li, D., Liu, C.M., Luo, R., Sadakane, K., and Lam, T.W. (2015) MEGAHIT: an ultra-fast single-node solution for large and complex metagenomics assembly via succinct de Bruijn graph. *Bioinformatics* 31: 1674-1676.

Li, J., Cui, J., Yang, Q., Cui, G., Wei, B., Wu, Z. *et al.* (2017) Oxidative weathering and microbial diversity of an inactive seafloor hydrothermal sulfide chimney. *Front Microbiol* 8.

Liao, Y., Smyth, G.K., and Shi, W. (2014) featureCounts: an efficient general purpose program for assigning sequence reads to genomic features. *Bioinformatics* 30: 923-930.

Liu, J., Wang, Z., Belchik, S.M., Edwards, M.J., Liu, C., Kennedy, D.W. *et al.* (2012) Identification and characterization of MtoA: A decaheme *c*-type cytochrome of the neutrophilic Fe(II)-oxidizing bacterium *Sideroxydans lithotrophicus* ES-1. *Front Microbiol* 3: 37.

Liu, T., Chen, D., Li, X., and Li, F. (2019) Microbially mediated coupling of nitrate reduction and Fe(II) oxidation under anoxic conditions. *FEMS Microbiol Ecol* 95.

Llirós, M., García-Armisen, T., Darchambeau, F., Morana, C., Triadó-Margarit, X., Inceoğlu, Ö. *et al.* (2015) Pelagic photoferrotrophy and iron cycling in a modern ferruginous basin. *Scientific reports* 5: 13803-13803.

Love, M.I., Huber, W., and Anders, S. (2014) Moderated estimation of fold change and dispersion for RNA-seq data with DESeq2. *Genome Biol* 15: 550.

Lovley, D.R., and Phillips, E.J.P. (1988) Novel mode of microbial energy metabolism: organic carbon oxidation coupled to dissimilatory reduction of iron or manganese. *Appl Environ Microbiol* 54: 1472-1480.

Lovley, D.R., Ueki, T., Zhang, T., Malvankar, N.S., Shrestha, P.M., Flanagan, K.A. *et al.* (2011) Geobacter: the microbe electric's physiology, ecology, and practical applications. *Adv Microb Physiol* 59: 1-100.

Lueders, T., Manefield, M., and Friedrich, M.W. (2004) Enhanced sensitivity of DNA- and rRNA-based stable isotope probing by fractionation and quantitative analysis of isopycnic centrifugation gradients. *Environ Microbiol* 6: 73-78.

Lymperopoulou, D.S., Kormas, K.A., and Karagouni, A.D. (2012) Variability of prokaryotic community structure in a drinking water reservoir (Marathonas, Greece). *Microbes Environ* 27: 1-8.

Mahaffy, P.R., Webster, C.R., Atreya, S.K., Franz, H., Wong, M., Conrad, P.G. *et al.* (2013) Abundance and isotopic composition of gases in the martian atmosphere from the Curiosity rover. *Science* 341: 263-266.

Martin, F., Torelli, S., Le Paslier, D., Barbance, A., Martin-Laurent, F., Bru, D. *et al.* (2012) Betaproteobacteria dominance and diversity shifts in the bacterial community of a PAH-contaminated soil exposed to phenanthrene. *Environ Pollut* 162: 345-353.

Martin, M. (2011) Cutadapt removes adapter sequences from high-throughput sequencing reads. *EMBnet journal* 17: 3.

McAllister, S.M., Polson, S.W., Butterfield, D.A., Glazer, B.T., Sylvan, J.B., and Chan, C.S. (2020) Validating the Cyc2 neutrophilic iron oxidation pathway using meta-omics of *Zetaproteobacteria* iron mats at marine hydrothermal vents. *mSystems* 5: e00553-00519.

McBeth, J.M., Fleming, E.J., and Emerson, D. (2013) The transition from freshwater to marine iron-oxidizing bacterial lineages along a salinity gradient on the Sheepscot River, Maine, USA. *Environ Microbiol Rep* 5: 453-463.

Melton, E.D., Swanner, E.D., Behrens, S., Schmidt, C., and Kappler, A. (2014) The interplay of microbially mediated and abiotic reactions in the biogeochemical Fe cycle. *Nat Rev Microbiol* 12: 797-808.

Michalski, J.R., Cuadros, J., Niles, P.B., Parnell, J., Deanne Rogers, A., and Wright, S.P. (2013) Groundwater activity on Mars and implications for a deep biosphere. *Nat Geosci* 6: 133-138.

Ming, D.W., Archer, P.D., Glavin, D.P., Eigenbrode, J.L., Franz, H.B., Sutter, B. *et al.* (2014) Volatile and organic compositions of sedimentary rocks in Yellowknife Bay, Gale crater, Mars. *Science* 343: 1245267.

Mitchell, P. (1961) Coupling of phosphorylation to electron and hydrogen transfer by a chemi-osmotic type of mechanism. *Nature* 191: 144-148.

Mori, J.F., Scott, J.J., Hager, K.W., Moyer, C.L., Küsel, K., and Emerson, D. (2017) Physiological and ecological implications of an iron- or hydrogen-oxidizing member of the Zetaproteobacteria, *Ghiorsea bivora*, gen. nov., sp. nov. *ISME J* 11: 2624-2636.

Moss, E.L., Maghini, D.G., and Bhatt, A.S. (2020) Complete, closed bacterial genomes from microbiomes using nanopore sequencing. *Nat Biotechnol* 38: 701-707.

Mumford, A.C., Adaktylou, I.J., and Emerson, D. (2016) Peeking under the iron curtain: development of a microcosm for imaging the colonization of steel surfaces by *Mariprofundus* sp. Strain DIS-1, an oxygen-tolerant Fe-oxidizing bacterium. *Appl Environ Microbiol* 82: 6799-6807.

Murray, A.E., Freudenstein, J., Gribaldo, S., Hatzenpichler, R., Hugenholtz, P., Kämpfer, P. *et al.* (2020) Roadmap for naming uncultivated Archaea and Bacteria. *Nat Microbiol* 5: 987-994.

Murray, R.G., and Stackebrandt, E. (1995) Taxonomic note: implementation of the provisional status *Candidatus* for incompletely described procaryotes. *Int J Syst Bacteriol* 45: 186-187.

Myers, C.R., and Nealson, K.H. (1990) Respiration-linked proton translocation coupled to anaerobic reduction of manganese(IV) and iron(III) in *Shewanella putrefaciens* MR-1. *J Bacteriol* 172: 6232-6238.

Nakagawa, K., Murase, J., Asakawa, S., and Watanabe, T. (2020) Involvement of microaerophilic iron-oxidizing bacteria in the iron-oxidizing process at the surface layer of flooded paddy field soil. *J Soils Sediments* 20: 4034-4041.

Nordhoff, M., Tominski, C., Halama, M., Byrne, J.M., Obst, M., Kleindienst, S. *et al.* (2017) Insights into nitrate-reducing Fe(II) oxidation mechanisms through analysis of cell-mineral associations, cell encrustation, and mineralogy in the chemolithoautotrophic enrichment culture KS. *Appl Environ Microbiol* 83: e00752-00717.

Nurk, S., Meleshko, D., Korobeynikov, A., and Pevzner, P.A. (2017) metaSPAdes: a new versatile metagenomic assembler. *Genome Res* 27: 824-834.

Parada, A.E., Needham, D.M., and Fuhrman, J.A. (2016) Every base matters: assessing small subunit rRNA primers for marine microbiomes with mock communities, time series and global field samples. *Environ Microbiol* 18: 1403-1414.

Peduzzi, S., Storelli, N., Welsh, A., Peduzzi, R., Hahn, D., Perret, X., and Tonolla, M. (2012) *Candidatus* "Thiodictyon syntrophicum", sp. nov., a new purple sulfur bacterium isolated from the chemocline of Lake Cadagno forming aggregates and specific associations with *Desulfocapsa* sp. *Syst Appl Microbiol* 35: 139-144.

Perez-Riverol, Y., Csordas, A., Bai, J., Bernal-Llinares, M., Hewapathirana, S., Kundu, D.J. *et al.* (2019) The PRIDE database and related tools and resources in 2019: improving support for quantification data. *Nucleic Acids Res* 47: D442-d450.

Pertea, M., Kim, D., Pertea, G.M., Leek, J.T., and Salzberg, S.L. (2016) Transcript-level expression analysis of RNA-seq experiments with HISAT, StringTie and Ballgown. *Nat Protoc* 11: 1650-1667.

Porsch, K., and Kappler, A. (2011) FeII oxidation by molecular O_2 during HCl extraction. *Environmental Chemistry* 8: 190-197.

Prakash, O., Green, S.J., Jasrotia, P., Overholt, W.A., Canion, A., Watson, D.B. *et al.* (2012) *Rhodanobacter denitrificans* sp. nov., isolated from nitrate-rich zones of a contaminated aquifer. *Int J Syst Evol Microbiol* 62: 2457-2462.

Price, A., Pearson, V.K., Schwenzer, S.P., Miot, J., and Olsson-Francis, K. (2018) Nitrate-dependent iron oxidation: a potential Mars metabolism. *Front Microbiol* 9.

Price, M.N., Deutschbauer, A.M., and Arkin, A.P. (2020) GapMind: automated annotation of amino acid biosynthesis. *mSystems* 5: e00291-00220.

Pruesse, E., Quast, C., Knittel, K., Fuchs, B.M., Ludwig, W., Peplies, J., and Glockner, F.O. (2007) SILVA: a comprehensive online resource for quality checked and aligned ribosomal RNA sequence data compatible with ARB. *Nucleic Acids Res* 35: 7188-7196.

Rabus, R., and Widdel, F. (1995) Anaerobic degradation of ethylbenzene and other aromatic hydrocarbons by new denitrifying bacteria. *Arch Microbiol* 163: 96-103.

Rappsilber, J., Mann, M., and Ishihama, Y. (2007) Protocol for micro-purification, enrichment, pre-fractionation and storage of peptides for proteomics using StageTips. *Nat Protoc* 2: 1896-1906.

Rentz, J.A., Kraiya, C., Luther, G.W., 3rd, and Emerson, D. (2007) Control of ferrous iron oxidation within circumneutral microbial iron mats by cellular activity and autocatalysis. *Environ Sci Technol* 41: 6084-6089.

Rocha, D.J., Santos, C.S., and Pacheco, L.G. (2015) Bacterial reference genes for gene expression studies by RT-qPCR: survey and analysis. *Antonie Van Leeuwenhoek* 108: 685-693.

Rodriguez-R, L.M., and Konstantinidis, K.T. (2016) The enveomics collection: a toolbox for specialized analyses of microbial genomes and metagenomes. *PeerJ Prepr* 4: e1900v1901.

Sauter, L. (2018) The competition between nitrate-reducing Fe(II)-oxidizing and photoferrotrophic microorganisms in the environment. In *Center for Applied Geoscience*: Eberhard-Karls-University Tübingen, pp. 12-13, 25.

Schmidt, C., Nikeleit, V., Schaedler, F., Leider, A., Lueder, U., Bryce, C. *et al.* (2020) Metabolic responses of a phototrophic co-culture enriched from a freshwater sediment on changing substrate availability and its relevance for biogeochemical iron cycling. *Geomicrobiol J*: 1-15.

Schmitt, M., Sinnberg, T., Nalpas, N.C., Maass, A., Schittek, B., and Macek, B. (2019) Quantitative proteomics links the intermediate filament nestin to resistance to targeted BRAF inhibition in melanoma cells. *Mol Cell Proteomics* 18: 1096-1109.

Schoch, C.L., Ciufo, S., Domrachev, M., Hotton, C.L., Kannan, S., Khovanskaya, R. *et al.* (2020) NCBI Taxonomy: a comprehensive update on curation, resources and tools. *Database (Oxford)* 2020.

Shelobolina, E., Konishi, H., Xu, H., Benzine, J., Xiong, M.Y., Wu, T. *et al.* (2012) Isolation of phyllosilicate-iron redox cycling microorganisms from an illite-smectite rich hydromorphic soil. *Front Microbiol* 3: 134.

Singer, S.J. (1990) The structure and insertion of integral proteins in membranes. *Annu Rev Cell Biol* 6: 247-296.

Song, X., Wang, S., Wang, Y., Zhao, Z., and Yan, D. (2016) Addition of Fe^{2+} increase nitrate removal in vertical subsurface flow constructed wetlands. *Ecol Eng* 91: 487-494.

Spät, P., Maček, B., and Forchhammer, K. (2015) Phosphoproteome of the cyanobacterium *Synechocystis* sp. PCC 6803 and its dynamics during nitrogen starvation. *Front Microbiol* 6: 248.

Stackebrandt, E., Frederiksen, W., Garrity, G.M., Grimont, P.A.D., Kämpfer, P., Maiden, M.C.J. *et al.* (2002) Report of the ad hoc committee for the re-evaluation of the species definition in bacteriology. *Int J Syst Evol Microbiol* 52: 1043-1047.

Steinert, G., Whitfield, S., Taylor, M.W., Thoms, C., and Schupp, P.J. (2014) Application of diffusion growth chambers for the cultivation of marine sponge-associated bacteria. *Mar Biotechnol* 16: 594-603.

Stern, J.C., Sutter, B., Freissinet, C., Navarro-González, R., McKay, C.P., Archer, P.D. *et al.* (2015) Evidence for indigenous nitrogen in sedimentary and aeolian deposits from the *Curiosity* rover investigations at Gale crater, Mars. *PNAS* 112: 4245-4250.

Straub, D., Blackwell, N., Langarica-Fuentes, A., Peltzer, A., Nahnsen, S., and Kleindienst, S. (2020) Interpretations of environmental microbial community studies are biased by the selected 16S rRNA (gene) amplicon sequencing pipeline. *Front Microbiol* 11: 550420.

Straub, K.L., and Buchholz-Cleven, B.E. (1998) Enumeration and detection of anaerobic ferrous iron-oxidizing, nitrate-reducing bacteria from diverse European sediments. *Appl Environ Microbiol* 64: 4846–4856.

Straub, K.L., Rainey, F.A., and Widdel, F. (1999) *Rhodovulum iodosum* sp. nov. and *Rhodovulum robiginosum* sp. nov., two new marine phototrophic ferrous-iron-oxidizing purple bacteria. *Int J Syst Bacteriol* 49 Pt 2: 729-735.

Straub, K.L., Benz, M., Schink, B., and Widdel, F. (1996) Anaerobic, nitrate-dependent microbial oxidation of ferrous iron. *Appl Environ Microbiol* 62: 1458.

Straub, K.L., Schönhuber, W.A., Buchholz-Cleven, B.E.E., and Schink, B. (2004) Diversity of ferrous iron-oxidizing, nitrate-reducing bacteria and their involvement in oxygen-independent iron cycling. *Geomicrobiol J* 21: 371-378.

Su, J.F., Shi, J.X., Huang, T.L., Ma, F., Lu, J.S., and Yang, S.F. (2016) Effect of nitrate concentration, pH, and hydraulic retention time on autotrophic denitrification efficiency with Fe(II) and Mn(II) as electron donors. *Water Sci Technol* 74: 1185-1192.

Su, J.f., Shao, S.c., Huang, T.l., Ma, F., Yang, S.f., Zhou, Z.m., and Zheng, S.c. (2015) Anaerobic nitrate-dependent iron(II) oxidation by a novel autotrophic bacterium, *Pseudomonas* sp. SZF15. *J Environ Chem Eng* 3: 2187-2193.

Tamura, K., and Nei, M. (1993) Estimation of the number of nucleotide substitutions in the control region of mitochondrial DNA in humans and chimpanzees. *Mol Biol Evol* 10: 512-526.

Team, R. (2019) RStudio: integrated development for R. *RStudio, Inc Boston, MA*

Team, R.C. (2020) R: A language and environment for statistical computing. *R Foundation for Statistical Computing, Vienna, Austria*.

Team, R.D.C. (2018) R: A language and environment for statistical computing. *Generic*.

Temple, K.L., and Colmer, A.R. (1951) The autotrophic oxidation of iron by a new bacterium, *Thiobacillus ferrooxidans*. *J Bacteriol* 62: 605-611.

Tominski, C. (2016) Genetic and physiological mechanisms of nitrate-dependent Fe(II) oxidation in the chemolithoautotrophic enrichment culture KS. In *Department of Geosciences*. Tuebingen: Eberhard Karls University of Tuebingen, p. 158.

Tominski, C., Heyer, H., Lösekann-Behrens, T., Behrens, S., and Kappler, A. (2018a) Growth and population dynamics of the anaerobic Fe(II)-oxidizing and nitrate-reducing enrichment culture KS. *Appl Environ Microbiol* 84: e02173-02117.

Tominski, C., Lösekann-Behrens, T., Ruecker, A., Hagemann, N., Kleindienst, S., Mueller, C.W. *et al.* (2018b) Insights into carbon metabolism provided by fluorescence *in situ* hybridization-secondary ion mass spectrometry imaging of an autotrophic, nitrate-reducing, Fe(II)-oxidizing enrichment culture. *Appl Environ Microbiol* 84: 19.

Valdés, J., Pedroso, I., Quatrini, R., Dodson, R.J., Tettelin, H., Blake, R., 2nd *et al.* (2008) *Acidithiobacillus ferrooxidans* metabolism: from genome sequence to industrial applications. *BMC Genomics* 9: 597.

Varghese, N.J., Mukherjee, S., Ivanova, N., Konstantinidis, K.T., Mavrommatis, K., Kyrpides, N.C., and Pati, A. (2015) Microbial species delineation using whole genome sequences. *Nucleic Acids Res* 43: 6761-6771.

von Meijenfeldt, F.A.B., Arkhipova, K., Cambuy, D.D., Coutinho, F.H., and Dutilh, B.E. (2019) Robust taxonomic classification of uncharted microbial sequences and bins with CAT and BAT. *Genome Biol* 20: 217.

Wagner, C., Mau, M., Schlömann, M., Heinicke, J., and Koch, U. (2007) Characterization of the bacterial flora in mineral waters in upstreaming fluids of deep igneous rock aquifers. *J Geophys Res Biogeosci* 112.

Wang, J., Muyzer, G., Bodelier, P.L.E., and Laanbroek, H.J. (2009) Diversity of iron oxidizers in wetland soils revealed by novel 16S rRNA primers targeting *Gallionella*-related bacteria. *ISME J* 3: 715-725.

Waterhouse, R.M., Seppey, M., Simão, F.A., Manni, M., Ioannidis, P., Klioutchnikov, G. *et al.* (2018) BUSCO applications from quality assessments to gene prediction and phylogenomics. *Mol Biol Evol* 35: 543-548.

Weber, K.A., Pollock, J., Cole, K.A., O'Connor, S.M., Achenbach, L.A., and Coates, J.D. (2006) Anaerobic nitrate-dependent iron(II) bio-oxidation by a novel lithoautotrophic betaproteobacterium, strain 2002. *Appl Environ Microbiol* 72: 686-694.

Weiss, J.V., Rentz, J.A., Plaia, T., Neubauer, S.C., Merrill-Floyd, M., Lilburn, T. *et al.* (2007) Characterization of neutrophilic Fe(II)-oxidizing bacteria isolated from the rhizosphere of wetland plants and description of *Ferritrophicum radicicola* gen. nov. sp. nov., and *Sideroxydans paludicola* sp. nov. *Geomicrobiol J* 24: 559-570.

Widdel, F., Schnell, S., Heising, S., Ehrenreich, A., Assmus, B., and Schink, B. (1993) Ferrous iron oxidation by anoxygenic phototrophic bacteria. *Nature* 362: 834-836.

Widdison, P.E., and Burt, T.P. (2008) Nitrogen cycle. In *Encyclopedia of Ecology*. Jørgensen, S.E., and Fath, B.D. (eds). Oxford: Academic Press, pp. 2526-2533.

Wilmes, P., Heintz-Buschart, A., and Bond, P.L. (2015) A decade of metaproteomics: where we stand and what the future holds. *Proteomics* 15: 3409-3417.

Winogradsky, S. (1888) *Beiträge zur Morphologie und Physiologie der Bacterien: hft. I.: Zur Morphologie und Physiologie der Schwefelbacterien*: Verlag von Arthur Felix.

Zdobnov, E.M., Tegenfeldt, F., Kuznetsov, D., Waterhouse, R.M., Simão, F.A., Ioannidis, P. *et al.* (2017) OrthoDB v9.1: cataloging evolutionary and functional annotations for animal, fungal, plant, archaeal, bacterial and viral orthologs. *Nucleic Acids Res* 45: D744-d749.

Zhang, H., Wang, H., Yang, K., Sun, Y., Tian, J., and Lv, B. (2015) Nitrate removal by a novel autotrophic denitrifier (*Microbacterium* sp.) using Fe(II) as electron donor. *Annals of Microbiology* 65: 1069-1078.

Zhang, X., Li, A., Szewzyk, U., and Ma, F. (2016) Improvement of biological nitrogen removal with nitrate-dependent Fe(II) oxidation bacterium *Aquabacterium parvum* B6 in an up-flow bioreactor for wastewater treatment. *Bioresour Technol* 219: 624-631.

Zhang, Y., Ma, A., Liu, W., Bai, Z., Zhuang, X., and Zhuang, G. (2018) The occurrence of putative nitric oxide dismutase (Nod) in an alpine wetland with a new dominant subcluster and the potential ability for a methane sink. *Archaea* 2018: 6201541.

Zhimiao, Z., Zhufang, W., Mengyu, C., Xinshan, S., Mengqi, C., and Yinjiang, Z. (2020) Adding ferrous ions improved the performance of contaminant removal from low C/N coastal wastewater in constructed wetlands. *Environ Sci: Water Res Technol* 6: 3351-3360.

Zhou, J., Wang, H., Yang, K., Ji, B., Chen, D., Zhang, H. *et al.* (2016) Autotrophic denitrification by nitrate-dependent Fe(II) oxidation in a continuous up-flow biofilter. *Bioprocess Biosyst Eng* 39: 277-284.

Zhu, B., Wang, J., Bradford, L.M., Ettwig, K., Hu, B., and Lueders, T. (2019) Nitric oxide dismutase (*nod*) genes as a functional marker for the diversity and phylogeny of methane-driven oxygenic denitrifiers. *Front Microbiol* 10: 1577.

Zhu, B., Bradford, L., Huang, S., Szalay, A., Leix, C., Weissbach, M. *et al.* (2017) Unexpected diversity and high abundance of putative nitric oxide dismutase (Nod) genes in contaminated aquifers and wastewater treatment systems. *Appl Environ Microbiol* 83: e02750-02716.

Zilli, J.E., Barauna, A.C., da Silva, K., De Meyer, S.E., Farias, E.N.C., Kaminski, P.E. *et al.* (2014) *Bradyrhizobium neotropicale* sp. nov., isolated from effective nodules of *Centrolobium paraense*. *Int J Syst Evol Microbiol* 64: 3950-3957.

ZoBell, C.E., and Upham, H. C. (1944) *A list of marine bacteria including descriptions of sixty new species.* Berkeley, CA, USA: University of California Press.

8. Appendix

List of abbreviations

Abbreviations	Full name
ASVs	amplicon sequencing variants
AG	Altingen groundwater
BLAST	basic local alignment search tool
BP	Bremen pond
Ca.	Candidatus
CO_2	carbon dioxide
DAPI	4′,6-Diamidino-2-phenylindole
DNA	deoxyribonucleic acid
DOC	dissolved organic carbon
EET	extracellular electron transfer
EPS	extracellular polymeric substances
F.	Ferrigenium
FC	log_2 fold change
Fe	iron
Fe-EDAS	ferrous ethylenediammonium sulfate
FeOB	Fe(II)-oxidizing bacteria
Fig.	figure
FISH	fluorescence in situ hybridization
GC-MC	gas chromatography coupled to mass spectrometry
HPLC	high-performance liquid chromatography
IMG	Integrated Microbial Genomes & Microbiomes
IMG/MER	Joint Genome Institute's Integrated Microbial Genome and Microbiome Expert Review
KS	Kristina Straub
LC-MS/MS	liquid chromatography–mass spectrometry/mass spectrometry
MAG	metagenome-assembled genomes
N_2	nitrogen
N_2O	nitrous oxide
NCBI	National Center for Biotechnology Information
NO	nitric oxide
NO_2^-	nitrite
NO_3^-	nitrate
NRFeOx	nitrate reduction coupled to Fe(II) oxidation
PacBio	Pacific Biosciences
PCR	polymerase chain reaction

PCT	Quantitative Proteomics & Proteome Center, Tuebingen
PFA	paraformaldehyde
QBiC	Quantitative Biology Center
RNA	ribonucleic acid
RT	room temperature
RuBisCO	ribulose 1,5-bisphosphate carboxylase/oxygenase
SI	supplementary information
TPM	transcripts per kilobase million

List of figures

Fig. S3.3. Phylogenetic trees of MtoA (A) and MtoB (B) of *Noviherbaspirillum* sp. and other Fe(II)-oxidizing bacteria based on amino acid sequences with bootstrap values, calculated on 1000 replicates using the Maximum Likelihood method.

Fig. S3.4. Phylogenetic trees of RuBisCO from culture BP, flanking members and other Fe(II)-oxidizing bacteria: RbcL (A) and RbcS (B) based on amino acid sequences with bootstrap values, calculated on 1000 replicates using the Maximum Likelihood method.

Fig. S3.5. Phylogenetic tree of the *Gallionellaceae* spp. ASVs detected in the environmental sediments compared to isolated *Gallionellaceae* spp. and Fe(II)-oxidizing bacteria based on nucleotide sequences with bootstrap values, calculated on 1000 replicates using the Maximum Likelihood method.

Fig. S3.6. Bubble plot showing the relative abundance of amplicon sequence variants (ASVs) of microbial populations from culture BP (identical ASV and genus or family level, respectively), detected in environmental sediments.

Fig. S3.7. Heatmap of normalized transcripts per kilobase million (TPM) of the *Gallionellaceae* sp., *Noviherbaspirillum* sp., *Thiobacillus* sp., *Rhodoferax* sp. and *Ramlibacter* sp. metagenome-assembled genomes. Visualized are normalized TPM values for the pathways of Fe(II) oxidation, carbon fixation, denitrification and oxygen respiration.

Fig. 4.1. Phylogenetic tree of seven isolated *Gallionellaceae* spp. and six metagenome assembled genomes (*Candidatus* species), using available full or nearly full-length 16S rRNA gene sequences and calculated on 1000 replicates using the Maximum Likelihood method.

Fig. 4.2. Nearly full-length 16S rRNA gene identity, average amino acid identity (AAI), average nucleotide identity (ANI), alignment fraction (AF; genome x aligned to genome y [upper no.], genome y aligned to genome x [lower no.]) of strains from '*Candidatus* Ferrigenium straubiae' (strain KS) sp. nov., '*Candidatus* Ferrigenium bremense' (strain BP) sp. nov. and '*Candidatus* Ferrigenium altingense' (strain AG) sp. nov. compared to their top three closely related isolated strains affiliating with the genera *Ferrigenium*, *Sideroxydans* and *Gallionella*.

Fig. 4.3. Phylogenetic tree of nine concatenated house-keeping genes amino acid sequences of *rpoA, gyrA, secA, ileS, rho* and *infB* of isolated and *Candidatus* members

of the *Gallionellaceae* family and other FeOB, calculated on 1000 replicates using the Maximum Likelihood method.

Fig. 4.4. Summary of key gene copy numbers involved in putative Fe(II)-oxidation, denitrification and carbon fixation of '*Ca.* Ferrigenium straubiae', '*Ca.* Ferrigenium bremense' and '*Ca.* Ferrigenium altingense', *Ferrigenium kumadai* An22, *Sideroxydans lithotrophicus* ES-1, *Gallionella capsiferriformans* ES-2, *Ferriphaselus* sp. R-1, *Ferriphaselus amnicola* OYT1.

Fig. 4.5. Scanning electron microscopy (SEM) pictures of culture KS, culture BP and culture AG during the mid Fe(II)-oxidation stage (exponential growth phase) and at the end of the Fe(II)-oxidation stage (lag phase).

List of tables

Statement of personal contribution, authorship and copyright

The work described in this thesis was supported by the German Research Foundation (Deutsche Forschungsgemeinschaft, DFG)-funded research training group RTG 1708 “Molecular principles of bacterial survival strategies”. The concept background and experimental design was discussed with Junior Prof. Sara Kleindienst, Dr. Nia Blackwell and Prof. Andreas Kappler. The experiments and data analysis for biological meaning were carried out by myself. The bioinformatic work and data discussion in this thesis was conducted by Daniel Straub. All these four supervisors wrote, reviewed and revised the manuscript for the publication related to chapter 2, chapter 3 and chapter 4. Prof. Karl Forchhammer and Prof. Klaus Hantke provide their objective and critical discussion of the concepts and results of this work. Ellen Roehm, Lars Grimm and Franziska Schaedler trained me to conduct all the experiments in the lab. The detail contribution of other people were:

Chapter 2: Metaproteomic analysis by Irina Droste-Borel from proteomic center, nitrate, nitrite and acetate measurement by Ellen Roehm, DAPI cell counts by Katrin Wunsch, Libera Lo-Presti and Katharine Thompson for initial manuscript draft review.

Chapter 3: Nicole Smith carried out partial metagenomic and 16S rRNA amplicon sequencing data interpretation, wrote and revised of the manuscript for the publication related to this chapter. The sediment sample from Bremen for cultivation was obtained by Shun Li, and Wiebke Ruschmeier later set up the enrichment culture. Jens Harder, Ingrid Kunze, Timm Bayer, Lea Sauter and Casey Bryce assisted obtaining the environmental samples in Bremen. Natalia Jakus prepare the PacBio samples from extracted DNA. The PacBio library preparation and sequencing were done by Zhe Wang. Irina Droste-Borel conducted metaproteomic measurement and partial raw data analysis. Nitrate, nitrite and acetate measurement were done by Ellen Roehm, Verena Nikeleit and Franziska Schaedler. Stefanie Becker developed the cell count methods for flow cytometry.

Chapter 4: Stefan Fischer conduct scanning electron microscopy with the infrastructural support by the DFG under Germany’s Excellence Strategy, cluster of Excellence EXC2124, project ID 390838134 and the Tübingen Structural Microscopy Core Facility (funded by the Excellence Strategy of the German Federal and State Governments) (INST 37/1027-1 FUGG) for financial support provided for the acquisition of the cryogenic focused ion beam scanning electron microscope.

Chapter 5: This work was mostly done by other researchers and the co-authors. My personal contribution to this review was writing partial paragraphs of nitrate-reducing Fe(II) oxidation section, reviewing and revising the table 1 and preparing the figures 3 and 4.

I hereby declare that I have written this thesis independently with the revision of the publication manuscripts by the co-authors. I have used the indicated references, and have not plagiarized any of the text. Chapters 2, 3 and 5 have been published in scientific journals. Chapters 4 will be submitted to another scientific journal and thus, it may be published in a slightly modified version elsewhere in the future.

Publications and conferences

A. Accepted and published peer-reviewed publications

First author:

Huang, Y., Straub, D., Blackwell, N., Kappler, A., and Kleindienst, S. (2021) Meta-omics reveal *Gallionellaceae* and *Rhodanobacter* as interdependent key players for Fe(II) oxidation and nitrate reduction in the autotrophic enrichment culture KS. *Appl Environ Microbiol*: AEM.00496-21. https://doi.org/10.1128/AEM.00496-21

Huang, Y., Straub, D., Kappler, A., Smith, N., Blackwell, N., and Kleindienst, S. (2021) A novel enrichment culture highlights core features of microbial networks contributing to autotrophic Fe(II) oxidation coupled to nitrate reduction. *Microbial Physiol*. https://doi.org/10.1159/000517083

Co-author:

Bryce, C., Blackwell, N., Schmidt, C., Otte, J., **Huang, Y.**, Kleindienst, S. Tomaszewski, E., Schad, M., Warter, V., Peng, C., Byrne, J. M., Kappler, A. (2018) Microbial anaerobic Fe(II) oxidation - Ecology, mechanisms and environmental implications. *Environ Microbiol* 20: 3462-3483. https://doi.org/10.1111/1462-2920.14328

B. Submitted manuscript

Huang, Y., Jakus N., Straub, D., Konstantinidis K. T., Blackwell, N., Kappler, A., and Kleindienst, S. '*Candidatus* Ferrigenium straubiae' sp. nov., '*Candidatus* Ferrigenium bremense' sp. nov., '*Candidatus* Ferrigenium altingense' sp. nov., are autotrophic Fe(II)-oxidizing bacteria of the family *Gallionellaceae*. *Syst Appl Microbiol*

C. Conferences

Goldschmidt 2020: online

Meta-omics reveal insights into microbial Fe(II) oxidation coupled to nitrate reduction in freshwater enrichment cultures

Goldschmidt 2019: 18-23 August in Barcelona, Spain

Mechanisms of Fe(II) oxidation coupled to nitrate reduction in a freshwater enrichment culture: a metagenome-based approach